Imperial College London

Faculty of Medicine

Department of Cellular and Molecular Neuroscience

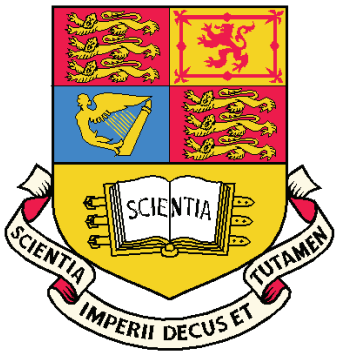

Role of inflammation in 6- hydroxydopamine model of Parkinson's disease and its modulation by Peroxisome Proliferator Activated receptor gamma (PPAR-γ) agonist as a neuroprotective strategy.

Mona Sadeghian

A thesis submitted in fulfilment of the requirements for the degree of Doctor of Philosophy in the Faculty of Medicine of Imperial College London

Declaration

I declare that this thesis is my own work and has not been submitted in any form for another degree or diploma at any university or other institution of tertiary education. Information derived from the published or unpublished work of others has been acknowledged in the text and a list of references is given.

Acknowledgements

There are many individuals who contributed to the production of this thesis through their support, advice and patience whom I would like to acknowledge here.

Firstly, I am indebted to Dr David T. Dexter and Dr Lilia Marinova for their patience, encouragement and supervision throughout my studies. It has been a pleasure to work on this challenging project. In addition thanks to GSK for funding this project.

Secondly, for their friendship, support, encouragement and contributions, I am indebted to my immediate colleagues, Miss Lauren Broom, Miss Rachel Allen and Mr Hugh Chan.

Finally, I would like to express my profound appreciation to my family and friends, in particular to Mum and Dad and my finace Neysun, thank you for always encouraging me to do my best and supporting me all the way.

Abstract

Parkinson's disease is an age related progressive neurodegenerative disorder affecting ~2% of the population over the age of 65. The aetiology of Parkinson's disease is not fully understood and treatment limited. Hence, the goal of ongoing research is to understand and target the mechanisms underlying the disease process to halt or slow down its progression. Parkinson's disease is pathologically characterised by the loss of dopaminergic neurons in the substantial nigra that leads to the loss of innervation to the striatum, subsequently leading to the motor complications observed in Parkinson's sufferers.

Recent clinical and experimental evidence suggests that inflammation, characterised by over activation of the brain's resident immune cells such as microglia/macrophages, play a detrimental role in Parkinson's pathology. This project, for the first time aims to explore the time course of microglial activation in association with dopaminergic neuronal cell death in the substantia nigra utilising the 6-hydroxy dopamine rat model of Parkinson's. The dynamics of morphological, immunophenotypic and phagocytic properties of activated microglia in the substantia nigra was assessed immunohistochemically. In addition we explored the cellular events between activated microglia and degenerating neurons in this model that had not been previously well defined. The role of matrix metalloproteinases as signalling molecules that activate microglia were also studied. Finally the significance of local microglial activation in the substantia nigra was elucidated by modulation of the microglial response via activation of the gamma subtype of peroxisome proliferator activated receptors. This project provided evidence that microglial activation preceded dopaminergic neuronal cell death in the substantia nigra and inhibition of microglial response serves as a neuroprotective strategy in Parkinson's disease.

Table of content

Chapter 1 Introduction 12

1.1 Parkinson's disease 13
1.2 Neuropathological features of idiopathic PD 14
1.2.1 Dopaminergic neuropathology in PD 17
1.2.2 Non-dopaminergic neuropathology in PD 18
1.3 Current pharmacological treatments for PD and their limitations 18
1.4 Epidemiology of PD 19
1.5 Aetiology and pathogenesis of PD 20
1.5.1 Environmental risk factors for idiopathic PD 20
1.5.1 Environmental risk factors for idiopathic PD 20
1.5.2 Genetic risk factors 22
1.5.3. Pathogenesis of PD 23
Oxidative stress and neurodegeneration in PD 23
Ubiquitin-proteasome system dysfunction 24
1.6 Inflammation in the brain 25
1.6.1 Microglia and their function 27
1.6.2 Inflammation inducing risk factors and development of PD 29
1.6.3 Inflammation in PD 30
1.6.3.1 Atypical glial pathology in PD 30
1.6.4 Evidence for involvement of inflammation in PD pathology 31
1.6.4.1 Evidence from human studies 31
1.6.4.2 Evidence from animal models of PD 32

Inflammation in MPTP model of PD 32
Inflammation in 6-Hydroxydopamine (6-OHDA) model of PD 33
Inflammation in Lipopolysaccaride (LPS) model of PD 33

1.7 Triggers for microglial activation 35
1.8 Aims of the study 35

Chapter 2 Material and Methods 38

2.1 In vivo methods 39
2.1.1 6-hydroxydopamine (6-OHDA) experimental model of Parkinson's disease 39
2.1.1.1 Overview 39
Benefits and limitations of 6-OHDA rat model 40
2.1.1.2 Medial forebrain bundle lesions 41
2.1.1.3 Mechanism of 6-OHDA neurotoxicity 43
2.1.1.4 Motor impairments in 6-OHDA lesion induced model of PD 44
2.1.2 Stereotaxic surgery 45
2.1.2.1 Animals 45
2.1.2.2 Stereotaxic injection of 6-OHDA into the MFB 45
2.1.3 Post-mortem procedures and brain tissue collection 48
2.2 Ex-vivo methods 48
2.2.1 Avidin-Biotin Immunohistochemistry 48
2.2.1.1 Overview 48
2.2.1.2 General standard protocol for ABC immunohistochemistry 51
2.2.1.3 Tyrosine hydroxylase (TH) immunohistochemistry protocol 52

2.2.1.4 Immunostaining for markers of glial cell activation in the SNc..... 52
2.2.1.5 Immunostaining for matrix metalloproteinase 3 (MMP3) expression in SNc 53
2.2.2 Double immunofluorescence..... 55
2.2.2.1 General immunofluorescence protocol..... 55
2.2.3 Cell counting and morphological assessment of immunostained cells 58
2.2.3.1 Quantitative cell counting for TH+ve, glial cells , MMP-3+ve and MMP-9 +ve in SNc and VTA 58
2.2.3.2 Morphological assessment of glial cells..... 58
2.2.4 Assessment of striatal catecholamine/monoamine neurotransmitters by High Performance Liquid Chromatography (HPLC) 61
2.2.4.1 HPLC methodology..... 61
2.3 Statistical analysis of the data 64

Chapter 3..... 65

A time course study into the relationship between microglial activation and dopaminergic neuronal cell loss in the substantia nigra of 6-hydroxydopamine model of Parkinson's disease. 65

3.1 Introduction 66
3.2 Experimental design..... 69
3.2.1 Dopaminergic neuronal loss in the SNc following 6-OHDA lesion induction in relation to the dynamic of microgliaactivation……73
3.2.1.1 Assessment of the nigrostriatal lesion progression induced by 6-OHDA injected into the MFB..... 69
3.2.1.2. Assessment of the kinetics of microglial activation and changes in morphology following..... 69
3.3 Statistical analysis..... 71
3.4 Results..... 72
3.4.1 6-OHDA induces a progressive loss of dopaminergic neurons and striatal Dopamine, with local activation of microglia in the SNc 72
3.4.1.1 Effect of 6-OHDA on TH+ve dopaminergic neurons in the SNc and dopamine 72
content in the striatum 72
3.4.1.1 Effect of 6-OHDA on TH+ve dopaminergic neurons in the SNc and dopamine content in the striatum..... 72
3.4.2 The extent of activation of microglia and their localisation in the SNc following 6-OHDA lesioning……..78
3.4.2.1 Effect of 6-OHDA on the number OX42+ve microglial cells in the SNc……..78
3.4.2.2 Effect of 6-OHDA lesioning on the number OX42+ve microglial cells in the VTA..... 78
3.4.2.3 Effect of 6-OHDA lesioning on the number of OX6+ve microglial cells in the SNc 80
3.4.2.4 Effect of 6-OHDA lesioning on the number of OX-6+ve microglial cells in the VTA..... 80
3.4.2.5 iNOS expression by OX6+ve microglia cells in the SNc following 6-OHDA lesion induction..... 81
3.4.2.5 iNOS expression by OX6+ve microglia cells in the SNc following 6-OHDA lesion induction..... 81

3.4.2.6 Effect of 6-OHDA on the number of CD68+ve microglial cells in the SNc 84
3.4.3 Morphological and phenotypic characteristics of the activated microglia following 6-OHDA lesion induction 86
3.4.3.1 Morphological and phenotypic characteristics of OX6+ve and OX42+ve microglia in the SNc 86
3.4.3.2 Morphological and phenotypic characteristics of CD68+ve cells in the SNc 86
3.4.4 The dynamic of MHC class II expressing OX6+ve microglial cell proliferation in the SNc 88
3.4.5 Close interaction between activated microglia and degenerating dopaminergic neurons in the SNc following 6-OHDA lesion induction 88
3.4.5.1 Interaction between TH+ve dopaminergic and OX6+ve microglia cells in the SNc following 6-OHDA lesion induction 88
3.4.5.2 Interaction between TH+ve dopaminergic and CD68+ve macrophages in the SNc following 6-OHDA lesion induction 90
3.5 Discussion 92
3.5.1 Microglial activation preceded dopaminergic neuronal loss in the SNc and dopamine depletion in the striatum 92
3.5.2 Morphological and phenotypic characteristics of activated microglia 94
correlates with their function 94
3.5.3 Dynamics of activated microglia in the SNc 96
Conclusions 97

Chapter 4 99

The role of Matrix metalloproteinases and CD200 receptor in the neurodegenerative process in the substantia nigra of 6-hydroxydopamine model of Parkinson's disease 99

4.1 Introduction 100
4.1.1 Maintaining microglia quiescence 100
4.2 Matrix metalloproteinases (MMPs) and Parkinson's disease 102
4.2.1 Overview 102
4.2.2 Evidence of involvement of MMPs in PD pathology 103
4.2 Experimental design 107
4.2.1 Relationship between MMP-3 and MMP-9 expression and dopaminergic neuronal cell death in the SNc following 6-OHDA lesioning 107
..4.2.1.1 Assessment of the kinetics of MMP-3 and MMP-9 expressions in the SNc after 6-OHDA lesion induction 107
4.2.1.2 Assessment of the dopaminergic neuronal cell death progression induced by 6-OHDA injected into the MFB 108
4.2.2 Relationship between microglial activation and MMP-3 and MMP-9 expression in the SNc following 6-OHDA lesion induction 108
4.2.2.1 Assessment of the kinetics of microglial activation in the SNc after 6-OHDA lesion induction 109
4.2.2.2 Assessment of MMP-microglial interaction in the SNc after 6-OHDA lesion induction 109
4.2.3 Role of CD200R expression during the progression of 6-OHDA lesion in the SNc 110

4.2.3.1. Assessment of the kinetics of CD200R expressing cells in the SNc after 6-OHDA lesion induction 110
4.2.3.2 Assessment of the interaction between neurons and CD200R expressing cells in the SNc following 6-OHDA lesion induction 110
4.3 Results 111
4.3.1 Involvement of neuronal MMP-3 and MMP-9 activities in the progression of dopaminergic neuronal cell death in the SNc following 6-OHDA lesioning 111
4.3.1.1. Extent and localisation of MMP-3 expressing cells following 6-OHDA or sham lesioning in the SNc 111
4.3.1.2 Morphological characteristics of MMP-3 expressing cells in the SNc following 6-OHDA or sham lesioning 114
4.3.1.3 Extent and localisation of MMP-9 expressing cells following 6-OHDA or sham lesioning in the SNc 116
4.3.1.4. Morphological characteristics of MMP-9 expressing cells in the SNc following 6-OHDA lesioning 118
4.3.1.5 Kinetics of MMP-3 and MMP-9 expressions in relation to loss of TH+ve dopaminergic in the SNc following 6-OHDA lesion 120
4.3.2 Kinetics of MMP-3 expression in relation to OX6+ve and CD68+ve activated microglia/macrophages in the SNc following 6-OHDA lesion induction 123
4.3.2.1. Comparison between the kinetics of MMP-3 expression and OX6+ve activated microglia in the SNc after 6-OHDA lesion induction 123
4.3.2.2 Comparison between the kinetics of MMP-3 expression and CD68+ve activated microglia in the SNc after 6-OHDA lesion induction 126
4.3.2.3 Interaction between MMP-3 expressing cells and OX6+ve microglia in the SNc after 6-OHDA lesion induction 129
4.3.2.4 Interaction between MMP-3 expressing cells and CD68 +ve macrophages in the SNc after 6-OHDA lesion induction 129
4.3.3 Expression of CD200R during lesion progression in the SNc after 6-OHDA injection 131
4.3.3.1 Effect of 6-OHDA lesion induction on the number of CD200R expressing cells in the SNc 131
4.3.3.2 Localisation of CD200R+ve cells in the SNc following 6-OHDA lesion induction 133
4.3.3.3 Interaction between TH+ve dopaminergic neurons and CD200R+ve cells in the SN after 6-OHDA lesion induction 133
4.3.3.4 Interaction between MMP-3 expressing cells and CD200R+ve cells in the SNc after 6-OHDA lesion induction 135
4.4 Discussion 137
4.4.1 MMP-3 and MMP-9 expressions preceded dopaminergic neuronal loss in the SNc following 6-OHDA lesion induction 137
4.4.2 Interaction between activated microglia and MMP-3 expressing neurons in the SNc following 6-OHDA lesion induction 140
4.4.2 The dynamic of CD200R expression in relation MMP-3 expression and dopaminergic neuronal cell death in the SNc 142
Conclusions 143

Chapter 5 145

Neuroprotective effects of modulation of glial activity by peroxisome proliferator activated receptor gamma (PPAR-γ) agonists in the 6-hdroxydopamine model of Parkinson's disease..... 145

5.1 Introduction 146
5.1.1 PPAR-γ and inflammation..... 146
5.1.2 Anti-inflammatory role of PPAR-γ in PD 148
5.2 Experimental design..... 152
5.2.1 Treatments with GW855266X, pioglitazone and PPAR-δ agonist 152
A. Treating pre and post 6-OHDA lesion induction..... 152
B. Post 6-OHDA lesion treatment regime..... 152
B1. Drug withdrawal following post lesion treatment 153
5.2.2 Assessment of effects of GW855266X, pioglitazone and PPAR-δ in the 6-OHDA model..... 153
5.2.2.1 Assessment of the effects of GW855266X, pioglitazone and PPAR-δ on the nigrostriatal tract functionality after 6-OHDA lesion induction..... 153
5.2.2.2 Assessment of the effects of GW855266X, pioglitazone and PPAR-δ on the integrity of dopaminergic neurons in the SNc after 6-OHDA lesioning 154
5.2.2.3 Assessment of the effect of GW855266X, pioglitazone and PPAR-δ on the extent of microglia/macrophages activation in the SNc after 6-OHDA lesion induction**……**161
5.2.2.4 Assessment of the effects of GW855266X or pioglitazone on the extent of MMP-3 and 9 activation in the SNc after 6-OHDA lesion induction..... 154
5.2.2 Statistical analysis of data 155
5.2.2.2 Assessment of the effects of GW855266X, pioglitazone and PPAR-δ on the integrity of dopaminergic neurons in the SNc after 6-OHDA lesioning.. treatments to be neuroprotective and anti-inflammatory 195
Conclusions 196

Chapter 6 198

General Discussion and Future work 198

6.1 A brief overview of the project……198

6.2 The summary of the key findings presented in this thesis ……....200

6.3 Reappraisal of the 6-OHDA model employed in this study and some methodological considerations……200

6.4 General discussion of the main findings and possible future directions……..203

6.5 Future directions……213

6.6 Conclusion 214

Table of figures

Figure number	Page numbers
1.1	16
1.2	24
2.1	42
2.2	47
2.3	50
2.4	60
2.5	63
3.1	74
3.2	75
3.3	76
3.4	77
3.5	79
3.6	82
3.7	83
3.8	85
3.9	87
3.10	89
3.11	91
4.1 graph	112
4.1picture	113
4.2	115
4.3	117
4.4	119
4.5	121
4.6	122
4.7	124
4.8	125
4.9	127
4.10	128
4.11	130
4.12	130
4.13	132
4.14	134
4.15	136
4.16	144
5.1	158
5.2	161
5.3	164
5.4	166
5.5	169
5.6	172
5.7	175
5.8	178
5.9	181
5.10	184
5.11	188
6.1	215
6.2	216

List of tables

Chapter 2

Table 2.1
Details of all primary and secondary antibodies utilised in ABC immunohistochemistry, *page* 54.

Table 2.2
Details of all antibody co-localisation experiments and working dilutions in addition to their relevant secondary antibodies , *page* 57.

Cheaper 5

Table 5.1
Treatment with pioglitazone and GW855266X administered 7 days pre and 7 days post 6-OHDA lesion induction led to preservation of the mean concentration of striatal dopamine metabolites in addition to dopamine turnover in the lesioned hemisphere compared to the unlesioned hemisphere in drug and vehicle treated animals, *page 159.*

Table 5.2
Treatment with pioglitazone and GW855266X administered for 7 days post 6-OHDA lesion induction led to preservation of the mean concentration of striatal dopamine metabolites in addition to dopamine turnover in the lesioned hemisphere compared to the unlesioned hemisphere in drug and vehicle treated animals *page 167.*

Table 5.3
Withdrawal of treatment with pioglitazone and GW855266X administered for 7 days post 6-OHDA lesion induction led to depletion of the mean concentration of striatal dopamine metabolites in the 6-OHDA lesioned hemisphere compared to the unlesioned hemisphere in drug treated and lesioned hemisphere in the vehicle treated animals, *page 179.*

Publications

1-Marinova-Mutafchieva L., **Sadghian M**., Broom L., Davis J.B., Medhurst A.D., Dexter D.T. (2007) Relationship between microglial activation and dopaminergic neuronal loss in substantia nigra: A time course study in a 6-hydroxidopamine model of Parkinson's disease (submitted to J Neuroscience).

2- **Sadghian M**., Marinova-Mutafchieva L., Broom L., Davis J.B., Medhurst A.D., Dexter D.T. (2008) Peroxisome proliferator activated gamma receptor agonists rescue dopaminergic neuron in the 6-hydroxydopamine parkinsonian model through inhibition of microglial activation and matrix metalloproteinase expression in the Substantia nigra. (Submitted to J Neuroscience).

3- Broom L , Marinova-Mutafchieva L., **Sadghian M**., Davis J.B., Medhurst A.D., Dexter D.T. (2008) Selective inhibition of iNOS by GW274150 down regulates the inflammatory response and is neuroprotectory in a 6-hydroxydopamine model of Parkinson's disease.(To be submitted to *J Neurochemistry*)

4- **Sadghian M**, Broom L, Marinova-Mutafchieva L., Davis J.B., Medhurst A.D., Dexter D.T. The role of Matrix metalloproteinases and CD200 receptor in the neurodegenerative process in the substantia nigra of 6-hydroxydopamine model of Parkinson's disease. (2008). (To be submitted to *J Neuroscience*).

Chapter 1- Introduction

1.1 Parkinson's disease

A textbook definition of PD is given as ' a progressive neurodegenerative disorder characterised by the clinical symptoms of muscle rigidity, resting tremor and bradykinesia due to the depletion of dopamine (DA) in the corpus striatum as a result of the degeneration of DA neurons in the Substantia Nigra Pars Compacta (SNc) (Zigmond et al., 1999). The clinical features of Parkinson's disease (PD) were first described in 1817 by Dr. James Parkinson in an essay entitled, 'An Essay of the Shaking Palsy'. The definition of PD given by James Parkinson's described the disease as:

''*Involuntary tremulous motion, with lessened muscular power, in parts not in action and even when supported; with a propensity to bend the trunk forwards, and to pass from a walking to a running pace: the senses and intellects being uninjured.* ''

It was not until 1953 that the principal brain lesion in PD was identified as degeneration of DA neurons in the SNc (Greenfield and Bosanquet, 1953). The biochemical and pharmacological understanding of the disease began in the 1960s. Ehringer and Hornykiewicz (1961) documented the dramatic loss of dopamine in the striatum of brains from patients dying with post-encephalitic and idiopathic Parkinson's disease. Ever since its initial description by James Parkinson the aetiological mechanisms underlying the selective destruction of the nigrostriatal dopaminergic pathway have remained unknown (Langston 2002; Di Monte and Lawler 2001). Currently, clinical diagnosis of PD is based on movement-related behavioural abnormalities (Rao et al., 2003; Sethi, 2002). However, the absence of distinct biomarkers for the presymptomatic diagnosis of the disease, because of the lack of clear understanding of the disease process, has significantly hampered efforts to identify and treat PD patients early in the disease course. Therefore, the goal of ongoing research in this field is to identify the underlying mechanisms involved in the pathogenesis of PD to be able to stop or slow down its progression. Current pharmacological treatment of PD is focussed on DA replacement therapy, which aims to either replace the lost DA in the striatum or mimic the action of DA by the use of selective DA receptor agonists. These strategies provide long-term symptomatic control of the cardinal motor features of PD and the use of these drugs significantly improves the motor function of PD patients and improves patient quality of life (Lang and Obeso, 2005). However, the long term use of

these drugs is associated with severe side effects that signifies the need for new therapeutic interventions that act as neuroprotective or neurorestoretive agents.

1.2 Neuropathological features of idiopathic PD

PD is characterised neuropathologically by the progressive and profound loss of neuromelanin containing dopaminergic neurons in the SNc with presence of eosinophillic, intracytoplasmic, proteinaceous inclusions termed as Lewy bodies (LB) and dystrophic Lewy neurites in surviving neurons throughout the central and autonomic nervous systems (Forno et al., 1996; Gelb et al., 1999) (Fig 1.1). Lewy bodies were first described by Friederich H. Lewy in the nucleus basalis of Meynert and the dorsal vagal nucleus in patients with PD (Lewy, 1912) and were named Lewy bodies in his honour. Morphologically LBs are classified to two types: The classical brainstem type and the cortical type. The classical type is intracytoplasmic, single or multiple, eosinophillic masses that are spherical or elongated, possessing a dense core and a peripheral halo. The cortical type is eosinophillic, irregular in shape, often without a conspicuous halo or central core (Takahashi and Wakabayashi, 2001). LBs are composed of several proteins, including ubiquitin, α-synuclein (Spillantini et al., 1997) and other ubiquitin-like proteins, such as torsinA (Wakabayashi et al., 2000; McNaught, et al, 2004). In PD, LB are found in many regions of the nervous system, including the substantia nigra, locus coeruleus, hypothalamus, nucleus basalis, cranial nerve motor nuclei, and the central and peripheral divisions of the autonomic nervous system (Iwanaga et al., 1999). In addition, it has been reported that LB inclusions may form in glial cells, known as glial cell inclusions (GCI) that were found in the midbrain of PD patients and were immunoreactive for α-synuclein (Wakabayashi, et a., 1998). The precise role of LB in PD pathology is not fully known, however recent evidence suggest that LB formation could be a cytoprotective phenomenon (Olanow et al., 2004). This hypothesis is based on studies showing LBs are made in a very similar way to aggrosomes (Kopito, 2000; McNaught et al., 2002). Aggresomes are proteinaceous inclusions formed at the centrosome that segregate and facilitate the degradation of excess amounts of damaged, mutated and cytotoxic proteins. These findings suggest that LBs could be cytoprotective by accumulating the damaging and toxic misfolded and mutant proteins. However, this could be a double edged sword, if LB formation represents a response to degrade the toxic proteins; the numbers of LBs continue

to increase as long as the host cells produce toxic proteins. Increase in LBs or their overload could on its own be cytotoxic and lead to further cell death.

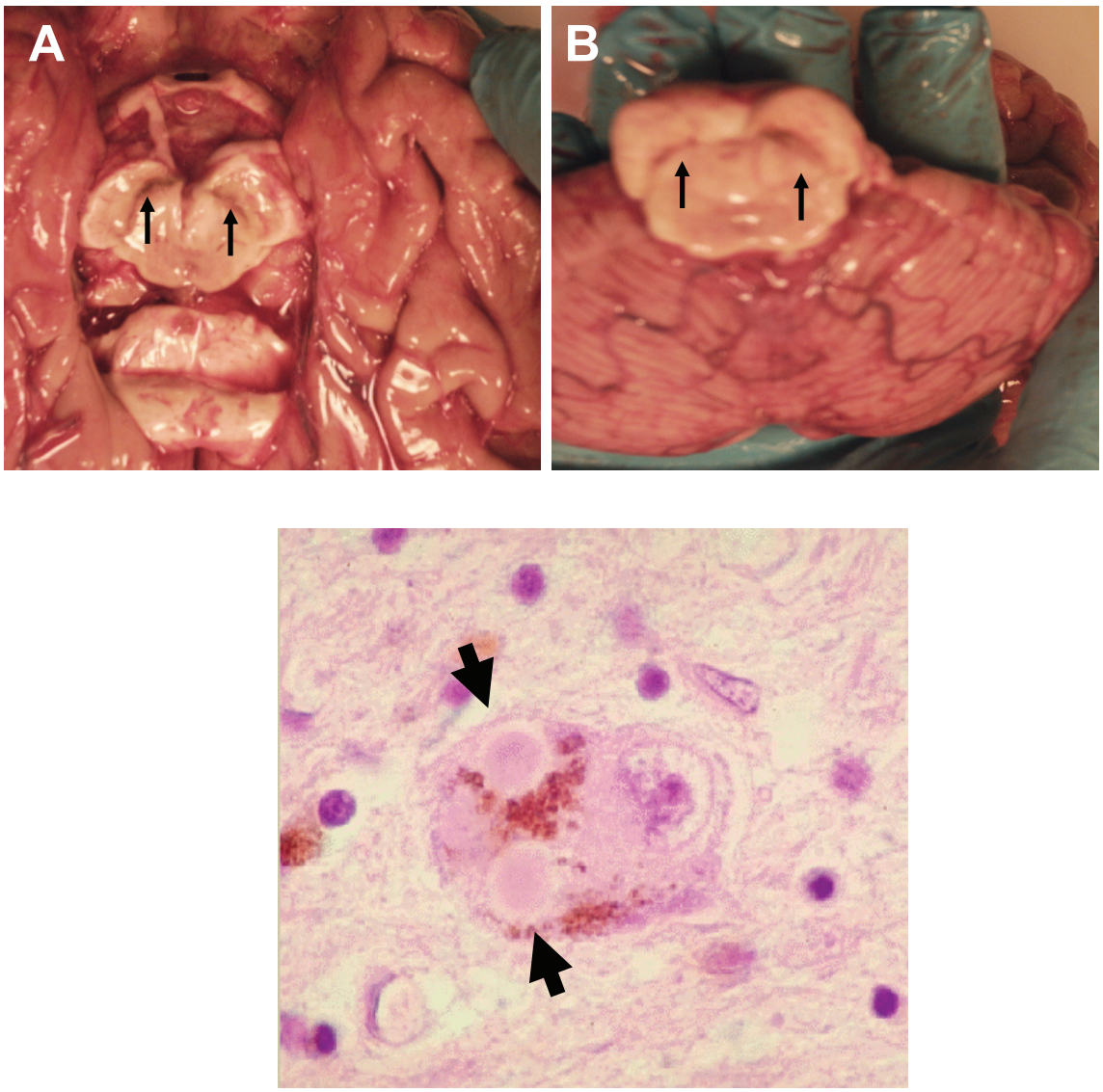

Fig 1.1 Neuropathological features of Parkinson's disease

A: Substantia nigra from a control case, note the darkened, pigmented nuclei (black arrows). **B:** Substantia nigra from a PD case, note the substantia nigra has lost its pigmentation, indicative of nigral cell loss. **C:** Histological section from the substantia nigra of a PD case, illustrating a dopaminergic neurone containing Lewy Bodies (black arrows). Images kindly provided by UK PDS Tissue Bank, Hammersmith Hospital, Imperial College, London.

1.2.1 Dopaminergic neuropathology in PD

The most prominent and consistent pathology in PD is the loss of the dopaminergic neurons in the SNc. The regional loss of SNc dopaminergic neurons results in the decrease of striatal dopamine concentrations in a regional pattern. Within the midbrain, three dopaminergic cell groups exist: the A8 group (retrorubral area) in the lateral reticular formation, the A9 group in the SNc and the A10 group in the ventral tegmental area (Pearson et al., 1983). The (A9) SNc neurons send projections along the medial forebrain bundle (MFB) to the putamen and caudate nucleus of the striatum to influence the basal ganglia pathway (Pollak et al., 2001). The striatum itself is divided into dorsal (caudate nucleus and the putamen) and ventral (nucleus accumbens). The dorsal and ventral parts of the striatum are segregated anatomically by the internal capsule. The pattern of SNc cell loss appears to correspond to the level of expression of the DA transporter (DAT) (Uhl et al., 1994) and is consistent with the finding that depletion of dopamine is most pronounced in the dorsolateral putamen the main site of projection for these neurons (Bernheimer et al., 1973). Within the SNc itself, cell loss follows a specific pattern, affecting ventral in preference to dorsal SNc cells (Damier et al., 1999). The cause of this brain regional vulnerability has remained unclear. However, a recent micro array study of PD and control brains indicated increased expression of genes encoding pro-inflammatory cytokines and subunits of the mitochondrial electron transport chain and decreased expression of several glutathione-related genes in the more vulnerable lateral tier region of the SN (Duke et al., 2006). These factors have implicated in the pathogenesis of PD (*see section 1.4*). The onset of parkinsonian symptoms occurs when ~60% of putamenal dopamine is depleted and ~80% of dopaminergic neurons in the SNc are lost. However, the adjacent mesolimblic dopaminergic neurons, with their cell bodies residing in the ventral tegmental area (VTA), are much less affected in PD. This is mirrored in significantly less depletion of dopamine in the caudate that is the main site of projection for these neurons (Price et al., 1978). It is not yet clear why the dopaminergic neurons in the VTA are less susceptible to degeneration in PD. Recent evidence suggests that genes potentially related to 'neuroprotection' are higher in VTA dopamine neurons, including four neuropeptide-related genes, and the calcium binding protein, calbindin. In fact, profiling experiments have confirmed that neuropeptide genes [e.g. Calcitonin gene related peptide (CGRP), Gastrin releasing peptitide (GRP) and Pituitary adenylate cyclase activating peptide (PACAP)] are more highly expressed in VTA dopamine neurons than in those from the SN (Chung et al., 2005; Greene et al., 2005)

.These findings potentially provides an explanation for why SN dopaminergic neurons are more susceptible to damaging factors that leads to their degeneration in PD.

1.2.2 Non-dopaminergic neuropathology in PD

The progressive degeneration of dopaminergic neurons in the SNc is the predominant pathologic feature of PD that leads to motor symptoms and diagnosis of this disease. Previously it was thought that the neuropathology of PD was solely confined to the lesions in the dopaminergic neurons of the SNc. However, evidence suggests that there is also non-dopaminergic pathology in PD. Indeed, neuronal cell loss in PD affects other neurotransmitter systems both in the periphery and the brain (Gerlach and Riederer, 1999; Goldstein et al., 2001, 2002). In the brain, the neurodegenerative process affects the noradrenergic system in the locus coeruleus (LC) with presence of LBs (Jellinger et al., 1987), the serotonergic Raphe nuclei and the cholinergic nucleus basalis Meynert (Whitehouse et al., 1983). In addition, damage occurs to gamma aminobutyric acid (GABA)-ergic and peptidergic neurons in the cerebellum (Halliday et al., 1990). Another brain area which is affected in PD even before the symptoms of the disease manifest is the loss of neurons in the olfactory bulb and the anterior olfactory nucleus that could give rise to the disturbances in the sense of smell, which are a very common feature of idiopathic PD (Braak et al., 2003; 2004).

It seems likely that Parkinson's disease is not a single disease but a number of phenotypically similar illnesses. A variable range of genetic and environmental interactions may produce these conditions and it may be that any individual risk factor will only affect susceptible subjects.

1.3 Current pharmacological treatments for PD and their limitations

Current pharmacological treatment of PD is focussed on DA replacement therapy, which aims to either replace the lost DA in the striatum or mimic the action of DA by the use of selective DA receptor agonists. These strategies provide relatively long-term symptomatic control of the cardinal motor features of PD and the use of these drugs significantly improves the motor function of PD patients, lowers morbidity and mortality and improves the patients quality of life (Karlson et al., 2000; Rajput, 2005; Lang and Obeso, 2005).

One of most frequently used drugs for symptomatic control of PD is Levadopa (L-DOPA). L-DOPA is DA precursor that provides effective relief of bradykinesia and rigidity (Yahr et al., 1968) of PD by replacing lost DA in the putamen (Agnati and Fuxe, 1980). However, prolonged L-DOPA treatment results in development of L-DOPA induced dyskinesias (LIDs), which are disabling involuntary movements (Brotchie et al., 2005). These complications occur in 90% of PD patients receiving L-DOPA, usually with 5-10 years of the initiation of L-DOPA treatment (Ahlskog and Muenter, 2001).

Alternative to L-DOPA is the use of DA D_2 receptor agonists such as, pramipexole, which are effective at managing the motor symptoms of PD either as a monotherapy or as an adjunct to L-DOPA use, which allows lower doses of L-DOPA be to administered (Kondo, 2002). As a monotherapy, DA receptor agonists provide effective relief of motor symptoms over a prolonged period of time, thus delaying the need for L-DOPA therapy and onset of motor complications (Holloway et al., 2004). However, DA agonists are associated with side effects, which are also common to L-DOPA, including cognitive disturbances, hallucinations, confusion episodes, sleepiness and potentially oedema (Nutt et al., 2000).

Another group of drugs which are prescribed in PD are Monoamine Oxidase inhibitors such as: rasagiline that also provide symptomatic relief of PD (Rabey et al., 2000). However, similar to DA agonists, patients will eventually require L-DOPA supplementation (Schapira, et al, 2006).

Taken together, dopamine replacement therapy in PD provides a relatively long period of symptomatic control of PD which improves the patients quality of life. However, long term use of these drugs is associated with severe motor complications. Importantly all current PD treatments are symptomatic in nature and do not halt the relentless progression of neurodegeneration in PD. Therefore, development of neuroprotective therapy for PD is one of the most important goals of research in this field.

1.4 Epidemiology of PD

Epidemiological studies suggest that the prevalence of idiopathic PD is estimated at 0.3% of the general population and 1-2% of people aged over 60 (Nussabum and Ellis, 2003). The prevalence of PD increases with age since the idiopathic form is rare before 50 years of age whilst the prevalence increases to up to 4% in people aged over 75 (deRijk et al., 2000), demonstrating that the primary risk factor for sporadic PD is aging. In support of

this, the incidence of PD is reported 1 in 1000 people below the age of 50, that increase dramatically to 1-2 in 100 people over the age of 60 (deLau and Bertler, 2006). In addition recent studies report a higher prevalence of PD in males compared to females (Swerdlow et al., 2001). The incidence of PD is reported to be approximately 1.5 times higher in men than in women (Elbaz et al., 2002); this finding may be related to risk factors more frequently found in men than in women (*e.g.*, occupational risk factors), or to protective factors in women (*e.g.*, hormonal factors).

1.5 Aetiology and pathogenesis of PD

The aetiology of PD is not yet fully known. The development of idiopathic PD might be the outcome of complex interplay between the innate vulnerabilities of the nigrostriatal dopaminergic pathway alongside genetic predisposition and environmental risk factors. The following section is an out line of some environmental risk factors that have been associated to developing idiopathic PD.

1.5.1 Environmental risk factors for idiopathic PD

To date a number environmental risk factors have been associated with development of PD later in life. The most compelling evidence for involvement of environmental risk factors in the development of PD came from the discovery of the neurotoxin, 1-Methyl-4-phenyl-1, 2, 3, 6-tetrahydropyridine (MPTP) (Langston et al., 1983). MPTP is a by-product of an illicit synthetic meperidine derivative developed by a group of young drug addicts that upon exposure to this drug developed clinical and pathological symptoms of idiopathic PD (Langston et al., 1983). The neuropathologic study of the brains of three MPTP-exposed subjects showed cell loss in the SNc and microglial activation with an ongoing inflammatory reaction 3–6 years after the toxic exposure (Langston et al., 1999). In addition, brain biopsy from non-human primates exposed to MPTP 5-14 years before death showed, cell loss in the SNc and reactive microglia and extracellular melanin in the SNc (McGeer et al., 2003). These findings indicate an active, ongoing neuronal loss, suggesting that toxic exposure happening at a single point in time many years before the onset of clinical symptoms of PD may result in a slowly progressive neurodegenerative process in

the SNc with a permanent inflammatory reaction in the brain of PD patients. The exact mode of action of MPTP is not fully known, however, MPTP is readily catalysed by monoamine oxidase type-B (MAO-B) in astrocytes to its active form the pyridinium ion MMP+. MPP+ is then taken up by dopaminergic neurons via the dopamine transporter (DAT). MPP+ then accumulates in mitochondria causing a profound inhibition of mitochondrial complex I that eventually leads to cellular energy failure and dopaminergic neuronal cell death (Blum et al., 2001).

Epidemiological studies have shown that other environmental risk factors include exposure to pesticides and herbicides, increase the risk of PD (Gorrell et al., 1996; Priyadarshi et al., 2000). The drinking of well-water that was shown to be contaminated with pesticides has also been investigated as an additional rural factor (Tanner et al, 1996). In agreement with these findings animal studies have also shown that chronic exposure of rodents to the pesticide, rotenone produces selective nigrostriatal degeneration and more importantly, the formation of LB-like inclusion bodies which are highly immunoreactive for α-synuclein. Rotenone treatment also induces microglial activation in the SNc of rodents (Betarbet et al., 2000; Sherer et al., 2003). Exposure to heavy metals such as iron, manganese, copper, lead, amalgam, zinc or aluminium have also been suggested as possible risk factors for the development of PD due to accumulation of metals in the SNc and increased oxidative stress (*see section 1.4.3*) (Olanow , 2004). Indeed, manganese is neurotoxic to the BG and individuals exposed to manganese dioxide ore have an increased risk of developing a parkinsonian-like syndrome, due to chronic inhalation of manganese dust (Huang et al., 2003). Additionally exposure to manganese fumes from welding has been suggested to increase the incidence of PD amongst welders, but this remains unsubstantiated (Jankovic, 2005). Interestingly, manganese is also a constituent of many pesticides, further suggesting a link between pesticide exposure and PD (Schapira, 2006).

An interesting finding demonstrated that the herbicide paraquat which is structurally similar to MPTP (McCormack et al., 2002), causes nigrostriatal degeneration in rodents by inhibition of complex I (Richardson et al., 2005). Additionally, paraquat increases the rate at which α-synuclein forms fibrils *in vitro* (Uversky et al., 2001; 2004) and increases α-synuclein expression *in vivo* leading to formation of inclusion bodies in nigral DA neurones (Manning-Bog et al., 2002). It is interesting to note that all of the environmental risk factors mentioned so far are either inhibitors of mitochondrial complex I or induce some form of

protein aggregation, suggesting a proteasomal deficit, both of which have been suggested to be involved in the pathogenesis of idiopathic PD (*see section 1.4.3*). Interestingly, compounds which inhibit proteasome activity appear to induce pathology and symptoms similar to PD in experimental models of PD (McNaught et al., 2002; 2004; Zeng et al., 2006). The relevance of these findings to idiopathic PD is further confirmed by the observation of specific complex I and proteasomal deficits in post-mortem tissue from PD patients (Schapira et al., 1990; McNaught and Jenner, 2001; McNaught et al., 2001; 2002).

1.5.2 Genetic risk factors

Sporadic PD accounts for 90-95% cases and approximately 5-10% of cases are hereditary with clear genetic origins, which are termed familial PD (Farrer, 2006). The discovery of genes linked to rare familial forms of PD during the last decade have confirmed the role of genetics in development of PD, and provided vital clues in understanding the molecular pathogenesis of the common sporadic illness. Studies have shown that relatives of PD patients have an approximate 2-3 fold higher risk of developing PD in comparison to age-matched controls (Gasser et al., 1998; Bonifati et al., 1995). Comparative studies on twins with age of PD onset before 50 years old demonstrated a significant concordance, suggesting that young-onset PD may have a genetic component (Schragg and Scott, 2006 ;Tanner and Aston 2000). Additionally, imaging studies in both affected and unaffected mono- and dizygotic twin pairs revealed a significant concordance for PD in identical twins. Taken together, these findings suggest that genetics is important in PD aetiology (Farrer, 2006). Importantly, a major breakthrough in this respect involved large scale linkage analysis studies which have led to the mapping and cloning of several genes that cause monogenetically inherited forms of the disease in an autosomal dominant or recessive fashion. Namely *PINK1*, PTEN-induced kinase 1, *SNCA*, gene that encodes the protein α-synuclein, *UCHL1*, ubiquitin carboxyl-terminal esterase 1, *PARK2*, locus which encodes the protein Parkin, *LRRK2*, leucine rich repeat kinase 2, NFT, neurofibrillary tangles (Farrer et al., 2006). Interestingly, all the identified gene mutations which cause inherited PD are genes encoding proteins involved in DA synthesis and transmission, oxidative stress, protein accumulation and degradation, mitochondrial function, and xenobiotic metabolism, implicating these cellular processes in PD pathogenesis (*see section 1.4.3*).

Thus, taken together the current consensus is that sporadic PD may result from a combination of interacting genetic and environmental factors although the nature and time course of these interactions is debated (BenMoyal-Segal and Soreq, 2006; Allam et al., 2005).

1.5.3. Pathogenesis of PD

Initially it was believed that neurodegeneration in PD was caused by necrotic cell death, but studies and use of modern techniques have shown that apoptosis (programmed cell death) is one of the main mechanisms of neuronal loss (Anglade et al., 1996; Tatton et al., 1998). There is a growing body of evidence suggesting that many factors are involved in PD pathogenesis such as: oxidative stress, protein handling dysfunction and inflammation. These factors participate in the cascade of events leading to neurodegeneration seen in PD (Jenner and Olanow, 1998; Olanow and Tatton, 1999; Jenner and Olanow, 2006). Below is a brief description of oxidative stress induced cell death and protein handling dysfunction leading to neuronal demise. However, the main focus of this thesis is on the role of inflammation in PD pathogenesis that is discussed in section 1.5.

Oxidative stress and neurodegeneration in PD

In the brain and specially the SNc the neurotransmitter dopamine, which is the main transmitter present in the SNc, normally, is subject to oxidative metabolism. It also has the potential to generate reactive oxygen species (ROS) and cytotoxic free radicals (Jenner, 1996). Enzymatically, both the synthesis of dopamine by tyrosine hydroxylase (TH) and catabolism by monoamine oxidases (MAO) can lead to hydrogen peroxide (H_2O_2) production (Fig 1.2) (Jenner and Olanow, 1996). Under normal circumstances H_2O_2 is cleared by glutathione (GSH). GSH plays an important role in the adult brain by removing H_2O_2 formed during normal cellular metabolism which stops its further reaction with ferrous iron and formation of toxic hydroxyl radicals (Fig 1.2). However, in the Parkinsonian brain there is a marked deficiency in chemically reduced glutathione levels and thus the brain's capacity to clear H_2O_2 is diminished (Sian et al., 1994). This becomes important since the nigra has high iron content, and further the iron levels are increased in

the brains of PD patients (Dexter et al., 1989). Iron might then react with excess H_2O_2 leading to production of toxic hydroxyl radicals (Fig.1.2) and potentially lead to oxidative damage and neuronal cell death (Perry and Yong, 1986).

Toxic free radicals are also generated during non-enzymatic oxidation of dopamine. These free radicals include: quinone, semiquinone (SQ) molecules and reactive oxygen species (ROS) that lead to oxidative damage of different neuronal components and eventually cell death (Fig. 1.2) (Adapted from Jenner & Olanow, 1998).

Evidence suggesting that the SN is in a of state of oxidative stress came from post-mortem studies on human PD brain tissue that showed increased iron, decreased GSH levels and evidence of lipids peroxidation and oxidation of proteins and DNA (reviewed in Jenner and Olanow, 2006). Therefore in recent years anti-oxidant compounds have received considerable attention for their potential neuroprotective properties.

a) Enzymatic dopamine oxidation

$$\text{1. } DA+O_2+H_2O \xrightarrow{MAO} 3,4DHPA+NH_3+H_2O_2$$

$$\text{2. } H_2O_2+2GSH \rightarrow GSSG+2H_2O$$

$$\text{3. } H_2O_2+Fe^{+2} \rightarrow OH^{\cdot}+OH^{-}+Fe^{+3}$$

b) Auto-oxidation of dopamine

$$\text{4. } DA+O_2 \rightarrow SQ^{\cdot} + {}^{\cdot}O2^{-} + H^{+}$$

$$\text{5. } DA+{}^{\cdot}O2+2H^{+} \rightarrow SQ^{\cdot} + H_2O_2$$

Fig 1.2: a) The enzymatic metabolism of dopamine. b) Dopamine auto-oxidation. Under normal circumstances hydrogen peroxide generated during dopamine metabolism by MAO (1)is cleared by glutathione (GSH) (2) this stops its further reaction with ferrous iron and formation of hydroxyl radicals (3).

Ubiquitin-proteasome system dysfunction

One of the main consequences of oxidative stress is the resultant dysregulation of protein metabolism in the cells (Berlett and Stadtman, 1997). Under normal circumstances

damaged intracellular proteins and cell fragments are tagged, usually by ubiquitin, which triggers their breakdown and clearance by the proteasome. This will enable cell function to continue and provides a balance between the rate of damage and clearance of these proteins inside the cell. Once cell death occurs in the brain, the levels of unwanted cell fragments and damaged proteins increase. The ubiquitin-proteasome system (UPS) is the primary non lysosomal system, responsible for degradation and clearance of mis-folded, short-lived, mutant, damaged by oxidative or excitotoxic injury or misplaced proteins in eukaryotic cells (Sherman and Goldberg, 2001).

Evidence for involvement of UPS dysfunction in PD came from familial cases of PD where specific gene defects were linked to inhibition of the UPS resulting in aggregation of abnormal proteins and associated loss of biological function (Jenner & Olanow, 1998). In sporadic PD, quantitative western blot analyses have shown a marked increase in the levels of aggregates of α-synuclein in the SNc (Baba et al., 1998). Many other proteins in addition to α-synuclein have also been demonstrated to accumulate in the SNc and other brain regions in PD. For example, a several-fold increase in the levels of ubiquitin–protein conjugates and phosphorylated proteins in the SNc has also been demonstrated (McNaught et al., 2002; and Zhu et al., 2002). *In vitro* and *in vivo* studies of McNaught et al., (2001) have shown that build up of un-processed proteins resulting from compromised UPS can lead to initiation of an inflammatory response that may lead to the death of dopaminergic neurones (Wyss-Coray and Mucke, 2002; Jenner et al.,2006) .

1.6 Inflammation in the brain

Inflammation is the first line of defence against injury and infection. However, an excessive inflammatory response can be a source of additional injury to host cells (Wyss-Coray and Mucke, 2002).The brain has a relatively low adaptive immune response but is vulnerable to innate immune reactions. Neurons, owing to a lack of ability to divide and little ability to recover from injury, are extremely vulnerable to auto destructive immune and inflammatory processes (Carson et al., 2006).This might hinder the recovery of neurological function at sites of inflammation or even exacerbate neuronal injury. Conventionally, it was believed that the brain is an immune privileged organ following a number of observations including the absence of professional antigen presenting dendritic cells in the brain that act as primary immune-surveyors in other tissues (Aloisi et al., 2001).

In addition, the lymphatic system that delivers antigen to lymph nodes and organs, and thus to the attention of general immune surveillance; is absent in the brain, although slow circulation of soluble antigens does occurs towards cervical lymph nodes (Aloisi et al., 2001). Moreover, there is a very low level of constitutive expression of major histocompatibility complex (MHC) molecules within the brain, and in particular MHC I expression which is required in order to present either self or foreign antigen to T cells, to initiate the adaptive immune response (Chew et al., 2006). However, the notion of the brain being an immune privileged organ was challenged by number of studies and observations. One of the main studies that challenged this idea demonstrated that transplanted tissue did not elicit a primary immune response when inoculated directly into the brain; however, upon peripheral challenge with the same antigen, a robust immune response was induced both in the periphery and to the previously tolerated inoculum in the brain (Perry et al., 1998). This and similar observations initiated a change in the concept of the brain as being entirely separate from immune surveillance, and over the last few years, it has become clear that the immune system and the central nervous system do indeed interact, but the immune response in the brain is much more tightly regulated than in the periphery. Furthermore, it was demonstrated that the BBB is not a completely impenetrable barrier, and that in health activated T cells do continuously, albeit in low numbers, circulate throughout the brain from the blood vessels and meninges towards cervical lymph nodes (Aloisi et al., 2000). Antigen presentation within the healthy brain does occur but is mediated exclusively through microglia, which have inducible antigen presenting ability, rather than through professional antigen presenting cells like dendritic cells found in the periphery (Kreutzberg et al., 1996). The antigen presenting ability of microglia is considerably suppressed however with very little or no constitutive MHC expression in the healthy brain. The microenvironment of the brain has developed specialised properties that limit potentially harmful inflammatory reactions which are to protect the largely irreplaceable post mitotic neurons. However under pathological conditions inflammatory reactions takes place that are characterised by activation of the microglia. Pro-inflammatory cytokines, released by microglia act on the endothelium to induce up-regulation of cell adhesion molecules including vascular cell adhesion molecule-1 (VCAM-1) and intercellular adhesion molecule-1 (ICAM-1) (Neumann and Wekerle, 1998). This up-regulation recruits passing T cells and monocytes expressing the counter receptors such as leukocyte function antigen-1 (LFA-1 or CD54) (Neumann and Wekerle, 1998). Activated T cells themselves release further pro-inflammatory cytokines like IFNγ and TNFα, which induce expression of MHC class II and

co-stimulatory molecules on the microglial cells (Gebicke-Haerter, 2001). When these activated microglial molecules bind to their respective receptors on T cells, they can then cause the transformation of the activated T cells into effector cells. Activated CD8 T lymphocytes can then mediate the direct cytotoxic lysis of target cells, recruit and activate accessory cells via pro-inflammatory mediators, while activated CD4 T lymphocytes instruct B cells to produce high affinity antibodies (Raivich et al., 1999). These functions are controlled and balanced by the production of an array of pro-inflammatory cytokines such as IL1, TNFα and IFNγ, and anti-inflammatory cytokines including IL10 and transforming growth factor-β (TGFβ) by the T cells and the microglia. The cascade of events during an inflammatory reaction in the brain suggests that microglia play a significant role in this process therefore, the following section is an outline of the main functions of microglia during homeostasis and pathological conditions such as PD.

1.6.1 Microglia and their function

Microglia, initially identified by Del Rio Hortega, constitute about 10% of all glial cells in the brain. They are found throughout the brain parenchyma and are the resident macrophage population of the brain. In healthy brain they usually display a ramified morphology signifying their non-activated state but recent in vivo imaging by Nimmerjahn, et al (2005) demonstrated that microglia even in their resting state are in constant activity and surveillance of the extracellular environment by extending and retracting their ramifications. As demonstrated by Nimmerjahn, et al (2005), following a laser beam injury to a blood vessel the surrounding microglia were activated as their processes thickened and retracted. Their phenotypic characteristic underwent a dramatic transformation as they migrated to the site of injury and accumulated around the injured vessel that was followed by phagocytosis of the injured vessel. Over the past few years an increasing body of evidence has emerged suggesting that microglia are the key components in immune surveillance of the brain. Traditionally, microglia were considered merely to have a housekeeping function where it was believed that they were principally involved in the removal of cellular debris (Barron et al., 1995). Microglia, not only act as phagocytic cells but also perform other roles in tissue repair and cellular homeostasis. During homeostasis microglial cells monitor the physiological integrity of their microenvironment to promote tissue repair by secreting growth factors, acquisition of macrophage differentiation markers

and effector properties thus, maintain the homeostasis of the brain parenchyma (Kreutzberg et al., 1996). In normal, healthy brain microglia have a ramified morphology and do not display an activated macrophage array of receptors. There is low expression of the membrane ligands and receptors that are essential for mediating typical macrophage functions, such as leukocyte common antigen (LCA/CD45), CD14, and mac-1 (Kreutzberg et al., 1996). Under conditions of brain infection, exposure to inflammatory stimuli or interaction with blood-derived cells, microglia become activated to perform several innate immune functions including production of pro-inflammatory cytokines, cytotoxicity and regulation of T cell responses through antigen presentation (Aloisi et al., 2001). Microglial activation involves an increase in a range of molecules with immune function (Raivich et al., 1999). There is increased microglial IgG reactivity and up-regulation of complement receptors and cell adhesion molecules like LFA-1, ICAM-1 (CD54), VCAM-1 (CD106) and CD1 (Kreutzberg et al., 1996). This is considered to represent a state of alert (Kreutzberg et al., 1996). If the inducing stimulus persists, microglial morphological and functional transformation continues with the up-regulation of MHC molecules alongside changes in the internal cytoskeleton of the microglial cell, enlarging the cell body and withdrawing processes to a more macrophage-like phenotype. Fully activated microglia then release large amounts of pro-inflammatory cytokines and cytotoxic factors including reactive oxygen and nitrogen species (Aloisi et al., 2001). Production of these neurotoxic factors causes neurodegeneration which in-turn could lead to further microglial activation and inflammation. When neuronal death occurs, microglia can recognize the expression of phosphatidylserine on the surface of apoptotic cells and will remove cellular debris from region by phagocytosis (Witting et al., 2000; Hirt and Leist, 2003). In Parkinson's disease the localisation of activated microglial cells in areas of neurodegeneration is indicative of their role in perpetuating the disease process that could lead to further damage to neurons. Recent evidence suggests a pivotal role of inflammation that is characterised by microglial activation in the initiation and progression of PD (Nguyen et al., 2002). Moreover, several studies have demonstrated that neuronal cell loss in the SNc in PD is accompanied by an inflammatory response with a dramatic proliferation of reactive microglial cells (McGeer et al., 1988; Forno., 1992; Forno, 1996; Knott et al., 2000). In such PD patients, higher levels of pro-inflammatory cytokines such as, TNF-α, IL-1ß and INF-γ were detected in the striatum and cerebrospinal fluid (Mogi et al., 1994, 1996). It is not yet known what factors are involved in the induction of the inflammatory response and over-activation of microglia.

However, a number of inflammation inducing risk factors in developing PD have been studied that are discussed in the following section (*see section 1.6.2*).

1.6.2 Inflammation inducing risk factors and development of PD

Epidemiological case control studies have demonstrated that some cases of PD are associated with head trauma or certain viruses or infections, suggesting that microglial activation caused by preceding brain inflammation may trigger the onset of a cascade of events leading to progressive degeneration of DA neurons (Liu and Hong 2003, Herrera et al., 2005). The correlation between closed head injury and development of PD later in life has been studied by many groups. Analysis of the medical histories of a large group of World War II veterans pointed to an association between the occurrence of severe head injuries and the development of PD in later life (Plassman et al., 2000). This notion is supported by several other studies, including several case–control studies that have identified head injury as a major risk factor for the development of PD (Stern et al., 1991; Taylor et al., 1999; Tsai et al., 2002). A very recent study demonstrated a significant increase in the risk of developing PD in twins with a history of prior head injury (Goldman et al., 2006). This study in accordance with the previous studies reported a long latency between injury and disease manifestation. This offers a long window for implementation of protective or preventive strategies, such as the use of anti-inflammatory agents. In support of the notion of head injury being a risk factor in development of PD later in life it is worth noting the so called ‘ Boxer’s parkinsonian syndrome’’ that suggests a higher incidence of PD-like movement disorders in boxers, due to their profession that is related to higher chance of suffering head injuries (Friedman et al., 1989). Although the mechanism underlying this head trauma–related development of permanent damage to the nigrostriatal pathway remains unclear, it is possible that the initial neuronal damage leads to the activation of glial cells that may exacerbate the neurodegenerative process. A number of biologically plausible mechanisms could explain the reason that head injury may lead to a neurodegenerative process such as PD. Mild-to-moderate closed-head injury induces an inflammatory cascade that begins within minutes of the injury and may persist for months. In addition the break down of the blood-brain barrier is an early response to traumatic brain injury, followed rapidly by oedema, leukocyte infiltration, and microglial activation (Schmidt et al., 2005). A number of animal studies also support the deleterious role of inflammation following head injury. Shohami et al., (1997) have demonstrated significant

elevations in the levels of a number of cytokines (including IL-1, IL-6, and TNF-α) after head injury in rats. The production and accumulation of such pro-inflammatory factors may exacerbate the neuronal damage initially induced by the head injury. In addition epidemiologic studies have shown an association between early-life viral or bacterial infections to postencephalitic PD; case reports have shown development of acute Parkinsonism following viral infections (Tsui et al., 1999; Ghaemi et al., 2000). The possibility that viruses can induce PD is also suggested by studies in rodents where rats infected with Japanese encephalitis virus exhibited neuronal loss with microglial activation which was confined mainly to the SNc (Ogata et al., 1997). In addition to viruses certain bacterial infections have also been associated with development of PD. Evidence suggests that peptic ulcer is more frequent in PD patients and one bacteria that is known to cause peptic ulcers is the *Helicobacter pylori*. Therefore, a study was performed to determine whether *H. pylori* seropositivity was associated with development of PD. Interestingly it was shown that siblings of PD patients had an increased probability of *H. pylori* seropositivity compared to control subjects (Charlett et al., 1999). Taken together, these studies suggest that early life incidences that are linked to an inflammatory component, increase the risk of developing PD in later life. Therefore, the following section focuses on the role of microglia in PD and the evidence suggesting that inflammation plays a significant role in PD pathogenesis.

1.6.3 Inflammation in PD

1.6.3.1 Atypical glial pathology in PD

The glial cells in the brain are composed of two major types. Macroglia, which include astrocytes and oligodendrocytes, and the microglia. So far evidence suggests that oligodendrocytes, which are involved in the process of myelination, are not implicated in Parkinson's disease pathology, whereas both astrocytes and microglial cells are involved (Wilkin and Knott, 1999). Astrocytes provide homeostatic control of the neuronal extracellular environment and respond to a diversity of damaging insults, including physical damage, disease or chemicals. Even damage to astrocytes themselves elicits reactive changes such as hypertrophy and proliferation of surviving astrocytes (Wilkin and Knott, 1999). An accumulating body of evidence suggests that there is a significant glial reaction

in the SNc in PD (Vila et al., 2001) but the gliosis observed in PD is an atypical form in which reactive astrocytes are largely absent in the SNc of post mortem parkinsonian brain tissue (Banati et al., 1998). However, only one type of glial cells seems to be highly activated in the SN of parkinsonian brains and that is microglia (Vila et al., 2001).

1.6.4 Evidence for involvement of inflammation in PD pathology

1.6.4.1 Evidence from human studies

A glial response has been observed in the vicinity of dying dopamine-containing neurons in human post-mortem SN from PD patients (McGeer et al., 1988) and MPTP-intoxicated individuals (Langston et al., 1999). Markers of elevated accumulation of NO, ROS and pro-inflammatory cytokines such as TNF-α, IL-1b and IFN- γ in the SN of PD patients have been demonstrated (Liu et al., 2003) indicating a state of chronic inflammation in the PD brain. In addition IgG from patients with PD can induce injury of dopaminergic neurons following stereotaxic injection into rat SNc (Chen et al., 1998). Furthermore, recent *in vivo* positron emission tomography (PET) studies demonstrated microglial activation using the peripheral benzodiazepine receptor binding ligand [^{11}C]-(*R*) PK11195. This study revealed that patients with idiopathic PD have markedly elevated neuroinflammation in the pons, basal ganglia, striatum, and frontal and temporal cortical regions compared to age-matched healthy controls irrespective of the number of years with the disease. These observations indicated that changes in microglia activation in the affected nigrostriatal pathway in early PD are likely to occur in parallel or prior to the loss of dopaminergic terminals (Gerhard et al., 2006). Moreover, epidemiological studies demonstrated that regular users of non-steroidal anti-inflammatory drugs (NSAIDs) are at lower risk of developing PD (Wahner et al., 2007; Ton et al., 2006; Chen et al., 2005).

Taken together, these findings are indicative of an ongoing inflammatory process in the brain of PD patients suggesting that inflammation plays a significant role in the pathogenesis of this disease.

1.6.4.2 Evidence from animal models of PD

Involvement of inflammation in PD is also evident from toxin induced experimental animal models of this disease. The neurotoxins employed include, 6-hydroxydopamine (6-OHDA), 1-methyl-4-phenyl-1, 2, 3, 6-tetrahydropyridine (MPTP), and the inflammogen Lipopoysaccharide (LPS) that have suggested an aetiological mechanism that involves inflammatory processes (Kurkowska-Jastrzebska et al., 1999; Carvey et al., 2005 and Iravani et al., 2001).

Inflammation in MPTP model of PD

As mentioned earlier MPTP is a neurotoxin that selectively injures the nigrostriatal system and post-mortem examination of MPTP-intoxicated humans years after exposure revealed dopaminergic cell loss without Lewy body formation and a marked microglial reaction in the SNc (Langston et al., 1999). The presence of this ongoing inflammatory reaction years after the original toxic exposure supports the idea that an environmental insult to the brain can set in motion a self-perpetuating process of neurodegeneration mediated by focal inflammatory processes. Following systemic administration, MPTP readily enters the brain and is metabolised by astroglia to the active metabolite 1-methyl-4-phenylpyridinium (MPP^+). MPP^+ enters cells via the dopamine transporter, and inhibits complex I of the mitochondrial electron transport chain (Murphy et al., 1995) leading to SNc cell death, depletion of striatal dopamine and interestingly early activation of microglia in both regions (Liberatore et al., 1999). Following MPTP administration to mice microglia not only activate, as evidenced by altered morphology from ramified to macrophage-like, but also increase in their number suggesting recruitment and/ or proliferation. There is markedly increased expression of both MHC class I and II antigens and the up regulation of inducible nitric oxide synthase (iNOS) expression (Liberatore et al., 1999). Inflammation is also a noted contributor to direct neuron damage, as MPTP toxicity is significantly reduced in mutant mice deficient in pro-inflammatory factors, such as superoxide (Zang et al.,2000; Wu et al., 2003) myeloperoxidase (Choi et al., 2005), prostaglandins (Feng et al., 2002; Vijitruth et al., 2006; Wang et al., 2005), NO (Wu et al., 2002) and TNFα (Sriram et al., 2002; Sriram et al., 2006). The effects of microglial inhibitors and anti-inflammatory drugs on MPTP administered mice provide further evidence for an active role of the microglial immune response in pathogenesis of PD. Minocycline, a semisynthetic tetracycline, is a potent inhibitor of microglial activation.

Minocycline acts on MPTP-activated microglia to prevent iNOS up regulation, inhibit phosphorylation of p38 mitogen activated protein kinase (Du et al., 2001) and reduce production of IL1β (Wu et al., 2002). Other anti-inflammatory agent and a preferential cyclooxygenase-2 inhibitor, also significantly attenuates dopaminergic cell loss in the MPTP mouse model of PD (Teisman and Ferger, 2001).

Inflammation in 6-Hydroxydopamine (6-OHDA) model of PD

6-OHDA is another neurotoxin capable of inducing regional degeneration of dopaminergic neurons in the SNc and depletion of dopamine in striatum very similar to idiopathic PD when injected intracranially in rodents (Rodriguez et al., 2001). There is also evidence that 6-OHDA toxic effects are in part mediated via the activation of microglia. Intra-striatal administration of 6-OHDA into mice causes microglial cells to activate and increase in number in the SNc post-injection. Dopaminergic cell loss follows and is accompanied by a further increase in microglial cell numbers (He et al., 2001). Analogous to the MPTP findings, co-administration of the microglial inhibitor minocycline protects dopaminergic cells, strongly favouring a pathogenic role for microglia (He et al., 2001). Activation of microglial cells is also shown to lead to production of pro-inflammatory cytokines such as: TNF-α in rats following 6-OHDA lesion induction.

These observations further emphasise the possible deleterious role of inflammation characterised by activation of microglial cells in the SNc in PD pathogenesis.

Inflammation in Lipopolysaccaride (LPS) model of PD

The bacterial endotoxin LPS is a potent microglial activator that binds to the LPS cell membrane receptor complex on microglia, triggering nuclear localisation of transcription factor NFκB, and subsequent activation of genes in the pro-inflammatory pathways (Kim et al., 2000). Injection of LPS into rat SNc produces a strong microglial response followed by death of dopaminergic neurons, whereas the same injection into rat hippocampus or cortex does not cause any cell death (Kim et al., 2000; Iravani et al., 2002). Interestingly, the midbrain dopaminergic neurons are not affected by midbrain injections of LPS, analogous to the sparing of these neurons by other neurotoxins including MPTP and 6-OHDA in animal models, and in human PD (Iravani et al., 2002). One possible explanation for this observed regional specificity of response to LPS is suggested to be a higher population of microglia in the SNc compared to other regions of the brain (Lawson et al.,

1990). Moreover even systemic injection of LPS in female rats led to reduced striatal dopamine, increased TNFα, and reduced dopaminergic cell count in the mesencephalon in their 21-day-old pups (Ling et al., 2002). Indicating that even a systemic inflammatory insult could lead to a localised degeneration of dopaminergic neurons in the SNc. The cellular events that leads to inflammation mediated dopaminergic neuronal cell death following LPS administration involves the activation of microglial cells, concomitant with up regulation of iNOS in SNc (Iravani et al., 2002; Gao et al., 2002) production of NO (Kim et al., 2000) and peroxinitrite which is toxic to dopaminergic neurons. Moreover production of pro-inflammatory cytokines such as, TNFα and IL1β from activated microglia (Kim et al., 2002) leads to further damage and cell death in the SNc. The production of these microglial derived neurotoxic factors precedes the death of dopaminergic neurons (Gao et al., 2002).

Taken together, these findings, from both human and animal studies strongly suggest that activated microglia play an important role in the pathogenesis and progression of PD. Moreover, DA neurons in the SN appear to be easily affected by microglial-derived neurotoxic factors, because the SN region is particularly rich in microglia and DA neurons are particularly sensitive to pro-inflammatory stimuli in the brain, such as LPS. Such evidence also indicates a possible role of activated microglia in the early stage of disease pathogenesis. More importantly, several studies have confirmed that microglia can play a causal role in DA neuron death. For example, LPS, is toxic to neurons but only in the presence of microglia (Gao et al., 2002; Gibbons and Dragunow, 2006). Also, an increasing number of experimental observations in animal models of PD indicate that inhibition of the inflammatory reaction could attenuate degeneration of nigrostriatal dopaminergic neurons (Liu et al., 2000; Teismann and Ferger et al., 2001; Wu et al., 2002). As such, pharmacological inhibition of iNOS (Iravani et al., 2002) or inhibition of microglial production of superoxide *in vivo* (Liu et al., 2000) reduces the LPS-induced SNc cell death. Naloxone, an opioid receptor antagonist, interferes with LPS binding to the LPS cell membrane receptor complex, CD14, on microglia preventing LPS from binding to its receptor complex inhibits activation of microglia and subsequent production and release of the pro-inflammatory factors, protecting the neuron-glia cell culture (Liu et al., 2000). These studies further support the concept that environmental insults can trigger prolonged microglial activation inducing pro-inflammatory cytokine production, lymphocyte recruitment, and alterations in cellular metabolism. This leads to the death of SNc neurons,

and can be a prolonged process mimicking idiopathic PD. The anti-inflammatory medications that down-regulate the microglial response and reduce neuronal loss strongly suggest that localised inflammation is pathogenic in the SNc rather than merely a late response to neuronal death.

1.7 Triggers for microglial activation

Post-mortem and experimental evidence indicates that microglial activation is indeed involved in PD pathogenesis. However, very little is known about the signals and triggers that leads to reactive gliosis. A number of studies have demonstrated that microglia are influenced primarily by direct neuronal-microglial interactions. Microglia are kept in a quiescent state in the intact CNS by local interactions between the microglia receptor CD200 and its ligand among other factors, which is expressed on neurons (Neumann et al., 2001). Indeed damage to neurons by neurotoxins led to the induction of MHC molecules on microglia and astrocytes. Thus, over-activation of microglial cells in the CNS is inhibited by the local microenvironment, in particular by physiologically active neurons, to prevent unwanted immune mediated damage of neurons. Other signalling molecules involved in glial activation are Matrix metalloproteinases (MMPs) such as: MMP-3. As demonstrated by Kim, et al, (2005) MMP-3 may be a microglia-activating signalling molecule released from neurons in early apoptosis.

1.8 Aims of the study

The working hypothesis in this project is that the microglial response associated with neurodegenerative process in PD is detrimental to remaining neurons and targeted immune modulators may act as neuroprotective agents. The presence of activated microglia in the SNc of post-mortem brain tissue signifies their association with dopaminergic neuronal cell death in PD. However, it only reflects their state in the terminal hours of the patient's life. What their activity was in previous days, months, or years remains completely unknown. Considering the evidence for the involvement of inflammation and microglial activation in PD pathology, a crucial factor in determining the fate of activated microglia following an insult is time. To date limited information is available on the time frame of activation of microglia in PD and whether inflammation precedes dopaminergic cell loss or

is it a consequence of it? The mechanism by which activated microglia might specifically target dopaminergic neurons and the cell to cell interaction between activated microglia and degenerating dopaminergic neurons in the *in vivo* models of PD also remains a critical missing link. Therefore the aims of this project were to address the following questions:

1) What are the kinetics (time course) of the immunophenotypic changes of activated microglia and the subsequent fate of activated microglial cells during the initiation and progression of dopaminergic neuronal loss in the SNc of 6-hydroxydopamine (6-OHDA) rat model of PD?

2) What signal(s) are released from neurons and how do these signal(s) modulate microglial activation in the 6-OHDA model of PD. What is the kinetic of signalling molecules such as: matrix metalloproteinases during the progression of dopaminergic lesion in the SNc? How does the expression of these signalling molecules correlate with the degree of microglial activation and what are the neuron-microglia interactions, with focus on the role of CD200R in dopaminergic cell death in the SNc after 6-OHDA lesion induction.

3) Finally, whether modulation of glial activity by anti-inflammatory compounds namely peroxisome proliferator activated gamma receptor (PPAR-γ) agonists leads to dopaminergic neuroprotection in 6-OHDA model of PD.

In order to satisfy these aims, the classical 6-OHDA rat model of PD will be employed, which produces selective degeneration of the rodent nigrostriatal system (Betarbet et al, 2002; Deumens et al, 2002). The effect of focal unilateral 6-OHDA lesion induction into the medial forebrain bundle (MFB) will be assessed on both the integrity and functionality of the nigrostriatal tract. Nigrostriatal integrity will be assessed by immunohistochemical studies quantifying the number of dopaminergic neuronal cells utilising the antigen Tyrosine hydroxylase (rate limiting enzyme in dopamine synthesis) in the SNc. Additionally, to quantify the effects of the 6-OHDA lesion on nigrostriatal functionality, the concentrations of DA and its metabolites dihydroxyphenylacetic acid (DOPAC) and homovanillic acid (HVA) in the corpus striatum will be quantitatively measured by High Performance Liquid Chromatography with Electrochemical Detection (HPLC-ECD). The relative amount of striatal DA metabolism will also be calculated. Furthermore to investigate the time course of microglial activation following 6-OHDA lesion induction in relation to dopaminergic neuronal cell death, animals will be sacrificed on days 1,3,5,7,9,13 and 15 after lesioning. To detect nigral microglial/macrophage

activation following 6-OHDA lesion induction, immunohistochemistry will be performed with OX-6 antibody targeted against MHC class II expressing activated microglia, OX-42, , antibody that is a general marker for microglial activation and CD-68 antibody that detects phagocytic macrophages. To study the potential signalling molecules that are involved in the initiation of microglial activation in the SNc after 6-OHDA lesion induction, immunohistochemistry will be performed for the active forms of MMP-3 and MMP-9 in addition to CD200R+ve cells. Finally, the significance of microglial response will be assessed by orally treating animals with different PPAR- γ agonists using different treatment regimes. The effect of each treatment on microglial activation and nigrostriatal functionality and integrity will be assessed as mentioned above.

Chapter 2- Material and Methods

2.1 In vivo methods

2.1.1 6-hydroxydopamine (6-OHDA) experimental model of Parkinson's disease

2.1.1.1 Overview

Experimental models of neurodegenerative diseases including PD are valuable tools that enable us to study the underlying pathophysiological mechanisms involved in the neurodegenerative processes observed during the course of these diseases. Research into the pathogenesis of PD has advanced very rapidly using animal models that are indispensable for the testing of novel therapeutic and neuroprotective strategies. However, up to date none of these models can mimic all the pathophysiological and clinical aspects of the disease as it is observed in humans. A model that utilises the toxin 6-OHDA *in vivo* is used in this project to replicate certain aspects of PD. 6-OHDA was the first chemical toxin discovered that destroyed catecholaminergic neurons both *in vivo* and *in vitro*. 6-OHDA that was originally isolated by Senoh and Witkop (1959) is a hydroxylated analogue of the neurotransmitter dopamine (Axlerod et al., 1998). The biological effects of 6-OHDA were first demonstrated by Porter et al,(1963), who showed that 6-OHDA induces efficient and long lasting noradrenalin depletion in sympathetic nerves to the heart (Porter et al., 1963). 6-OHDA is mainly used in rodents, to induce nigrostriatal damage and replicate the loss of striatal dopamine as seen in PD patients. 6-OHDA induced neuronal death is shown to be by both apoptotic (Silva et al., 2005; Vila and Przedborski, 2003) and non-apoptotic pathways (Jeon et al., 1995). If administered systemically 6-OHDA does not cross the blood-brain barrier (BBB) except in neonatal rats when the BBB is still permeable (Podkletnova et al., 1998; 2001). Hence to mimic the pathological changes observed in the nigrostriatal pathway in PD, 6-OHDA must be stereotaxically injected into one of the following distinct structures in the brain, corpus striatum, substantia nigra and the medial forebrain bundle (MFB) that comprises the nigrostriatal tract. In rodents, 6-OHDA injection into the substantia nigra directly, produces a rapid degeneration of dopaminergic neurons, within 24 h with subsequent depletion of striatal dopamine levels (Faull and Laverty, 1969). Intrastriatal injection of 6-OHDA causes a retrograde neuronal cell death in the SNc that (Berger et al., 1991; Sauer and Oertel, 1994; Przedborski et al., 1995) was shown to be progressive up to 5 weeks post lesion (Yuan et al., 2005). However, striatal injections of 6-OHDA results in the small focal losses of dopaminergic cells in the SNc and multiple injections of 6-OHDA are

required to create a model mimicking the early stages of clinical PD. Such multiple injections can induce unwanted mechanical damage. Whereas, 6-OHDA injection into the MFB leads to the loss of dopamine content in the striatum as early as 3 days after lesion induction followed by progressive loss of dopaminergic neurons in the SN up to 8 weeks (Yuan et al., 2005). This closely mimics the progressive nature of PD in humans. Injections of 6-OHDA into the MFB also allow the investigation of the effect of 6-OHDA on the nigrostriatal and the mesolimbic system. The magnitude of the lesion depends on the concentration of 6-OHDA injected, the site of the injection, the species used (Betarbet et al., 2002) and whether noradrenalin uptake blockers such as desipramine are employed (Luthman et al., 1989). In mice, rats and cats, 6-OHDA is a highly effective toxin for dopaminergic (DAergic) neurons (Beal, 2001).

Since PD pathology is observed bilaterally in the human brain, bilateral PD models are considered more appropriate. Bilateral 6-OHDA lesions induce, in part, parkinsonian motor symptoms; however, the bilateral lesion does not represent the most frequently used model, due to the fact that bilaterally affected animals are associated with high morbidity rate due to aphagia caused by the severity of the lesion, therefore these animals require intensive nursing care (Cenci ,et al., 2002). Hence, unilateral lesions with 6-OHDA are the most reproducible and commonly used method to model PD with the un-lesioned hemisphere of the brain serving as internal control. Taken together, to be able to replicate the progressive and partial lesion of the nigrostriatal system, unilateral 6-OHDA injection into the MFB was employed as the animal model of PD in this project.

Benefits and limitations of 6-OHDA rat model

The clinical and widespread neuropathological alterations seen in PD patients are not entirely replicated in any animal model including the intra-cerebral injection of 6-OHDA in rodents. Although, 6-OHDA induces a significant decrease in dopamine and dopaminergic fibres in the striatum and leads to degeneration of dopaminergic neurons in the SNc with preservation of non-dopaminergic neurons 6-OHDA does not affect other brain regions that are affected in human PD such as: anterior olfactory structures, lower brain stem areas or the locus coeruleus (Betarbet et al., 2002). In addition formation of cytoplasmic inclusion bodies known as Lewy bodies that are hallmarks of PD pathology is not observed in 6-OHDA lesioned animals. However, *in vivo* the 6-OHDA partial lesion

model has been used routinely for the purpose of screening potential therapeutic (Lundblad et al., 2002; Asin et al., 1995) and neuroprotective drugs (Zbarsky et al., 2005). 6-OHDA robustly mimics and reflects the molecular changes such as, oxidative stress, accumulation of iron in the SNc as observed in human PD and it is a suitable model for studying the underlying mechanisms involved in the process that leads to dopaminergic neuronal loss including the involvement and role of inflammation (Cicchetti et al., 2002; Depino et al., 2003) in the course of the disease. Despite the mentioned limitations of this model it is one the most reliable, reproducible and widely used models of PD.

2.1.1.2 Medial forebrain bundle lesions

In order to study the role of inflammatory processes in the early phases of PD pathology, at which time point use of neuroprotective treatments would be most beneficial, it was decided that a partial lesion model of PD was the most suitable approach. To create a model that mimics the early phases of PD pathology, a unilateral partial lesion in the nigrostriatal system was induced by injection of 6-OHDA into the MFB rather than SN or the striatum (Fig 2.1). MFB comprises the dopaminergic axon projections from substantia nigra (SN) pars compacta and the ventral tegmental area (VTA) to the dorsal striatum (Fallon et al., 1978). These cells release dopamine at the somatodendritic level as well as at the terminal region. Studies by other colleagues in this laboratory have shown that 7 days after unilateral 6-OHDA injection into the MFB 60-70% of dopamine content in the striatum is lost with retrograde loss of 40-50% of dopaminergic neurons in the SN (Datla et al., 2001; 2003; 2004; Zbrasky et al., 2005) sparing the ventral tegmental area (VTA). These observations reflect the nigrostriatal pathology of PD as seen in human cases (Damier et al., 1999; Braak et al., 2004). As mentioned earlier the partial lesion model not only enables us to study the pathological mechanism involved in early phases of PD but it is also a suitable model for testing potential neuroprotective compounds that exert their beneficial effects when administered early in the degenerative process. In addition, 6-OHDA lesion induction to the MFB avoids local mechanical trauma to the SNc or the striatum and initiates degeneration at the axon terminals leading to retrograde damage of the DA neurons in the SN.

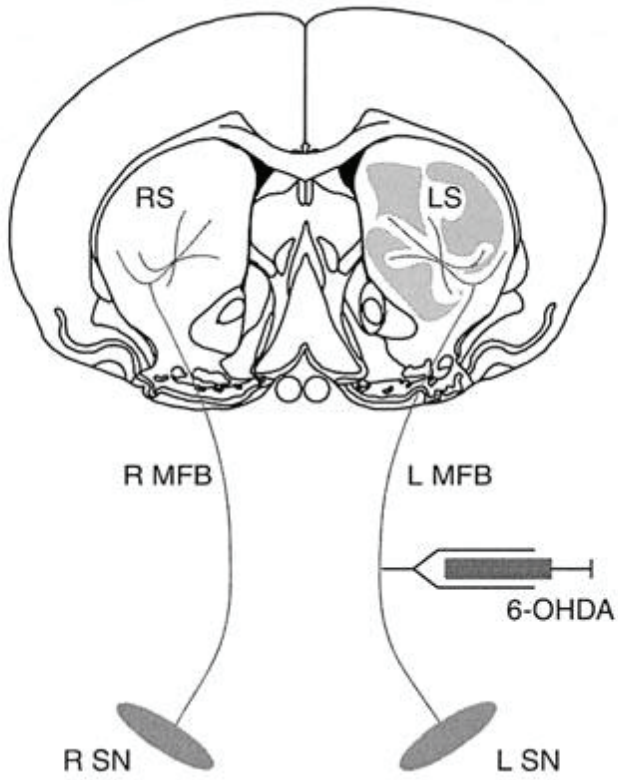

Fig 2.1 Schematic diagram of the nigrostriatal pathway

Shaded areas in the left striatum indicate the loss of DA due to a MFB injection of 6-OHDA. Abbreviations: RS, right striatum; LS, left striatum; R MFB, right medial forebrain bundle; L MFB, left medial forebrain bundle; 6-OHDA, 6-hydroxydopamine; R SN, right substantia nigra; L SN, left substantia nigra.

2.1.1.3 Mechanism of 6-OHDA neurotoxicity

One of the potential mechanisms by which 6-OHDA is shown to cause neurotoxicity to dopaminergic neurons is oxidative stress (Heikkila and Cohen, 1971; Sachs and Jonsson, 1975). 6–OHDA undergoes auto-oxidation very rapidly and generates hydrogen peroxide and para-quinons that leads to generation of reactive oxygen species (ROS).In addition evidence shows that 6-OHDA disturbs the endogenous antioxidant mechanisms in the basal ganglia by depleting the reduced glutathione (GSH) and reducing the activity and the mRNA levels of super-oxide dismutase (SOD) (Perumal et al., 1992), which results in production of high levels of hydrogen peroxide (H_2O_2). H_2O_2 reacts with iron via the Fenton reaction leading to production of toxic hydroxyl radicals ($OH^{\cdot}$) (Ben-Shachar and Youdim, 1991). 6-OHDA also leads to iron accumulation in the SN and directly stimulates the release of Fe^{2+} from ferritin (Ben-Shachar and Youdim, 1991; Youdim et al., 1993). These observations suggest that 6-OHDA renders the basal ganglia to the state of an on-going oxidative stress that is measured by increased levels of malondialdehyde indicative of lipid peroxidation in the SNc (Kumar et al., 1995). The biochemical defects in the brain, specifically the SNc caused by 6-OHDA are similarly observed in post-mortem brain tissue of PD patients. These defects include, increased membrane peroxidation in the SNc and widespread ROS-induced protein modification (Dexter et al., 1989; Dexter et al., 1994). In addition evidence shows that 6-OHDA acts as a direct inhibitor of mitochondrial electron transport chain enzymes, the complex IV (cytochrome c) and the complex I (NADH dehydrogensae) resulting in cellular energy failure and depletion of adenosine triphosphate (ATP) subsequently cell death (Glinka et al., 1996; 1997; Youdim et al., 1995). Mitochondrial Complex I defects have similarly been observed in the SNc from post-mortem brain tissue of PD patients (Schapira et al., 1990 and 2006). Evidence shows that oxidative stress and mitochondrial dysfunction are not the only mechanisms involved in 6-OHDA induced neurotoxicity; activation of microglia has also been shown to play a key role in neuronal death after 6-OHDA lesion induction. Direct administration of 6-OHDA into the SNc of mice activates microglia and increases the number of activated microglia in the SNc with the subsequent loss of dopaminergic neurons 1 week after 6-OHDA administration (He et al., 2001). Furthermore, 6-OHDA-lesioned rats have been demonstrated to have increased levels of TNFα in both the SNc and the striatum (Mogi et al., 1999). These observations are in accord with evidence from post-mortem brain tissue from the SNc of PD patients showing the presence of similar inflammatory response

characterized by activated microglia (McGeer et al., 1988; Mogi et al., 1995). Mitochondrial inhibition, oxidative stress and inflammatory response induced by 6-OHDA are mechanisms that could work synergistically *in vivo* leading to neuronal cell death in the SNc (Rodriguez-Pallares et al., 2007).

2.1.1.4 Motor impairments in 6-OHDA lesion induced model of PD

Rats with severe unilateral 6-OHDA lesions including lesions to the MFB show significant signs of motor impairments similar to akinesia and bradykinesia observed in human cases of PD when 80-90% of the striatal dopamine is lost and more than 80% of dopaminergic neurons in the SN have degenerated. Akinetic movements are observed in rats in their reaction time to challenges such as: adjusting step test and paw retraction test (Barneoud et al., 1995). In addition severe 6-OHDA lesions cause an asymmetric and quantifiable rotating motor behavior in the longitudinal axis of the body, which can be quantified in a rotation-box (Hefti et al., 1980). This rotational asymmetry is induced by systemic administration of drugs that have direct or indirect agonistic effect on dopamine release (Hefti et al., 1980). For example, systemic administration of apomorphine (APO), a dopamine agonists, induces contralateral turning behavior to the side of the lesion in rats with severe 6-OHDA lesions. APO stimulates both classes of dopamine receptors (D_1, D_2). The degeneration of the nigro-striatal dopaminergic neurons leads to super-sensitivity of post-synaptic dopamine receptors in the striatum. Thus receptors on the lesioned side are more sensitive to dopamine agonists than those on the intact side. Consequently when challenged with APO contralateral response is attributed to the stimulation of supersensitive D_1-receptor and D_2-receptors (Schwarting and Huston, 1996). Another class of dopamine releasing drugs are the indirect agonists that include amphetamines. Amphetamines are considered indirect dopamine agonists, since they bind to the monoamine transporters and increase extracellular levels of endogenous striatal dopamine (Schwarting and Huston, 1996). Systemic amphetamine treatment after 6-OHDA lesion induction induces a dose dependent ipsilateral turning behavior to the side of the lesion that could be explained by stimulation of post-synaptic dopamine receptors on the contralateral un-lesioned side. It is noteworthy however to mention that shortly after 6-OHDA lesion, amphetamine treatment can induce contralateral turning that is in response to the release of non-functional dopamine pools in the lesioned hemisphere. When dopamine pools are depleted, the direction of turning switches to the contralateral side. This phenomenon could be explained

by the release of dopamine in the unlesioned hemisphere after amphetamine injection (Schwarting and Huston, 1996). The characteristic rotating behaviour is often used as a measure for the degree of lesion induced by 6-OHDA and to test potential beneficial effects of the anti-parkinsonian therapeutic agents.

It should be emphasised that such testing is not suitable in the partial lesion model employed in this project, since degree of dopamine depletion in the striatum and dopaminergic neuronal loss in SNc are not sufficient enough to be able to observe sever and significant rotational behaviour.

2.1.2 Stereotaxic surgery

2.1.2.1 Animals

Male (Sprague-Dawley (SD) rats (Harlan, UK) weighing 200-210(g) on arrival were housed in groups of three per cage at a temperature of 21± 1ºC on a 12hr light: dark cycle (lights on 07:00 am, lights off 07:00 pm). Rats had free access to standard rat chow and water *ad libitum*. Animals were allowed to acclimatize for 7 days in the Charing Cross Central Biomedical Unit (CBU) before any experiments were carried out. During this time the weight of the animals increased to the most suitable weight of 220-250g for sterotaxic surgery. The stereotaxic surgical coordinates adapted from Paxinos and Watson rat brain atlas are calculated for rats weighing up to 290g. Male rats were used through out this project because recent evidence shows; the incidence of PD is greater in males than females (Scharg et al., 2000; Swerdlow et al., 2001). In addition evidence from experimental models of PD also support this observation and suggests that oestrogen might have neuroprotective properties on dopaminergic neurons after 6-OHDA lesion (Gillies et al., 2004; Murray et al., 2003; Dluzen, 1997; Dubal et al., 1998).

2.1.2.2 Stereotaxic injection of 6-OHDA into the MFB

Groups of rats (n=6) received unilateral injection of 6-OHDA into the MFB according to the protocol of Datla and colleagues, (2001). Rats were weighed on the day of surgery and pre-operative weight was recorded. Generalised anaesthesia was induced using 5% Isoflurane (Abbott, U.K.) in oxygen (2l/min) (BOC, U.K.) in an induction chamber.

Once stable anaesthesia was established by testing the loss of paw pinch reflex, animals were then placed into a stereotaxic frame (David Kopf instrument, USA) with incisor bar set at 5mm below the interaural line. To maintain their body temperature at 37 ºC rats were kept on a thermostatically controlled heated mat. Anaesthesia was maintained thereafter with isoflurane (1-3%) in oxygen (1l/min). The scalp area was shaved and swabbed with iodine solution (Betadine, Seton Healthcare Group Plc, Oldham, UK) to sterilise the skin. 0.1 ml bupivacain hydrochloride (Marcain, AstraZeneca, Chester, UK) was then administered by subcutaneous (s.c.) injections at four sites on the scalp as local anaesthetic and 5ml 4% glucose in 0.18% saline intraperitoneal (i.p.) was given to prevent dehydration. A single incision was made sagittally along the scalp starting from behind the eyes and going up to the ears to expose the skull. The skin was retracted and the periosteum removed, the cranium was then dried to ensure clear view of the bregma. All subsequent stereotaxic coordinates were measured in millimetres with anterior and lateral coordinates made relative to bregma and ventral coordinates made relative to the dura. A small hole was made in the skull with a sterile dental drill above the level of the MFB (2.2mm posterior, 1.5mm lateral from bregma and 7.9mm ventral to the dura, according to Paxinos and Watson, 1986) (Fig 2.2). 6-hydroxydopamine hydrobromide (dissolved in 0.1% ascorbic acid in 0.9% sodium chloride solution; Sigma, U.K.) was injected into the left MFB, delivered in 4min using a 10µl manual, microinjection syringe (Hamilton, USA) and the needle left *in situ* for 4min to prevent reflux along the injection needle. The concentration of 6-OHDA was calculated from its free base in an injection volume of 4µl. Post-surgery, animals were placed in a heated recovery chamber for 1 hour to recover from the anaesthetic. Post-operative care included individual caging and a mashed diet.

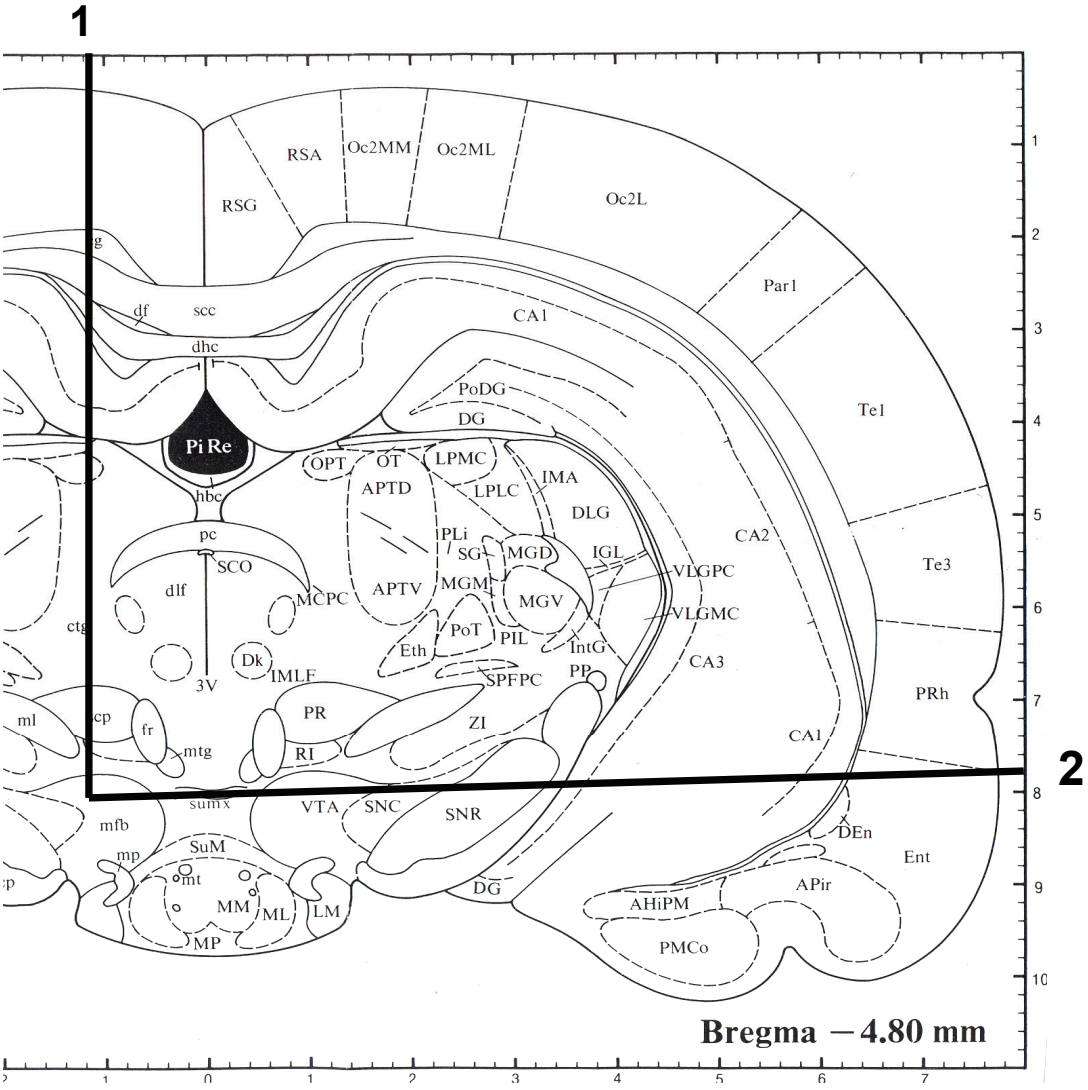

Fig 2.2 Diagrammatized coronal brain section (plate 37 of the standard rat brain atlas, Paxinos and Watson, 1986) to illustrate the stereotaxic coordinates used to inject 12µg 6-OHDA into the left MFB. Coordinate 1 is equal to 1.5 mm lateral to the midline and coordinate 2 is equal to –7.8mm ventral to dura. The anterior coordinate is not shown, but is equal to –2.2 mm anterior to bregma. These co-ordinates were measured with the incisor bar set 5 mm above the interaural line. The Paxinos and Watson atlas (1986) diagrams are based on incisor bar set 3 mm above the interaural line, hence these markers are purely illustrative and not intended to be to exact scale.

2.1.3 Post-mortem procedures and brain tissue collection

At the end of each individual experiment animals were sacrificed by CO_2 over dose. Brains were quickly removed and cut coronally at the level of infundibular system (-4.16 mm from bregma) on a chilled platform using a rodent brain matrix. Hindbrain and forebrain blocks were then separated. Hindbrain blocks containing the SNc were transferred to 4% paraformaldehyde solution made up in 0.1M PBS (pH 7.4) and kept for 6-7 days for fixation. Then the brains were cryoprotected in 30% sucrose solution containing 0.1% sodium azide as preservative until the block had sunk (48-72 hours). The brains were then stored at -80^{0}C freezer until subsequent cryostat sectioning. From the forebrain block corpus striata were dissected out on ice and flash frozen on dry ice, the striata were stored at -80^{0}C until processed for measurement of the monoamine content by High Performance Liquid Chromatography with Electrochemical detection (HPLC-ECD) (*see section 2.2.4.1*).

2.2 Ex-vivo methods

2.2.1 Avidin-Biotin Immunohistochemistry

2.2.1.1 Overview

Immunohistochemistry is the process of localizing proteins (antigens) in cells of tissue sections exploiting the principle of antibody binding specifically to antigens. The antigen-antibody interaction can then be visualized by markers such as: dye, enzyme, fluorescent dye, radioactive element and colloidal gold. Albert H. Coons and his colleagues (Coons et al., 1955) were the first to label antibodies with fluorescent dye and use it to identify antigens in tissue sections. With the expansion and development of immunohistochemistry technique, enzyme labels were introduced such as peroxidase (Nakane and Pierce, 1966). Other methods included colloidal gold (Faulk and Taylor, 1971) label that was used to identify immunohistochemical reactions at both light and electron microscopy level.

One of the immunohistochemical methods employed in this project to analyse antigen localisation is standard avidin-biotin complex (ABC) immunoperoxidase technique. Avidin is a large glycoprotein, with 68kDa molecular weight that has a very high affinity for biotin. Biotin, a low molecular weight vitamin, can be conjugated to a variety of biological molecules such as antibodies. In addition to the high affinity between avidin and biotin, avidin has four binding sites for biotin thus several molecules of biotin could be conjugated to proteins including enzymes and antibodies. Exploiting these properties provides potential for formation of molecular complexes between biotinylated proteins and avidin hence, immunoperoxidase method was developed to localise antigens in tissue sections. The technique builds three layers of macromolecules, the first layer is the addition of the unlabeled primary antibody to the tissue, second layer is biotinylated secondary antibody and the third layer is a complex of avidin-biotin peroxidase. The binding can be visualised by addition of the substrate for the peroxidase. The traditional substrates include diaminobenzidine tetrachloride (DAB) and 3 –amino-9-athyl carbazole (AEC). DAB produces a brown precipitate in tissue sections or purple/grey colour in the presence of divalent cations such as nickel or cobalt that are insoluble in alcohol (Fig 2.3). ABC is a simple and rapid method that has several advantages over other methods such as: directly coupling a marker to an antibody or using nucleic acid probes and lectins. The high affinity constant ($>10^{15}\ M^{-1}$), between avidin and biotin leads to rapid formation of an irreversible stable complex of avidin conjugate and biotinylated secondary antibody. In addition, since avidin has more than one binding site for biotin, a large amount of peroxidase can bind to a single antigen site. This leads to a very high sensitivity of the staining performed, allowing lower concentration of primary antibody to be used.

The general protocol for ABC immunohistochemistry technique for detection of specific proteins is out-lined in the following section. Modifications to this standard immunohistochemistry protocol are covered in the individual experiments.

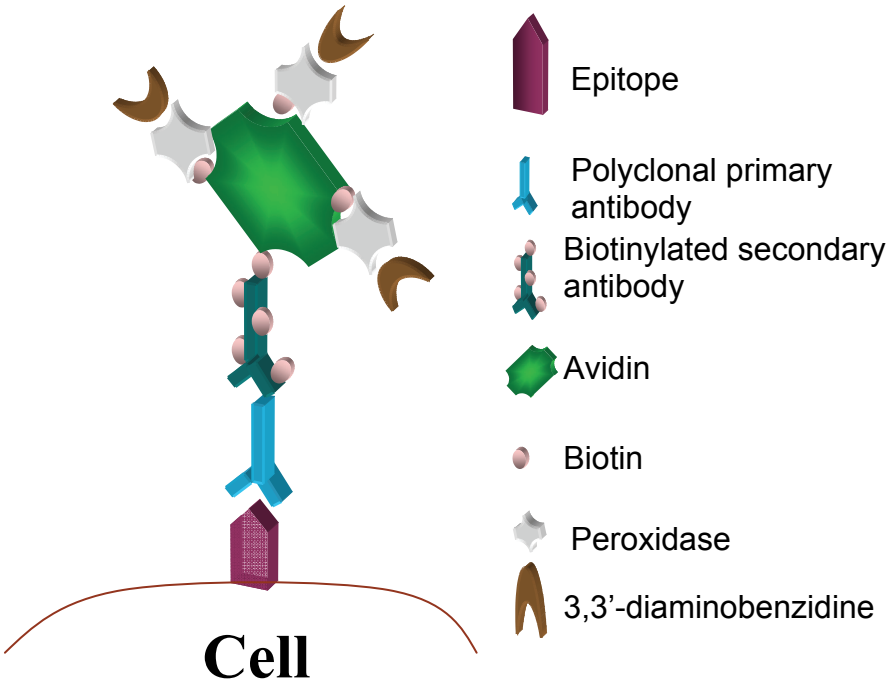

Fig 2.3 Illustration of the avidin-biotin immunoperoxidase immunohistochemistry technique.

In brief, the unlabelled primary antibody is applied to the tissue sections followed by biotinylated secondary antibody. A preformed avidin-biotin-horseradish peroxidase macromolecular complex is then applied to form a molecular scaffold bound to the secondary antibody. Antibody binding is then visualised by the addition of the chromagen 3, 3'-diaminobenzidine (DAB) which, in the presence of the peroxidase substrate hydrogen peroxide, forms an insoluble brown precipitate.

2.2.1.2 General standard protocol for ABC immunohistochemistry

All primary and secondary antibodies were titrated to obtain the optimum working dilution (Table 2.1). Coronal sections of the entire SNc, that expands from -4.80 to 6.30 mm from bregma, was cut at 20µm thickness on a cryostat (Bright Instruments, UK) maintained at -20 ºC. Sections were collected and free floated in 24 well plates (Beckton Dickenson, UK) and were stored at 4°C in 0.1M phosphate buffered saline (PBS) containing 0.05% sodium azide as preservative, pH 7.4. Prior to staining minimum three and maximum six tissue sections were transferred to individual wells in 2mls of 0.1M PBS. Excess sodium azide was washed out by rinsing section 3x 5min in 0.1M PBS on a shaking platform. Endogenous peroxidase activity was then quenched by incubating tissue section in 1% H_2O_2 for 30-50min. To facilitate antibody penetration sections were incubated for total of 15min in 0.1 M PBS containing 0.05% Triton X-100 (Sigma-Aldrich-UK). In order to eliminate any non-specific antibody binding tissue sections were blocked for 1 hour in the appropriate non-immune serum diluted in 0.1M PBS. Normal goat serum (Vector Labs, Peterborough, UK) was used when the secondary antibody was raised in goat and normal horse serum (Vector Labs, Peterborough, UK) was used when the secondary antibody was raised in horse, this information may be found in Table 2.1. After blocking, tissue sections were incubated in appropriate primary antibody, diluted in 0.1M PBS Triton X-100 at room temperature (20-21°C) over night (~ 18 hours). This was followed by 60-90 min incubation in the appropriate biotinylated secondary antibody diluted in 0.1M PBS Triton X-100. Secondary antibodies were chosen according to the host in which the primary antibody was raised, the list of primary and corresponding secondary antibodies may be found in Table 2.1. Sections were then incubated in a pre-formed avidin conjugated horseradish peroxidase macromolecular complex (Vactastain Elite ABC kit PK-6100, Vector Labs, UK) for 45min. ABC was prepared according to the manufacturer's instructions, diluted in 0.1M PBS Triton X-100 30min before use. Antibody binding was then visualised by incubating sections in DAB, using a DAB peroxidase kit [(DAB peroxidase kit SK-4100), Vector Labs, UK], as per manufacturer's instructions. DAB incubation time was optimised depending on the specific protein under study. DAB reactivity was visually determined by characteristic DAB brown precipitate. To terminate DAB reaction tissue sections were rinsed in distilled water for 5min. Where appropriate Nickel/DAB staining enhancer was used as per manufacturer's guide in order to enhance the density of the staining [(DAB peroxidase kit SK-4100), Vector Labs, UK].

For each immunostaining a negative control was added in which the primary antibody was omitted. In none of the cases immunoreactivity was observed (data not shown). Tissue sections were then mounted onto poly-L-lysine coated slides and left to dry at room temperature before being dehydrated in ascending concentration of ethanol for 3 min each. Sections were then immersed into two changes of xylene for 3min each to de-fat the tissue. DPX mounting medium was used to cover-slip the tissues sections on slides. All dehydration stages including cover slipping was performed in a fume hood and slides were allowed to dry overnight before being analysed.

2.2.1.3 Tyrosine hydroxylase (TH) immunohistochemistry protocol

To visualise dopaminergic neurons in the SN, TH immunohistochemistry was utilised. TH is cytosolic rate limiting enzyme which is involved in dopamine synthesis by catalyzing the conversion of the amino acid L-tyrosine to dihydroxyfenilalnine (DOPA). DOPA is a precursor for dopamine which in turn is a precursor for noradrenalin and adrenaline. Hence, TH antibody labels both dopaminergic and noradrenergic neurons. However, in the SNc the only chatecholaminergic neurons present are dopaminergic (Pickel et al., 1977; Wassef et al, 1981) thus, TH is a suitable marker for quantification of dopaminergic neurons in the SN. TH immunostaining is an accurate and rapid method to assess the integrity of the SN after 6-OHDA lesion induction and /or to asses the effect of potential neuroprotective/neurorestorative treatments on the integrity of dopaminergic neurons. The staining was performed on 20µm thick, free-floating nigral sections as described in (see *section 2.2.1.2*). The details of primary and secondary antibodies and their working dilution may be found in (Table 2.1). The staining was performed on 6-OHDA lesioned, sham operated and/or drug treated animals. Once the immunostaining was completed sections were analysed under a light microscope (Nikon Eclipse E400) and the number of TH+ve dopaminergic neurons was counted at both ipsi and contralateral sides of the 6-OHDA lesion or sham operated animals.

2.2.1.4 Immunostaining for markers of glial cell activation in the SNc

To monitor the effect of 6-OHDA and/or drug treatments on the activational state of microglial cells in the SNc, resident microglia and macrophages were detected using three different antibodies outlined below. The working dilution and secondary antibodies used

may be found in Table 2.1. Staining was performed on 20μm thick consecutive free floating sections of the SNc of 6-OHDA lesioned, sham operated and/or drug treated animals as previously described (see section 2.2.1.2). The immunostained sections were analysed microscopically and were assessed both quantitatively and qualitatively, the details of the criteria used for their analysis are outlined in *section 2.2.3.1 and 2.2.3.2*.

OX-6: to detect the activation of a population of microglial cells that express major histocompatibility complex II (MHC II) surface receptor.

OX-42 (CD11b): to monitor the activation of brain resident monocytes/microglial cells. This antibody recognises the presence of leukocyte integrin complement receptor type 3 (CR3) on microglia.

CD-68: to detect the presence of macrophages with phagocytic function, this antibody recognises a glycoprotein that is expressed predominantly on the lysosomal membrane of myeloid cells.

2.2.1.5 Immunostaining for matrix metalloproteinase 3 (MMP3) expression in SNc

MMPs belong to a family of zinc-dependent proteases. The main function associated with MMPs is degradation and remodeling of extracellular matrix proteins. They are known to be involved in the cleavage of cell surface receptors, the release of apoptotic ligands and chemokine activation. Immunostaining for MMP-3 and MMP-9 was performed to monitor the effect of 6-OHDA on the number of MMP-3 and MMP-9 expressing cells in the SNc. The working dilutions and secondary antibodies used may be found in Table 2.1. Staining was performed on 20μm thick consecutive free floating sections from the SNc of 6-OHDA lesioned and sham operated animals as described in *section 2.2.1.2*. The immunostained sections were analysed microscopically. MMP-3 and MMP-9 positive cells were analysed morphologically and quantitatively, the details of the criteria used for their analysis are outlined in *section 2.2.3.3*.

Epitope	Antibody and its working dilution	Source	Secondary antibody	Secondary antibody working dilution	Source
Tyrosine Hydroxylase (TH)	Polyclonal rabbit α-rat TH *1:000*	Pel-freez (USA)	Biotinylated rabbit α-rat made in goat	*1:200*	Vectorlabs Peterborough, UK
OX42	Monoclonal mouse α-rat OX42 *1:750*	Serotec (UK)	Biotinylated mouse α–rat made in horse	*1:100*	Vectorlabs Peterborough, UK
OX6	Monoclonal mouse α–rat OX6 *1:750*	Serotec (UK)	Biotinylated mouse α–rat made in horse	*1:100*	Vectorlabs Peterborough, UK
CD68	Monoclonal mouse α-rat CD68 *1:750*	Serotec (UK)	Biotinylated mouse α-rat made in horse	*1:100*	Vectorlabs Peterborough, UK
MMP-3	Polyclonal rabbit α-rat MMP-3 *1:100*	Santa-Cruz (USA)	Biotinylated rabbit α-rat made in goat	*1:200*	Vectorlabs Peterborough, UK
MMP-9	Polyclonal rabbit α-rat MMP-9 *1:100*	Santa-Cruz (USA)	Biotinylated rabbit α–rat made in goat	*1:200*	Vectorlabs Peterborough, UK

Table 2.1 Details of all primary and secondary antibodies utilised in ABC immunohistochemistry. Sources as well as optimal working dilutions are also shown.

2.2.2 Double immunofluorescence

Double-labelling immunofluorescence techniques detect the localization of a protein relative to another protein and allow analysis of co-localization at a cellular and sub-cellular level. Immunofluorescence staining methods can also be used successfully for labelling multiple antigens in the same preparation. Such methods are especially useful for co-localization of antigens in the same compartment of a cell, and in this regard offer a distinct advantage over enzyme-based detection systems. In this project the traditional approach to double fluorescent labelling has been used in which fluorescently conjugated secondary antibodies are targeted against primary antibodies from different species. Although this technique in general tends to be less sensitive than enzymatic staining, the sensitivity of the fluorescent stain can be increased by using a (strept) avidin-biotin system for amplification of the label. The dyes chosen for immunofluorescence are excited by a specific wavelength of light, usually blue or green, and emit light of a different wavelength in the visible spectrum. By using selective filters, only the light coming from the dye or flurochrome used is detected in the fluorescence microscope. By attaching different dyes to different antibodies, the distribution of two or more molecules can be determined in the same cell or tissue section. The general protocol for double fluorescence immunostaining is out-lined in the following section (see *section 2.2.2.1*).

2.2.2.1 General immunofluorescence protocol

One of the immunohistochemical methods used throughout this project was double immunofluorescence technique. All primary and secondary antibodies were titrated to obtain the optimum working dilution (Table 2.2). Any modifications made to this protocol are mentioned in individual experiment. Coronal sections of the entire SN that expands from -4.80 to 6.30 mm from the bregma were cut at 20µm thickness on a cryostat (Bright Instruments, Cambridge, UK) maintained at -20 ºC. Free floating sections were collected in a 24 well plates (Falcon, Beckton Dickenson, Cowley, UK) and were stored at 4°C in 0.1M phosphate buffered saline (PBS) containing 0.05% sodium azide as preservative, pH 7.4. Prior to staining minimum three and maximum six tissue sections were transferred to individual wells in 2mls of 0.1M PBS. Excess sodium azide was washed out by rinsing section 3x 5min in 0.1M PBS on a shaking platform. To facilitate antibody penetration

sections were incubated for total of 15min in 0.1 M PBS containing 0.05%. Triton X-100. In order to eliminate any non-specific antibody binding tissue sections were blocked for 1 hour in the appropriate non-immune sera diluted in 0.1M PBS. Normal goat serum (Vector Labs, Peterborough, UK) was used when the secondary antibody was raised in goat and normal horse serum (Vector Labs, Peterborough, UK) was used when the secondary antibody was raised in horse (Table 2.2). Sections were then incubated for 18 hours (over-night) with two different primary antibodies that recognise two different antigens of interest, for the purpose of determination of co-localisation. The primary antibodies that were co-incubated were not made in the same animal species to eliminate cross-reactivity. In all cases negative controls were included and non showed immunoreactivity (Data not shown). Tissue sections were then incubated in appropriate secondary antibodies in the dark for 60 minutes. Secondary anti-bodies had fluorescent dye attached to the antibody so that they are detected by UV light. Sections were then wet mounted onto Poly-l-lysine coated slides in dark and left to dry at room temperature. Once dry sections were cover-slipped using Vectasheild Hard Set mounting medium with DAPI with is a marker for cell nucleus (Vector Laboratories, Peterborough, U.K.) before being examined on a Nikon Eclipse E1000 fluorescence microscope using appropriate filter sets. DAPI (4', 6-diamidino-2-phenylindole) bind to the DNA and is used to mark cell nucleus. DAPI produces a blue fluorescence with excitation emission at about 460 nm when bound to DNA. The details of all primary antibody co-incubations, working dilution, secondary antibodies and their working dilution and the wavelength at which the fluorescent dyes attached emit light that is in visible spectrum may be found in (Table 2.2). Table 2.2 provides details of co-localisation studies that were performed through out this project, specificity and choice of each marker is discussed in individual studies and experiments.

1st AB	Source	2nd AB	source	1st secondary AB	Emission (nM)	2nd secondary AB	Emission (nM)	source
Polyclonal rabbit α-rat TH 1:500	Pel-freez (USA)	Monoclonal mouse α-rat OX6 1:750	Serotec (UK)	Alexa fluor 488 goat α-rabbi 1:300	519	Cy3 conjugat goat α-mouse 1:300	670	Invitrogen (UK)
Polyclonal rabbit α-rat TH 1:500	Pel-freez (USA)	Monoclonal mouse α-rat CD68 1:750	Serotec (UK)	Alexa Fluor 488 goat α-rabbi 1:300	519	Cy3 conjugat goat α-mouse 1:300	670	Invitrogen (UK)
Polyclonal rabbit α-rat TH 1:500	Pel-freez (USA)	Monoclonal mouse α-rat NeuN 1:2000	Chemico (UK)	Alexa Fluor 488 goat α-rabbi 1:300	519	Cy3 conjugat goat α-mouse 1:300	670	Invitrogen (UK)
Polyclonal rabbit α-rat Ki67 1:200	Clone TEC-3 Dako CA (USA)	Monoclonal mouse α–rat OX-6 1:750	Serotec (UK)	Alexa Fluor 488 goat α-rabbi 1:300	519	Cy3 conjugat goat α-mouse 1:300	670	Invitrogen (UK)
Polyclonal rabbit α-rat iNOS 1:400	Calbiochen (UK)	Monoclonal mouse α-rat OX-6 1:750	Serotec (UK)	Alexa Fluor 488 goat α-rabbi 1:300	519	Cy3 conjugat goat α-mouse 1:300	670	Invitrogen (UK)
Polyclonal rabbit α-rat MMP-3 1:200	Santa-Cruz (USA)	Monoclonal mouse α-rat GFAP 1:500	Sigma (UK)	Alexa Fluor 488 goat α-rabbi 1:300	519	Cy3 conjugat goat α-mouse 1:300	670	Invitrogen (UK)
Polyclonal rabbit α-rat MMP-9 1:200	Santa-Cruz (USA)	Monoclonal mouse α-rat GFAP 1:500	Sigma (UK)	Alexa Fluor 488 goat α-rabbi 1:300	519	Cy3 conjugat goat α-mouse 1:300	670	Invitrogen (UK)
Polyclonal rabbit α-rat MMP-9 1:200	Santa-Cruz (USA)	Monoclonal mouse α-rat NeuN 1:2000	Chemico (UK)	Alexa Fluor 488 goat α-rabbi 1:300	519	Cy3 conjugat goat α-mouse 1:300	670	Invitrogen (UK)
Polyclonal rabbit α-rat MMP-3 1:200	Santa-Cruz (USA)	Monoclonal mouse α-rat NeuN 1:2000	Chemico (UK)	Alexa Fluor 488 goat a-rabbi 1:300	519	Cy3 conjugat goat α-mouse 1:300	670	Invitrogen (UK)
Polyclonal rabbit α-rat Caspase-3 1:300	Serotec(UK)	Monoclonal mouse α-rat NeuN 1:2000	Chemico (UK)	Alexa Fluor 488 goat α-rabbi 1:300	519	Cy3 conjugat goat α-mouse 1:300	670	Invitrogen (UK)
Polyclonal rabbit α-rat MMP-3 1:200	Santa-Cruz (USA)	Monoclonal mouse α-rat CD200R 1:100	Serotec (UK)	Alexa Fluor 488 goat α-rabbi 1:300	519	Cy3 conjugat goat α-mouse 1:300	670	Invitrogen (UK)
Polyclonal rabbit α-rat Caspase-3 1:300	Serotec(UK)	Monoclonal mouse α-rat CD68 1:750	Serotec (UK)	Alexa Fluor 488 goat α-rabbi 1:300	519	Cy3 conjugat goat α-mouse 1:300	670	Invitrogen (UK)

Table 2.2 Details of all antibody co-localisation experiments and working dilutions in addition to their relevant secondary antibodies**.**

2.2.3 Cell counting and morphological assessment of immunostained cells

2.2.3.1 Quantitative cell counting for TH+ve, glial cells, MMP-3+ve and MMP-9 +ve in SNc and VTA

In order to quantify the number of TH+ve dopaminergic neuronal bodies the counting was performed manually using a Nikon Eclipse E800 microscope (Nikon, Tokyo, Japan) connected to a JVC analogue camera at x100 magnification. TH+ve neurons were counted in both ipsi and contralateral hemispheres of the brain in each of the stereotaxic regions of the SN and adjacent VTA area, (-4.80,-5.30,-5.60,-5.80 and -6.30 mm from bregma) (Carman et al., 1991) to ensure complete sampling of the entire structures; ventral tegmental area (VTA) and SNc. The stereotaxic region in each section was determined by examination of the shape and distribution of TH+ve neurons at low magnification (x40) with reference to the standard rat brain atlas of Paxinos and Watson (1986). The SNc was delineated from the VTA by reference to specific anatomical landmark of the third cranial nerve rootlet as previously described by Iravani et al., (2002). To minimise bias the operator was assessed for the consistency of counting in each stereotaxic level of the SNc prior to cell counting. Cells that were intact with a nucleus, clear cytoplasm and axonal processes were included into the counts and cells that appeared deformed with no obvious axonal processes were excluded from the counts (Iravani, et al, 2002). For each animal, cell counts were carried out through the entire structure of the SN. The counts were pooled together to give a total mean cell count for ipsi and contralateral hemispheres in each group. To ensure an unbiased cell counts the operator was blinded to the treatment under analysis. The same approach was employed for quantitative counting of MMP-3+ve and MMP-9+ve cell. Representative photomicrographs were captured at x100, x400 magnifications using Image ProPlus v5.0 software (Media Cybernetics, UK). A similar approach was utilized for quantitative counting of the inflammatory markers using x200 magnification.

2.2.3.2 Morphological assessment of glial cells

The criteria that was used for the assessment of the activational state of glial cells in the SNc and VTA is outlined below. It should be noted that criteria for assessment of any other non glial markers which had a glial expression are dealt with in individual sets of experiments in relevant sections.

Glial cells acquire different morphologies depending on their function. Therefore alongside quantitative counting, assessment of their morphology and pattern of expression is necessary when their functional properties are being studied. The pattern of expression of microglia (OX6 and OX42+ve cells) and macrophages (CD68+ve cells) was divided into three categories that are referred to as, no expression, focal expression and widespread. No expression: no immunoreactivity for OX6, OX42 and CD68 was observed in the SN and VTA. Focal expression: OX6, OX42 and/or CD68 immunoreactive cells were observed to be present in the SN and/or VTA and their expression is confined to these areas only. Widespread: the immunoreactivity is observed in other regions of the brain tissue sections as well as the SNc and the VTA. Microglia/macrophages (OX6 and OX42 and CD68+ve cells) go through a morphologically graded response, from resting to activated. These cells are considered activated when they show intense expression of either OX42 or OX6 or CD68, their cell soma is hypertrophied and they have thickened and shortened processes (Fig 4.2C). These cells are fully active when they have amoeboid morphology with very short and thick processes (Fig 4.2B). Microglial cells were considered to be at rest when they had moderate expression of either OX42 or OX6 or CD68, a small cell body with very thin but numerous processes with ramifications (Fig 4.2A). The pattern and morphology of microglial cells was analysed using Nikon Eclipse E800 light microscope (Nikon, Tokyo, Japan) under x200 magnification. Figure 2.4 shows representative photomicrographs of OX6+ve and OX42+ve microglia taken at x400 magnification.

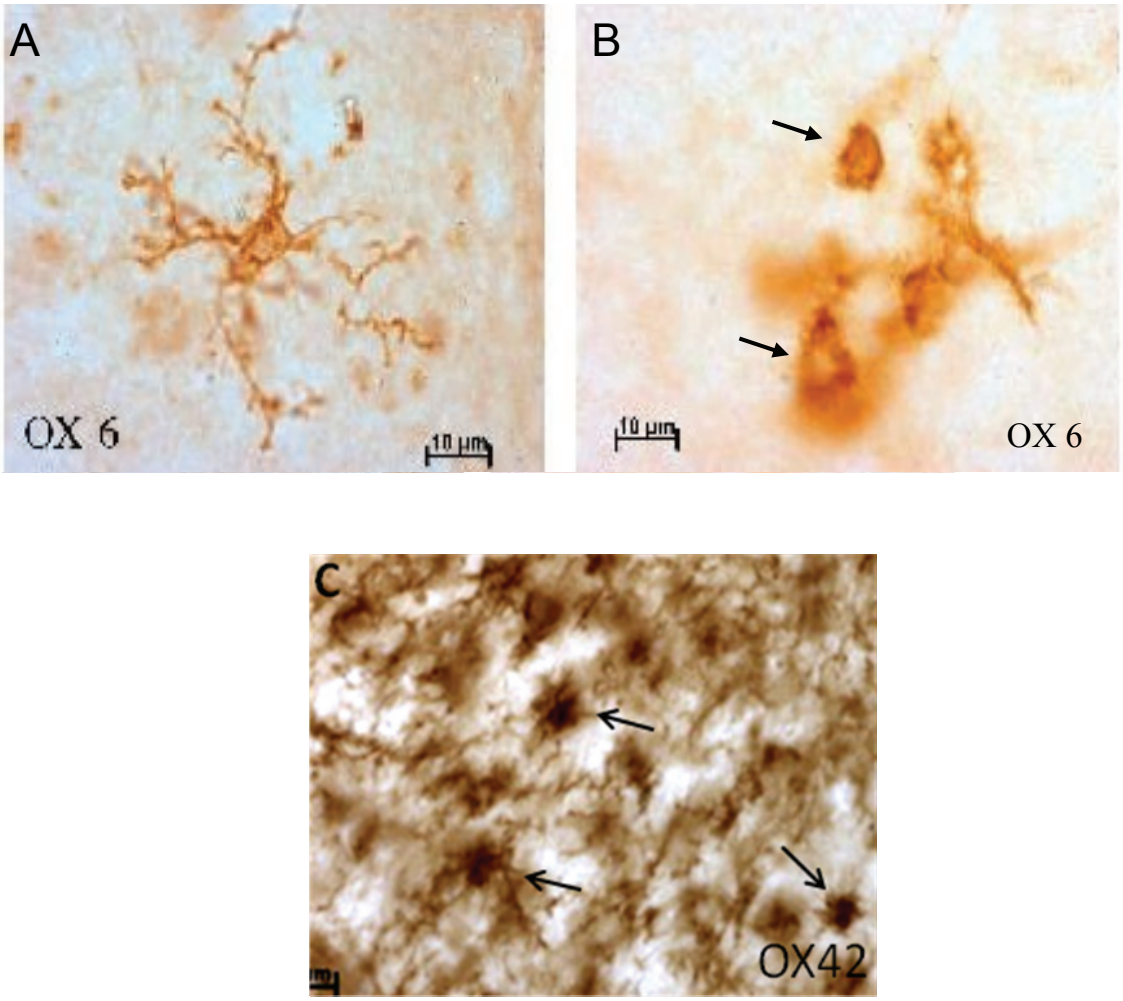

Figure 2.4 Representative photomicrographs of DAB peroxidase immunostaining for OX6+ve and OX42+ve microglia in the SNc following 6-OHDA lesion induction.

A) Activated OX6+ve microglial cell with hypertrophied cell body and very few processes.

B) Fully activated OX6+ve microglia (black arrows) with amoeboid morphology and no processes.

C) Activated microglia with intense expression of OX42 antibody and hypertrophied cell bodies with thickened and shortened processes.

Images were taken at x400, scale bar represents 10µm.

2.2.4 Assessment of the concentrations of striatal monoamine by High Performance Liquid Chromatography (HPLC)

HPLC with electrochemical detection (ECD) was performed to measure the concentration of monoamines in the brain in order to assess the functionality of the nigrostriatal tract. Therefore concentrations of striatal monoamines, specifically dopamine (DA) and its metabolites, dihydroxyphenylacetic acid (DOPAC) and homovanillic acid (HVA) were measured.

2.2.4.1 HPLC methodology

HPLC procedure was performed as previously described by Datla et al., (2002). Briefly, individual samples from left and right striatum were weighed and homogenised in 500 µl of ice-cold homogenising buffer (50 mM trichloroacetic acid, 0.5 mM disodium ethylenediaminetetraacetic acid (EDTA) and 0.5 pmol/µl 3,4-dihydroxybenzylamine hydrobromide as an internal standard, for 20 sec using an ultrasonicator (Soniprep, Sanyo, UK). Samples were placed on ice for 10 min to allow complete extraction of monoamines and then centrifuged at 13,000 rpm for 10 min at 4°C (Heraeus, UK). The resultant supernatant was then filtered through a 0.45 µM syringe pore filter (Whatman, UK) into glass HPLC vials (Chromacol, UK) and loaded onto an autosampler (Gina 50 Dionex, UK) maintained at 5°C and connected to a PC-based control system running Chromeleon software (Dionex UK). From each sample 20 µl was injected and chromatographically separated on an Altex ultrasphere 5 µM column (4.6 mm x 7.5 cm; Beckman, UK) using a mobile phase consisting of 0.1 mM KH_2PO_4, 0.1 mM EDTA, 1 mM octyl sodium sulfonate, 18% methanol V/V, adjusted to pH 2.5 with orthophosphoric acid, at a flow rate of 1.2 ml/min. To reduce background current and improve base line noise samples passed through a guard cell (model 5020,ESA Bioscience, UK) containing a porous graphite electrode set at +400mV to remove any electroactive impurities before reaching the column and the detector. Samples were quantified by an analytical cell (model 5011, ESA Bioscience UK) attached to a Coulochem II electrochemical detector (ESA Analytical) with electrode one at -0.20 V and electrode two at +0.34 V with respect to the palladium reference electrode. Calibration curve were calculated for each monoamine to ensure a linear relationship between the solute and the concentration of each monoamine. In addition, to facilitate the

quantification of monoamines and to determine the exact retention time for each monoamine in the samples, external standards of known concentration were analysed prior to each sample run (Fig 2.5). Chromatographic data were collected and analysed using PC-based Chromeleon software (Dionex, UK). The levels of monoamines in the lesioned and unlesioned rats for control and drug treated groups were then compared and analysed statistically as described below (*see section 2.3*).

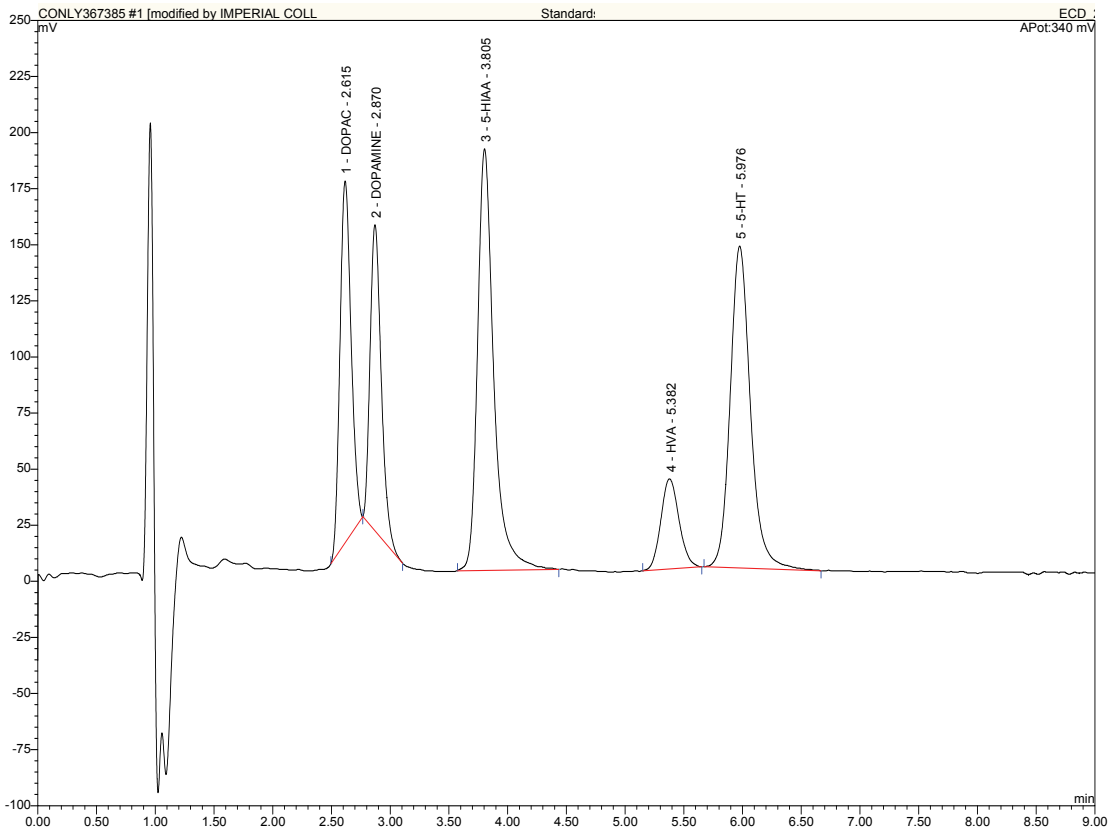

Figure 2.5 Representative chromatogram trace, showing detection of monoamines in the external standards by HPLC-ECD. Typical retention times were: Internal std 1.75 min, dihydroxyphenylacetic acid (DOPAC) 2.6 min, dopamine (DA) 2.8 min, 5-hydroxyindoleacetic acid (5-HIAA) 3.8 min, homovanillic acid (HVA) 5.3 min and 5-hydroxytryptamine (5-HT) 6.0 min.

2.3 Statistical analysis of the data

All data (except where stated) are presented as the mean ± SEM based on *n* independent observations. Multiple comparisons were made within and between different groups of 6-OHDA lesioned and/or drug treated animals. The significance levels for the extent of cell loss in SNc and VTA and increase or decrease in the number of inflammatory cells were calculated by two-way analysis of variance (ANOVA) and post- tested with *post-hoc* parametric Newman-Keuls Multiple Comparison test using GraphPad Prism v5.00 (GraphPad software, USA) software. The significance of monoamines loss in the striatum within and between different groups of animals was calculated by two-way analysis of variance (ANOVA) and post- tested with *post-hoc* parametric Newman-Keuls Multiple Comparison test using GraphPad Prism v5.00 software (Graphpad software, USA). The concentration of monoamines are presented in (ng monoamine/mg striatal tissue) as mean ± SEM. Differences were considered statistically significant at $p < 0.05$.

All the above mentioned methods and data analysis were carried out by the author, however due to the large number of animals technical assistance was received from Miss Lauren Broom in oral dosing of the experimental animals.

Chapter 3

A time course study into the relationship between microglial activation and dopaminergic neuronal cell loss in the substantia nigra of 6-hydroxydopamine model of Parkinson's disease.

3.1 Introduction

Inflammation is the first line of defence against injury and infection. However, an excessive inflammatory response can be a source of additional injury to host cells (Wyss-Coray and Mucke, 2002). The brain has a relatively low adaptive immune response but is vulnerable to innate immune reactions. Neurons, as a result of a lack of ability to divide and little ability to recover from injury, are extremely vulnerable to auto destructive immune and inflammatory processes (Carson et al., 2006). This might hinder the recovery of neurological function at sites of inflammation or even exacerbate neuronal injury. The hallmark of brain inflammation is the activation of glia, particularly microglia. Studies into the role of microglia in PD pathology are recent and little is known about the cellular events between activated microglia and degenerating neurons in the *in vivo* models of PD. Indeed, convincing evidence of a pathogenic role for activated microglia in PD has already begun to emerge. Microglia comprise approximately 12% of cells in the brain that are derived from myeloid cells in the periphery with the highest concentrations being found in the substantia nigra, basal ganglia and hippocampus (Lawson et al., 1990). Microglia, are the resident innate immune cells in the brain that during homeostasis perform a dynamic surveillance of the CNS environment. Although phenotypically down regulated, recent imaging studies *in vivo* show that microglial cells, even in their so-called resting state, are highly active, with their fine processes continually surveying their local microenvironment (Fetler and Amigorena, 2005).

Conversely under pathological conditions such as neurodegenerative diseases activated microglia contribute to neuronal damage in which the over activation and dysregulation of microglia results in progressive neurotoxic consequences (Kim et al., 2007). The exact cause and cellular events that leads to microglial activation is not yet fully understood however factors including, brain bacterial and viral exposure, pesticides, drug contaminants, and repeated head trauma lead to an active glial response. Once activated, microglia display conspicuous functional plasticity and transform into a macrophage-like phenotype, which involves morphological changes, proliferation, increased expression of cell surface receptors and the production of neurotrophic and neurotoxic factors. Activated microglia, are thought to contribute to neuronal damage, particularly via the release of pro-inflammatory and neurotoxic factors. In PD, nigral microglia are not only highly activated but also highly clustered around dystrophic dopaminergic neurons. A glial response has

been observed in the vicinity of dying dopamine-containing neurons in human post-mortem SN from PD patients (McGeer et al., 1988) and MPTP-intoxicated individuals (Langston et al., 1999). In PD patients higher levels of the pro-inflammatory cytokines such as: IL-1β and interferon-γ (IFN- γ) were detected in the cerebrospinal fluid (CSF) and the striatum (Liu et al., 2003) indicating a state of chronic inflammation in the PD brain.

Inflammation has also been implicated in the neurodegenerative process in animal models of PD created by using neurotoxic compounds such as MPTP, 6-OHDA or rotenone. Many studies indicate that in addition to the impairment of dopamine-containing neurons following MPTP intoxication there is also microglial and astroglial reaction in the damaged regions that is associated and co-localised with increased iNOS expression and nitrotyrosine formation (Wu et al., 2002). Reduction in MPTP-induced toxicity that was observed after genetic inactivation or pharmacological inhibition of iNOS (Dehmer et al., 2000) further supports important role of glia-derived NO in mediating MPTP toxicity. Additionally, inactivation of genes involved in inflammation such as those encoding cyclooxygenase 2 (COX-2) (Feng et al., 2002), NADPH oxidase (Gao, 2003) and both TNF-α receptors (Ferger et al., 2004) protects dopamine-containing neurons against MPTP-induced neurotoxicity, indicating that inflammation is an important component of the MPTP mediated neurodegenerative process. 6-OHDA-induced degeneration of the dopamine-mediated pathway is associated with a microglial response in the nigrostriatal system (Cicchetti et al., 2002). Elevated levels of TNF-α have also been observed in both the striatum and the SNc of 6-OHDA-injected rats (Mogi et al., 1999). Another line of evidence supporting glial involvement in PD is that microglial activation induced by pro-inflammatory lipopolysaccharide (LPS) is capable of initiating the degeneration of dopamine-containing neurons in the SNc of experimental animals and in cell cultures (Iravani et al., 2002; Liu, 2003). Furthermore, LPS and the pesticide rotenone synergistically induce a selective degeneration of dopamine-containing neurons in primary midbrain neuron–glia cultures (Gao et al., 2003), further supporting an important role of inflammation in the pathogenesis of PD. Post-mortem and experimental models of PD all indicate that chronic inflammation is an on going process in the pathogenesis of PD. Particularly, nearly all the proposed aetiologies of PD, including brain bacterial and viral exposure, pesticides, and repeated head trauma, are known to cause brain inflammation suggesting that microglial activation caused by preceding brain inflammation may trigger

the onset of a cascade of events leading to chronic, progressive degeneration of dopaminergic neurons (Liu and Hong 2003; Herrera et al., 2005). Indeed evidence shows that an inflammatory response in the brain is not always deleterious; in acute neuroinflammatory conditions such as stroke or acute brain injury, microglial activation is accompanied by secretion of anti-inflammatory and trophic factors to promote tissue repair and minimise the damage (Wyss-Coray and Mucke, 2002). Following an acute insult the innate immunity primes the microglia to exert phagocytic activity in removal of cell debris and dead neurons to reduce secondary damage (Glezer et al., 2006; Neumann et al., 2006; Simard and Rivest, 2006; Simard et al., 2006; Sriram et al., 2006). Therefore, a crucial factor in determining the fate of activated microglia following an insult is time. To date , limited information is available on the time frame of activation of microglia in PD. It is not known whether inflammation precedes dopaminergic cell loss or is a consequence of it? The mechanism by which activated microglia might specifically target dopaminergic neurons and the cell to cell interaction between activated microglia and degenerating dopaminergic neurons in the *in vivo* models of PD remains a critical missing link .Therefore the aim of this study was to address the following questions: what is the kinetic (time course) of immunophenotypic changes of activated microglia and the subsequent fate of activated microglial cells during the initiation and progression of dopaminergic neuronal loss in the SNc after unilateral injection of 6-hydroxydopamine (6-OHDA) into the medial forebrain bundle (MFB).

To satisfy these aims each group (n=6) of animals was sacrificed on days 1,3,5,7,9,13 and 15 after 6-OHDA lesion induction. The integrity of dopaminergic neurons in the SNc was determined by counting the number TH+ve dopaminergic neurons in the SNc in each group compared to control sham operated animals. The functionality of the nigrostriatal tract was determined by measuring the amount of striatal dopamine in each group utilising HPLC-ECD. In addition, the time course of microglial activation and their morphological characteristics were determined by immunostaining for different glial markers such as: OX42, OX6 and CD68, detailed experimental design may be found in the following section (see section 3.2). Finally the association of microglial activation with dopaminergic neuronal cell death was studied by carrying out different double immunofluorescent stainings for co-localisation of different markers, which is described in detail in the following section (see section 3.2.1.2).

3.2 Experimental design

3.2.1 Dopaminergic neuronal loss in the SNc following 6-OHDA lesion induction in relation to the dynamic of microglial activation

3.2.1.1 Assessment of the nigrostriatal lesion progression after 6-OHDA injection into the MFB

To investigate the relationship between the kinetics of reactive gliosis and the extent of dopaminergic neuronal cell loss in the SNc, male Sprague-Dawley rats were divided into experimental groups (n=6) and a unilateral 6-OHDA lesion was induced stereotaxically into the MFB (*see section 2.1.2.2*). Subsequently animals were sacrificed by CO_2 over dose at day 1 (*24 hours after 6-OHDA injection*), 3, 5, 7,9,13 and 15 after 6-OHDA or sham (4µl 0.1% ascorbic acid) lesion induction and the brains were removed (*see section 2.1.3)*. To assess the integrity of dopaminergic neurons in the SNc and the VTA at different time points following 6-OHDA lesioning immunohistochemistry was performed for Tyrosine hydroxylase (TH) positive dopaminergic neurons (*see section 2.2.1.3*). The number and morphology of TH+ve cells were then determined according to the criteria described in (*see section 2.2.3*). To investigate the effect of 6-OHDA lesioning on the functionality of the nigrostriatal system on days 1, 3, 5, 7,9,13 and 15 after lesioning concentration of dopamine in the striatum was measured using HPLC-ECD (*see section 2.2.4*). To further assess the kinetic of microglial activation at different time points following 6-OHDA or sham lesion induction immunohistochemistry was performed for OX42, OX6 and CD68 expression that is outlined in the following section (*see 3.2.1.2*).

3.2.1.2. Assessment of the kinetics of microglial activation and changes in morphology following 6-OHDA lesion induction

To assess the number of activated microglial cells and their morphology in the SNc on days 1 ,3,5,7,9,13 and 15 after 6-OHDA lesioning, peroxidase immunohistochemistry was performed using the following antibodies, details of staining procedure is outlined in (*see section 2.2.1.4*).

OX6: was used to detect the population of activated microglial cells that express major histocompatibility complex II (MHC II) surface receptor.

OX42 (CD11b): to monitor the activation of a population of brain resident monocytes/microglial cells that express the leukocyte integrin complement receptor type 3 (CR3).

CD68: to detect the activation of a population of macrophages with phagocytic function, that expresses CD68 glycoprotein predominantly on their lysosomal membrane.

Microglial cells expressing OX6, OX42 and CD68 were morphologically assessed and counted in the SNc according to the criteria described in (see *section 2.2.3*). To investigate the interaction between TH+ve dopaminergic neurons and microglial cells at different time points following 6-OHDA or sham double immunofluorescence staining was performed which is outlined in the following section.

3.2.1.3 Assessment of neuron-glia interactions following 6-OHDA/sham lesion induction in the SNc

To be able to explore the effect of neuron-microglia interactions on dopaminergic cell loss the following double immunofluorescence stainings were performed; detailed description of immunofluorescence protocol is described in (see *section 2.2.2)*

TH+ Neuronal-N (NeuN)

To determine the expression of TH in neurons and to be able to associate any observed loss of TH immunoreactivity to neuronal loss rather than the enzyme down-regulation.

TH + OX6

To observe the interaction between TH+ve dopaminergic neurons and MHC II antigen presenting microglial cells at different time points following 6-OHDA lesioning in the SNc.

TH + CD68

To observe the interaction between TH+ve dopaminergic neurons and CD68+ve phagocytic macrophages in the SNc at different time points following 6-OHDA lesioning.

OX6 + Ki67

To assess the proliferative activity of MHC II antigen presenting microglial cells following 6-OHDA/sham lesion induction at different time points.

OX6+iNOS

To determine the expression of iNOS by the activated microglial cells in the SNc following 6-OHDA lesion induction.

Caspase 3 + NeuN

To assess the occurrence of neuronal apoptosis following 6-OHDA or sham lesion induction in the SNc. Therefore co-localisation of NeuN antibody, a neuron-specific nuclear protein with caspase3, a key protease that is activated during the early stages of apoptosis was studied.

Caspase 3 + CD68

To assess the interaction between CD68+ve phagocytic microglia and apoptotic cells in the SNc following 6-OHDA lesion induction.

3.3 Statistical analysis

Manual cell counts for dopaminergic neurons and different populations of glial cells were carried out on serial sections through the entire nigra for each animal .The data from each time point are expressed as the mean $\pm$ SEM based on *n* independent observations (*n*=6). Multiple comparisons were made comparing different time points and the statistical significance between and within groups was assessed using repeated measures two-way ANOVA followed by *post-hoc* Newman-Keuls Multiple Comparison test as described in (*see section 2.3*). A value of $P < 0.05$ was considered statistically significant.

3.4 Results

3.4.1 6-OHDA induces a progressive loss of dopaminergic neurons and striatal Dopamine, with local activation of microglia in the SNc

3.4.1.1 Effect of 6-OHDA on TH+ve dopaminergic neurons in the SNc and dopamine content in the striatum

To detect the effects of 12µg 6-OHDA (in 4µl) injection into the MFB on neuronal survival in the SNc, the number of TH+ve dopaminergic neurons in the SNc were monitored. The results are shown as the mean number of cell counts for TH+ve neurons in the SNc at different time points after toxin injection. As shown in (Fig. 3.1) 6-OHDA injection caused a progressive loss of nigral TH+ve neurons in the SNc. Comparison of the number of nigral TH+ve neurons between lesioned and unlesioned sides showed no significant loss of TH+ve neurons within the first 7 days after 6-OHDA injection. Cell counts on day 7 were lesioned: 73 ± 8.08, unlesioned 93 ± 8.80, $p>0.5$. However, significant loss of TH+ve neurons in the lesioned hemisphere started to manifest from day 9 compared to the unlesioned hemisphere (lesioned: 40 ±5.25, unlesioned: 86±5.25, $p<0.01$). Unilateral dopaminergic neuronal loss progressed up to day 15 after lesion induction comparing lesioned and unlesioned hemispheres. Cell counts on day 15 showed unlesioned: 75±12, lesioned 32.5±1.5, $p<0.01$. Whereas, TH+ve cells were not observed in the VTA (Fig 3.1). In particular, neurons in the lateral portion and ventral tier of the SNc were most vulnerable (Fig 3.2 panel B). At all time points studied the loss TH immunoreactivity was accompanied by a comparable loss of NeuN immunoreactivity, indicating that neuronal cell bodies are lost, rather than a down regulation of TH expression (Fig 3.3). In sham lesioned animals no significant loss of TH+ve dopaminergic neurons were observed compared to the unlesioned side (*data not shown*). Concomitant with the loss TH+ve dopaminergic neurons in the SNc injection of 12µg 6-OHDA (in 4µl) into the MFB was followed by significant depletion of striatal dopamine ipsilateral to the lesioned hemisphere compared to the unlesioned hemisphere (Fig 3.4). Dopamine depletion started to manifest itself from day 9 [lesioned: 4±1.68 (ng/mg), unlesioned: 11.1±0.14 (ng/mg), $p<0.001$] similar to the loss of TH+ve neurons in the SNc. Unilateral loss of dopamine was observed to the day 15 after lesion induction on the side of the lesion compared to the unlesioned hemisphere (lesioned : 4±2.2 , unlesioned: 13.02± 1.1, $p<0.001$) In the sham lesioned animals no significant loss

of dopamine content was observed in the lesioned hemisphere compared to unlesioned hemisphere (*data not shown*). Hence, progressive and partial lesion in the nigrostriatal system started to manifest from day 9 following 12µg 6-OHDA injection into the MFB. The lesion is characterised by dopaminergic neuronal loss in the SNc that is concurrent with progressive depletion of dopamine in the striatum.

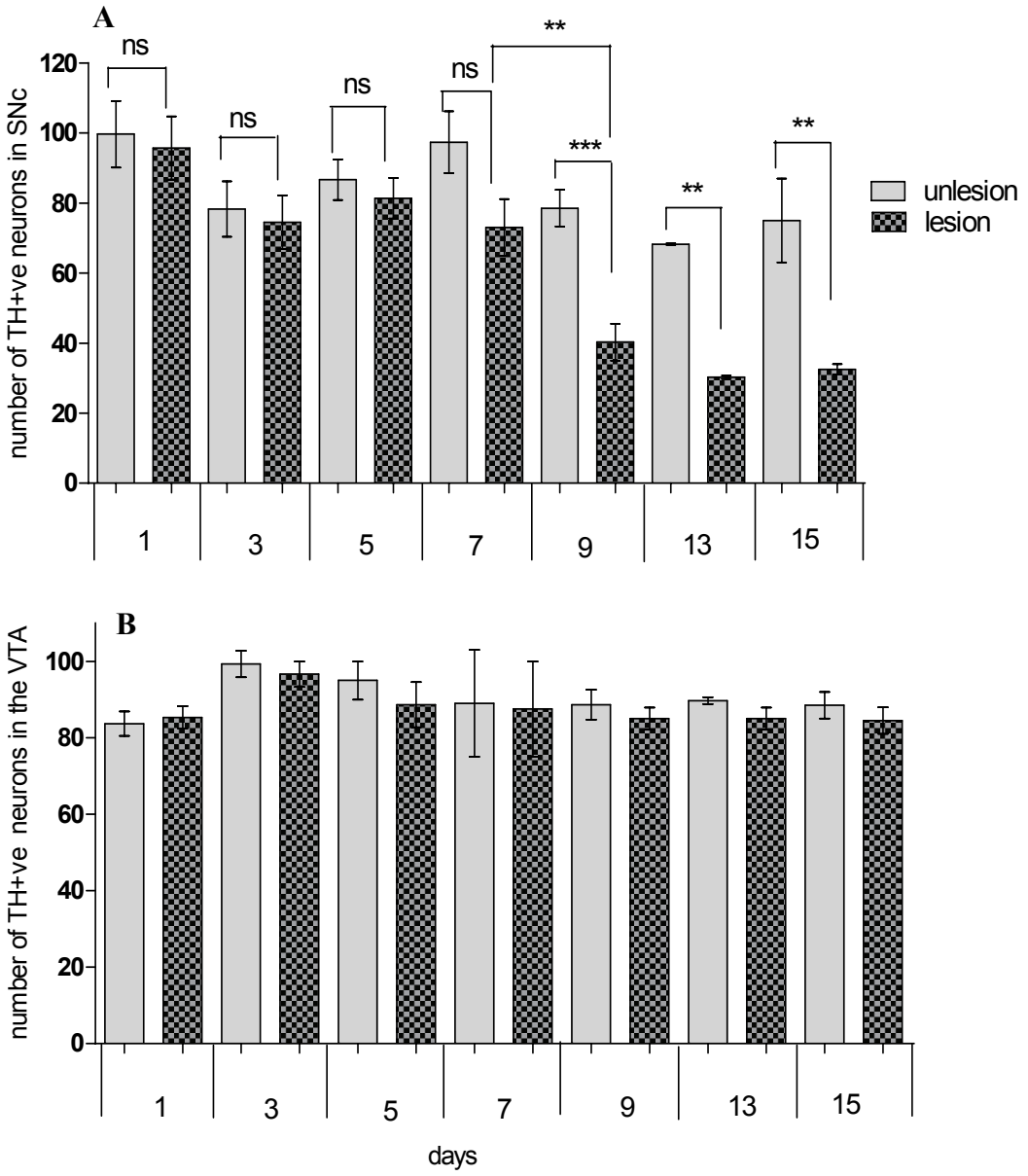

Fig 3.1 Time dependent TH+ve dopaminergic neuronal cell death in the SNc but not VTA following 6-OHDA lesion induction.

Male SD rats were injected with 12 μg 6-OHDA or with ascorbic acid (as sham) into the MFB and maintained under normal conditions. Animals were sacrificed at the indicated time points and coronal brain sections (20 μm thick) were cut through the nigra. Immunostaining was carried out with TH antibody and TH+ve neurons in SNc and in VTA were counted. Results are expressed as mean number of cells $\pm$ SEM. Panel (A) shows the number of TH +ve neurons in SNc at different time points after 6-OHDA injection, significant TH+ve dopaminergic neuronal cell death occurs from day 9 after 6-OHDA lesion induction onwards. Panel (B) shows the number of TH+ve neurons in VTA at different time points after 6-OHDA injection, no significant loss TH+ve dopaminergic neuronal loss is observed. ** $p< 0.01$,*** $p<0.001$ compared to the non lesioned side. ns= non-significant. Number of animals was 6/group per time point.

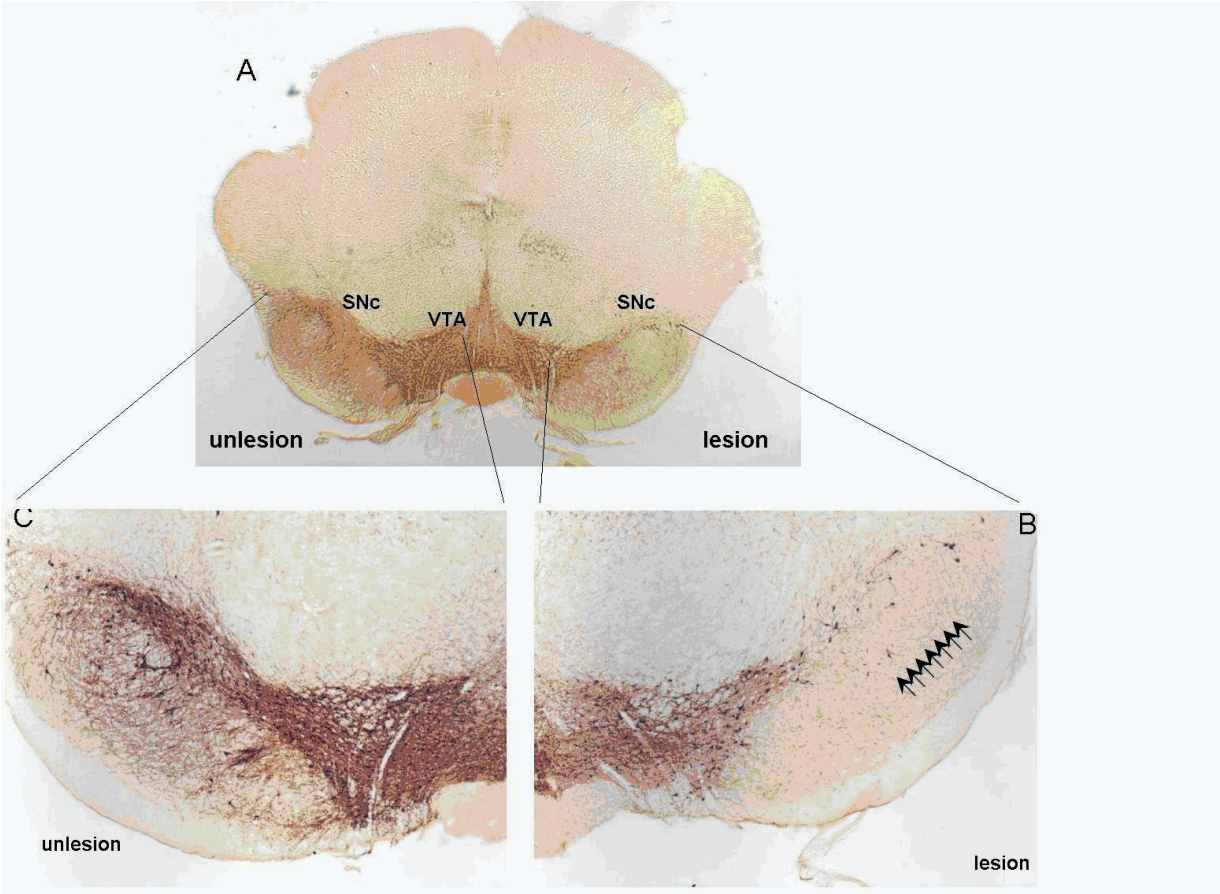

Fig 3.2 Injection of 6-OHDA into the left MFB resulted in a unilateral degeneration of dopaminergic neurons in the SNc. Sequential coronal brain section (20μm) taken at day 9 after lesion induction were immunostained for TH as marker for dopaminergic neurons.

A) Shows selective loss of TH immunoreactivity in the SNc ipsilateral to the side of injection. No apparent loss TH immunoreactivity in the VTA was observed (100x).

B) Unilateral loss of TH+ve dopaminergic neurons in the SNc after 6-OHDA lesion induction ipsilateral to the lesion side on day 9. Neurons in the lateral portion and ventral tier (arrows) of SNc were mostly affected and lost TH immunoreacativity (x200).

C) TH+ve dopaminergic neurons in the SNc contralateral to the 6-OHDA lesion side (x200).

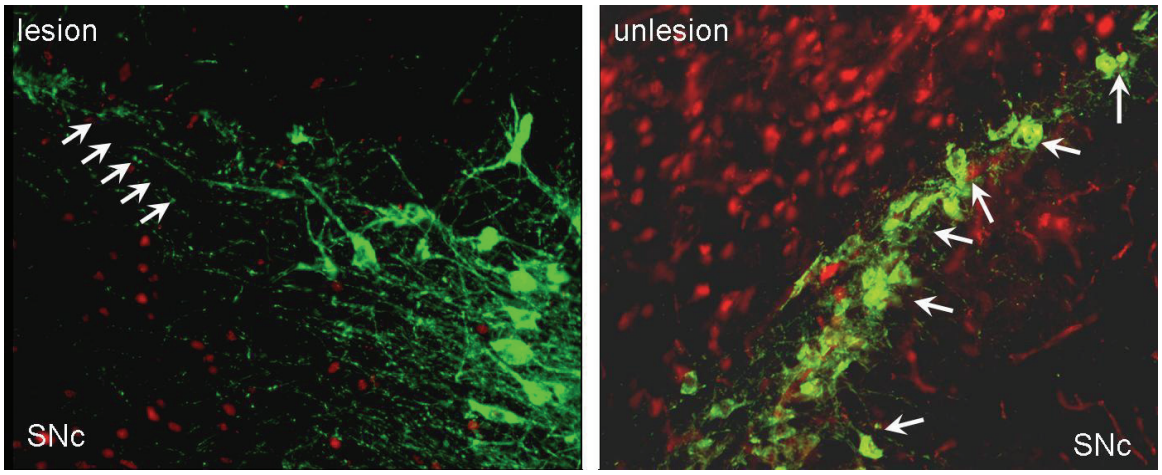

Fig 3.3 Injection of 6-OHDA into the left MFB resulted in a unilateral degeneration of dopaminergic neurons in the SNc ispsilateral to the lesion side on day 9 as indicated by the loss of TH+ve and NeuN+ve cell bodies.

Left panel: Co-localisation of TH+ve (green) and NeuN+ve (red) in dopaminergic neurons ispsilateral to the lesion side. White arrows points to loss of both TH and NeuN immunoreactivity in the SNc after 6-OHDA lesion induction (x100).

Right panel: Co-localisation of TH+ve (green) and NeuN+ve (red) in intact dopaminergic neurons in the SNc contralateral to lesion side. White arrows points to representative dopaminergic neurons that express TH and NeuN in the SNc (x100).

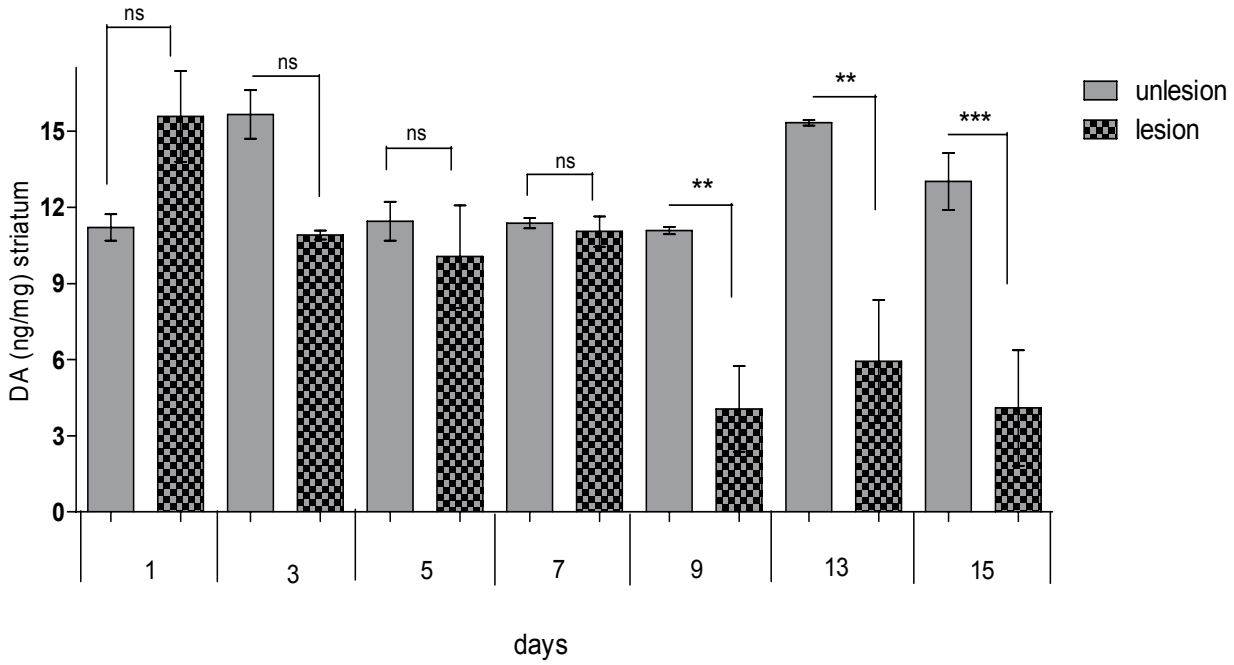

Fig 3.4 Time dependent unilateral depletion of striatal dopamine content (ng/mg) following 6-OHDA lesion induction.

Male SD rats were injected with 12 µg 6-OHDA or with ascorbic acid (as sham) into the MFB and maintained under normal conditions. Animals were sacrificed at the indicated time points and the striata were removed and processed for HPLC-ECD to measure the striatal dopamine content (ng/mg). Results are expressed as mean (ng/mg) $\pm$ SEM. Graph shows time dependent depletion of striatal dopamine content (ng/mg) after 6-OHDA lesion induction in lesion side compared to the unlesion side. Dopamine deletion manifests from day 9 after 6-OHDA lesion induction and progresses to day 15 after lesioning. ** $p< 0.01$, ***<0.001 compared to the non lesioned side. ns= non-significant. Number of animals was 6/group per time point.

3.4.2 The extent of activation of microglia and their localisation in the SNc following 6-OHDA lesioning

3.4.2.1 Effect of 6-OHDA on the number OX42+ve microglial cells in the SNc

Interestingly, staining for microglia using OX42 antibody, indicated that overall the SNc contained more activated OX42+ve cells on the lesioned side at all time points studied compared to the unlesioned side (Fig 3.5A). The number of OX42+ve microglial cells increased as early as day 1 after 6-OHDA lesion induction on the lesioned hemisphere to the compared to unlesioned hemisphere: (lesion: 7.8 ± 0.54 ; unlesion: 1.8 ± 0.79). Significant increase in the number of OX42+ve microglial cells in the lesioned hemisphere compared to the unlesioned side started to manifest on day 9 after lesion induction. The greatest number of OX42+ve cells was observed on day 15 (lesioned: 68±10.48, unlesioned: 11.50±2.21). This was concomitant with a significant loss of TH+ve dopaminergic neurons in the SNc (see *section 3.4.1.1*). In the sham lesioned animals no expression of OX42+ve cells was observed.

3.4.2.2 Effect of 6-OHDA lesioning on the number OX42+ve microglial cells in the VTA

OX-42+ve microglial cells also significantly increased in the VTA as early as 5 days after 6-OHDA lesion induction ipsilateral to the side of lesion compared to contralateral control side: (lesion: 8.70 ± 0.66 ; unlesion: 3.0 ± 0.57, $p<0.05$) (Fig 3.5B). Increase in the number OX-42+ve microglial cells progressed significantly up to day 15 after lesion induction ipsilateral to the lesion side compared to contralateral control side (lesion: 21.0± 1.79 , unlesion: 8.25 ± 1.31, $p<0.001$), however, this was not associated with dopaminergic neuronal cell loss . In the sham operated animals no expression of OX42+ve microglial cell was observed in the VTA. The presence of activated microglia in the SNc and VTA following 6-OHDA lesion induction at early days post lesioning indicates that microglial activation is a rapid response even before any dopaminergic neuronal loss has been observed. Preservation of TH+ve neurons in the VTA in presence activated microglia suggests that the SNc is more vulnerable to a toxic insult.

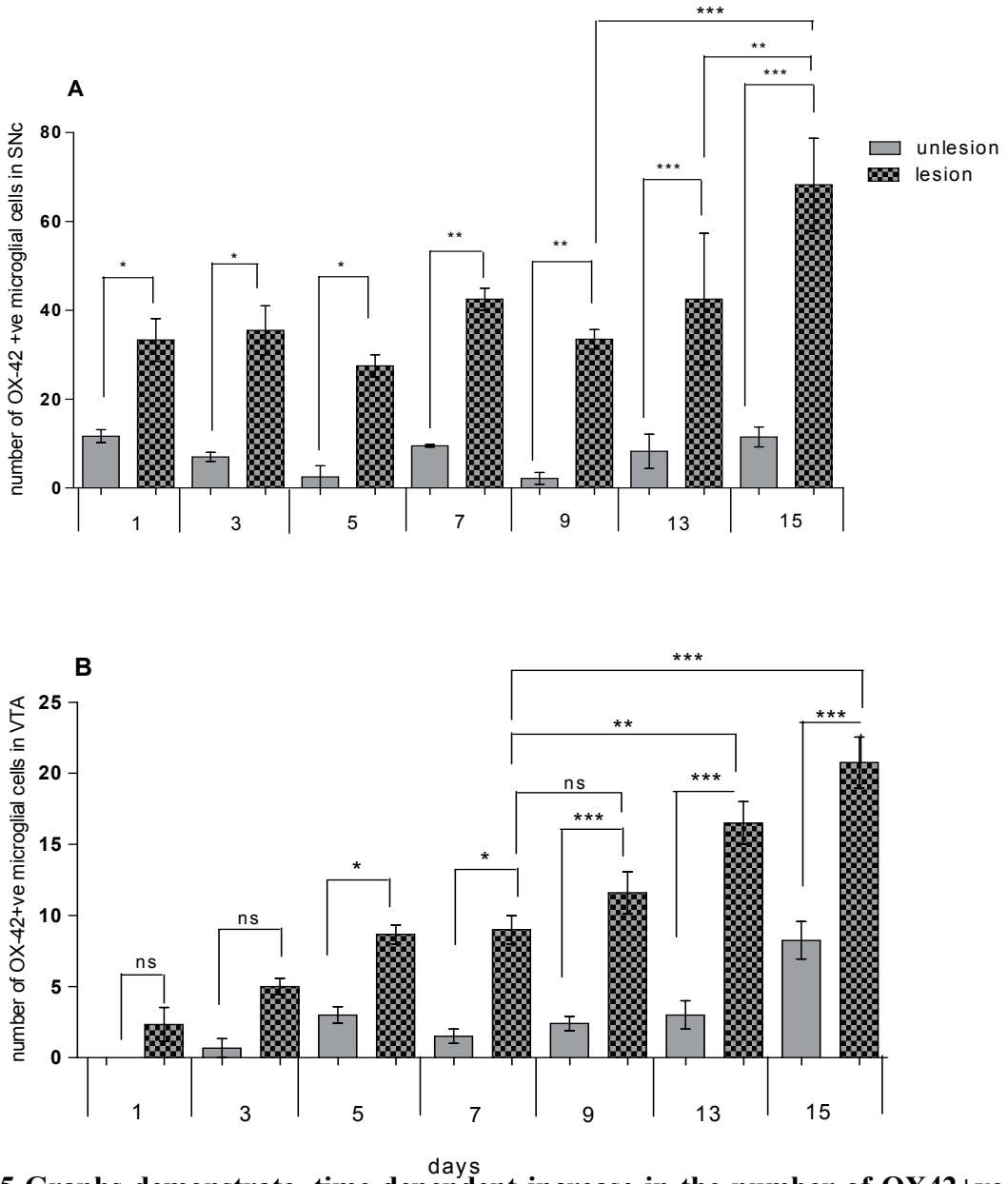

Fig 3.5 Graphs demonstrate, time dependent increase in the number of OX42+ve microglia in the SNc and VTA after 6-OHDA lesion induction.

A) Injection of 6-OHDA into the MFB induced an increase in the number of OX42+ve microglial cells in the SNc in a time dependent manner. Immunostaining was performed with OX42 antibody which is a general microglial marker and stains for CR3 receptor on microglial cells. The number of OX42+ve microglia increased significantly from day 1 after lesion induction and progressed up to day 15 ispsilateral to the side of lesion compared to the contralateral side. Cell counts were performed as described in (*see Chapter 2, section 2.2.3*). **B)** Injection of 6-OHDA into the MFB induced increase in the number of OX42+ve microglial cells in the VTA in time dependent manner. The number of OX42+ve microglia increased significantly from day 3 after lesion induction and progressed up to day 15 ispsilateral to the side of lesion compared to the contralateral side. Results are expressed as mean number of cells $\pm$ SEM, n=6. * $p<0.5$, ** $p<0.01$, *** $p< 0.001$, *ns*= not significant. . Number of animals was 6/group per time point.

3.4.2.3 Effect of 6-OHDA lesioning on the number of OX6+ve microglial cells in the SNc

OX6 +ve cells are the antigen presenting population of microglia. OX6+ve microglia were first observed in the medial part and ventral tier of the SNc at day 1 after 6-OHDA lesion induction when no apparent changes were observed in the number of TH+ve cells in the lesioned hemisphere compared to the non lesioned hemisphere. The number of OX6+ve cells gradually increased and a focal accumulation of these cells in both the lateral and medial portions of the SNc ipsilateral to the lesion was observed at day 7 (cell counts: lesion: 19.80± 2.85, unlesion: 1.25 ± 0.35, $p<0.01$) (Fig 3.6A). The number of OX6+ve cells increased significantly at day 9 following 6-OHDA lesion induction (lesioned: 46±2.25, unlesioned: 0.75± 0.4, $p<0.001$), with the greatest number of OX6+ve cells at day 13 (lesioned: 54±0.5, unlesioned: 0 ±0, $p<0.001$) in the lesioned side compared to the unlesioned side. At which time point a significant loss of TH+ve neurons in the SNc was also evident (Fig.3.1A). OX-6+ve microglia decreased significantly by day 15 after lesion induction compared to the lesion side on day 13 (Day 15 post-lesion: 35.5±11.8, Day 13 post-lesion: 54±0.5, $p<0.5$). In sham lesioned animals no expression of OX6+ve microglial cells was observed (*data not shown*). Thus, OX6+ve microglial cell were focally expressed in the SNc following 6-OHDA lesion induction before any dopaminergic neuronal loss was observed in the SNc.

3.4.2.4 Effect of 6-OHDA lesioning on the number of OX-6+ve microglial cells in the VTA

Activation and increases in the mean number of OX-6+ve microglial cells in VTA showed a similar dynamic pattern as observed in the SNc (*see section 3.4.2.1*). The overall mean number of OX6+ve cells in the VTA was less than the SNc. By day 9 OX6+ve microglial cells reached their greatest number on the 6-OHDA lesion side compared to unlesion side (lesion: 18.2 ± 2.37, unlesion 0.80 ±0.20 $p<0.001$). The number of OX6+ve cells decreased significantly by day 15 (lesion: 11.0 ± 2.2, unlesion: 2.2 ± 0.4) (Fig 3.6B). However activation of antigen presenting microglial cells in the VTA was not associated with TH+ve dopaminergic neuronal loss in this area.

3.4.2.5 iNOS expression by OX6+ve microglia cells in the SNc following 6-OHDA lesion induction

Double immunofluorescence staining demonstrated that a sub-population of OX6+ve microglial cells express iNOS in the SNc in the lesioned side of the brain from day 3 after 6-OHDA lesion induction (Fig 3.7, top and bottom panels). iNOS expression was observed up to day 9 after the lesion; on day 13 and 15 iNOS expression was not detected. This observation indicated that OX6+ve activated microglial could have the potential to up-regulate NO production.

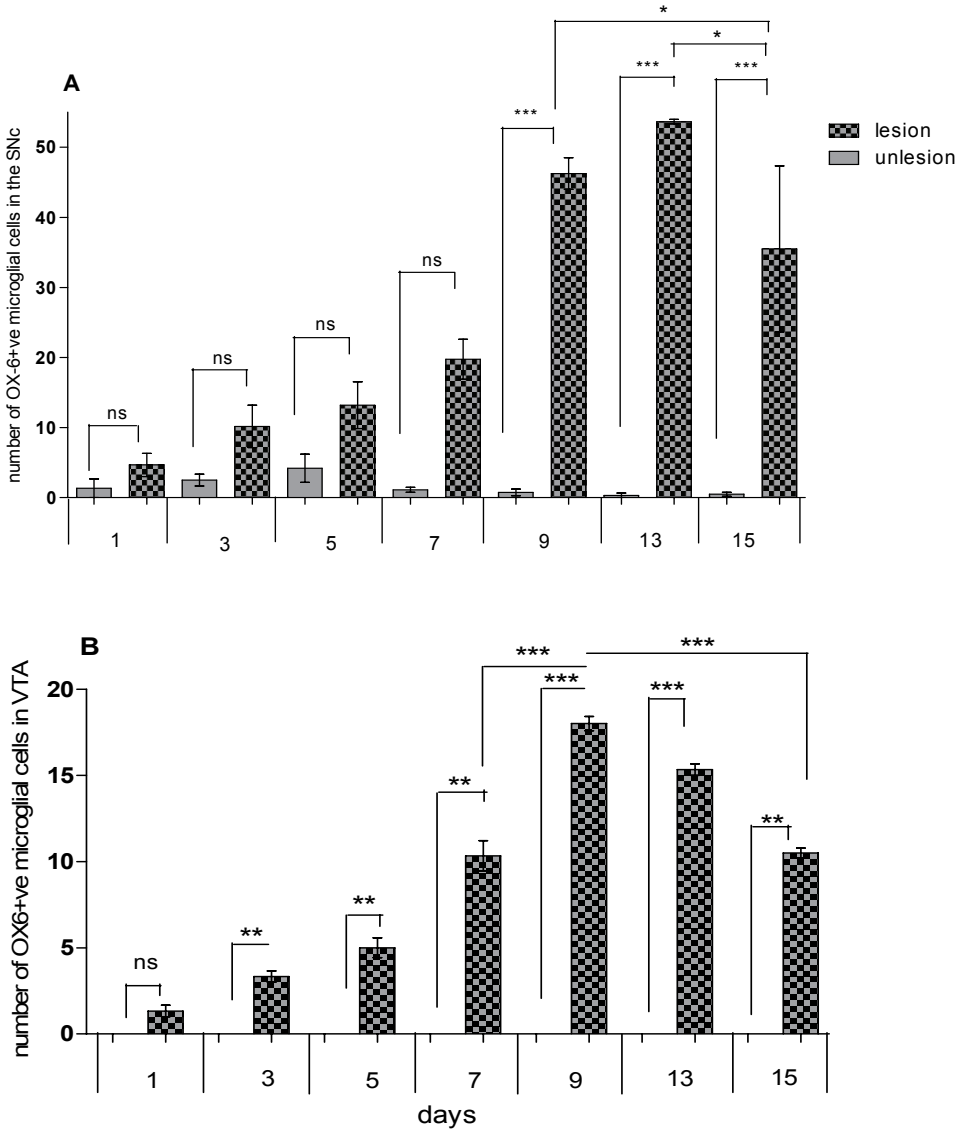

Fig 3.6 Unilateral time dependent increase in the number of OX6+ve microglial cells in the SNc and VTA following 6-OHDA lesion induction.

Injection of 6-OHDA induced accumulation of OX6+ve cells in the SNc and VTA in a time dependent manner. A) Time-course quantification of OX6+ve microglia in the SNc. Immunostaining was carried out with OX6 antibody as markers for MHC II expressing activated microglia. The number of OX6+ve cells reached its full manifestation on day 13 after 6-OHDA lesion induction in the lesioned hemisphere compared to the unlesioned hemisphere. OX6+ve microglia significantly decreased in number by day 15 after 6-OHDA lesion induction. Positive cells in the SNc were counted as described in (*see Chapter 2, section 2.2.3*). B) Time-course quantification of OX6+ve in the VTA. The number of OX6+ve cells reached its full manifestation on day 9 after 6-OHDA lesion induction in the lesioned hemisphere compared to the unlesioned hemisphere. OX6+ve significantly decreased in number by day 15 after 6-OHDA lesion induction. Results are expressed as mean number of cells $\pm$ SEM. * $p<0.5$, ** $p<0.01$, *** $p< 0.001$, *ns*= not significant. . Number of animals was 6/group per time point.

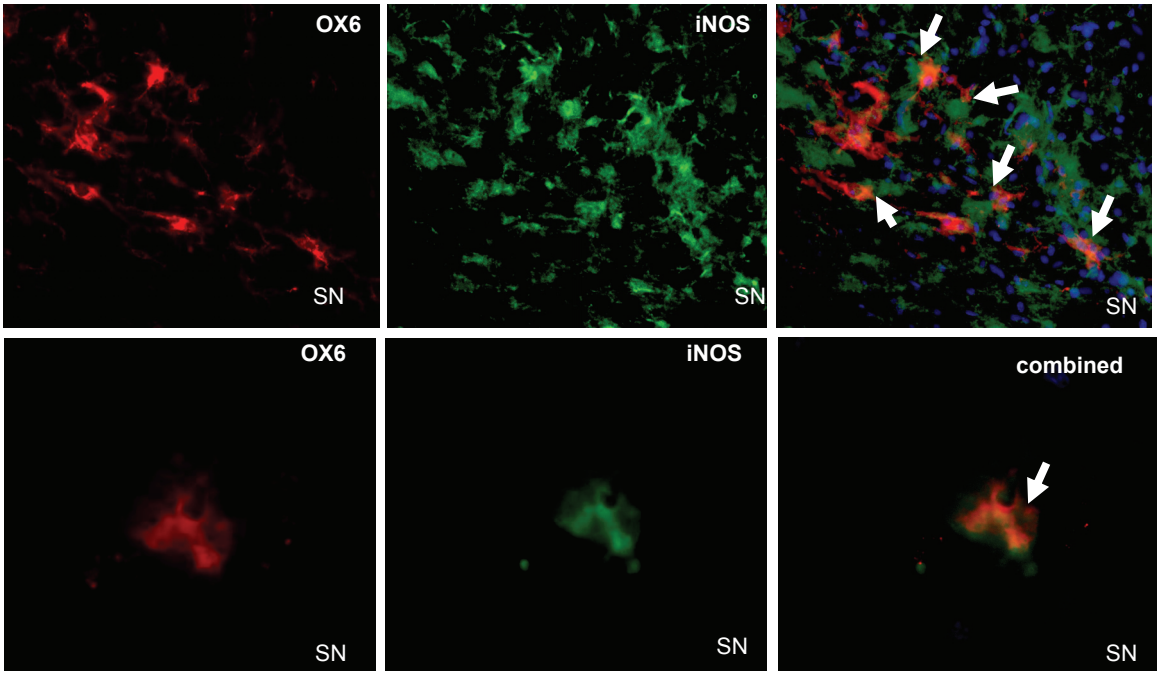

Fig 3.7 Unilateral 6-OHDA lesion induction into the MFB resulted in activation of OX6+ve microglial cells (red) in the SNc ispsilateral to the 6-OHDA lesioned hemisphere compared to the contralateral side. The photomicrograph shows that a sub population of OX6+ve microglia express iNOS (green) on day 3 after lesion induction.

Top panel: Shows double immunofluorescence staining for OX6+ve (red) and iNOS (green). The combined image shows co-localisation of a number of OX6+ve microglia with iNOS (white arrows) in the SNc on day 3 after 6-OHDA lesion induction in the lesioned hemisphere compared to the unlesioned hemisphere where no OX6+ve microglia where present (x200).

Bottom panel: Shows a higher magnification of a morphologically active OX6+ve microglia (red) that is fully co-localised with iNOS (green). Microglial cells once activated have the potential to express iNOS 3 days after 6-OHDA challenge ispsilateral to the lesioned hemisphere (x400).

3.4.2.6 Effect of 6-OHDA on the number of CD68+ve microglial cells in the SNc

CD68+ve phagocytic microglia were present ipsilateral to the side of the lesion 3 days after 6-OHDA induction compared to contralateral control side. Whereas in sham operated animals no CD68+ve cells were detectable. Their localisation was very similar if not identical to that of OX6+ve cells. CD68+ve cells were mainly confined to the medial portion of SNc until day 7. Thereafter, the number of CD68 expressing cells progressively increased up to day 15 and a large number of CD68+ve cells in the medial and lateral portion of SNc ipsilateral to the lesion was observed, no immunoreactivity was detected on the unlesion side (lesioned: 40.17±3.76) (Fig 3.8). Presence of CD68+ve microglia/macrophages indicated that phagocytic activity accompanied neuronal degeneration. CD68+ve macrophages were not detected in the VTA after 6-OHDA lesion induction.

Taken together, glial cell counts revealed that a unilateral reactive gliosis occurred in the SNc following 6-OHDA lesion induction. The focal activation of microglia/macrophages took place before any dopaminergic neuronal loss was observed. The number of activated microglia increased in a time-dependent manner indicating that their activation was associated with degeneration of dopaminergic neurons.

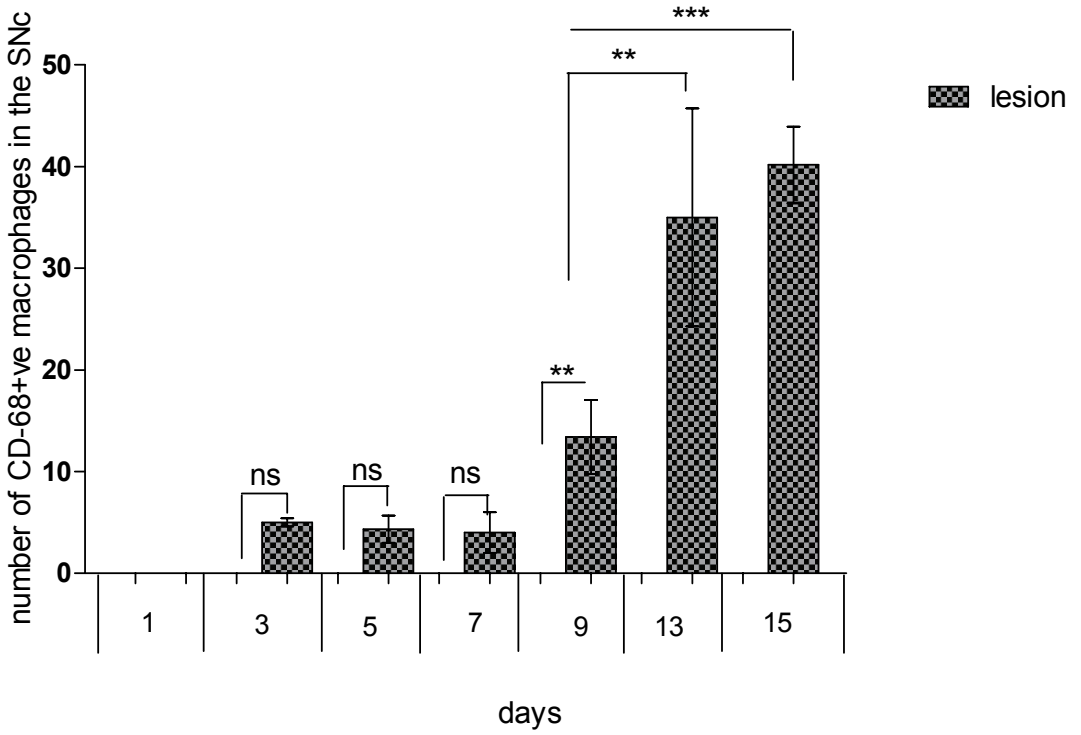

Fig 3.8 Graph showing a time dependent increase in the number of CD68+ve macrophages in the SNc after 6-OHDA lesion induction.

Injection of 6-OHDA induced accumulation of CD68+ve cells in the SNc in a time dependent manner. Immunostaining was carried out with CD68 antibody as markers for phagocytic macrophages. The number of CD68+ve cells reached its full manifestation on day 15 after 6-OHDA lesion induction in the lesioned hemisphere compared to the unlesioned hemisphere. CD68+ve cells significantly increased in number on day 9 after 6-OHDA lesion induction that progressed to day 15. Positive cells in the SNc were counted as described in (*see Chapter 2, section 2.2.3*). Results are expressed as mean number of cells $\pm$ SEM. ** $p<0.01$, *** $p< 0.001$, *ns*= not significant. . Number of animals was 6/group per time point.

3.4.3 Morphological and phenotypic characteristics of the activated microglia following 6-OHDA lesion induction

Morphological changes of the activated microglia following 6-OHDA lesion induction were studied in DAB-immunolabelled sections from the SNc.

3.4.3.1 Morphological and phenotypic characteristics of OX6+ve and OX42+ve microglia in the SNc

Following unilateral 6-OHDA administration into the MFB, OX6 and OX42+ve microglia not only increased in number but also appeared morphologically active. OX6 and OX42+ve cells were densely stained with an activated morphology characterised by an enlarged somas and thickened processes. OX6+ve microglia were focally accumulated in both the lateral and medial portions of the SNc ipsilateral to the lesion side from day 7 (Fig 3.9 panels A and B). The observed morphology of these cells was characteristic of activated microglial cells that are capable of producing pro-inflammatory and cytotoxic factors.

3.4.3.2 Morphological and phenotypic characteristics of CD68+ve cells in the SNc

CD68+ve microglia had a predominant amoeboid macrophage-like appearance. An accumulation of granular staining in the lysosomal membranes was observed in the cytoplasm of CD 68+ve cells indicating phagocytic activity. The observed morphology of CD68+ve cell was indicative of their role as active phagocytic macrophages.

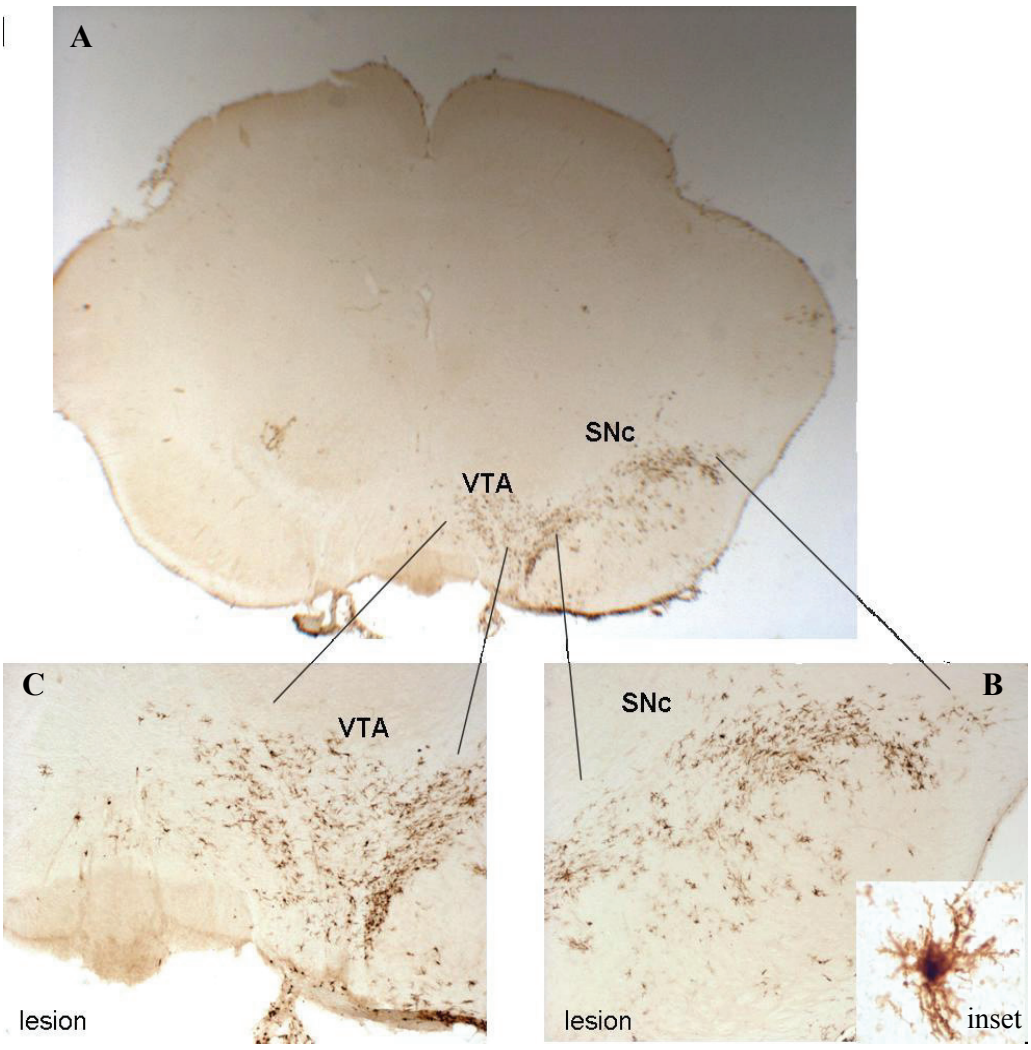

Fig 3.9 Injection of 6-OHDA into the left MFB resulted in a unilateral and focal accumulation of OX6+ve activated microglia in the SNc and the VTA. Sequential coronal brain section (20μm) taken at day 9 after lesion induction were immunostained for OX6 as marker for MHC II presenting activated microglia.

A) Shows focal accumulation of OX6+ve microglia in the SNc and VTA in the 6-OHDA lesioned hemisphere with no OX6+ve cells in the unlesioned hemisphere. In the lesioned hemisphere OX6+ve microglia are localised in both medial and lateral portions of the SNc (x10). **B)** Shows higher magnification of the SNc in the lesioned hemisphere. Activated OX6+ve microglia are densely stained with OX6 antibody and predominantly accumulated in the medial and lateral portions of the SNc and few microglial cells are observed in the ventral tier 9 days after 6-OHDA lesion induction (x100). **Inset**: Inserted box illustrates typical ramified morphology OX6+ve cells (x400). **C)** Shows 10x higher magnification of the VTA in the lesioned hemisphere. Activated microglia are densely stained with OX6 antibody (x100).

3.4.4 The dynamics of MHC class II expressing OX6+ve microglial cell proliferation in the SNc

The number of OX6+ve microglial cells increased locally in the SNc up to 13 days after 6-OHDA lesion induction (*see section 3.4.2*). To elucidate mechanism of proliferation double immunofluorescence staining was performed for cell nucleus mitotic protein marker, Ki67 and OX6 antibody. Microglial cells demonstrated active mitotic and proliferative activity on days 3, 5, 7 and 9 after 6-OHDA lesion induction. This was characterised by the co-localisation of the nuclear mitotic protein, Ki67 with OX-6+ve microglial cells on lesioned hemisphere of the brain (Fig 3.10 bottom panel). This observation further indicated that the glial response to 6-OHDA was a rapid response starting on day 3 after the toxin injection. A peak in proliferation was observed on day 7 when a large proportion of activated microglial cells were positive for OX6 and Ki67. Thus, a sub population of activated microglial cells that are OX6+ve do proliferate locally from 3 days after 6-OHDA lesion induction. To further assess the contribution of activated microglia to dopaminergic neuronal cell loss, neuron-glia interactions were studied as outline below (see *section 3.4.5*).

3.4.5 Close interaction between activated microglia and degenerating dopaminergic neurons in the SNc following 6-OHDA lesion induction

3.4.5.1 Interaction between TH+ve dopaminergic and OX6+ve microglia cells in the SNc following 6-OHDA lesion induction

The double- immunofluorescence staining of TH with OX6 revealed that in the lesioned hemisphere 3 and 5 days after 6-OHDA lesion induction considerable number of OX6 expressing cells were in the vicinity of the morphologically intact TH+ve neurones that had an intact nucleus and clear cytoplasm with axonal processes in the SNc (Fig 3.10 ,middle panel). However, on day 9 post 6-OHDA lesion, a large number of OX6 expressing cells were observed in close contact with the cell debris of TH+ve dopaminergic neurons as well as to the morphologically shrunken neurons. As shown in the photomicrograph in (Fig 3.10, top panel) TH immunoreactivity is preserved, however the morphology of the cells presents a damage neuron lacking dendritic processes. This observation suggests that activated microglial cells surround healthy looking neurons before they appear apoptotic.

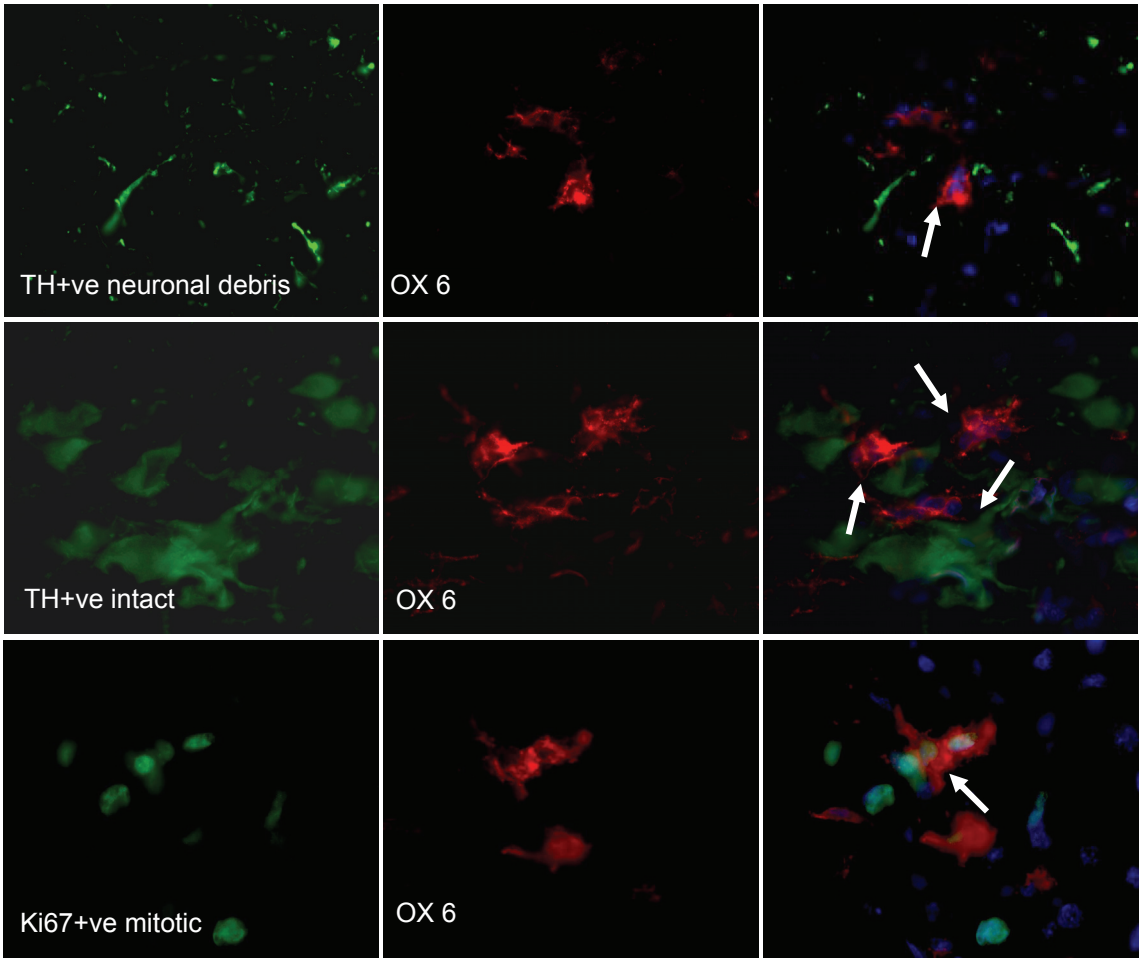

Fig 3.10 Locally proliferating activated OX6+ve microglia are attached to morphologically intact TH+ve dopaminergic neurons as well as neuronal debris on days 7 and 9 after 6-OHDA lesion induction respectively.

Top and middle panels show double immunofluorescence images of OX6 (red) and TH (green) on days 9 and 7 respectively, post 6-OHDA lesion in the lesioned hemisphere. Note that OX6+ve microglia are specifically adhered to dendrites of degenerating neurons (top panel) or are in close proximity to dendritic processes of structurally intact TH+ve neurons (middle panel, white arrows) (x400). Bottom panel shows double immunofluorescence photomicrograph of OX6 (red) and Ki 67 (green). Merge image indicates that some of OX6+ve cells are proliferating in the SNc ipsilateral to the lesion side on day 7 post lesion (x400).

3.4.5.2 Interaction between TH+ve dopaminergic and CD68+ve macrophages in the SNc following 6-OHDA lesion induction

CD68+ve cells were observed in close contact with morphologically normal appearing TH+ve dopaminergic neurons at day 3 following 6-OHDA lesion induction. However, CD68+ve cells were also observed to be in close proximity or adhered to the degenerating TH+ve cell bodies, axons and cell debris by day 9 to 15 post 6-OHDA lesion induction even engulfing the dying TH+ve dopaminergic neurons as shown in the representative photomicrograph shown in (Fig 3.11, top panel) Moreover, staining with apoptotic marker caspase3, which is the executioner enzyme of apoptosis, showed that CD68+ve cells were in close contact to caspase3 expressing cells from day 3 after 6-OHDA lesion induction (Fig 3.11, bottom panel). This evidence suggests that microglial phagocytic activity may be initiated prior to the TH+ve neuronal demise suggesting that phagocytosis of apoptotic cells may take place at very early stage of neuronal loss in SNc.

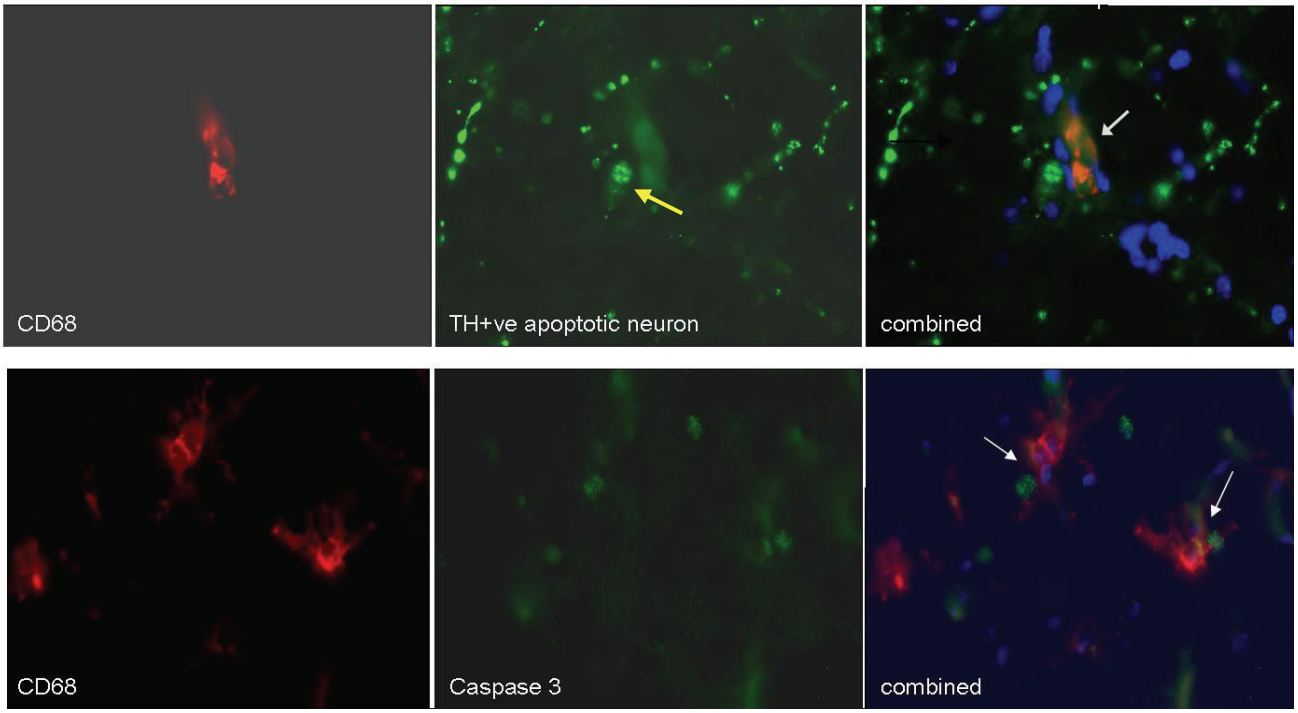

Fig 3.11 Phagocytosis of apoptotic dopaminergic neurons by CD68+ve macrophages in the SNc after 6-OHDA lesion induction. Double immunofluorescence image of CD68+ve macrophages (red) and TH (green) or Caspase3 (green) on days 9 and 3 respectively post 6-OHDA lesion

Top panel: Composite image shows engulfment of dopaminergic neurons by CD68+ve microglia. Note that the TH+ve dopaminergic neuron appears apoptotic (yellow arrow, middle image, top panel) (x400).

Lower panel: Composite image shows Caspase 3+ve apoptotic cells are in close contact with CD68+ve phagocytic microglia (white arrows) (x400).

3.5 Discussion

In the current study the kinetic (time course) of immunophenotypic changes of activated microglia and the subsequent fate of activated microglial cells during the initiation process of dopaminergic neuronal loss in the SNc after unilateral injection of 6-hydroxydopamine (6-OHDA) into the medial forebrain bundle (MFB) was determined. To be able to explore this aim, four aspects of the role of microglia were investigated. (1) The time course of microglial activation following 6-OHDA lesion induction, (2) morphological changes and immunophenotypic characteristics of activated microglial cells, (3) their interaction with dopaminergic neurons in the SN, and (4) the subsequent impact on neuronal loss.

3.5.1 Microglial activation preceded dopaminergic neuronal loss in the SNc and dopamine depletion in the striatum

Unilateral injection of 12µg 6- OHDA into the MFB led to a progressive partial lesion in the SNc that was evident by loss of >53% of TH+ve dopaminergic neurons. Significant neuronal loss started to manifest 9 days after 6-OHDA injection. It is well documented (Pickel et al., 1977; Wassef et al, 1981) that loss of TH-immunoreactivity in the SNc is indicative of degeneration of nigral dopaminergic neurones. However to rule out the possibility that the observed decrease in the number of TH+ve dopaminergic neurons was due to the down-regulation of the enzyme, TH, or a transient atrophy of cells following 6-OHDA, double staining for TH and NeuN was performed. The staining clearly demonstrated that 6-OHDA led to loss of both TH and NeuN immunoreactivity. This observation indicates neuronal cell bodies are lost in the lesioned hemisphere compared to the unlesioned hemisphere rather than down regulation of the enzyme per se or a transient atrophy of neurons. Studies have shown that another approach to ascertain that TH loss is indeed an indication of dopaminergic neuronal loss is to pre-label dopaminergic neurons with the retrograde neuronal tracer, Flurogold (FG). In this setting equal loss of TH immunoreactive neurons as well as FG immunoreactive neurons is indicative of neuronal loss rather than TH down regulation (Iravani et al., 2002). 6-OHDA injection into MFB led to concomitant partial depletion of dopamine in the striatum that also started to manifest on day 9 in the lesioned hemisphere compared to unlesioned hemisphere. Dopamine was

depleted by >62% 9 days post-lesion induction that progressed time dependently. This is in accord with the characteristics of the partial lesion model of PD (*see section 2.1.1.2*) Following 6-OHDA injection to the MFB the innervation of the striatum is gradually lost which consequently leads to the retrograde loss of dopaminergic cell bodies in the SNc, as demonstrated the groups previous studies (Datla et al., 2001; 2003; 2004; Zbarsky et al., 2005). Prior to any significant dopaminergic neuronal loss however, activated microglia (OX42+ve) appeared in the SNc ipsilateral to the lesion side as early as day 1–3 post 6-OHDA lesioning. Some activated microglia also adhered to the axons or cell bodies of morphologically intact dopaminergic neurons, although no significant decrease in the number of nigral TH+ve neurons was detected by 7 days after 6-OHDA. In addition OX6+ve microglia increased in number significantly in SNc from day 7 following 6-OHDA lesion induction and their full manifestation was observed on day 9 when dopaminergic neuronal loss was statistically significant. This finding indicates that activated microglia participate in the neurodegenerative process from a very early stage when there has been no apparent loss of dopaminergic neurons. Moreover significant number of activated microglia specifically adhered to axons, dendrites, and cell bodies of degenerating DA neurons throughout all time points of the study. This heavy adhesion of activated microglia to the various parts of DA neurons was followed by a significant decrease in the number of DA neuronal cell bodies indicating that activated microglia are directly associated with the cell loss at later time points.

To monitor the presence of different sub-populations of microglia/macrophages in the SNc and to distinguish between these sub-populations we utilise different antibodies, each targeted against a specific protein present on the surface of microglial cells. Microglia which, constitute the immune defence system of the CNS, share many properties with peripheral monocytes and macrophages, but retain unique morphological and molecular characteristics (Perry and Gordon, 1991; Sedgwick et al., 1991). For example, microglia can bind several lectins, including *Griffonia simplicifolia* agglutinin I B4, *Ricinus communis* agglutinin, and Mistletoe agglutinin as well as express complement receptor 3 (CR3), even in the resting state. Following CNS injury, microglial activation occurs within a few hours and activated microglia are characterised by an up regulation or *de novo* expression of several marker proteins, e.g. major histocompatibility complex (MHC) class I and II (Streit and Kreutzberg, 1988; Kaur and Ling, 1992; Kreutzberg, 1996). In this study, the expression of OX6 on a sub-population of activated microglia indicated, that microglial cells underwent immunological changes acquiring the ability to process and present an

antigen. In addition, expression of OX42 by activated microglia demonstrated the presence of leukocyte integrin complement receptor type 3 (CR3) on these microglia. Furthermore, a sub-population of activated rat microglia expressed an antigen in the lysosomal membranes that was recognized by the monoclonal antibody CD68 (ED1). The amount of CD68 expression in a single cell can be correlated to phagocytic activity of the respective cell type (Damoiseaux et al., 1994). In fact, it has been demonstrated that ED1+ve microglia are phagocytic in several types of neurodegenerative conditions, such as traumatic brain injuries (Rinaman et al., 1991; Frank and Wolburg, 1996). We found that OX6+ve microglia, which recognize rat MHC II, appeared at the 6-OHDA lesioned hemisphere of the brain in the very early stages of neurodegeneration. These cells appeared earlier than those labelled with CD68. Moreover, throughout all time points of our study it was found that the number of OX6+ve microglia was slightly greater than that of CD68+ve microglia, suggesting that the vast proportion of the OX6 +ve cells acquired a phagocytic phenotype. In fact, it has been demonstrated that a significant proportion of OX6+ve microglial cells are ED1+ve at the site of neurodegeneration after MFB transection (Cho et al., 2003; 2007). This finding implies that the transformation of microglia to antigen presenting cells expressing MHC II antigens precedes microglial phagocytosis.

Taken together, we have demonstrated that dopaminergic neuronal loss is preceded by microglial activation. Similarly, in MFB axotomised brain, it has also been demonstrated that the activation of microglia preceded neuronal loss and that activation of microglia was followed by a significant loss of neuronal fibres and nigral dopaminergic neurons (Cho et al., 2006). These findings strongly suggest that activated microglia play an important role in the progress of neurodegeneration.

3.5.2 Morphological and phenotypic characteristics of activated microglia correlates with their function

The highly ramified form of resting microglia observed the SNc of normal brains supports their immune surveillance function (Fetler and Amigorena, 2005). Pathological conditions lead to their activation and morphological changes. An increase in somal size, as well as the presence of thickened and shortened processes are observed in early stages of microglial activation, before their final transformation into amoeboid microglia with phagocytic activity (Streit and Kreutzberg, 1988; Mor et al., 1999; Stence et al., 2001).

These results demonstrated the presence of numerous activated microglia ipsilateral to the lesioned side of the SNc with both ramified and amoeboid like morphology. Both forms of activated microglia showed strong OX6 immunoreactivity and attachment to the TH+ve neurons, axons and dendrites which was followed by significant loss of dopaminergic neurons. This suggests that activated microglia with ramified and/or amoeboid morphology participated in neuronal cell death. Active participation and neurotoxic role of activated microglia was further supported by our data demonstrating the expression of inducible nitric oxide synthase (iNOS) by OX6 +ve microglial cells following 6-OHDA lesion induction. There is a strong body of evidence demonstrating that once microglial cells are active they produce neurotoxic factors such as reactive oxygen and nitrogen species, and nitric oxide (NO) from inducible nitric oxide synthase (iNOS) (Iravani et al., 2002). In addition, other pro-inflammatory cytokine are secreted including: tumour necrosis factor (TNF)-alpha, interleukin (IL)-1beta, and IL-6 which have also detected in cerebrospinal fluid (CSF) from patients with sporadic PD, and in animal models, such as MPTP and 6-OHDA- induced PD (Nagatsu T. et al., 2005). Since activated microglia express iNOS and nitrated protein aggregates are present in Lewy bodies (Good *et al.*, 1998; Hunot et al., 1996; Hunot et al., 2003) it has been suggested that part of the inflammatory response may be mediated by nitric oxide (NO) / peroxynitrite ($ONOO^-$). Under conditions of oxidative stress, NO reacts with superoxide anions ($^-O_2$) and produces peroxynitrite, (ONOO-). Peroxynitrite formation leads to production of highly toxic hydroxyl radicals (Beckman et al., 1990), neurotoxicity and cell death (Allan S.M and Rothwell N.J, 2001).

As demonstrated in the findings, injection of 6-OHDA produced apparent apoptosis of DA neurones. DAPI staining of the nuclei of DA neurons in the SNc at day 7 post lesioning showed multiple, rounded chromatin clumps similar to that observed during apoptosis (Tatton and Kirsh, 1997). However, distinguishing the apoptosis/necrosis dichotomy in the CNS is a difficult task, and many variations of apoptotic processes are possible (Roy and Salovsky, 2000). We observed DNA clumps in the nuclei of shrunken, apparently dead neurons in the lesioned side of SNc. Since a continuum of neuronal death occurs post 6-OHDA lesioning, it is reasonable to assume that a few of the dopaminergic neurons degenerate soon after toxin inoculation without having been phagocytosed by microglia. However, at days 3-5 post-lesion, the prevalence of phagocytic microglia in the SNc attached to DA neurons which were apparently morphologically intact with normal

nuclear chromatin distribution and were expressing tyrosine hydroxylase led to the conclusion that a majority of degenerating neurons were targeted for phagocytosis at very early apoptotic stage. In fact, we observed that the majority of Caspase 3+ve cells were in close contact with CD68+ve phagocytic microglia in SNc ipsilateral to the lesion as early as 5- 7 days post lesion. This observation is in accordance with recent reports demonstrating that apoptotic neurons could be phagocytosed by activated microglia in early neuronal apoptosis (Savil and Fadok, 2000, Cho et al, 2003, Sugama et al, 2003). Thus, early microglial phagocytosis of apoptotic neurons might preclude the possibility of their recovery. We observed that CD68+ve activated microglia appeared at day 3 post lesion induction, and the analysis of TH +ve neuron numbers at this time point indicated no significant difference between the SNc ipsilateral and contralateral to the lesion suggesting that microglial phagocytic activity preceded neuronal death. Moreover, observed engulfment of apoptotic neurons clearly demonstrate that the role of microglia in apoptotic neurodegeneration in the CNS is similar to that of macrophages in cellular apoptosis outside the brain. A major implication of these observations would be that early phagocytosis of apoptotic neurons might prevent neuronal survival by phagocytosing potentially recoverable neurons in neurodegenerative disorders such as PD. This is consistent with reports by Chao, et al (2006) where the ramified form of activated microglia showed strong expression of CD68 at the lesioned site where the MFB had been cut. Thus, adhesion of activated microglia to damaged DA neurons represents a process linked with the phagocytic clearance of those neurons.

3.5.3 Dynamics of activated microglia in the SNc

Activated microglia can also be characterized by their proliferative and migratory properties. Accumulation of activated microglia around regions of the brain undergoing degeneration may be attributed to migration of microglia to the affected sites (Akiyama et al., 1994; Heppner et al., 1998; Schiefer et al., 1999; Marella and Chabry, 2004; Rodriguez et al., 2007), as well as their local proliferation (Graeber et al., 1988; Amat et al., 1996; Schwab et al., 2001). We have observed a time-dependant unilateral relocation of activated microglia from the ventral tier to the medial and lateral portions of the SNc following 6-OHDA lesion induction suggesting that at least some of the activated microglia accumulated in the SNc might be derived as a result of migration. Similar to this

observation, movement of amoeboid microglia along dendrites of neurons has been identified in brainstem slices using infrared-gradient contrast microscopy and time-lapse video recording (Schiefer et al., 1999). In parallel , using nuclear mitotic protein marker Ki67, our data revealed numerous locally proliferating OX6+ve microglial cells in the SNc at day 3 to 7 post 6-OHDA lesioning. Thus, accumulation of activated microglia in the SNc ipsilateral to the lesion with 6-OHDA can be explained by both local proliferation and migration.

The data presented in this chapter provides evidence of the potentially damaging effects of microglial activation on the adjacent dopaminergic neurons. However, it is worth noting that in contrast to the harmful effects of microglial activation these cells have the capacity to secrete factors that can promote neuronal survival or regeneration. Transforming growth factor-beta (TGF-β),brain derive neurotrophic factor (BDNF,) and nerve growth factor (NGF), to name just a few examples, promote neuronal survival and are secreted by microglial cells .Microglial cells monitor the physiological integrity of their microenvironment to promote tissue repair and maintain the homeostasis of the brain parenchyma (Kreutzberg et al., 1996). Therefore, as presented in the results, the increase in microglia/macrophages cell numbers prior to neuronal loss could be an attempt to rescue neurons from the toxic effects of 6-OHDA by secreting anti-inflammatory cytokines and other protective factors. Future studies are necessary to examine the time course of production of pro *v* anti inflammatory factors by the microglial cells in the SNc following 6-OHDA challenge.

Conclusions

The present study clearly demonstrates that microglial activation preceded dopaminergic neuronal cell death in the SNc after 6-OHDA lesion induction. Moreover glial response was associated with dopaminergic cell loss in the SNc. CD68+ve and OX6+ve microglia specifically adhered to degenerating neurons throughout the whole neurodegenerative process, from an early stage to phagocytosing dying neurons. This process is probably in response to expression of apoptotic signals, such as phosphatidylserine (PS) and the expression of their receptors, including PS receptor (PSR), on the phagocyte membrane which initiate phagocytosis (Huynh, 2002; Ravichandran, 2003), or in response to contents released from dying neurons. Our results indicate that neurons undergoing neuronal cell death may be phagocytosed by activated microglia

concomitantly at various stages. The presence of microglia in neurodegeneration may not be limited to phagocytosis of dead neurons, but in fact microglia may actively contribute to neurodegenerative processes.

Chapter 4

The role of Matrix metalloproteinases and CD200 receptor in the neurodegenerative process in the substantia nigra of 6-hydroxydopamine model of Parkinson's disease.

4.1 Introduction

As concluded in chapter 3, microglial activation and phagocytosis of early stage apoptotic neurons preceded dopaminergic neuronal cell death in the SNc following 6-OHDA MFB lesions. Moreover, a sub-population of the activated microglia showed activation of iNOS, suggesting active microglia are involved in dopaminergic neuronal death in the SNc. However, very little is known about the mechanisms responsible for the activation of microglial cells following an insult to the CNS, particularly in PD pathology. Although research has focused on identifying triggers that lead to glial activation, it is becoming increasingly clear that interaction with other cells plays a significant role in modulating activation. In addition the changes that occur in the homeostasis of the brain leading to microglial activation and the cell to cell interactions regulating this process are not yet fully understood. The following sections will provide an outline of some mechanisms responsible for keeping microglia quiescent during homeostasis and events that leads to their activation following an insult to the CNS.

4.1.1 Maintaining microglia quiescence

The pro-inflammatory and damaging nature of microglial activation only applies to pathologic conditions. In homeostasis, the immune responsiveness of the microglia is tightly regulated in the CNS keeping them quiescent. The regulatory processes that are involved in keeping microglia in a resting state can be classified into those that rely on secreted factors and those that depend on the intimate communication of proteins on opposing cells such as neurons and astrocytes. Microglia receive cues from other cell types namely, neurons that enable them to remain quiescent in the absence of an immune stimulus. For example, neuronal electrical activity inhibits microglial activation, as demonstrated in neuron-glia co-cultures where blockade of neuronal electrical activity by tetrodotoxin induces microglial activity that was characterised by MHC II expression (Neumann et al., 2001). Other factors including, neuropeptides such as alpha-melanocyte stimulating hormone (α-MSH) and vasoactive intestinal peptide (VIP) inhibit proinflammatory cytokine and NO production by lipopolysaccharide-activated cultured microglia, while the neurotransmitter Gamma-aminobutyric acid (GABA) has

immunosuppressive effects on T and B-cell function (Reinke et al., 2006). Evidence suggests that neurons are not the only cell type that are capable of keeping microglia quiescent, interestingly astrocytes are able to suppress microglial activation by releasing soluble and insoluble factors such as TGFβ or anti-inflammatory IL-10 (Vincent, et al, 1997; Aloisi et al., 2001; Min et al., 2006).

In addition to various secreted factors from neurons and other cell types that regulate microglial activity a recently recognized local modulator of the inflammatory response, hence microglial activation, is the interaction between CD200 glycoprotein and its receptor, CD200R. CD200 is a type 1 membrane glycoprotein (Jenmalm et al., 2006) that is expressed on several cell types, including neurons, and exerts its effect by binding to the CD200R receptor triggering intracellular signalling cascades (Wright et al., 2003). CD200R is highly expressed on macrophages, neutrophils, monocytes, mast cells, and lymphocytes, and expression has also been localized on microglia (Barclay et al., 2002). The suppressive effect that neurons exert on microglia can explain how microglial activation is controlled during homeostasis through an interaction of the glycoprotein CD200 ligand on their surface with CD200R on microglia (Hoek et al., 2000). Under pathological conditions when the neuron-glia interactions are disturbed, the suppressive effect of neurons on microglia is inevitably compromised leading to activation and proliferation of microglia. Data from CD200 knockout mice, best demonstrate the CD200 interactions (Hoek et al., 2000). In these mice there are increased numbers of macrophages in the spleen (especially in young animals) and a defect occurs in the organization of the mesenteric lymph nodes. In addition, in such knockout mice, microglia were spontaneously activated. The activated microglia showed an activated phenotype with less ramified morphology. In addition, microglia in CD200 knockout mice showed the presence of clusters of differentiation on their surface including: CD11b and CD45 that are indicative of their activation. Moreover the expression of inducible nitric oxide synthase (iNOS) by microglia and macrophages in CD200 knockouts was significantly increased. These data indicates that CD200 expressed by resident CNS cells, including neurons, might silence or down regulate innate immune function of microglia. During an inflammatory reaction pro-inflammatory signals also play a major role in modulating microglial activation. Several factors, including LPS, IFN- γ, CD40L, chemokines, neurotransmitters and gangliosides, and several proteases such as thrombin, tissue plasminogen activator (tPA), matrix

metalloproteinase- 3 (MMP-3) and MMP-9 are found to be involved in microglial activation. Some of them are produced by neurons and others are from pathogens, immune cells or microglia (abd- el-Basset and Fedoroff, 1995; Tsirka, 1997; Suzumura et al., 1998; Tan et al., 1999; Aloisi et al., 1999). Other factors that are suggested to activate microglia include neuromelanin that is released from degenerating dopaminergic neurons (Wilms et al., 2003). Among these various molecules that lead to microglial activation, matrix metalloproteinases (MMPs) are currently being investigated as one of the signals responsible for activating microglial cells in neurodegenerative disorders like PD. Therefore the following sections will provide an overview of the importance and significance of MMPs in PD pathology.

4.2 Matrix metalloproteinases (MMPs) and Parkinson's disease

4.2.1 Overview

There are 23 MMPs, belonging to the matrixin subfamily of zinc metalloproteinases and are able to cleave extracellular matrix (ECM) as well as non-matrix proteins (Nagase et al., 2006). ECM is a complex macromolecular structure that occupies the extracellular space. This matrix is composed of a variety of polysaccharides and proteins and it is strongly associated with the cell surface. In the brain, the matrix is mainly developed as the basal lamina surrounding blood vessels. Local cells normally produce the extracellular matrix components and therefore the composition of the matrix is dependent on the cellular environment. MMPs are released from variety of cell types in the brain including astrocytes, neurons and microglia as well as leukocytes and macrophages and are involved in tissue remodelling such as wound healing and angiogenesis (Puistola et al., 1989; Turpeenniemi-Hujanen et al., 1992, Salo et al., 1994; Chambers & Matrisian, 1997) during development and homeostasis. All MMPs are secreted as pro-enzymes and require extracellular activation. In homeostasis, to avoid unwanted proteolysis MMP activation is tightly regulated at various levels, including regulation at the level of transcription by endogenous tissue inhibitors of metalloproteinases (TIMPs) (Rosenberg et al., 2002). The MMPs can be classified into five sub-groups, depending on their substrate specificity. These groups

include: the collagenases (MMP-1, MMP-8, MMP13, and MMP-14), which degrade the interstitial collagens, types I, II and III; the gelatatinases (MMP-2 and MMP-9), which degrade type IV collagen in basement membrane; the stromelysins (MMP-3, MMP-10, and MMP-11), which degrade non-collagen matrix proteins, such as fibronectin, laminin, aggregan, etc.; and a miscellaneous group, which include matrilysin (MMP-7) and MMP-12 (elastase).

Accumulating evidence indicates that MMPs are involved in the pathogenesis of various central nervous system disorders including bacterial meningitis (Paul et al., 1998), stroke (Clark et al., 1997), multiple sclerosis (Maeda and Sobel, 1996), and neurodegenerative diseases such as Alzheimer's disease (AD) (Asahina et al., 2001) and PD (Lorenzl et al., 2002).

4.2.2 Evidence of involvement of MMPs in PD pathology

The role MMPs in PD pathology is supported by their involvement in inflammation and neuronal death, two key components of the disease. MMP-3 (stromlysine1) is the main member of MMPs family that has been studied in the context of PD. Stromelysin-1, known also as MMP-3, degrades various collagens, elastin, fibronectin, laminin but also activates latent forms of other matrix metalloproteinases such as MMP-9 (Ramos-De Simone et al., 1999). First studies that supported a pathogenic role for MMPs came from post-mortem studies from PD patients. A study by Lorenzl et al, (2002) investigated the levels of MMP-2, MMP-9, MMP-1, tissue inhibitor of metalloproteinase 1 (TIMP-1) and TIMP-2 in post-mortem brain tissue from PD patients. This study revealed reduced levels of MMP-2, increased levels of TIMP-1 in the SN suggesting that alterations in MMPs/TIMPs may contribute to disease pathogenesis. The pathogenic role of MMPs in PD pathology is also supported by *in vivo* and *in vitro* studies. In the 6-OHDA model of PD a study by Sung and colleagues (2005) demonstrated that increased levels of MMP-3 are found in the SNc three weeks post lesion induction. Using immunohistochemistry, significant MMP-3 expression was seen arising from the SNc area into the nigrostriatal dopaminergic pathways after stereotactically injecting the toxin at three points in the right striatum. Cell culture studies by (Kim et al., 2005) have also shown that MMP-3 may be a microglia-activating signalling molecule released from neurons in early apoptosis. MMP-3 was

released from apoptotic cells incubated in serum deprived media (SDM) as early as 2 hours after serum deprivation and before cellular morphological change could be detected. Furthermore, cell culture studies have shown that MMP-3 appears to be induced in neurotoxin-stressed DA neurons and activated inside the cell before release. Whether this induction and activation of MMP-3 is specific to degenerating DA neurons or dying cells in general, still needs to be investigated (Kim et al., 2005). More recently Kim et al., (2007) have demonstrated a dose dependent release of MMP-3 in primary mesencephalic cultures treated with 1-methyl-4-phenylpyridinium (MPP+), a toxic metabolite of MPTP. Expression of MMP-3 occurred specifically in DA neurons. The release of MMP-3 resulted in microglial activation and superoxide generation as well as enhanced dopamine cell death.

Animal studies have demonstrated that activated microglia are highly visible in the striatum and the SN at 2 and 5 days after MPTP injection in wild type mice but were minimal in MMP-3 knockout mice, as was dopaminergic neuron degeneration (Kim et al., 2007). In mesencephalic culture, MMP-3 activated microglia, have been shown to produce NADPH oxidase (NADPHO) derived superoxide, which causes dopaminergic neuronal death. It was found that MMP-3 caused dopamine cell death in wild type mice; however in cells from NADPHO knockout mice death was attenuated. This suggests, NADPHO may mediate MMP-3 induced superoxide production and dopamine cell death (Wu et al., 2003; Gao et al., 2003). Furthermore, recent studies have suggested that MMPs play a role in cell death via apoptotic mechanisms, including caspase-dependent cascades (Mannello et al., 2005). Cell culture studies have also shown that MMP-3 activity stimulates the production of inflammatory cytokines by microglia, such as TNF-α. Administration of a specific MMP-3 inhibitor NNGH (N-isobutyl-N-(4-methoxyphenylsulfonyl) –glycylhydroxamic acid), resulted in inhibition of TNF-α release from activated microglia (Kim et al., 2005). Studies into the role of MMPs, in particular MMP-3, in PD pathology provide convincing evidence that MMP-3 may play a role in PD pathogenesis that is at least partially mediated by activation of inflammatory pathways.

In addition to the role of MMP-3 in PD pathology, MMP-9 is also being investigated. Elevated levels of MMP-9 were observed in the striatum and the SNc of MPTP treated mice (Lorenzl et al., 2004). Using immunohistochemistry and Western blot analysis, Lorenzl, et al (2004) demonstrated that the activity of MMP-9 was up regulated 3 hours after MPTP injection in the striatum and after 24 h in the substantia

nigra, activity remained elevated for up to 7 days. Furthermore, the significance of MMP-9 in PD pathology was determined when pharmacological inhibition of the enzyme led to significant dopaminergic neuroprotection following MPTP administration in mice (Lorenzl et al., 2004).

Thus, in *vivo* and *in vitro* studies suggest that MMPs, in particular MMP-3, play a crucial role in microglial activation in different models of PD leading to dopaminergic neuronal loss. Therefore we hypothesise that MMP-3 is a microglial activating signal released from dopaminergic neurons early in the disease process, and contributes to dopaminergic neuron degeneration. However, in the *in vivo* models of PD limited information is available on the time course of MMP-3 or MMP-9 expressions in relation to microglial activation and /or quiescence. To test our hypothesis we addressed the following aims:

1) Are MMPs released from neurons as signalling molecules and how are these signal(s) modulate microglial activation in the 6-OHDA model of PD.

2) What are the kinetics of MMP-3 and MMP-9 activation during the progression of dopaminergic cell loss in the SNc after 6-OHDA lesioning?

3) Does the expression of MMP-3 and MMP-9 correlate with the degree of microglial activation?

4) What are the neuron-microglia interactions with focus on the role of CD200R in dopaminergic cell death in the SNc after 6-OHDA lesion induction.

To satisfy these aims the classical 6-OHDA model of PD will be produced by unilateral injection of 6-OHDA into the MFB. The animals will be sacrificed on days 1(*24 hours after lesion induction*) ,3,5,7,9,13 and 15 after lesioning. MMP-3 and MMP-9 expression following 6-OHDA lesion induction in relation to dopaminergic neuronal cell death and microglial activation will be studied. Immunohistochemistry will be performed for active forms of MMP-3 and MMP-9 in addition to CD200R+ve cells. To assess the integrity of dopaminergic neurons in the SNc after 6-OHDA lesion induction, TH immunohistochemistry will be performed for dopaminergic neurons and cell counts performed for TH+ve neurons in the SNc. In addition, to assess the time course of microglia/macrophage activation in relation to MMP-3 and MMP-9 expression immunohistochemistry will be performed for OX6 and CD68 expressing microglia/macrophages in the SNc following 6-OHDA lesion induction. The complete

description of the experimental design may be found in the following section (*see section 4.2*). New batches of animals were used in this chapter's experiments compared to Chapter 3 experiments therefore certain key parameters were assessed again such as the expression of TH, OX6 and CD68.

4.2 Experimental design

4.2.1 Relationship between MMP-3 and MMP-9 expression and dopaminergic neuronal cell death in the SNc following 6-OHDA lesioning

4.2.1.1 Assessment of the kinetics of MMP-3 and MMP-9 expressions in the SNc after 6-OHDA lesion induction

To investigate the relationship between the expression of MMP3 and MMP-9 and the progression of dopaminergic neuronal cell loss in the SNc, male Sprague-Dawley rats were divided into experimental groups (n=6). Unilateral 6-OHDA lesion was induced stereotaxically into the MFB (*see section 2.1.2.2*). Subsequently animals were sacrificed by CO_2 over dose at day 1, 3, 5, 7,9,13 and 15 following 6-OHDA or sham (4µl 0.1% ascorbic acid) lesion induction and the brains were removed (*see section 2.1.3)*.

To assess the expression and morphology of MMP3+ve and MMP-9+ve cells at different time points following 6-OHDA or sham lesion induction peroxidase immunohistochemistry with Nickel enhancer was performed for the active form of MMP-3 and MMP-9 using the following antibodies, details of staining procedure is outlined in (*see Chapter 2, section 2.2.1.4*):

MMP-3: A polyclonal antibody was used against the active form of MMP-3 enzyme mapping at C-terminus of the enzyme of human origin. This antibody recognises the 45 and 28 kDa active forms of the enzyme.

MMP-9: A polyclonal antibody was used against the active form of MMP-9, also known as 92-kDa gelatinase/type IV collagenase, in mammals mapping near the C-terminus of MMP-9 of human origin.

To determine the cell types that express MMP-3 and MMP-9 in the SNc after 6-OHDA lesion induction the following double immunofluorescence stainings were performed. Details of antibody combinations are listed below. The full description of staining procedure is outlined in (see *Chapter section 2.2.2).*

MMP-3+NeuN

To investigate the expression of MMP-3 by neurons in the SNc following 6-OHDA or sham lesion induction.

MMP-3+ Glial fibrillary acidic protein (GFAP)

To investigate the expression of MMP-3 by astrocytes that express GFAP in the SNc following 6-OHDA or sham lesion induction. GFAP is a type III intermediate filaments protein that is expressed by astrocytes.

MMP-9 + NeuN

To investigate the expression of MMP-9 by neurons in the SNc following 6-OHDA or shame lesion induction.

MMP-9 and GFAP

To investigate the expression of MMP-9 by astrocytes in the SNc following 6-OHDA or sham lesion induction.

4.2.1.2 Assessment of the dopaminergic neuronal cell death progression induced by 6-OHDA injected into the MFB

Integrity of dopaminergic neurons in the SNc at different time points following 6-OHDA lesioning was assessed by using immunohistochemistry for Tyrosine hydroxylase (TH) positive dopaminergic neurons (*see section 2.2.1.3*). The number and morphology of TH+ve cells were then determined according to the criteria described in (*see section 2.2.3*).

4.2.2 Relationship between microglial activation and MMP-3 and MMP-9 expression in the SNc following 6-OHDA lesion induction

4.2.2.1 Assessment of the kinetics of microglial activation in the SNc after 6-OHDA lesion induction

As described in chapter 3, to asses the kinetics and morphology of microglial activation at different time points following 6-OHDA or sham lesion induction peroxidase immunohistochemistry was performed for OX6 and CD68 expression. Description of the antibodies used is listed below, details of staining procedure is outlined in (*see section 2.2.1.4*):

OX6: was used to detect the population of activated microglial cells that express major histocompatibility complex II (MHC II) antigens.

CD68**:** was used to detect the activation of a population of macrophages with phagocytic function that expresses CD68 glycoprotein on their lysosomal membrane.

4.2.2.2 Assessment of MMP-microglial interaction in the SNc after 6-OHDA lesion induction

To explore the potential interaction between the MMP-3 expressing cells and microglial cells in the SNc following 6-OHDA lesioning, the following double immunofluorescence stainings were performed; detailed description of immunofluorescence protocol is described in (see *section 2.2.2)*

MMP-3 +OX6

To observe the interaction and spatial association between MMP-3 expressing cells with MHC II antigen presenting microglial cells following 6-OHDA lesion induction at different time points.

MMP-3+ CD68

To study the interaction and spatial association between MMP-3 expressing cells and CD68+ve phagocytic macrophages at different time points following 6-OHDA lesioning in the SNc.

4.2.3 Role of CD200R expression during the progression of 6-OHDA lesion in the SNc

4.2.3.1. Assessment of the kinetics of CD200R expressing cells in the SNc after 6-OHDA lesion induction

The kinetics and morphology of CD200R+ve cells at different time points following 6-OHDA or sham lesion induction was assessed utilising peroxidase immunohistochemistry for CD200R expression. (*See chapter 2, section 2.2.1.4*).

CD200R**:** A mouse monoclonal antibody was used to detect cells that express CD200 receptor (R), a membrane glycoprotein, mainly found on the surface of myeloid cells, including microglia. Studies suggest that CD200-CD200R interaction may be involved in the control of myeloid cellular function.

4.2.3.2 Assessment of the interaction between neurons and CD200R expressing cells in the SNc following 6-OHDA lesion induction

To study the interactions between TH+ve and/or MMP-3+ve neurons with CD200R+ve cells in the SNc after 6-OHDA lesioning the following double immunofluorescence stainings were performed. Description of the antibodies used are listed below, details of staining procedures are outlined in (*see section 2.2.1.4*).

TH + CD200R

To investigate the spatial association and interaction of CD200R, a cell surface glycoprotein that is involved in regulation of microglial activation, in relation to TH+ve dopaminergic neurons in the SNc following 6-OHDA or sham lesioning.

MMP-3+ CD200R

To investigate the expression and spatial association of CD200R, a cell surface glycoprotein that is involved in regulation of microglial activation, with MMP-3 expressing cells in the SNc following 6-OHDA or sham lesioning.

4.3 Results

4.3.1 Involvement of neuronal MMP-3 and MMP-9 activities in the progression of dopaminergic neuronal cell death in the SNc following 6-OHDA lesioning

4.3.1.1. Extent and localisation of MMP-3 expressing cells following 6-OHDA or sham lesioning in the SNc

MMP-3+ve cells were observed in the SNc on both the lesioned and the unlesioned hemispheres from day 1 after 6-OHDA lesion induction. However, the number of cells expressing MMP-3 increased significantly in the lesioned hemisphere compared to the unlesioned hemisphere on day 7 after 6-OHDA lesion induction (lesioned: 25.0 ± 5; unlesioned: 10± 0.5 , $p < 0.5$) (Fig 4.1,Graph). This was concomitant with presence of significantly high numbers of OX6+ve microglia in the 6-OHDA lesioned hemisphere of the SNc. The number of MMP-3 +ve cells gradually increased up to day 13 after lesioning (lesioned: 30.5 ± 0.5; unlesioned: 6.0 ± 0.1, $p< 0.01$). However number of MMP-3+ve cells decreased significantly on day 15 after lesion induction compared to the lesioned side on day 13 (Day 15 post-lesion: 18.0±8.0, Day 13 post-lesion: 30.5 ± 0.5, $p<0.5$) (Fig 4.1, Graph). In sham operated animals the number of MPP-3+ve cells increased on the lesioned side compared to the unlesioned side, however, it did not reach significance level (*data not shown*), suggesting that the physical experimental procedures had no significant impact on MMP-3 expression only the presence of 6-OHDA. It is noteworthy that constitutive expression of MMP-3 was detected in control sections: levels of MMP-3 did not differ on either side of the SNc (*data not shown*).

MMP-3 expressing cells were not specifically confined to any particular area in the SNc, however the distribution was particularly dense in the dorsal tier of the SNc and clusters of cells were observed in lateral aspect of the ventral tier of the SNpc and pars reticulate (Fig 4.1, Photomicrograph).

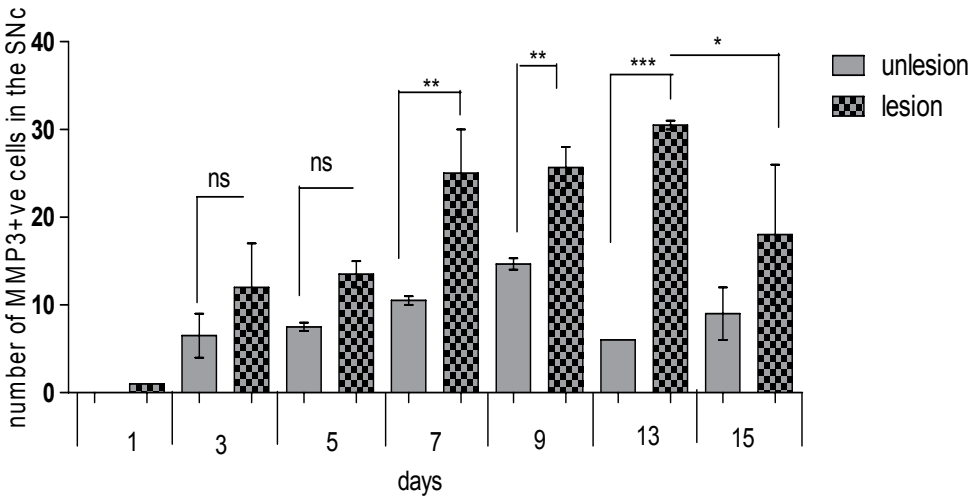

Fig 4.1 *Graph*-Time dependent increase in the number of MMP-3+ve cells in the SNc after 6-OHDA lesion induction.

Injection of 6-OHDA in to the MFB induced a significant increase in the number of MMP-3+ve cells in a time dependent manner. Graph demonstrates time-course quantification of MMP-3+ve cells in the SNc. Immunostaining was carried out with MMP-3 antibody as marker for active form of this enzyme. The number of MMP-3+ve cells significantly increased on day 7 after 6-OHDA lesion induction in the lesioned hemisphere compared to the unlesioned hemisphere. On day 13 after lesion induction the number of MMP-3+ve cells reached its maximum in the lesioned hemisphere compared to the unlesioned hemisphere. MMP-3+ve cells significantly decreased in number by day 15 after 6-OHDA lesion induction. Positive cells in the SNc were counted as described in (*see Chapter 2, section 2.2.3*). Results are expressed as mean number of cells $\pm$ SEM, n=6.*$p< 0.5$, ** $p<0.01$, *** $p< 0.001$, *ns*= not significant.

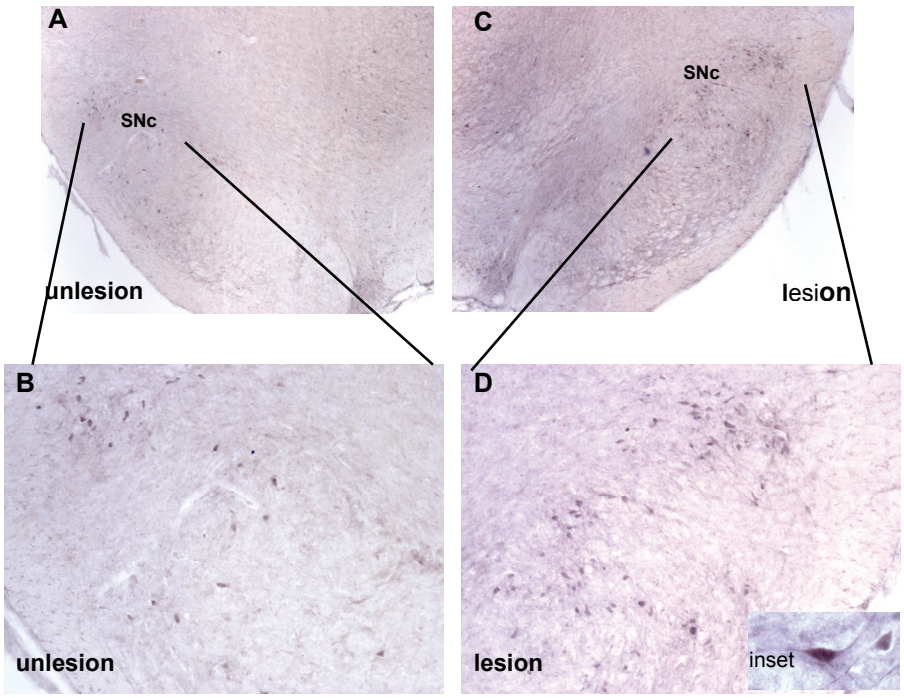

Fig 4.1 ***Photomicrograph*****- Representative photomicrographs of immunoperoxidase staining for MMP-3 with Nickel enhancer showing the localisation of up-regulated MMP-3+ve cells in the SNc on day 7 after 6-OHDA lesion induction in the lesioned hemisphere compared to the unlesioned hemisphere.**

A) Shows MMP-3+ve cells in the unlesioned hemisphere (x40). Few MMP-3+ve cells are present in the lateral and ventral portions of the SNc after 6-OHDA lesion induction (x40).

B) Higher magnification photomicrograph of (A) shows peroxidase immunostained MMP-3+ve cells that are present as cluster of very few cells in the lateral portion of the SNc with MMP-3+ve cells scattered in ventral and dorsal aspects of the SNc in the unlesioned hemisphere following 6-OHDA lesion induction (x100).

C) Shows increased number MMP-3+ve cells in the lesioned hemisphere after 6-OHDA lesion induction. At this low magnification dense staining is observed in the ventral lateral and dorsal portions of the SNc (x40).

D) Higher magnification photomicrograph of (C) shows peroxidase immunostained MMP-3+ve cells that are present as cluster of numerous cells accumulated in the lateral, ventral and dorsal portions of the SNc in the lesioned hemisphere following 6-OHDA lesion induction (x100).

Inserted box: Inset shows immunoperoxidase stained MMP-3+ve cell in the SNc of 6-OHDA lesioned hemisphere, MMP-3+ve cell represents a neuronal morphology with dendritic processes, staining of MMP-3 is present in the cytoplasm (x400).

4.3.1.2 Morphological characteristics of MMP-3 expressing cells in the SNc following 6-OHDA or sham lesioning

Morphological characteristics of MMP-3+ve cells following 6-OHDA lesion induction was studied in DAB immunolabelled sections with Nickel staining enhancer. Assessment of the sections revealed that most MMP-3+ve cells had neuronal morphology with a defined cell bodies and dendritic processes (Fig 4.2 A). To determine which cell types express MMP-3 following 6-OHDA lesion induction double immunofluorescence staining was performed for MMP-3 and NeuN or GFAP. The staining revealed that the majority of MMP-3 expressing cells were neurons (Fig 4.2B, Top panel). This observation was consistent at all time points studied. However no astrocytic expression of MMP-3 was detected since, MMP-3+ve cells were negative for GFAP expression (4.2B, Bottom panel).

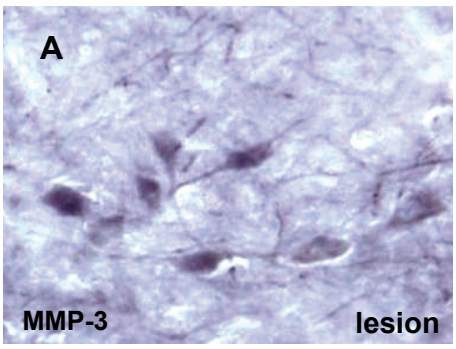

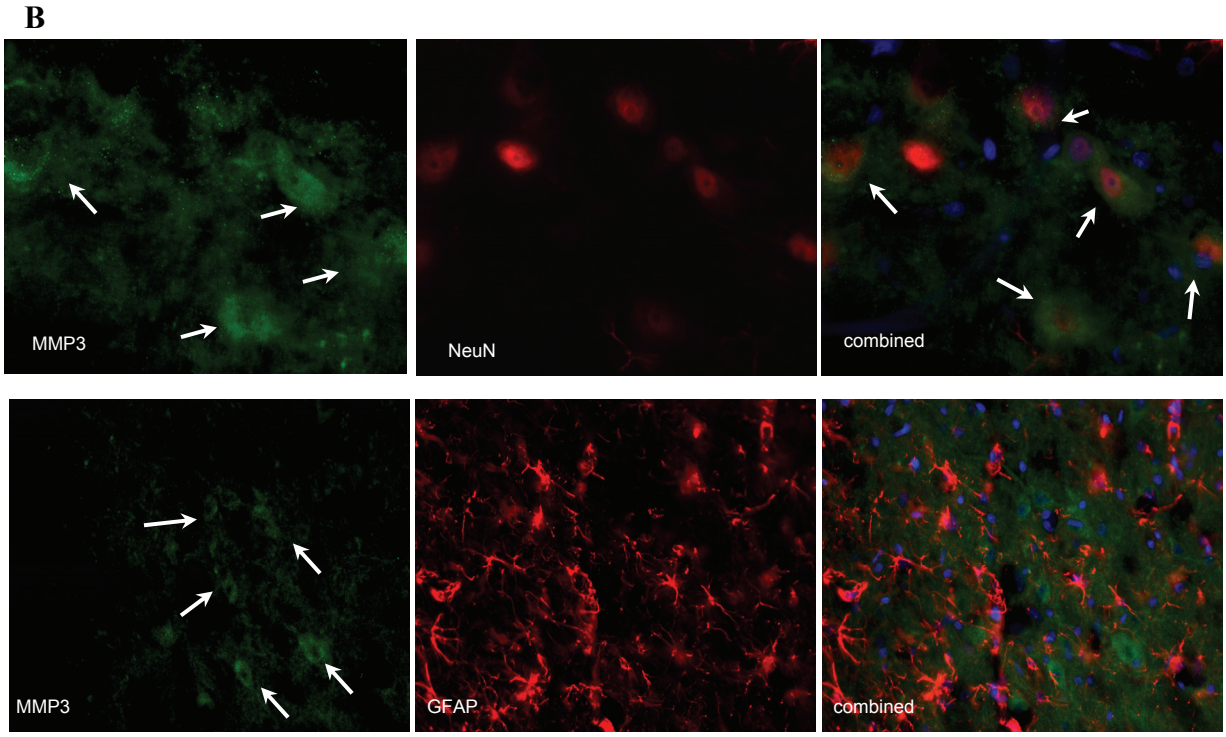

Fig 4.2A: Morphological characteristics of MMP-3+ve cells following 6-OHDA lesion induction DAB immunolabelled sections with Nickel staining enhancer.
Assessment of the sections revealed that most MMP-3+ve cells had neuronal morphology with a defined cell bodies and dendritic MMP-3 is mainly expressed in the cytoplasm of these neurons (x400).

Fig4.2B: To determine which cell types express MMP-3 (green) following 6-OHDA lesion induction double immunofluorescence staining was performed for MMP-3 and NeuN (Red-Top panel) or GFAP (Red-Bottom panel) Blue represent DAPI staining.
Top panel: The staining revealed that the majority of MMP-3 expressing cell were co-localised with neuronal cell marker NeuN (combined image) hence, MMP-3 was expressed by neurons in the SNc following 6-OHDA lesion induction. This observation was consistent at all time points studied (x400). **Bottom panel**: Staining revealed no co-localisation of GFAP expressing astrocytes and MMP-3+ve cells in the SNc following 6-OHDA lesion induction (x200). This was consistent at all time points studied.

4.3.1.3 Extent and localisation of MMP-9 expressing cells following 6-OHDA or sham lesioning in the SNc

MMP-9 expressing cells were present in the SNc as early as day 1 after 6-OHDA lesion induction in the lesioned side compared to the unlesioned side. Cell counts revealed that MMP-9 expressing cells were significantly increased in number from day 1 after 6-OHDA lesion induction in the lesioned hemisphere compared to the unlesioned hemisphere in the SNc: (lesioned: 40.35± 3.63; unlesioned: 22.0 ± 5.43, $p<0.5$). The number of MMP-9 +ve cells remained significantly increased in the lesioned hemisphere compared to the unlesioned hemisphere through out the rest of the study and cell counts on day 15 further confirmed this observation: (lesioned : 36.67 ± 4.25 ; unlesioned: 9.33± 0.6, $p <0.001$) (Fig 4.3A). MMP-9 expressing cells were localised in the SNc in a very similar manner to MMP-3+ve cells. MMP-9+ve cells were not confined to particular portion of the SNc. Being detected in the dorsal tier of the SNc and lateral aspect of the ventral tier in the SNc. A common observation was that MMP-9 expressing cells were denser in the SNc compared to the SN pars reticulata through out all time points studied (Fig 4.3B). In sham operated animals MMP-9 expressing cells increased in number on the side of the lesion however the increase did not reach significance (*data not shown*). These observations indicated that MMP-9 expressing cells were up regulated very early in the process and remained up regulated until the end of the study on day 15 on the side of lesion. This phenomenon suggested that MMP-9 activation might be a down-stream mechanism of MMP-3 activation. Therefore once MMP-3 was activated it primed MMP-9 expressing cells to express this enzyme. This is further supported by the lack of constitutive expression of MMP-9 in control brains.

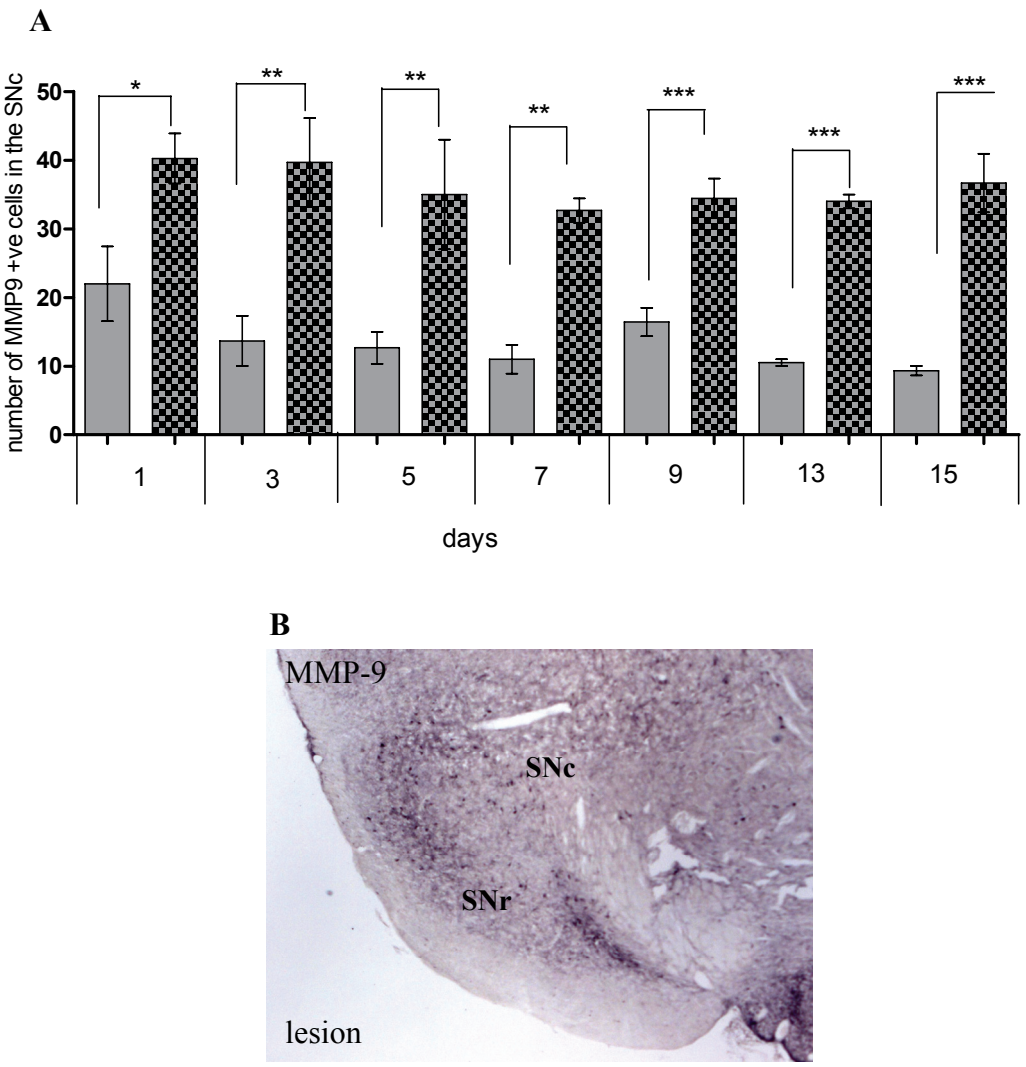

Fig 4.3 Unilateral MFB injection of 6-OHDA resulted in a significant increase in the number of MMP-9+ve cell in the SNc from day 1 after lesion induction that progressed up to day 15 on the lesioned hemisphere compared to the unlesioned hemisphere.

A) The graph shows the number of MMP-9+ve cells immunostained with MMP-9 antibody. The number of MMP-9+ve cells in the SNc significantly increased on day 1 after lesion induction in the lesioned hemisphere compared to the unlesioned hemisphere. MMP-9+ve cells reached their greatest number on day 9 post 6-OHDA lesioning that progressed up to day 15 after lesioning. Results are expressed as mean number of cells $\pm$ SEM, n=6.*$p< 0.5$, ** $p<0.01$, *** $p< 0.001$. Number of animals was 6/group per time point.

B) DAB immuperoxidase staining utilising Nickel staining enhancer was carried out for MMP-9 as a marker for the active form of this enzyme in the SNc following 6-OHDA lesion induction. The photomicrograph represents the SN in the lesioned hemisphere on day 9 after 6-OHDA lesion induction. MMP-9+ve cell are detected in the dorsal tier of the SNc and lateral aspect of the ventral tier in the SNc. A common observation was that MMP-9 expressing cells were denser in the SNc compared to the SN pars reticulate (SNr) through out all time points studied (x100).

4.3.1.4. Morphological characteristics of MMP-9 expressing cells in the SNc following 6-OHDA lesioning

Morphological characteristics of MMP-9+ve cells in the SNc following 6-OHDA lesion induction were studied in DAB immunolabelled sections with Nickel staining enhancer. Most MMP-9+ve cells had neuronal morphology with a defined cell bodies and dendritic processes very similar if not identical to MMP-3+ve cells. Neuronal expression of MMP-9 was observed in both the lesioned and unlesioned hemispheres following 6-OHDA or sham lesioning. Double immunofluorescence staining was performed to assess the expression of MMP-9 by neurons and/or astrocytes in the SNc. Double fluorescence staining for MMP-9 and NeuN revealed that the majority of MMP-9 expressing cell were neurons. However no astrocytic expression of MMP-9 was detected by GFAP and MMP-9 double immunofluorescence staining throughout all time points studied following 6-OHDA lesion induction.

Thus, a significant increase in the number of cells expressing both active form of MMP-3 and the downstream molecule, MMP-9 occurred very early after 6-OHDA lesion induction. This observation suggested that activation of these enzymes following 6-OHDA lesioning could be involved in dopaminergic neuronal loss in the SNc.

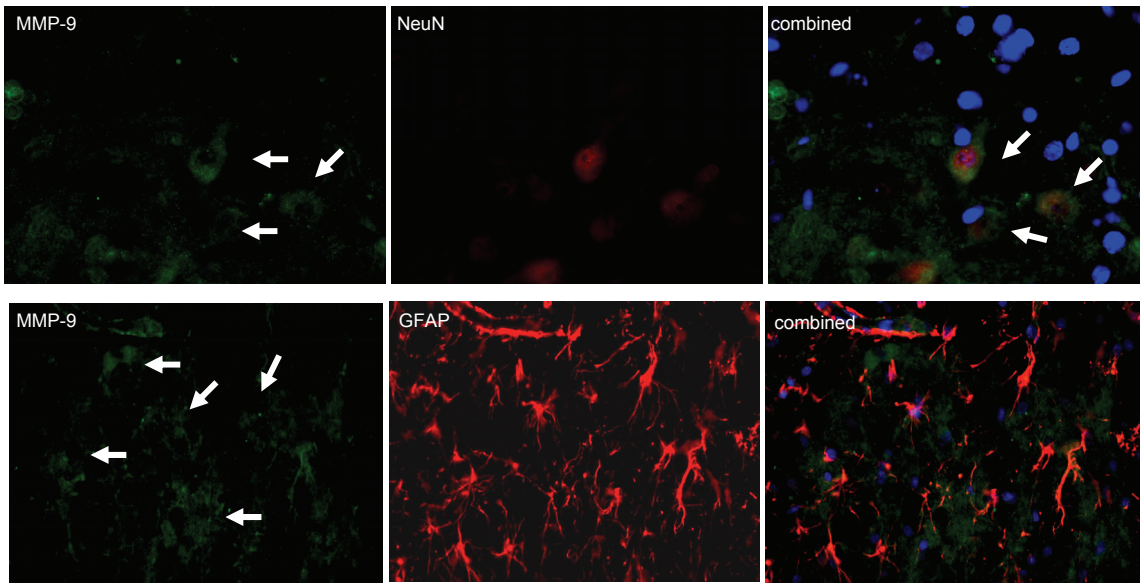

Fig 4.4: To determine which cell types express MMP-9 (green) following 6-OHDA lesion induction double immunofluorescence staining was performed for MMP-9 and NeuN (Red-Top panel) or GFAP (Red-Bottom panel) Blue represent DAPI staining.

Top panel: The staining revealed that the majority of MMP-9 expressing cell were co-localised with neuronal cell marker NeuN (combined image-white arrows) hence, MMP-3 was expressed by neurons in the SNc following 6-OHDA lesion induction. This observation was consistent at all time points studied (x400).
Bottom panel: Staining revealed no co-localisation of GFAP expressing astrocytes and MMP-9+ve cells (green-white arrows) in the SNc following 6-OHDA lesion induction (x200). This was consistent at all time points studied.

4.3.1.5 Kinetics of MMP-3 and MMP-9 expressions in relation to loss of TH+ve dopaminergic in the SNc following 6-OHDA lesion

To detect the effect of 12µg 6-OHDA (in 4µl) injection into the MFB on neuronal cell loss in the SNc, the number of TH+ve dopaminergic neurons in the SNc were monitored. The results are shown as the mean number of cell counts for TH+ve neurons in the SNc at different time points after toxin injection. As shown in (Fig 4.5) 6-OHDA injection caused a progressive loss of nigral TH+ve neurons in the SNc. Comparison of the number of nigral TH+ve neurons between lesioned and unlesioned sides showed no significant loss of TH +ve neurons within the first 7 days after 6-OHDA injection (lesioned: 73 ± 8.08, unlesioned 97.33 ± 8.80 $p>0.5$.). However, both MMP-3+ve and MMP-9+ve cell number significantly increased on day 7 after lesioning in the lesioned hemisphere compared to unlesioned hemisphere (Figures 4.1 and 4.3A, respectively). Significant loss of TH+ve neurons in the lesioned hemisphere started to manifest from day 9 compared to the unlesioned hemisphere (lesioned: 40 ±5.25, unlesioned: 86±5.25, $p<0.01$) when MMP-3 and MMP-9 expression were also significantly increased. Unilateral dopaminergic neuronal loss progressed up to day 15 after lesion induction comparing lesioned and unlesioned hemispheres. Cell counts on day 15 showed (unlesioned: 75±12, lesioned 32.5±1.5, $p<0.01$). In particular, neurons in the lateral portion and ventral tier of the SNc were most vulnerable to 6-OHDA toxicity. However, MMP-3 expression decreased significantly on day 15, whereas MMP-9 expression remained increased. At all time points studied the loss TH immunoreactivity was accompanied by a comparable loss of NeuN immunoreactivity, indicating that neuronal cell bodies are lost, rather than demonstrating a down regulation of TH expression (*data not shown in this chapter, see chapter 3, figure 3.3*). In sham lesioned animals no significant loss of TH+ve dopaminergic neurons were observed compared to the unlesioned side of the brain.

Taken together these observations indicated that following 6-OHDA lesion induction both MMP-3 and MMP-9+ve cells significantly increased in number in the SNc on the lesioned hemisphere before any dopaminergic neuronal loss was evident. In addition, neuronal expression of both MMP-3 and MMP-9 indicated that MMP-3 and MMP-9 released from neurons after lesioning might act as signalling molecules to activate microglia and/or directly affect the neighbouring dopaminergic neurons in the SNc leading to cell death.

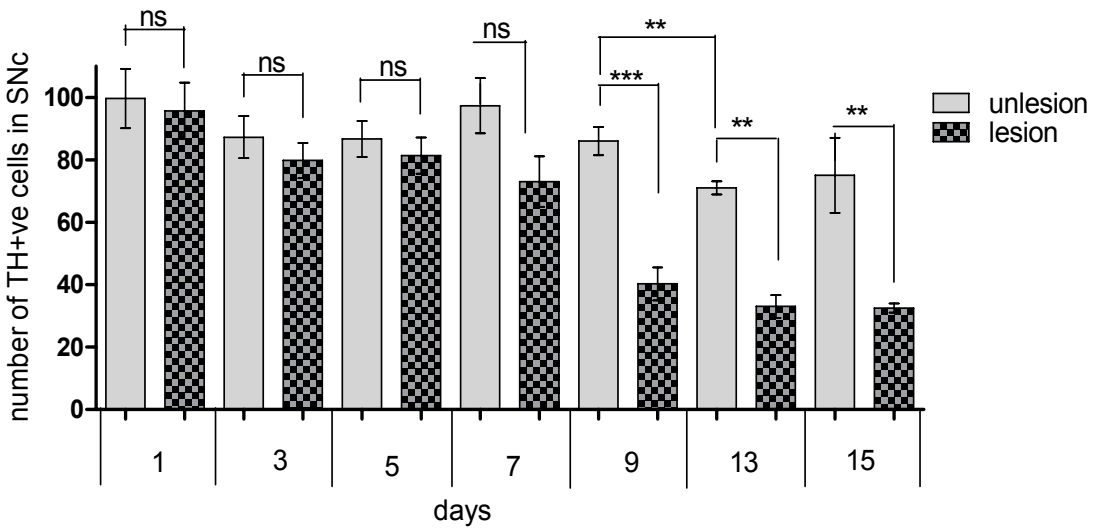

Fig 4.5 Time dependent TH+ve dopaminergic neuronal cell death in the SNc following 6-OHDA lesion induction.

Male SD rats were injected with 12 μg 6-OHDA or with ascorbic acid (as sham) into the MFB and maintained under normal conditions. Animals were sacrificed at the indicated time points and coronal brain sections (20 μm thick) were cut through the SNc. Immunostaining was carried out with TH antibody and TH+ve neurons in SNc were counted. Graph shows the number of TH +ve neurons in SNc at different time points after 6-OHDA injection. Significant TH+ve dopaminergic neuronal cell death occurs from day 9 after 6-OHDA lesion induction in the lesioned hemisphere compared to the unlesioned side that progresses to day 15 post lesioning. Results are expressed as mean number of cells ± SEM. ** $p< 0.01$, ***$p<0.001$, ns= non-significant. Number of animals was 6/group per time point.

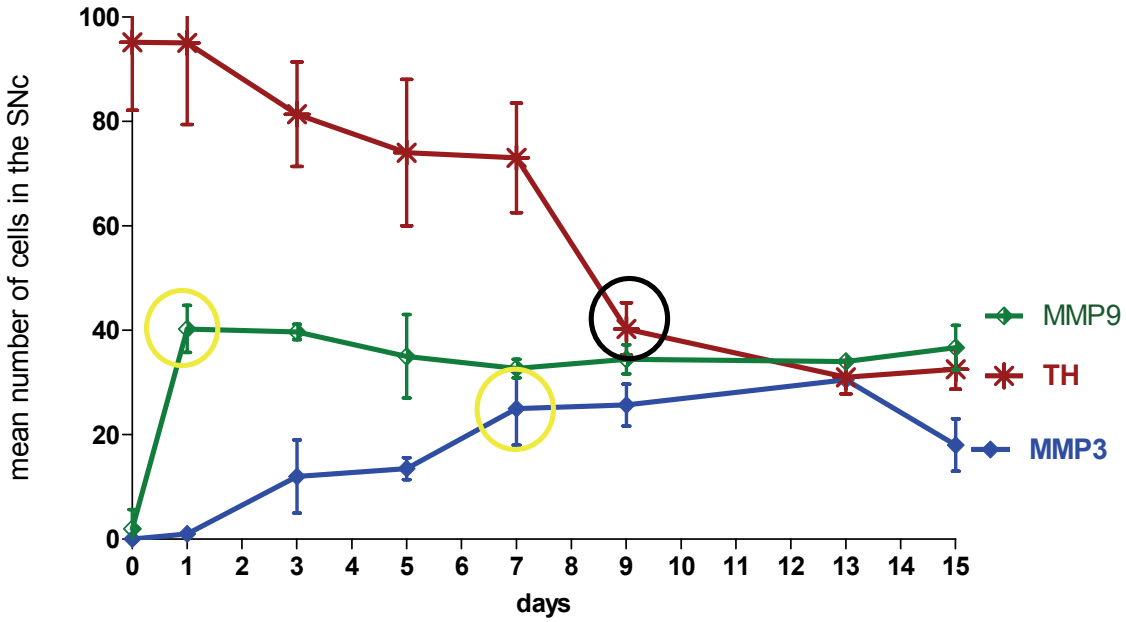

Fig 4.6 Graphical demonstration of the increase in the mean number of nigral MMP-3 and MMP-9 expressing cells in the 6-OHDA lesioned hemisphere prior to TH+ve nigral dopaminergic neuronal cell death in the 6-OHDA lesioned hemisphere.

Blue line demonstrates the time dependent increase in the mean number of MMP-3+ve cells in the SNc following 6-OHDA lesion induction in the lesioned hemisphere. On day 7 (yellow circle) the mean number MMP-3+ve cells increased significantly as shown in (Fig 4.1) compared to day 5 post lesion. **Green line** demonstrates the time dependent increase in the mean number of MMP-9+ve cells in the SNc following 6-OHDA lesion induction in the lesioned hemisphere. MMP-9+ve cells significantly up-regulate from day 1 after 6-OHDA lesioning (yellow circle) and remained up-regulated up to day 15 after 6-OHDA lesion induction (Fig 4.3A). **Red line** represent time dependent decrease in the number of TH+ve dopaminergic neurons in the SNc after 6-OHDA lesion induction in the lesioned hemisphere. Significant loss of dopaminergic neurons is observed on day 9 after lesioning (black circle) that progressed to day 15 post 6-OHDA lesioning (Fig 4.5). Hence it is graphically demonstrated that significant increase in the number MMP-3 and MMP-9 expressing cells precedes TH+ve dopaminergic neuronal cell death in the SNc after 6-OHDA challenge. Results are presented as mean number of cell± SEM. Number of animals was 6/group per time point.

4.3.2 Kinetics of MMP-3 expression in relation to OX6+ve and CD68+ve activated microglia/macrophages in the SNc following 6-OHDA lesion induction

4.3.2.1. Comparison between the kinetics of MMP-3 expression and OX6+ve activated microglia in the SNc after 6-OHDA lesion induction

Similar to the data reported in chapter 3, OX6+ve cells are the antigen presenting population of microglia. OX6+ve microglia were first observed in the medial part and ventral tier of the SNc at day 1 after 6-OHDA lesion induction when no apparent changes were observed in the number of TH+ve cells in the lesioned hemisphere compared to the non lesioned hemisphere. At which time point increased number of MMP-3 +ve cells were also observed in the SNc (see *section 4.3.1.1*). The number of OX6+ve cells gradually increased and a focal accumulation of these cells in both the lateral and medial portions of the SNc in the lesioned hemisphere was observed on day 7 (cell counts: lesion: 19.83± 6.16, unlesion: 0.83 ± 0.47, $p<0.01$) (Fig 4.7). At this time point MMP-3+ve cells were significantly increased in number in the lesioned hemisphere compared to the unlesioned side of the brain (*see section 4.3.1.1*). The number of OX6+ve cells increased significantly on day 9 following 6-OHDA lesion induction (lesioned: 55.57±4.71, unlesioned: 1.57± 0.75, $p<0.001$), when significant loss of TH+ve neurons in the SNc was also evident (Fig 4.5). The number of OX-6+ve microglia decreased significantly by day 15 after 6-OHDA lesion induction compared to the lesion side on day 9 (Day 15 post-lesion: 29.25±5.96, Day 9 post-lesion: 55.57±4.71, $p<0.001$). In sham lesioned animals no expression of OX6+ve microglial cells was observed.

Thus, focal expression of OX6+ve microglia in the SNc on the lesioned hemisphere from day 7 -13 after lesioning was concurrent with significant increase in the number of MMP-3+ve cells in the SNc following 6-OHDA lesion induction that preceded any dopaminergic neuronal loss in the SNc (Fig 4.8).

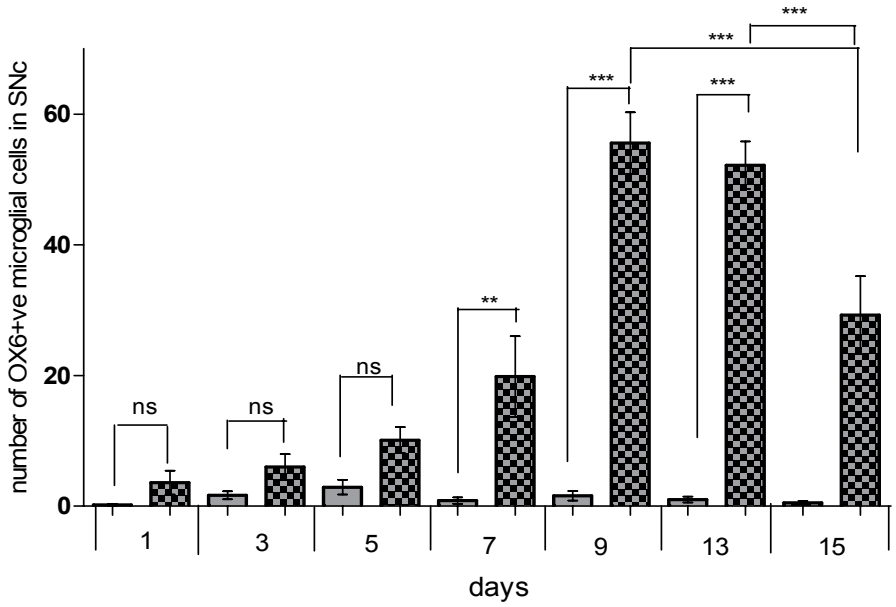

Fig 4.7 Unilateral time dependent increase in the number of OX6+ve microglial cells in the SNc following 6-OHDA lesion induction.

Injection of 6-OHDA induced accumulation of OX6+ve cells in the SNc in a time dependent manner. Graph shows at time-course quantification of OX6+ve microglia in the SNc. Immunostaining was carried out with OX6 antibody as markers for MHC II expressing activated microglia. The number of OX6+ve cells reached its full manifestation on day 9 after 6-OHDA lesion induction in the lesioned hemisphere compared to the unlesioned hemisphere. OX6+ve microglia significantly decreased in number by day 15 after 6-OHDA lesion induction. Positive cells in the SNc were counted as described in (*see Chapter 2, section 2.2.3*). Results are expressed as mean number of cells $\pm$ SEM. ** $p< 0.01$, ***$p<0.001$, ns= non-significant. Number of animals was 6/group per time point.

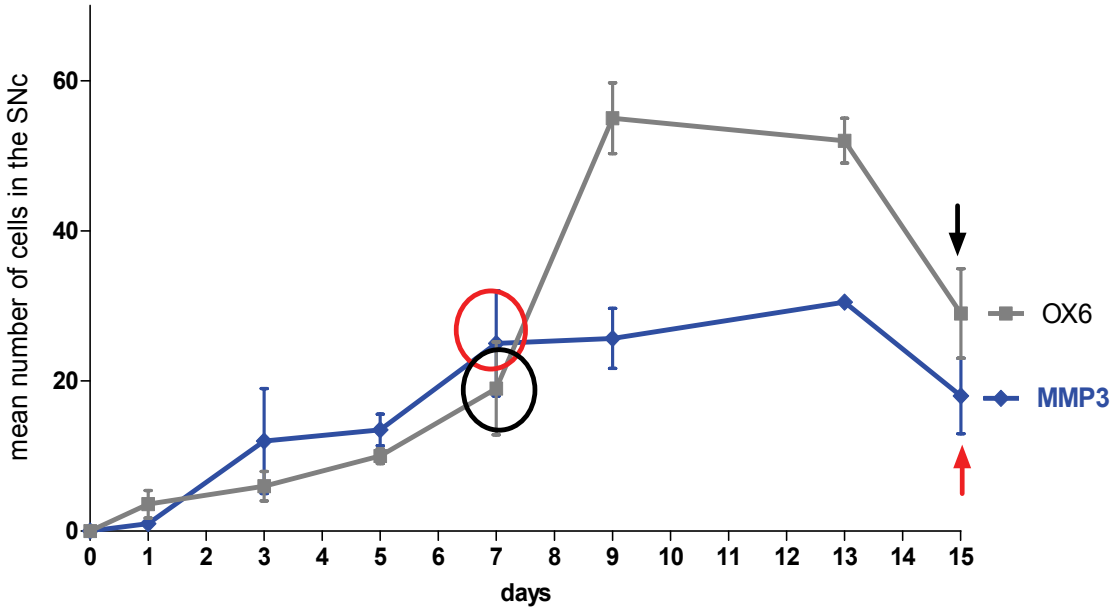

Fig 4.8 Graphical demonstration of the time dependent increase in the mean number of nigral MMP-3 expressing cells in the 6-OHDA lesioned hemisphere concomitant with significant increase in the number of OX6+ve microglia in the 6-OHDA lesioned hemisphere.

Blue line demonstrates the time dependent increase in the mean number of MMP-3+ve cells in the SNc following 6-OHDA lesion induction in the lesioned hemisphere. On day 7 (red circle) the mean number MMP-3+ve cells increased significantly as also shown in (Fig 4.1) compared to day 5 post lesion.
Grey line demonstrates the time dependent increase in the mean number of OX6+ve cells in the SNc following 6-OHDA lesion induction in the lesioned hemisphere. OX6+ve cells significantly up-regulate on day 7 after 6-OHDA lesioning (black circle) as also demonstrated in (Fig 4.7). The mean number of both MMP-3+ve cells and OX6+ve microglia decreased significantly on day 15 after 6-OHDA lesion induction in the SNc ipsilateral to the lesion side (red and black arrows respectively). Results are presented as mean number of cell± SEM. Number of animals was 6/group per time point.

4.3.2.2 Comparison between the kinetics of MMP-3 expression and CD68+ve activated microglia in the SNc after 6-OHDA lesion induction

CD68+ve phagocytic microglia were present ipsilateral to the side of the lesion 3 days after 6-OHDA induction compared to contralateral control side. Whereas, in sham operated animals no CD68+ve cells were detectable. Their localisation was very similar if not identical to that of OX6+ve cells. CD68+ve cells were mainly confined to the medial portion of SNc until day 7. Thereafter, the number of CD68 expressing cells progressively increased up to day 15 and a large number of CD68+ve cells in the medial and lateral portion of SNc ipsilateral to the lesion was observed, no immunoreactivity was detected in the unlesion side. Cell counts revealed that significant increase in the number of CD68+ve macrophages was observed on day 9 after lesion induction in the lesioned hemisphere compared to the unlesioned hemisphere (lesioned: 18.20± 1.43; unlesioned: no cells were detected, $p<0.001$) (Fig 4.9). At this time point MMP-3+ve cells also significantly increased in number in the lesioned hemisphere compared to the unlesioned side (*see section 4.3.1.1*). CD68+ve cells increased in number up to day 15 after 6-OHDA lesion induction in the lesioned hemisphere (lesioned: 40.57±3.2; unlesioned : no cells detected, $p<0.001$). Interestingly, the number of MMP-3+ve cells decreased on day 15 after 6-OHDA lesioning in the lesioned hemisphere compared to the unlesioned hemisphere (*see section 4.3.1.1*). The presence of CD68+ve microglia/macrophages indicated that phagocytic activity accompanied neuronal degeneration with simultaneous MMP-3 expression in the SNc following 6-OHDA lesioning.

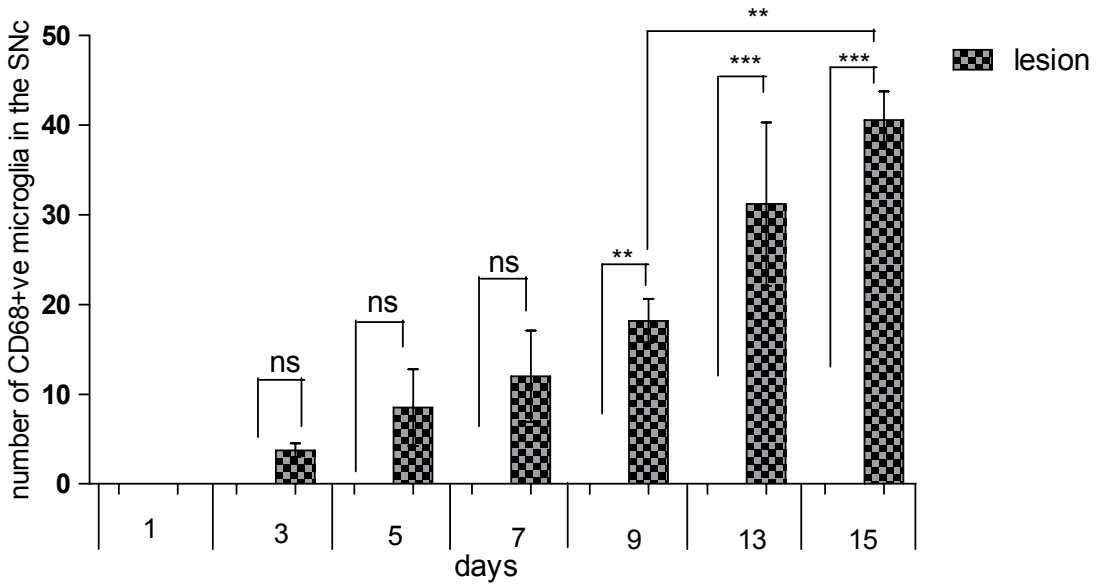

Fig 4.9 Graph showing a time dependent increase in the number of CD68+ve macrophages in the SNc after 6-OHDA lesion induction.

Injection of 6-OHDA induced accumulation of CD68+ve cells in the SNc in a time dependent manner. Immunostaining was carried out with CD68 antibody as markers for phagocytic macrophages. The number of CD68+ve cells reached its full manifestation on day 15 after 6-OHDA lesion induction in the lesioned hemisphere compared to the unlesioned hemisphere. CD68+ve cells significantly increased in number on day 9 after 6-OHDA lesion induction that progressed to day 15. Positive cells in the SNc were counted as described in (*see Chapter 2, section 2.2.3*). Results are expressed as mean number of cells $\pm$ SEM. ** $p<0.01$, *** $p< 0.001$, *ns*= not significant. . Number of animals was 6/group per time point.

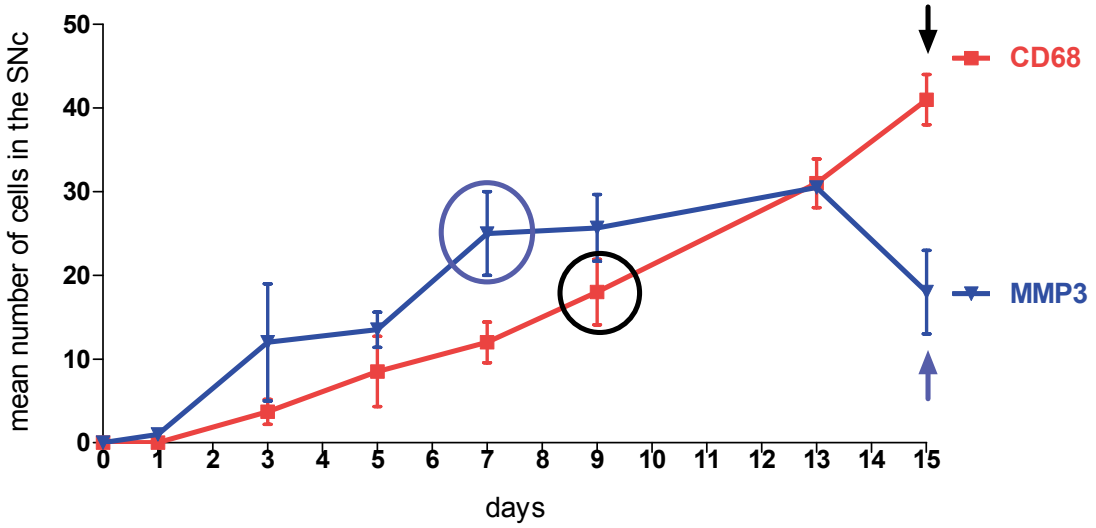

Fig 4.10 Graphical demonstration of the time dependent increase in the mean number of nigral MMP-3 expressing cells in the 6-OHDA lesioned hemisphere concomitant with significant increase in the number of nigral CD68+ve macrophages in the 6-OHDA lesioned hemisphere.

Blue line demonstrates the time dependent increase in the mean number of MMP-3+ve cells in the SNc following 6-OHDA lesion induction in the lesioned hemisphere. On day 7 (purple circle) the mean number MMP-3+ve cells increased significantly as also shown in (Fig 4.1) compared to day 5 post lesion.
Red line demonstrates the time dependent increase in the mean number of CD68+ve cells in the SNc following 6-OHDA lesion induction in the lesioned hemisphere. CD68+ve cells significantly up-regulate on day 9 after 6-OHDA lesioning (black circle) as also demonstrated in (Fig 4.8). The mean number of MMP-3+ve cells decreased significantly by day 15 after 6-OHDA lesion induction however, the mean number CD68+ve macrophages increased significantly compared to day 9 on day 15 after 6-OHDA lesion induction in the SNc ipsilateral to the lesion side (purple and black arrows respectively). Results are presented as mean number of cell± SEM. Number of animals was 6/group per time point.

4.3.2.3 Interaction between MMP-3 expressing cells and OX6+ve microglia in the SNc after 6-OHDA lesion induction

Double immunofluorescence staining revealed that OX6+ve activated microglia were in the vicinity of MMP-3 expressing cells on days 7-15 after lesion induction in the SNc on the lesioned side compared to the unlesioned side (Fig 4.11). The presence of activated OX6+ve microglia very close to the MMP-3+ve neurons was observed up to day 15 after 6-OHDA lesion induction but not in the sham lesioned animals. This observation indicated that MMP-3 expression was closely related to microglial activation.

4.3.2.4 Interaction between MMP-3 expressing cells and CD68 +ve macrophages in the SNc after 6-OHDA lesion induction

Double immunofluorescence staining revealed that MMP-3 expressing cells were in very close contact with CD68+ve macrophages on days 3, 7, 9 and 13 after 6-OHDA lesion induction on the side of the lesion (Fig 4.12). This indicated that MMP-3+ve cells are in nature mostly neuronal and interact with CD68+ve macrophages. Secretion of MMP-3 by neurons could act as a signal to activate CD68 expressing macrophages in the SNc following 6-OHDA lesion induction. As shown in chapter 3 (*see section 3.4.5.1*) microglial phagocytic activity may be initiated prior to the TH+ve neuronal demise, suggesting that phagocytosis of apoptotic cells may take place at very early stage of neuronal loss in SNc.

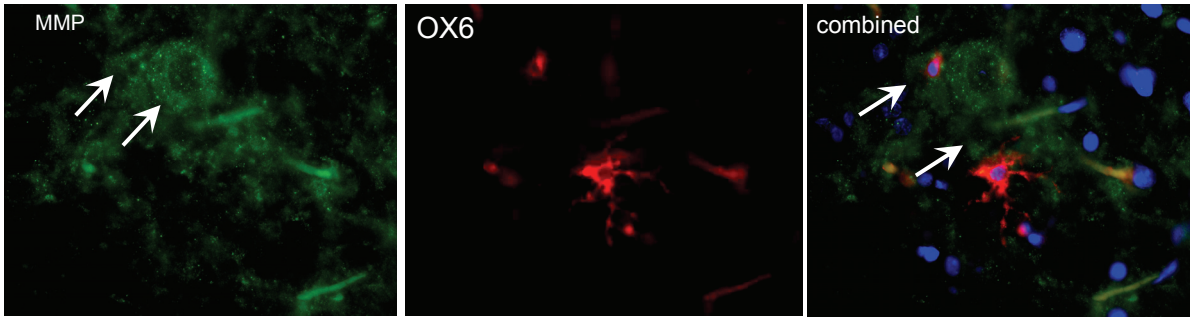

Fig 4.11 Spatial association between OX6+ve and MMP-3+ve on day 9 after 6-OHDA lesion induction.

Unilateral injection of 6-OHDA resulted in a time dependent increase in the number of MMP-3+ve and OX6+ve cells in the SNc ispsilateral to the side of the lesion. Double immunofluorescence staining for MMP-3 (green) and OX6 (red) shows spatial association between MMP-3+ve and OX-6+ve microglia in the SNc following 6-OHDA lesion induction in the lesioned hemisphere (combined image, white arrows) . OX6+ve microglia are in a close vicinity to MMP-3+ve cells indicating a possible interaction between them. Blue: Represents DAPI staining as marker of the cell nucleus (x400).

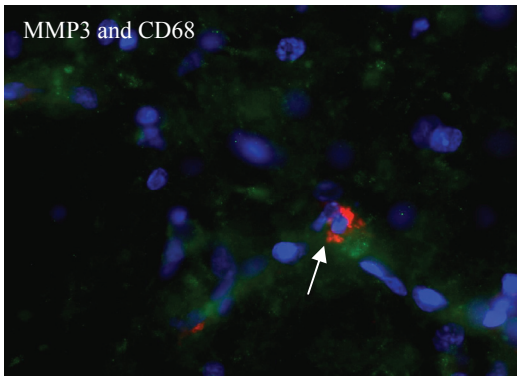

Fig 4.12 Spatial association between CD68+ve and MMP-3+ve on day 9 after 6-OHDA lesion induction.

Unilateral injection of 6-OHDA resulted in a time dependent increase in the number of MMP-3+ve and CD68+ve cells in the SNc ispsilateral to the side of the lesion. Double immunofluorescence staining for MMP-3 (green) and CD68 (red) shows a close contact between MMP-3+ve and CD68+ve macrophages on day 3 after 6-OHDA lesion induction in the SNc following 6-OHDA lesion induction in the lesioned hemisphere (white arrow). Indicative of possible phagocytosis of MMP-3+ve cells before dopaminergic neuronall cell death occurs. The combined image is presented due to corruption in the files containing the individual picture of MMP-3 and CD68 stained cells. Blue: Represents DAPI staining as marker of the cell nucleus (x400).

4.3.3 Expression of CD200R during lesion progression in the SNc after 6-OHDA injection

4.3.3.1 Effect of 6-OHDA lesion induction on the number of CD200R expressing cells in the SNc

CD200R +ve cells significantly increased in number in the SNc on day 3 after 6-OHDA lesioning in the lesioned hemisphere compared to the unlesioned hemisphere: (lesioned : 13.67±1.85 ; unlesioned: 5 ± 0.57, $p<0.5$) (Fig 4.13). CD200R expressing cells reached their highest number on day 13 after 6-OHDA lesion induction compared to the unlesion side: (lesioned: 33.67 ± 2.33 ; unlesioned: 14.0 ± 1.3, $p<0.001$) (Fig 4.13). The number CD200R+ve cells decreased significantly on day 15 compared to day 13 after 6-OHDA lesioning in the lesioned side (Day 15 post lesion: 11.67 ± 1.66 ; Day 13 post lesion : 33.67 ± 2.33, $p<0.01$) (Fig 4.13). Control animals did not demonstrate any CD200R immunoreactivity. Under homeostasis CD200R is bound to its ligand, CD200 which is expressed on neurons. Following a 6-OHDA challenge and the resultant disturbance of the ECM, CD200R will unbind from the CD200 glycoprotein and is detectible by CD200R antibody. This observation further suggested that CD200-CD200R interactions that exert an inhibitory effect on the microglial activation were disturbed following 6-OHDA lesion induction leading expression of uncoupled CD200R.

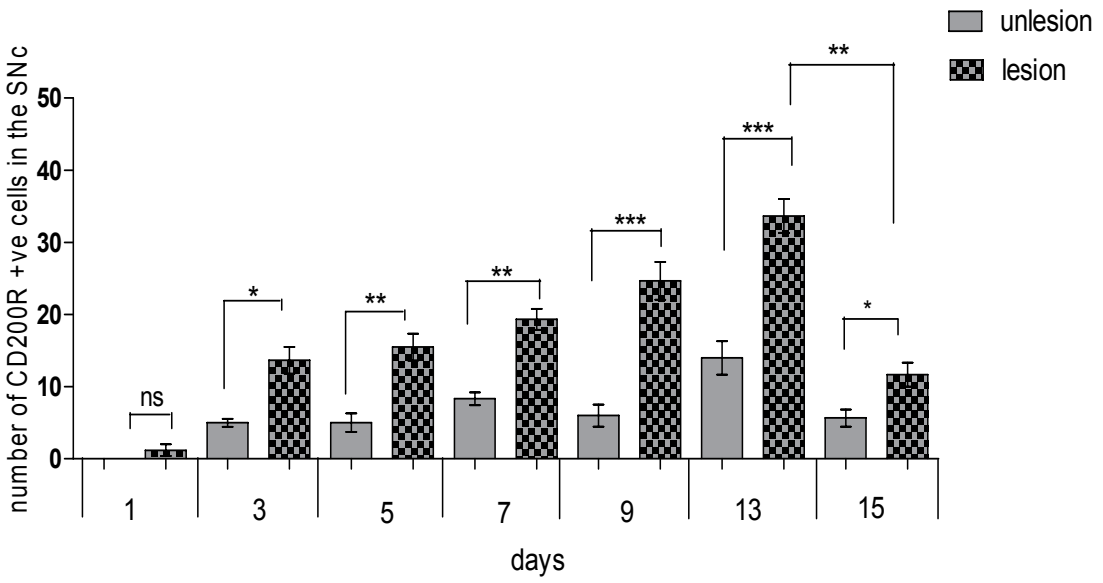

Fig 4.13 Time dependent unilateral increase in the number of CD200R expressing cells in the SNc following unilateral injection of 6-OHDA into the MFB.

Immunoperoxidase staining was performed on 20μm coronal sections of the SNc with CD200R antibody. Cell counts revealed that the number of CD200R+ve cells increased significantly in the lesioned hemisphere on day 3 after 6-OHDA lesion induction compared to the unlesioned hemisphere. The number of CD200R+ve cells in the lesioned hemisphere increased time dependently and reached its greatest on day 13 after 6-OHDA lesioning. By day 15 the number CD200R+ve cells decreased significantly. Results are expressed as mean number of cells $\pm$ SEM. * $p<0.5$, ** $p<0.01$, *** $p< 0.001$, *ns*= not significant. . Number of animals was 6/group per time point.

4.3.3.2 Localisation of CD200R+ve cells in the SNc following 6-OHDA lesion induction

CD200R expressing cells were mainly observed in the medial portion of the SNc up to day 7 after 6-OHDA lesion induction on the side of lesion. On day 9 after 6-OHDA lesioning CD200R+ve cells were observed in both the medial and the lateral portions of the SNc before they relocated to the ventrolateral portion of the SNc on days 13 and 15 after lesioning on the side of the lesion. In control animals no CD200R+ve cells were detected.

Thus, the kinetics and localisation of CD200R+ve cells were similar if not identical to CD68 and OX6 expressing microglia/macrophages. Both OX6+ve microglia and CD200R+ve cells relocated from the medial portion of the SNc to the lateral and ventral aspects of the SNc in a time dependent manner in addition to increase in their numbers following 6-OHDA lesion induction.

4.3.3.3 Interaction between TH+ve dopaminergic neurons and CD200R+ve cells in the SN after 6-OHDA lesion induction

Double immunofluorescence staining showed that on days 7,9,13 and 15 after 6-OHDA lesion induction, CD200R expressing cells were observed in a close vicinity to the morphologically intact TH+ve dopaminergic neurons in the SNc as well as attached to the cell bodies of morphologically damaged TH+ve neurons with round cell bodies and absence of dendritic processes in the lesioned hemisphere compared to the unlesioned hemisphere (Fig 4.14, bottom panel and top panel, respectively). The interaction between TH+ve dopaminergic neurons and CD200R+ve cells was very similar to the interaction observed between TH+ve dopaminergic neurons and OX6+ve microglial cells (see *chapter 3, section 3.4.5.1*). CD200R+ve cells surrounded morphologically intact dopaminergic neurons, in addition to damaged ones, suggesting that signals from traumatised or damaged neurons could trigger the activation of CD200R+ve cells which demonstrated a phenotype characteristic of activated microglia. To further explore the interaction between ECM disturbance and CD200R expression, the relationship between MMP-3+ve cells and CD200R expressing cells was investigated (*see section 4.3.2.7*).

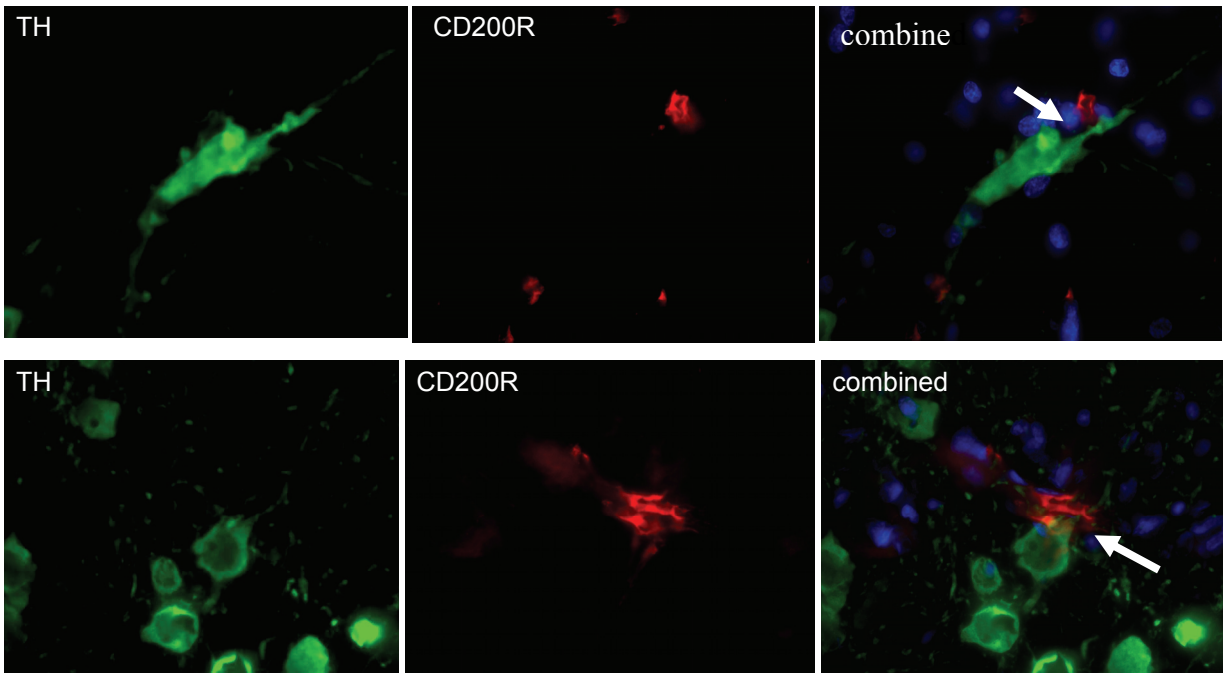

Fig 4.14 Close interaction between intact and morphologically damaged TH+ve dopaminergic neurons with CD200+ cell in the SNc on day 9 after 6-OHDA lesion induction in the lesioned hemisphere.

Top panel: The combined image shows double immunofluorescence staining for TH (green) and CD200R (red) on 20µm thick nigral sections. CD200R+ve cells are in very close vicinity almost attached to the dendrites of a morphologically intact TH+ve dopaminergic neuron (white arrow) in the SNc ipsilateral to the lesioned hemisphere (x400). Blue: Represents DAPI staining as marker of the cell nucleus.

Bottom panel: The combined image shows double immunofluorescence staining for TH (green) and CD200R (red) on 20µm thick nigral sections. CD200R+ve cells are attached to morphologically damaged TH+ve dopaminergic neurons in the SNc, TH+ve cell have lost their dendritic processes and have a round morphology (white arrow). This indicates that TH+ve dopaminergic neurons are damaged following 6-OHDA lesion induction(x400). Blue: Represents DAPI staining as marker of the cell nucleus.

4.3.3.4 Interaction between MMP-3 expressing cells and CD200R+ve cells in the SNc after 6-OHDA lesion induction

Double immunofluorescence staining revealed that on days 3 and 5 after 6-OHDA lesion induction CD200R expressing cells were attached to MMP-3+ve cells with neuronal morphology in the SNc (Fig 4.15, Top panel). On days 7-15 after 6-OHDA lesion induction CD200R +ve cells were observed to be in close proximity to MMP-3+ve cells that showed neuronal morphology in the SNc (Fig 4.15 Bottom panel). This observation indicated that during the early days post 6-OHDA lesioning the release of MMP-3 by neurons could lead to the dissociation of the CD200R expressing cells from the CD200 glycoprotein on neurons, hence CD200R expressing cells were detectable whilst still attached to MMP-3+ve neurons. However, at later time points after 6-OHDA lesion induction, CD200R +ve cells were dissociated from MMP-3+ve neurons. This observation suggested that disturbance in the ECM could have led to a disassociation of the CD200R from its ligand CD200, hence dysregulation in neuron-glia interaction contributing to microglial activation.

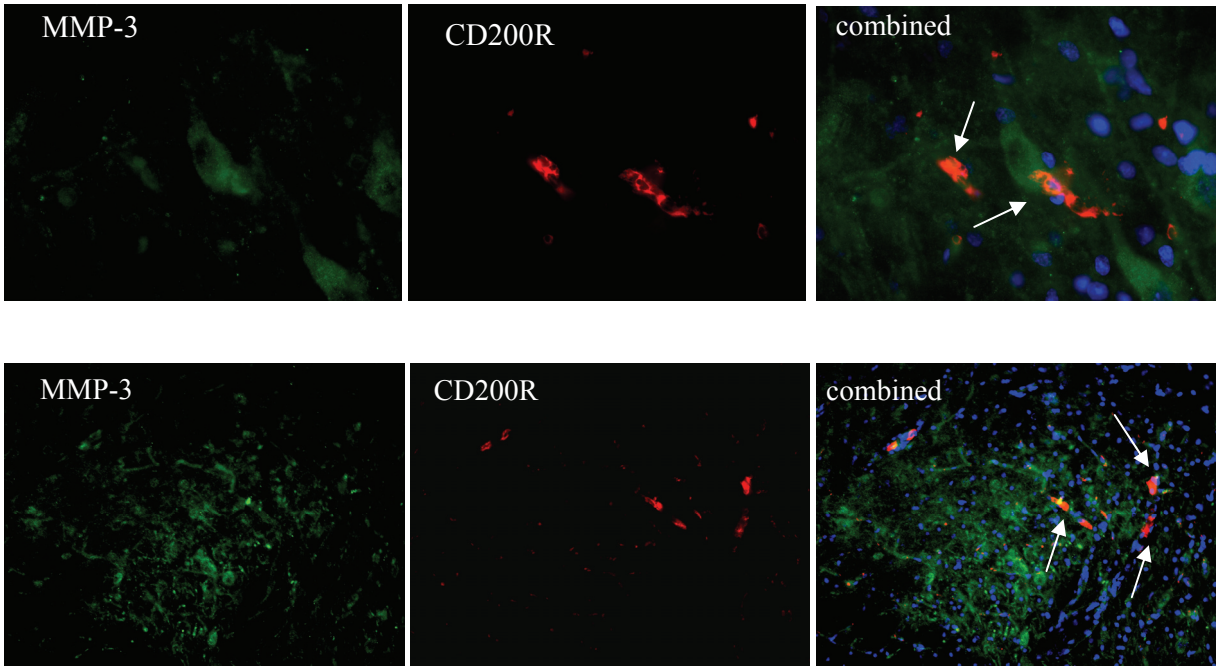

Fig 4.15 Spatial association between MMP-3+ cells and CD200R+ve microglia in the SNc following 6-OHDA lesion induction.

Top panel: The combined image shows double immunofluorescence staining for MMP3 (green) and CD200R (red) on 20µm thick nigral sections. CD200R+ve cells are attached to MMP-3+ve neurons (white arrows) in the SNc ipsilateral to the lesioned hemisphere on day 3 after 6-OHDA lesioning (x400). Blue: Represents DAPI staining as marker of the cell nucleus

Bottom panel: The combined image shows double immunofluorescence staining for MMP3 (green) and CD200R (red) on 20µm thick nigral sections. CD200R+ve cells are in close proximity to MMP-3+ve neurons (white arrows) but not attached to them in the SNc ipsilateral to the lesioned hemisphere on day 7 after 6-OHDA lesioning (x100). Blue: Represents DAPI staining as marker of the cell nucleus.

4.4 Discussion

The main aim of this study was to elucidate the mechanisms that are involved in initiation of microglial activation, with particular emphasis on signals released from neurons in the SNc after unilateral injection of 6-hydroxydopamine (6-OHDA) into the medial forebrain bundle (MFB). Hence, we studied the kinetics of MMP-3 and MMP-9 activation in relation to the extent of dopaminergic neuronal loss during the lesion progression in the SNc. In addition, we assessed how the expression of MMP-3 and 9 correlate with the extent of microglial activation in the SNc following 6-OHDA lesion induction. Finally, we have studied the association and spatial interactions between CD200R expressing cells and neurons in the SNc during the progression of dopaminergic neuronal loss in our PD model.

4.4.1 MMP-3 and MMP-9 expressions preceded dopaminergic neuronal loss in the SNc following 6-OHDA lesion induction

Limited constitutive MMP-3 expression was observed in the SNc, in both control and sham operated animals, however the numbers of cells were not significantly different between control and sham lesioned animals. Therefore, any significant increase in the number of MMP-3 +ve cells was considered to be due to the effects of 6-OHDA lesion induction. As our results demonstrate (*see section 4.3.1.1*) that MMP-3+ve cells are present in the SNc from day 3 after lesioning on the lesioned side and significantly increased in number in the SNc on day 7 after 6-OHDA lesion induction. Increases in the number of MMP-3+ve cells progressed up to day 13 followed by a significant decrease on day 15 after lesion induction. Concomitant with the increase in MMP-3+ve cell number, unilateral injection of 12µg 6- OHDA into the MFB led to a progressive partial lesion in the SNc that was evident by loss of >55% of TH+ve dopaminergic neurons as discussed in chapter 3 (see *section 3.5.1*). Significant neuronal loss started to manifest itself 9 days after 6-OHDA injection. It is well documented (Pickel et al., 1977; Wassef et al., 1981) that loss of TH-immunoreactivity in the SNc is indicative of degeneration of nigral dopaminergic neurones. However as mentioned in chapter 3, to rule out the possibility that the observed decrease in the number of TH+ve dopaminergic neurons was due to the down-regulation of TH following 6-OHDA, double staining for TH and NeuN was performed (*see Chapter 3, section 3.4.1.1*) that clearly demonstrated that 6-OHDA led to loss of neuronal cell bodies (*data not shown*

in this chapter). Our data clearly demonstrated that the up-regulation of MMP-3 expressing cells preceded dopaminergic neuronal cell death in the SNc. MMP-3 expression reached a maximum on day 9 after lesion induction when significant dopaminergic neuronal loss was also apparent; supporting our hypothesis that MMP-3 is associated with dopaminergic neuronal loss in PD pathology. Moreover, the loss of TH+ve dopaminergic neurons was observed to be mostly in the ventral tier of the SNc where MMP-3+ve cells were present in clusters, further emphasising MMP-3 involvement in dopaminergic neuronal cell death. To assess whether the observed MMP-3 expression is in fact the active enzyme, we monitored the expression of its downstream MMP, MMP-9. As our results demonstrate, a significant increase in the number of MMP-9 expressing cells was observed from days 1-15 after 6-OHDA lesion induction in the SNc ipsilateral to the lesioned hemisphere compared to the unlesioned hemisphere. Interestingly, in the control animals no constitutive expression of MMP-9 in the SNc was detected. Not only was MMP-9 expression very rapid following 6-OHDA lesioning but since no constitutive MMP-9 expression was observed, it is likely that MMP-9 expression is down-stream to MMP-3, further suggesting that MMP-3 is in its active form. This is in line with reports from Ogata et al., (1992) which demonstrated that MMP-3 was an activator for pro-MMP-9 *in vitro*. In addition, cell culture studies have shown that microglia-derived MMP-3 was critical for the activation of MMP-9 during LPS-induced inflammatory response (Rosenberg et al., 2001).

The observation that MMP-3+ve cells decreased in number by day 15 after 6-OHDA lesion induction when MMP-9+ve cells remained up-regulated through out the study indicated that MMP-3 activity might be involved in early cellular events and activates MMP-9 which subsequently may lead to cell death following 6-OHDA lesioning . However, it is worth noting that the significant increase in the number of MMP-9+ve cells in the SNc 24 hours after 6-OHDA lesioning could be through an MMP-3 independent pathway. To this end, other factors such as presence of pro-inflammatory cytokines such as, TNF-α and IFN–γ, are implicated in direct activation of MMP-9 (Lorenzl et al., 2004).

Morphological assessment and double immunofluorescence stainings revealed that MMP-3 and MMP-9+ve cells were expressed by neurons and not astrocytes. Indeed, *in vitro* studies demonstrated that astrocytes only express MMP-2 under basal conditions but not MMP-3 and MMP-9 (Colton et al., 1993; Wells et al., 1996). Our finding of the neuronal expression of MMP-3 and 9 in the SNc is in accord with

findings of Kim, et al, (2005, and 2007) who demonstrated that the active form of MMP-3 was in fact released from dopaminergic neurons and was most likely responsible for microglial activation and generation of NADPHO-derived superoxide, eventually enhancing nigrostriatal dopaminergic neuronal degeneration. We observed that the majority of neurons expressing MMP-3 or MMP-9 were morphologically intact, which may support the studies suggesting that MMP-3 release occurs early before any morphological changes indicative of apoptosis occur (Kim et al., 2007).

Specific expression of MMP-3 and 9 by neurons in the SNc following 6-OHDA administration could be an indication that the activation of MMP-3 and 9 in the SNc, following an insult, is not a heterogeneous response but rather it has a precise functional characteristic leading to the subsequent microglial activation and progression of dopaminergic neuronal cell death in the SNc. The exact role of MMPs in neuronal degeneration is however not clear. Previous reports by Yong et al., (1998) revealed that MMPs can exert direct neurotoxic effects to neurons *in vitro* by the destruction of component of the ECM, such as laminin. However, recent evidence suggests that although characterized for their ability to degrade matrix proteins, MMPs are becoming increasingly recognized as effectors of cell signalling (Conant et al., 2004). MMPs are able to cleave non-matrix proteins and thereby generate potential cell surface receptor signalling ligands. For example, MMP-1 can degrade insulin-like growth factor-binding proteins and thereby stimulate insulin-like growth factor signalling (Fowlkes et al., 1994**).** Another mechanism by which MMPs could affect cell survival might include direct effects on cell surface receptors raising the possibility that they may directly affect cell signalling. For example, MMP-9 and MMP-3 can both bind to CD44, a cell adhesion molecule involved in cell-cell and cell matrix interactions which regulate many pathological conditions such as brain tumour invasion (Stricker et al., 2001). In addition, MMP-1 can exert direct neurotoxic effects in neuronal cell cultures by dephosphorylation of Akt and through other non-proteolytic mechanism (Conant et al., 2004). MMPs not only exert direct neurotoxicity to neurons, but they can also lead to neurodegeneration indirectly. One indirect mechanism by which MMP-3 and MMP-9 activity leads to neurodegeneration in different brain diseases is by the activation of microglial cells. MMP-3 could potentially serve as a signalling molecule that mediates the interaction between apoptotic neurons, which are caspase-3+ve (*see Chapter 3*), and microglia in early apoptosis.

As demonstrated in our results microglial activation, characterised by up-regulation of MHC II and CD68 expressing microglia/macrophages, not only preceded dopaminergic cell death in the SNc following 6-OHDA lesioning but also occurred concomitant with an increase in MMP-3 and MMP-9 expression. Detailed discussion on the role MMPs in microglial activation in context of our findings may be found in the following section (*see section 4.4.2*)

4.4.2 Interaction between activated microglia and MMP-3 expressing neurons in the SNc following 6-OHDA lesion induction

6-OHDA MFB lesion induction led to the focal activation of microglia that was detected by their expression of OX6, a marker of major histocompatibility complex class II antigen presentation (Sugama et al., 2003) and CD68. CD68 is an antigen in the lysosomal membranes which stains phagocytic microglia (Croisier et al., 2005). The amount of CD68 expression in a single cell can be correlated to phagocytic activity of the respective cell type (Damoiseaux et al., 1994). Under normal conditions, microglia have a resting, ramified appearance with small somas and long fine processes (Vilhardt, 2004; Raivich et al., 1999). OX6 expressing activated microglia, were densely stained with enlarged cell bodies and thick contracted lamellipodia, while CD68 phagocytic microglia had an amoeboid macrophage-like appearance. OX6 expression was particularly dense in the medial aspect of the SNc, spreading laterally. CD68 expressing cells showed identical localisation and time dependent relocation to lateral portion of the SNc similar to OX6+ve microglia. A further indication of microglial activation is the increase in cell numbers (Raivich et al., 1999).

The increase in the number of OX6+ve activated microglia in the SNc was significant from day 7 after 6-OHDA lesion induction on the lesioned hemisphere compared to the unlesioned hemisphere. This coincided with a significant increase in the number of MMP-3+ve cells on the side of the lesion compared to the unlesioned side. Increases in the number of OX6+ve activated microglia and MMP-3+ve cells progressed in a time dependent manner and on day 9 after 6-OHDA lesioning concurred with significantly decrease in the number of dopaminergic TH positive neurons. This supports previous studies demonstrating that MMP-3 activated microglia may contribute to dopaminergic neuronal degeneration (Kim et al., 2007). In addition, the

early presence of phagocytic CD68 expressing microglia on day 3 after lesioning, when TH loss is not measurable, is an indication that early phagocytic activity may be taking place. MMP-3 expression not only occurred in parallel to OX6 expression but a significant increase in the number of CD68 expressing phagocytic microglia was also observed on day 9 after 6-OHDA lesioning . These findings indicated MMP-3 expression might be associated with microglial activation in the neurodegenerative process from a very early stage when there has been no apparent loss of dopaminergic neurons.

The kinetics of microglial activation and MMP-3 expression indicated that these two phenomena coincide in the SNc after 6-OHDA lesion induction, suggesting an involvement of MMP-3 activity and its downstream MMP, MMP-9, in microglial activation. This is further supported by our results showing the spatial interaction between activated microglia and MMP-3 expressing neurons. This was characterised by presence of OX6 and/or CD68+ve microglia/macrophages in close vicinity and even in contact with MMP-3+ve neurons. This interaction between OX6+ve microglia and MMP-3 expressing neurons was observed from 7-15 days after 6-OHDA lesioning. The continuous presence of MMP-3 +ve neurons and OX6+ve microglia at close proximity indicates that once MMP-3 was expressed in the SNc, it progressively contributed to the activation of microglia, which preceded the initiation of dopaminergic neuronal cell death.

Interaction between MMP-3+ve neurons and CD68+ve macrophages was observed from days 3-13 after 6-OHDA lesioning, suggesting that phagocytosis of damaged and/or apoptotic neurons is initiated very early in the process following 6-OHDA lesion induction. Up regulation of MMP-3 and MMP-9, that coincided with CD68 expression, plays a possible role in activation of phagocytic activity in the SNc. It has been demonstrated that in MMP-$3^{-/-}$ knockout mice, microglial activation and subsequent dopaminergic neuronal loss in the SNc and the striatum were attenuated following MPTP administration (Kim et al., 2007). The mechanism by which MMP-3 expression leads to microglial activation is not yet fully understood. Indeed, ECM molecules, such as laminin and fibronectin, are substrates of MMPs and can be modified or cleaved by MMPs to release soluble forms. Soluble ECM molecules have been demonstrated to regulate microglia/macrophages function (Chamak and Mallat, 1991; Tate et al., 2007). Studies on BV2 cell lines, demonstrated that in addition to

degradation of the ECM macromolecules by MMP-3, MMP-3 is involved in microglial activation through its enzymatic activity (Kim et al., 2005). It has been demonstrated that MMP-3 expression by chondorocytes was required for the generation of a macrophage chemoattractant and the subsequent infiltration of proteolytically active macrophages (Haro et al., 2000).

An additional finding of our study was a decrease in the levels of MMP-3 at day 15 to levels similar to the unlesion side. This could be due to the reduced levels of dopaminergic neurons present at this point, thus implicating MMP-3 as an early microglial activator. It also supports that dopaminergic neurons are releasing MMP-3 since their declining content leads to decreased MMP-3 expression. To further investigate the interaction between MMP-3 expressing neurons and microglia that lead to microglial activation in the SNc following 6-OHDA lesion induction we studied the dynamics of CD200R and its relation to both dopaminergic cell loss and MMP-3 expression.

4.4.2 The dynamics of CD200R expression in relation MMP-3 expression and dopaminergic neuronal cell death in the SNc

Interaction between neurons and microglia is a local modulator of microglial activation (Wang et al., 2007). In this study, we assessed both the kinetics of CD200R expression and the interaction between the CD200R expressing cells and dopaminergic neurons in the SNc following 6-OHDA lesion induction. CD200R belongs to the immunoglobulin super-family that received immunoregulatory signals from CD200 glycoprotein to regulate the activation of microglia. We demonstrated that the number of CD200R expressing cells increased in the SNc, on the lesioned hemisphere compared to the unlesioned hemisphere, in a time dependent manner following 6-OHDA lesioning. The number of these cells reached their maximum on day 13 but decreased there after. In sham and control animals CD200R was not expressed to a significant level. The kinetics of CD200R was very similar to that of MMP-3+ve neurons and OX6+ve microglia. The presence of CD200R+ve cells attached to the cell bodies and dendrites of dopaminergic neurons from 7-15 days after 6-OHDA lesion induction indicated that CD200-CD200R dysregulation occurs following 6-OHDA lesioning which leads to

expression of CD200R by microglia. Furthermore activated CD200R+ve cells demonstrated very similar properties to OX6+ve cells. These data support the immunomodulatory role of neuron-microglia interaction that keeps the microglia quiescence during homeostasis.

The time dependant relocation of C200R+ve cell from the medial portion of the nigra from day 7 up to day 15 to the more ventrolateral parts of the SNc is also similar to the dynamics of OX6+ve and CD68+ve microglia. However, the total number of CD200R+ve on average was lower than the OX6+ve microglia in our study. This might be an indication that CD200-CD200R interaction is a local modulator of microglial activation where it regulates the resident sub-population of microglia in the SNc.

Our study for the first time reports on a spatial relationship between MMP-3+ve neurons and CD200R+ve cell in the SNc (Fig 4.12). Attachment of CD200R+ve cells to MMP-3+ve neurons on days 3-7 after lesioning suggested that distribution in the ECM and expression of MMP-3 could play a role in the dissociation of CD200R from its ligand and subsequent activation of microglia. In addition, the observed dissociation of CD200R+ve cells from the MMP-3+ve neurons on day 9-15 further indicated that MMP-3 might be an early signalling molecule for activation of microglia in the initiation process of PD pathology that mediates the interactions with the ECM or cell surface receptors (Schlondorff and Blobel, 1999). Increased MMP activity leads to enhancement of proteolytic activity with simultaneous degradation of ECM component such as laminin. This might result in the alteration of adhesive contact with the extracellular matrix, and consequently the expression of cell- cell interaction proteins such as CD200/CD200R glycoprotein or other members of the IgG super family such as ICAMS (Hubbard and Rothlein, 2000).

Conclusions

Our results, clearly demonstrated that there is a temporal relationship between MMP-3/MMP-9 expressions and microglial activation followed by degeneration of dopaminergic neurons in the SNc in the 6-OHDA model. MMP-3 and MMP-9 may be released from injured dopaminergic neurons leading to the disturbance of the neuron-microglia interactions. Which was evident by CD200R up-regulation and activation of microglial cells that contributed to progressive dopaminergic neuronal cell death in SNc.

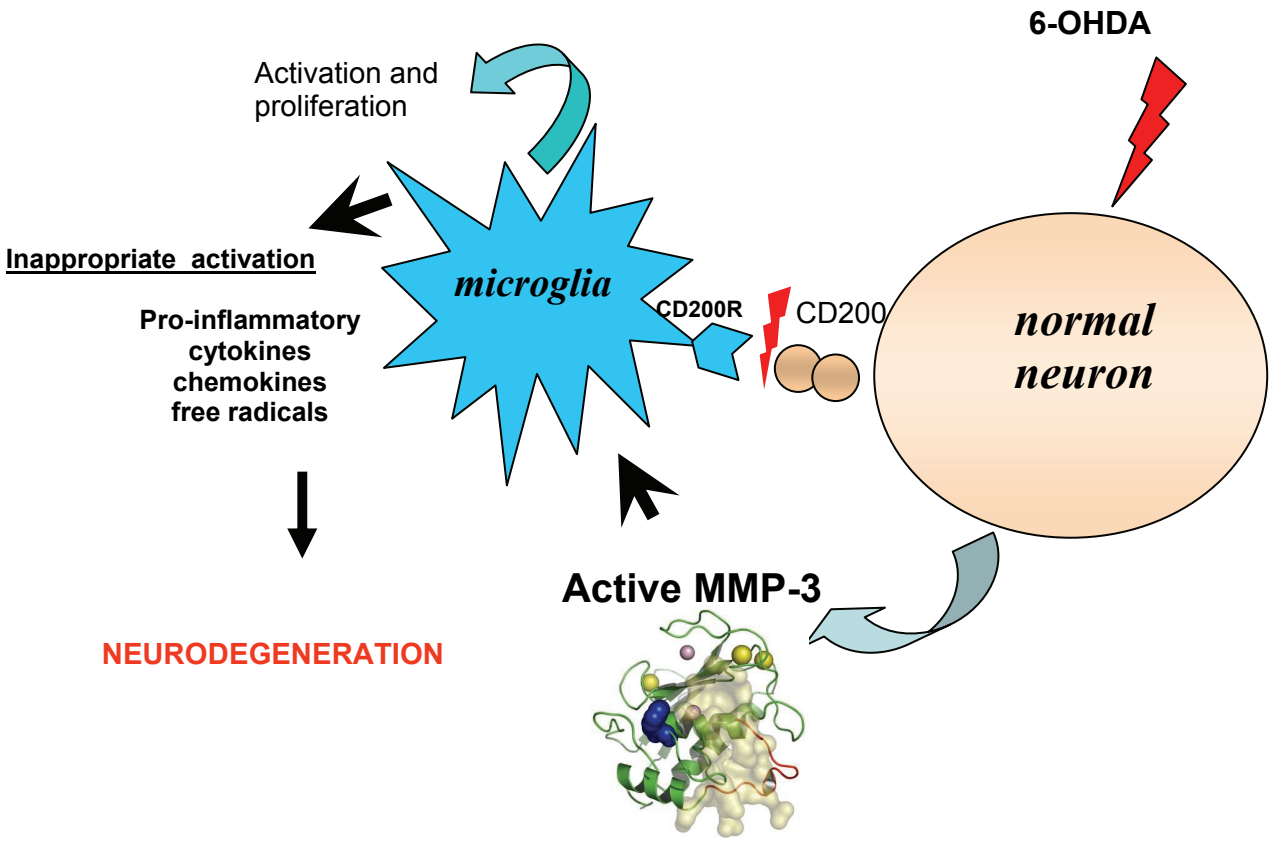

Fig 4.16 Cartoon showing the involvement of MMP-3 expression in microglial activation upon neuronal damage.

Upon 6-OHDA induced neuronal damage microglia are rapidly activated as a result of both a weakening neuronal inhibitory signals and activating stimulatory signals. Loss of neuronal integrity results in breakdown of microglial inhibitory molecules such as CD200-CD200R interaction. Instead, microglial stimulatory signals including MMP-3 are rapidly turned on and activate microglia. Activated microglia phagocytose at sites of neuronal damage, and increase in numbers, either from proliferation or recruitment, in order to remove damaged tissue and promote repair. However, their inappropriate activation as in neurodegenerative disorders causes direct damage to the CNS either by releasing potentially toxic substances such as proinflammatory cytokines, chemokines, NO, superoxide and prostanoids or by early phagocytosis against normal neurons

Chapter 5

Neuroprotective effects of modulation of glial activity by peroxisome proliferator activated receptor gamma (PPAR-γ) agonists in the 6-hdroxydopamine model of Parkinson's disease.

5.1 Introduction

Data from preceding chapters demonstrated that activation of microglia/macrophages prior to dopaminergic neuronal demise is strongly associated with the initiation and progression of dopaminergic neuronal cell death in the SNc following 6-OHDA lesioning. To elucidate the significance of microglial activation in dopaminergic neuronal loss in the SNc, the potential neuroprotective effects of modulation of glial activation was studied by targeting one of the players in the inflammatory process, the peroxisome proliferator activated receptor gamma sub-type (PPAR-γ).

5.1.1 PPAR-γ and inflammation

PPARs are members of a super-family comprising of the nuclear hormone receptors for steroids, thyroid hormones and retinoids, that were cloned more than 15 years ago (Issemann and Green, 1990) . Three different but structurally homologous PPAR isotypes (PPAR-α, PPAR-β, also known as δ, and PPAR-γ) have been identified in various species. PPARs (α,β/δ and γ) bind to specific DNA regions, the peroxisome proliferator response elements (PPREs) and enhance the expression of regulated genes that are mainly involved in reproduction, metabolism, development and the immune response. In addition, PPARs control gene expression, such as inhibition of pro-inflammatory genes independent of PPAR binding, through a poorly understood mechanism termed transrepression. This results in the inhibition of several transcription factors, including nuclear factor kB (NF-kB), activator protein-1 (AP-1) and activator of transcription-1 (STAT-1) (Kielian and Drew, 2003).

The distribution of PPARs in different organs has been studied in many species including humans and rodents. In both species, PPAR-α is mainly expressed in organs with high catabolic rates of fatty acids such as hepatocytes and cardiomiocytes (Palmer et al., 1998). PPAR-γ is mainly found in brown and white adipocytes and the nervous system. PPAR-β/δ is ubiquitously expressed, with a higher expression in the digestive tract and the placenta (Desvergne and Wahli, 1999; Escher et al., 2001).

Reflecting their distribution, PPARs act principally as lipid sensors and regulate whole-body metabolism in response to dietary intake of lipids (Michalik et al., 2006). PPAR-γ in particular stimulates lipid metabolism and adipocyte differentiation. In addition, activation of PPAR-γ is linked to reduction of serum glucose levels. This property has led to

the development of specific PPAR-γ agonists for the treatment of type 2 diabetes (Willson et al., 2001). The best-characterized synthetic PPAR-γ agonists belong to the insulin sensitizers, thiazolidinedione class of drugs, which includes pioglitazone (Actos®, Takeda Pharmaceutical Company Ltd, Osaka, Japan) and rosiglitazone (Avandia®, GlaxoSmithKline, Philadelphia, PA), both are used for treatment of type 2 diabetes. Other synthetic PPAR-γ agonists include, non-steroidal anti-inflammatory drugs (i.e. indomethacin, fenoprofen and flufenamic acid), (Lehmann et al., 1995). Endogenous ligands for PPARs include naturally occurring molecules, such as fatty acids and the prostaglandin D_2 metabolite, 15-deoxy-$\Delta^{12,14}$prostaglandin J_2 (15d-PGJ_2) that bind to PPAR-γ and stimulate transcription of target genes (Kliewer et al., 1994 ; Forman et al., 1995).

PPAR-γ despite having a major role in metabolic tissues, it is also expressed in several other cell types, including cells of the immune system such as macrophages, dendritic cells, eosinophils, T cells and B cells. Interestingly, it was documented that this receptor is expressed at high levels in mouse spleen (Kliewer et al., 1994) indicating its role in the immune system. In recent years, parallel to investigations on the functions of PPAR-γ in lipid metabolism, a new aspect of PPAR-γ function has been revealed and developed that is its potential anti-inflammatory activity (Bernardo et al., 2006). Studies by Ricote et al., (1998) demonstrated that murine activated peritoneal macrophages express high levels of PPAR-γ. Therefore, macrophages were the first cell type that linked PPAR-γ and inflammatory diseases. One of the first pieces of evidence suggesting a role for PPAR-γ in inflammation, came from the observation of an antagonistic effect of PPAR-γ on metabolic/pro-inflammatory effects of TNFα in adipocytes (Zhang et al., 1996). Furthermore Ricote et al., (1998) showed that natural and synthetic PPAR-γ agonists inhibit the expression of the inducible nitric oxide synthase (iNOS), matrix metalloproteinase 9 (MMP-9) and scavenger receptor A (SR-A) mRNAs *in vitro*. These and other similar *in vitro* observations led to a series of studies on anti-inflammatory effects of PPAR-γ ligands. Park et al., (2003) demonstrated that the PPAR-γ agonists including the naturally occurring, 15d-PGJ_2 and synthetic agonists such as rosiglitazone inhibit the phosphorylation of Janus kinase-signal transducers and activators of transcription (STAT1, STAT3, JAK1, and JAK2) in microglia and astrocytes. The authors further demonstrated that these agonists induce the expression of suppressor cytokine signalling (SOCS) 1 and 3, which alters JAK/STAT phosphorylation and JAK/STAT mediated signalling. Suggesting that activation of PPAR-γ is associated with an inhibitory effect on microglial response.

The dominant site of PPAR-γ action is the peripheral tissue, however in recent years considerable evidence has emerged on their role in the CNS. The role of PPARs in the CNS is mainly been related to lipid metabolism, however these receptors have been implicated in neural cell differentiation and death as well as in inflammation and neurodegeneration. The expression of PPAR-γ in the brain has been extensively studied in relation to inflammation and neurodegeneration (Heneka et al., 2000). The following section is an overview of the role of PPAR-γ in the brain with particular emphasis on its role in PD pathology.

5.1.2 Anti-inflammatory role of PPAR-γ in PD

There is increasing evidence to indicate that PPAR-γ has important roles in modulating neuroinflammation and neurodegeneration, therefore PPAR-γ represents a valuable therapeutic target in diseases such as PD, Alzheimer's disease (AD) and Multiple sclerosis (MS) where inflammation plays an integral role in their pathogenesis. A number of *in vitro* and *in vivo* studies have shown that PPAR-γ agonists are potent inhibitors of microglia-mediated production of cytotoxic factors. In LPS treated cortical neuron–glial co-cultures, PPAR-γ agonists reduced LPS induced expression of iNOS and COX-2 and protected neurons (Kim et al., 2002). In addition, studies on stimulated mouse microglia and astrocytes revealed that synthetic PPAR-γ agonists such as: rosiglitazone, pioglitazone, and ciglitazone alongside the naturally occurring 15d-PGJ(2) ligand, inhibited the production of nitric oxide, the pro-inflammatory cytokines TNFα, IL-1*β*, and IL-6, and the chemokine monocytes chemotactic protein 1 MCP-1 from microglia and astrocytes (Storer et al., 2005). Administration of PPAR-γ agonists to animals who have had LPS administered to the cerebellum, resulted in a significant inhibition of iNOS and other inflammatory genes that yielded neuroprotection (Heneka et al., 2000). These results suggest that PPAR-γ agonists play an anti-inflammatory role following an insult to the brain that leads to neuroprotection.

In experimental models of AD, the expression of iNOS in neurons was associated with a time-dependent neuronal cell death, which was prevented by activation of PPAR-γ *in vitro* and *in* vivo (Heneke et al., 1999; Heneka et al., 2000). In a model of MS, known as experimental allergic encephalomyelitis (EAE) induced in mice, Niino et al, (2001) demonstrated that PPAR-γ activation limited the development of clinical symptoms and the infiltration of the brain by peripheral leukocytes in EAE induced by myelin oligodendrocyte

glycoprotein peptide 35–55 ($MOG_{35–55}$). These newly appreciated anti-inflammatory actions of PPAR-γ agonists, may not only allow novel therapies for AD and MS but any other central nervous system diseases with an inflammatory component, including PD. PPAR-γ agonists inhibit several functions associated with microglial activation (Bernardo et al., 2000 and 2003), suggesting that these natural and synthetic compounds can have important roles in controlling brain inflammation. This could be of particular relevance in the case of endogenous molecules such as 15d-PGJ2 that can be produced within the brain and act in paracrine and/or autocrine manners (Bernardo et al., 2003) to modulate inflammation.

Given the *in vivo* and *in vitro* anti-inflammatory/neuroprotective effects of PPAR-γ agonists, the first studies to elucidate possible neuroprotective role of PPAR-γ agonists in models of PD utilised the MPTP mouse model of PD. MPTP treated mice were orally treated with synthetic PPAR-γ ligands to test the hypothesis that PPAR-γ mediated anti-inflammatory effects would exert neuroprotection. Breidert and colleagues (2002) found that pioglitazone (PPAR-γ agonist) treatment protected from MPTP-induced dopaminergic cell death in the SNc. This finding was confirmed by Dehmer, et al (2004) demonstrating that oral pioglitazone treatment also protected tyrosine hydroxylase-positive SNc neurons from MPTP-induced cell death. In both studies, pioglitazone decreased microglial and astrocyte activation and reduced the number of iNOS-positive cells in both the striatum and SNc. *In vitro* studies showed that PPAR-γ agonists act by blocking the differentiation of monocytes into reactive macrophages (Ricote et al., 1998) and the activation of microglia (Combs et al., 2000). The molecular mechanisms by which PPAR-γ activation inhibits inflammatory response are not yet fully understood. However, Dehmer, et al (2004) demonstrated that in MPTP treated mice this may have been achieved by reduced NFκB dependent signal transduction, since pioglitazone treatment induced a striatal increase of IκB-α, a direct inhibitor of NFκB nuclear translocation. Similar data have been generated using an intrastriatal LPS induced inflammation driven rat model of dopaminergic neurodegeneration, where pioglitazone effectively reduced microglial activation and protected dopaminergic neurons on the SNc (Hunter et al., 2007).

Recent epidemiological evidence, suggests that medication with non-steroidal anti-inflammatory drugs (NSAIDs), and in particular ibuprofen, may delay or prevent the development of PD (Chen et al., 2005). Since Ibuprofen crosses the blood–brain barrier and potentially acts as a PPAR-γ agonist (Lehmann et al., 1997), it is possible that PPAR-γ

activation contributes to the observed beneficial effect of Ibuprofen. Taken together, these data suggest that treatment with PPAR-γ agonists may offer a new therapeutic approach to the treatment of PD.

Given the neuroprotective properties of PPAR-γ agonists, this study for the first time investigated the potential anti-inflammatory effects of PPAR-γ agonists and their modulatory effect on the inflammatory cascade leading to dopaminergic cell death in 6-OHDA rat model of PD. To test whether activation of the gamma sub-type of PPARs is the only sub-type that exerts neuroprotective properties we also tested a PPAR-δ agonist.

Our hypothesis was that downgrading inflammation may have a neuroprotective impact on PD pathology. To address this hypothesis we set up our study with the following aims:

-To investigate the effect of different treatment regimes of PPAR-γ agonists (GW855266X) and pioglitazone on the extent of dopaminergic cell and striatal dopamine loss and glial response in the SNc following 6-OHDA lesion induction into the MFB (*see chapter 2 section 2.1.2*).

To satisfy these aims we studied two PPAR-γ agonists and one PPAR-δ agonist for their anti-inflammatory and neuroprotective properties in 6-OHDA rat model of PD. The first PPAR-γ agonist (GW855266X) tested was a compound developed and granted to us under the licence of GlaxoSmithKline (GSK). The dose used for this compound was determined and recommended by GSK according to their *in vitro* studies carried out internally. The second compound, which was also provided by GSK, was the clinically used PPAR-γ agonist, pioglitazone that was mainly used as our reference compound. The third GSK licensed compound was a PPAR-δ agonist (GW610742X) that was tested to determine whether the PPAR-γ sub-type was the only sub-type responsible for the beneficial effects observed. As described in the next section (*see section 5.2* Experimental design), the two PPAR-γ agonists and PPAR-δ agonist were tested in different treatment regimes in order to determine the most beneficial treatment strategy. Firstly, we have replicated the treatment regime used by Breidert at al, (2002), administering PPAR agonists prior to and after lesion induction with 6-OHDA. Secondly, in a highly novel and more clinically relevant regime has been exploited by administering the compounds post lesion induction. Finally, to assess

whether the potential neuroprotective effect of the PPAR-γ agonists is long lasting we have conducted drug withdrawal studies. The neuroprotective effects of different treatment regimes were assessed by investigating the integrity and functionality of the nigrostriatal tract as described in section 5.2 below. In addition as descried in section 5.2 the effects of different treatment regimes were assessed on the inflammatory response by investigating the activation and up-regulation of glial cells, as well as members of the matrix metalloproteinases in the SNc.

5.2 Experimental design

5.2.1 Treatments with GW855266X, pioglitazone and PPAR-δ agonist

To assess the potential anti-inflammatory/neuroprotective effects of GW855266X, pioglitazone and PPAR-δ agonist in the 6-OHDA model the effects of different treatment regimes on the integrity of the nigrostriatal system and the inflammatory response were compared. All treatments were administered orally via a gavage twice daily (p.o.b.i.d). The weight of the animals was monitored through out the study. The treatment regimes were chosen as follows:

A. Treating pre and post 6-OHDA lesion induction

These compounds were to be used for the first time in our study and thus we did not know which treatment regime would be most effective. To answer this question, in this initial study we chose to administer the compounds before 6-OHDA lesion induction (*see chapter 2 section 2.1.2)* and continue post lesion to test whether presence of either of these PPAR-γ and δ agonists would be neuroprotective in the 6-OHDA lesioned animals. Animals were divided into 4 groups (n=6). One group of animals was treated with pioglitazone (20mg/kg), another group was treated with GW855266X (5 mg/kg). The next group was treated with PPAR-δ agonist (10mg/kg) and the last group of animals served as controls and were treated with 0.5% methylcellulose as drug vehicle. Treatments were given p.o.b.i.d. for 14 consecutive days starting 7 days before 6-OHDA lesion induction and were continued for a further 7 days post lesioning. Animals were sacrificed on day 15 after 6-OHDA lesion induction. Upon achieving encouraging results with the PPAR-γ compounds we then administered them post 6-OHDA lesion induction a more clinically relevant treatment regime.

B. Post 6-OHDA lesion treatment regime

Our findings from the initial studies with PPAR-γ agonists, pioglitazone (20mg/kg) and GW855266X (5mg/kg) but not PPAR-δ agonist, administered pre and post 6-OHDA lesion induction were encouraging therefore, in this study the PPAR-γ agonists were administered after 6-OHDA lesion induction . To determine the neuroprotective and anti-

inflammatory effects of GW855266X and pioglitazone after 6-OHDA lesion induction, rats were divided into 3 groups (n=6). One group of animals was treated with pioglitazone (20mg/kg), another group was treated with GW855266X (5 mg/kg) and the last group of animals served as controls and were treated with 0.5% methylcellulose as drug vehicle. Treatments were given p.o.b.i.d. for 7 consecutive days starting from day 2 after 6-OHDA lesion induction (*see chapter 2 section 2.1.2)*. Animals were sacrificed on day 9 after lesioning and specimens were collected for HPLC-ECD and immunohistochemical analysis.

B1. Drug withdrawal following post lesion treatment

To investigate whether the neuroprotective effects of GW855266X and pioglitazone were long lasting or whether the continuous presence of the drugs was necessary to maintain their beneficial effect, rats were divided into 3 groups (n=6). One group of animals was treated with pioglitazone (20mg/kg), another group was treated with GW855266X (5mg/kg) and the last group of animals served as controls and were treated with 0.5% methylcellulose as vehicle. Treatments were given p.o.b.i.d. for 7 consecutive days starting from day 2 after 6-OHDA lesion induction, thereafter treatments were ceased for 7 consecutive days, animals were eventually sacrificed on day 16 after 6-OHDA lesion induction and specimens were collected for HPLC-ECD and immunohistochemical analysis.

5.2.2 Assessment of effects of GW855266X, pioglitazone and PPAR-δ in the 6-OHDA model

5.2.2.1 Assessment of the effects of GW855266X, pioglitazone and PPAR-δ on the nigrostriatal tract functionality after 6-OHDA lesion induction.

The effects of treatment with both PPAR-γ and PPAR-δ agonists and on the functionality of the nigrostriatal system was assessed by measuring the concentration of dopamine and its metabolites (ng/mg) in the striatum using HPLC-ECD and compared to the vehicle treated group. Detailed description of the HPLC procedure is found **(***see section 2.2.4)*.

5.2.2.2 Assessment of the effects of GW855266X, pioglitazone and PPAR-δ on the integrity of dopaminergic neurons in the SNc after 6-OHDA lesioning

For this purpose immunohistochemistry was performed for Tyrosine hydroxylase (TH) positive dopaminergic neurons (*see section 2.2.1.3*). The number and morphology of TH+ve cells were then determined according to the criteria described in (*see section 2.2.3*).

5.2.2.3 Assessment of the effect of GW855266X, pioglitazone and PPAR-δ on the extent of microglia/macrophages activation in the SNc after 6-OHDA lesion induction

To investigate the effects of treatment with GW855266X and pioglitazone on the extent of microglial/macrophages activation in the SNc and to compare it to the vehicle treated group, peroxidase immunohistochemistry was performed for both OX6 and CD68 expressions. Description of the antibodies used is listed below and details of the staining procedure are outlined in (*see section 2.2.1.4*):

OX6: was used to detect the population of activated microglial cells that express major histocompatibility complex II (MHC II) antigens.

CD68**:** was used to detect the activation of a population of macrophages with phagocytic function that expresses CD68 glycoprotein on their lysosomal membrane.

5.2.2.4 Assessment of the effects of GW855266X or pioglitazone on the extent of MMP-3 and 9 activation in the SNc after 6-OHDA lesion induction

To assess the effects GW855266X and pioglitazone on the expression of MMP3+ve and MMP-9+ve cells following 6-OHDA induction, peroxidase immunohistochemistry with Nickel enhancer was performed to detect the expression of the active form of MMP-3 and MMP-9 using the following antibodies, details of staining procedure is outlined in (*see chapter 2, section 2.2.1.4*):

MMP-3: A polyclonal antibody was used against the active form of MMP-3 enzyme mapping at C-terminus of the enzyme of human origin. This antibody recognises the 45 and 28 kDa active forms of the enzyme. MMPs are mainly responsible for the degradation of extracellular matrix components

MMP-9: A polyclonal antibody was used against the active form of MMP-9, also known as 92-kDa gelatinase/type IV collagenase, in mammals mapping near the C-terminus of MMP-9 of human origin. MMP-9 degrades the collagen of the extracellular matrix.

5.2.3 Statistical analysis of data

All data are presented as the mean ± SEM based on *n* independent observations. Multiple comparisons were made between and within groups using two-way ANOVA with *post-hoc* Newman-Keuls test. Striatal dopamine turnover, expressed as the mean values ± SEM calculated using the equation [DOPAC (pmol/ml +HVA (pmol/ml)/DA (pmol/ml)]. Differences were considered statistically significant at $p<0.05$ and all statistical analysis were performed using GraphPad Prism v5.00 software (GraphPad software, San Diego, CA, USA).

5.3 Results

5.3.1 Neuroprotective effects of treatment with GW855266X and pioglitazone but not PPAR–δ agonist administered 7 days before and continued for 7 days after 6-OHDA lesion induction

5.3.1.1 Effect of treatment with GW855266X (5mg/kg) and Pioglitazone (20mg/kg) and PPAR-δ agonist (10mg/kg) administered before and after 6-OHDA lesion induction on striatal dopamine concentration (ng/mg).

To assess whether presence of GW855266X (5mg/kg), pioglitazone (20mg/kg) and PPAR-δ agonist (10mg/kg) in the brain before and after 6-OHDA lesion induction was neuroprotective, the PPAR agonists were administered p.o.b.i.d. for 14 consecutive days starting 7 days before 6-OHDA lesion induction that was continued for further 7 days post lesioning. It is noteworthy to mention that the weight of animals did not show any unexpected changes throughout all the treatment regimes in this study.

As Fig 5.1 shows, in vehicle treated animals the striatal dopamine content was significantly decreased by ~62% in the lesioned hemisphere compared to the unlesioned hemisphere following 6-OHDA lesion induction [lesioned: 4.88 ± 2.31 (ng/mg), unlesioned: 12.99 ± 0.93 (ng/mg), $p<0.001$]. In addition, striatal levels of dopamine metabolites, DOPAC and HVA were also significantly decreased by ~45% and ~ 52% respectively in the lesioned hemisphere compared to the unlesioned hemisphere following 6-OHDA lesioning (Table 5.1). In the vehicle treated animals, dopamine turn over increased significantly by ~70% in the lesioned hemisphere compared to the unlesioned hemisphere, indicative of compensatory dopamine production by the surviving neurons. However, treatment with GW855266X (5mg/kg) before and after lesion induction led to a significant preservation of the dopamine content in the striatum in the lesioned hemisphere compared to the lesioned hemisphere in vehicle treated 6-OHDA lesioned animals [Drug treated-lesioned: 9.39 ± 0.52 (ng/mg), vehicle treated-lesioned: 4.88 ± 2.31 (ng/mg),$p<0.05$]. In addition, treatment with GW855266X (5mg/kg) led to preservation of both DOPAC and HVA in the lesioned hemisphere compared to the lesioned hemisphere in the vehicle treated animals. This was concurrent with a significant decrease in dopamine turnover in the striatum compared to the lesioned hemisphere in vehicle treated animals (Table 5.1). Similarly, treatment with pioglitazone (20mg/kg) before and after lesion induction led to a

significant preservation of the striatal dopamine content in the lesioned hemisphere compared to the lesioned hemisphere in vehicle treated animals [Drug treated-lesioned: 9.37 ± 0.96 (ng/mg), vehicle treated-lesioned: 4.88 ± 2.31 (ng/mg),*p<0.01*] (Fig 5.1). This was concomitant with significant preservation of striatal dopamine metabolites, DOPAC and HVA (Table 5.1). In addition, dopamine turn over was also decreased significantly and normalised in the lesioned hemisphere following pioglitazone treatment compared to the lesioned hemisphere in vehicle treated animals (Table 5.1). Unlike PPAR-γ agonists treatment with PPAR-δ agonist did not show any protective properties which was evident in a significant depletion of striatal dopamine content in the lesioned hemisphere compared to the lesioned hemisphere in the vehicle treated animals following 6-OHDA lesion induction [(Drug treated-lesioned: 3.87 ± 1.39 (ng/mg), vehicle treated-lesioned: 4.88 ± 2.31 (ng/mg), *p<0.05*]. In addition striatal dopamine metabolites, DOPAC and HVA were significantly depleted (Table 5.1)

Hence, PPAR-δ agonist (10mg/kg) did not have any neuroprotective properties; therefore we did not pursue the studies on this compound further. However, treatment with GW855266X (5mg/kg) and pioglitazone (20mg/kg), before and after the 6-OHDA lesion induction, led to the preservation of striatal dopamine and its metabolites.

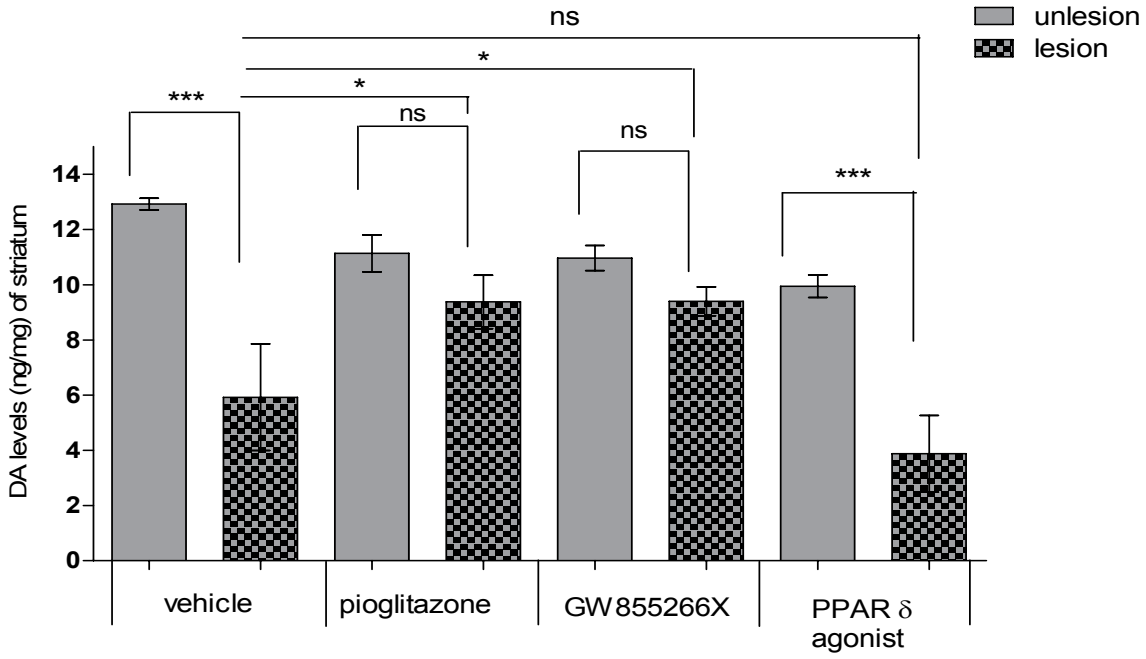

Fig 5.1 Protective effect of treatment with pioglitazone and GW855266X administered 7 days pre and 7 days post 6-OHDA lesion induction on nigrostriatal functionality in the lesioned hemisphere compared to the lesioned hemisphere in the vehicle treated animas. Graph demonstrates the concentration of striatal dopamine ng/mg in different groups of treatment.

In vehicle treated animals the striatal dopamine content was significantly decreased in the lesioned hemisphere compared to the unlesioned hemisphere following 6-OHDA lesion induction. However, treatment with pioglitazone (20mg/kg) and GW855266X (5mg/kg) before and after lesion induction led to a significant preservation of the dopamine content in the striatum in the lesioned hemisphere compared to the lesioned hemisphere in the vehicle treated 6-OHDA lesioned animals. Unlike PPAR-γ agonists treatment with PPAR-δ agonist did not show any protective properties which was evident in a significant depletion of striatal dopamine content in the lesioned hemisphere compared to the lesioned hemisphere in the vehicle treated animals following 6-OHDA lesion induction. Results are presented as mean striatal dopamine ng/mg of wet tissue weight ±SEM. * $p<0.5$ ** $p<0.01$, *** $p< 0.001$, *ns*= not significant. Number of animals was 6/group per treatment group. ***Treatment regime:***

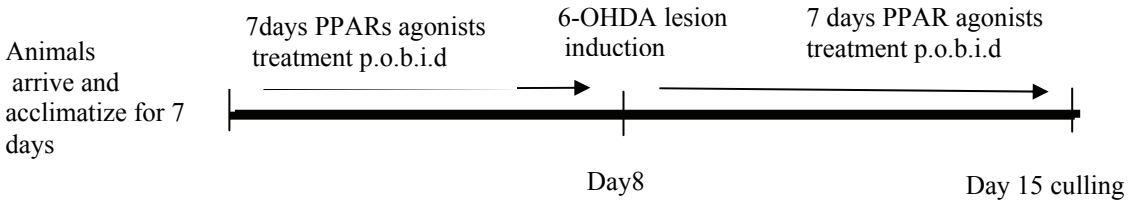

	DOPAC (ng/mg)	HVA (ng/mg)	Dopamine turnover (pmol/mg)
Vehicle	Lesion: 0.924 ± 0.2 Unlesion: 1.67 ± 0.27 *p<0.5*	Lesion: 0.49 ± 0.06 Unlesion: 1.02 ± 0.34 *P<0.5*	Lesion: 40.29 ± 21.66 Unlesion: 12.46 ± 1.41 *p<0.1*
GW855266X (5mg/kg)	Lesion: 1.19 ± 0.67 Unlesion: 1.55 ± 0.62 *p>0.5*	Lesion: 0.36 ± 0.13 Unlesion: 0.44 ± 0.17 *p>0.5*	Lesion: 24.17 ± 2.52 Unlesion: 22.07 ± 3.15 *P>0.5*
Pioglitazone (20mg/kg)	Lesion: 1.20 ± 0.19 Unlesion: 1.43 ± 0.17 *p>0.5*	Lesion: 0.48 ± 0.30 Unlesion: 0.60 ± 0.49 *p>0.5*	Lesion: 22.68 ± 5.75 Unlesion: 23.51 ± 4.70 *p>0.5*
PPAR-δagonis (10mg/kg)	Lesion: 0.60 ±0.20 Unlesion: 1.19 ±0.05 *p<0.5*	Lesion: 0.17 ± 0.05 Unlesion: 0.40 ± 0.03 *p<0.5*	Lesion: 28.28 ±2.99 Unlesion: 16.46 ±2.26 *P<0.5*

Table 5.1 Treatment with pioglitazone and GW855266X administered 7 days pre and 7 days post 6-OHDA lesion induction led to preservation of the mean concentration of striatal dopamine metabolites: DOPAC and HVA in addition to dopamine turnover in the lesioned hemisphere compared to the unlesioned hemisphere in drug and vehicle treated animals.

Table shows that in the vehicle treated animals, striatal levels of dopamine metabolites, DOPAC and HVA were significantly decreased in the 6-OHDA lesioned hemisphere compared to the unlesioned hemisphere. In addition, in these animals following 6-OHDA lesion induction striatal dopamine turn over increased significantly in the lesioned hemisphere compared to the unlesioned hemisphere. Treatment with GW855266X (5mg/kg) and pioglitazone (20mg/kg) before and after lesion induction led to a significant preservation of both DOPAC and HVA in the lesioned hemisphere compared to the lesioned hemisphere in the vehicle treated animals. That was concurrent with a normalisation of striatal dopamine turn over in the 6-OHDA lesioned hemisphere compared to lesioned hemisphere. Treatment with PPAR-δ agonist pre and post 6-OHDA lesion induction did not show any protective properties which was evident in a significant depletion of striatal DOPAC and HVA and an increase in dopamine turn over in the lesioned hemisphere compared to the unlesioned hemisphere. Concentration of striatal dopamine metabolites are shown as ng/mg of wet tissue weight ±SEM. Mean striatal monoamine turnover ratio was calculated using the expression ((DOPAC+HVA)/DA). Number of animals was 6/group per treatment group. $p<0.5$ was considered significant.

5.3.1.2 Effect of treatment with GW855266X (5mg/kg) and pioglitazone (20mg/kg) administered before and after 6-OHDA lesion induction on the number of TH+ve dopaminergic neurons in the SNc

TH+ve dopaminergic cell counts in vehicle treated animals showed a significant decrease in the number of TH+ve dopaminergic neurons in the lesioned hemisphere compared to the unlesioned hemisphere (lesioned: 40.69 ± 3.73, unlesioned: 66.38 ± 2.9, $p<0.001$) (Fig. 5.2). However, treatment with GW855266X (5mg/kg) p.o.b.i.d before and after 6-OHDA lesion induction led to amelioration of the loss of TH+ve dopaminergic cells in the SNc in the lesioned hemisphere compared to the lesioned hemisphere in vehicle treated animals (Drug treated-lesioned: 51.14 ± 3.24 , vehicle treated-lesioned: 40.69 ± 3.73, $p<0.05$). Thus, the presence of GW855266X (5mg/kg) in the brain prior to 6-OHDA lesioning was neuroprotective in the SNc and prevented dopamine depletion in the striatum. In addition, similar neuroprotective properties were observed with pioglitazone (20mg/kg) administered p.o.b.i.d before and after 6-OHDA lesion induction. Nigral TH+ve dopaminergic cell counts revealed a significant amelioration of dopaminergic cell death in the lesioned hemisphere compared to the lesioned hemisphere in vehicle treated animals (Drug treated-lesioned: 49.70 ± 2.62 , vehicle treated-lesioned: 40.69 ± 3.73, $p<0.05$).

Thus, presence of GW855266X and pioglitazone in the brain before and after 6-OHDA lesioning exerted beneficial effects that were characterised by significant protection of dopaminergic neurons in the SNc and inhibition of dopamine depletion in the striatum. We further assessed the effects of GW855266X and pioglitazone on the microglia/macrophage activation in the SNc, the data obtained are presented in the following sections.

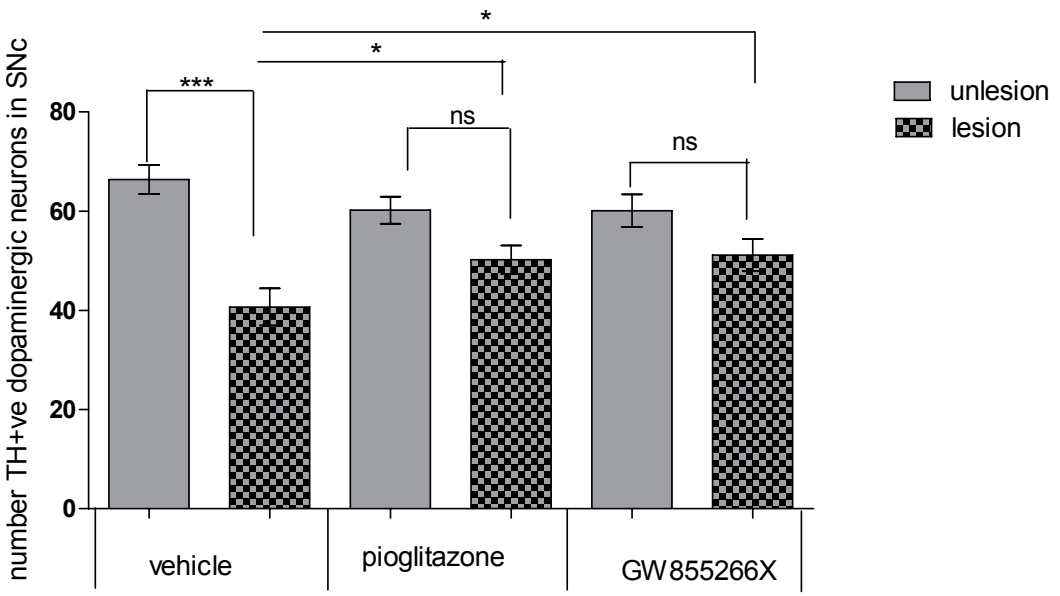

Fig 5.2 Treatment with pioglitazone and GW855266X administered 7 days pre and 7 days post 6-OHDA lesion induction protected nigral TH+ve dopaminergic neurons in the lesioned hemisphere compared to the lesioned hemisphere in the vehicle treated animals. Graph demonstrates the number mean number of TH+ve dopaminergic neurons in the SNc of different treatment groups

In vehicle treated animals the number of TH+ve dopaminergic neurons significantly decreased in the lesioned hemisphere compared to the unlesioned hemisphere following 6-OHDA lesion induction. However, treatment with both pioglitazone (20mg/kg) and GW855266X (5mg/kg) before and after lesion induction led to a significant decrease in TH+ve dopaminergic neuronal cell demise in the lesioned hemisphere compared to the lesioned hemisphere in vehicle treated 6-OHDA lesioned animals.. Results are presented as mean number of cells ±SEM. * p<0.5 ** *p<0.01*, *** *p< 0.001*, *ns*= not significant. Number of animals was 6/group per treatment group.

5.3.2 Treatment with GW855266X and pioglitazone administered 7 days before and continued for 7 days after 6-OHDA lesion induction exerted anti-inflammatory properties

5.3.2.1 GW855266X (5mg/kg) and pioglitazone (20mg/kg) treatment for 7 days before and 7 days after 6-OHDA lesion induction inhibited the activation of OX6+ve and CD68+ve microglia/macrophages in the SNc

To assess whether the presence of GW855266X (5mg/kg) and pioglitazone (20mg/kg) in the brain before and after 6-OHDA lesion induction would inhibit or reduce the number of activated microglia/macrophages in the SNc treatments were given p.o.b.i.d. for 14 consecutive days starting 7 days before 6-OHDA lesion induction that was continued for further 7 days post lesioning.

Cell counts in the SNc demonstrated that in the vehicle treated animals, OX6+ve microglial cells significantly increased in number in the 6-OHDA lesioned hemisphere compared to the unlesioned hemisphere (lesioned: 23.14± 3.57, unlesioned: 0.45± 0.31, $p<0.001$). OX6+ve microglia were morphologically active with enlarged somas and thickened processes. These cells were focally accumulated in the medial and lateral portions of the SNc in the lesioned hemisphere. Interestingly, treatment with GW855266X (5mg/kg) before and after 6-OHDA lesion induction led to a significant decrease in the number of activated OX6+ve microglia in both lateral and medial potions of the SNc in the lesioned hemisphere compared to lesioned hemisphere in the vehicle treated animals (Drug treated-lesioned 7.53± 3.13, vehicle treated-lesioned 23.14± 3.57, $p<0.001$) (Fig 5.3A). In parallel, in vehicle treated animals cell count for CD68+ve macrophages in the SNc demonstrated a significant increase in CD68+ve cell numbers in the lesioned hemisphere compared to the unlesioned hemisphere following 6-OHDA lesion induction (lesioned: 14.80 ± 4.57, unlesioned: 0.0, $p<0.001$) (Fig 5.3B) . As mentioned in previous sections these cells had an activated amoeboid morphology and were located similarly to OX6+ve microglia in lateral and medial portions of the SNc. Treatment with GW855266X (5mg/kg) before and after 6-OHDA lesion induction led to a significant inhibition of the number of CD68+ve macrophages in the lesioned hemisphere in the SNc compared to the lesioned hemisphere in the vehicle treated animals (Drug treated-lesioned: 1.83 ± 1.09, vehicle treated-lesioned: 14.80 ± 4.57, $p<0.001$) (Fig 5.3B). CD68+ve macrophages were inhibited in both medial

and lateral portions of the SNc. Thus, treatment with GW855266X (5mg/kg) for 7 days before 6-OHDA lesion induction and 7 days after led to a significant inhibition of active gliosis characterised by inhibition of both OX6 and CD68+ve microglia/macrophages activity in the SNc. Similarly, treatment with pioglitazone (20mg/kg) before and after 6-OHDA lesion induction led to a significant decrease in the number of activated OX6+ve microglia in both lateral and medial portions of the SNc in the lesioned hemisphere compared to lesioned hemisphere in the vehicle treated animals (Drug treated-lesioned 9.33± 2.34, vehicle treated-lesioned 23.14± 3.57, $p<0.001$) (Fig 5.3A). In addition cell counts for CD68+ve macrophages in the SNc showed that treatment with pioglitazone (20mg/kg) before and after 6-OHDA lesion induction led to a significant inhibition of CD68+ve macrophages in the lesioned hemisphere compared to the lesioned hemisphere in the vehicle treated animals (Drug treated-lesioned: 1.83 ± 0.77, vehicle treated-lesioned: 14.80 ± 4.57, $p<0.001$) (fig 5.3B). CD68+ve macrophages were inhibited in both medial and lateral portions of the SNc.

Thus, treatment with pioglitazone (20mg/kg) for 7 days before 6-OHDA lesioning and 7 days after led to a significant inhibition of active gliosis characterised by inhibition of both OX6 and CD68+ve microglia/macrophages activity in the SNc.

Taken together, the presence of GW855266X and pioglitazone in the brain before 6-OHDA lesion induction and continued drug administration for 7 days after lesioning exerts neuroprotective properties and a modulation of the inflammatory response. Having obtained positive results with GW855266X and pioglitazone using the above mentioned treatment regime, which also replicated the findings of Dehmer at al (2004) in the MPTP model, we then decided to administer these compound in a more clinically relevant regime and assess their neuroprotective and anti-inflammatory effects. Therefore, the following section presents our findings on therapeutic treatment regime with these compounds where they are administered post 6-OHDA lesion induction.

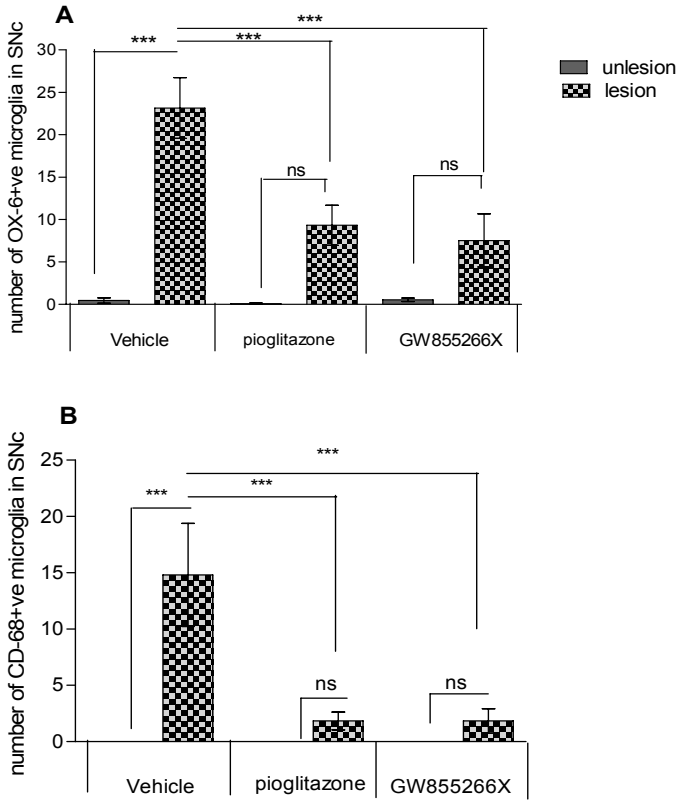

Fig 5.3 Graphs shows anti-inflammatory effect of treatment with PPAR-γ agonists for 14 consecutive days starting 7 days before 6-OHDA lesion induction and continuing for further 7 days. This is demonstrated as significant decrease in the number of OX6+ve and CD68+ve microglia/macrophages in the SNc ipsilateral to the 6-OHDA lesioned hemisphere compared to the lesioned hemisphere in the vehicle treated animals.

Graph A: Shows the number of OX6+ve microglia in the SNc in the vehicle and PPAR-γ agonists [pioglitazone (20mg/kg) and GW855266X (5mg/kg)] treated animals. Immunohistochemistry was performed with OX6 antibody that detects the population of microglial cells expressing MHC II antigens. In the vehicle treated animals the number of OX6+ve microglial cells increased significantly following 6-OHDA lesion induction. Treatment with both pioglitazone (20mg/kg) and GW855266X (5mg/kg) resulted in a significant decrease in the number OX6+ve microglial cells in the SNc ipsilateral to 6-OHDA lesion side compared to the lesioned hemisphere in vehicle treated animals. Results are presented as mean number of cell± SEM. * p<0.5 ** *p<0.01*, *** *p< 0.001*, *ns*= not significant. Number of animals was 6/group per time point.

Graph B: Shows the number of CD68+ve macrophages in the SNc in the vehicle and PPAR-γ agonists [pioglitazone (20mg/kg) and GW855266X (5mg/kg)] treated animals. Immunohistochemistry was performed with CD68 antibody that detects phagocytic macrophages. In the vehicle treated animals the number of OX6+ve microglial cells increased significantly following 6-OHDA lesion induction. Treatment with both pioglitazone (20mg/kg) and GW855266X (5mg/kg) resulted in a significant decrease in the number CD68+ve microglial cells in the SNc ipsilateral to 6-OHDA lesion side compared to the lesioned hemisphere in vehicle treated animals. Results are presented as mean number of cell± SEM. * p<0.5 ** *p<0.01*, *** *p< 0.001*, *ns*= not significant. Number of animals was 6/group per time point.

5.3.3 Neuroprotective effects 7 day continuous treatment with PPAR-γ agonists post 6-OHDA lesion induction

5.3.3.1 Effects of GW855266X (5mg/kg) and pioglitazone (20mg/kg) on the concentration (ng/mg) of dopamine in the striatum administered for 7 days after 6-OHDA lesion induction

In the vehicle treated animals, striatal dopamine content was significantly decreased by ~67% in the lesioned hemisphere compared to the unlesioned hemisphere following 6-OHDA lesion induction [lesioned: 4.92 ± 2.5 (ng/mg), unlesioned: 14.99 ± 2.37 (ng/mg), $p<0.001$] (Fig 5.4). In addition, 6-OHDA lesion induction in vehicle treated animals led to depletion of dopamine metabolites, DOPAC and HVA by ~65% and ~51% respectively in the lesioned hemisphere compared to the unlesioned hemisphere. This was concomitant with a significant increase in dopamine turn over in the lesioned hemisphere compared to the unlesioned hemisphere by ~60% (Table 5.2). However, 7 days treatment with GW855266X (5mg/kg) p.o.b.i.d starting 2 days after 6-OHDA lesioning led to a significant preservation of the dopamine content in the striatum in the lesioned hemisphere compared to the lesioned hemisphere in the vehicle treated animals [Drug treated-lesioned: 11.79 ± 1.44 (ng/mg), vehicle treated-lesioned: 4.92 ± 2.5 (ng/mg), $p>0.05$] (Fig 5.4). This was concomitant with the preservation of striatal dopamine metabolites, DOPAC and HVA compared to vehicle treated animals (Table 5.2). Thus, post-lesion continuous treatment for 7 days with GW855266X (5mg/kg) protected the functional integrity of the nigrostriatal system. Very similar effects were also observed when animals were treated for 7 days with pioglitazone (20mg/kg) p.o.b.i.d starting 2 days after 6-OHDA lesioning. Treatment led to a significant preservation of striatal dopamine concentration in the lesioned hemisphere compared to the lesioned hemisphere in vehicle treated animals [Drug treated-lesioned: 10.24 ±0.97 (ng/mg), vehicle treated-lesioned: 4.92 ± 2.5 (ng/mg), p<0.001] (Fig 5.4). Dopamine metabolites, DOPAC and HVA were also significantly preserved in the lesion hemisphere compared to vehicle treated animals (Table 5.2). Evidently, dopamine turn over was also reduced significantly and normalised in the lesioned hemisphere compared to the vehicle treated animals (Table 5.2). Thus, treatment with GW855266X (5mg/kg) and pioglitazone (20mg/kg) starting 2 days post 6-OHDA lesion induction was shown to have significant neuroprotective properties and inhibit dopamine depletion in the striatum.

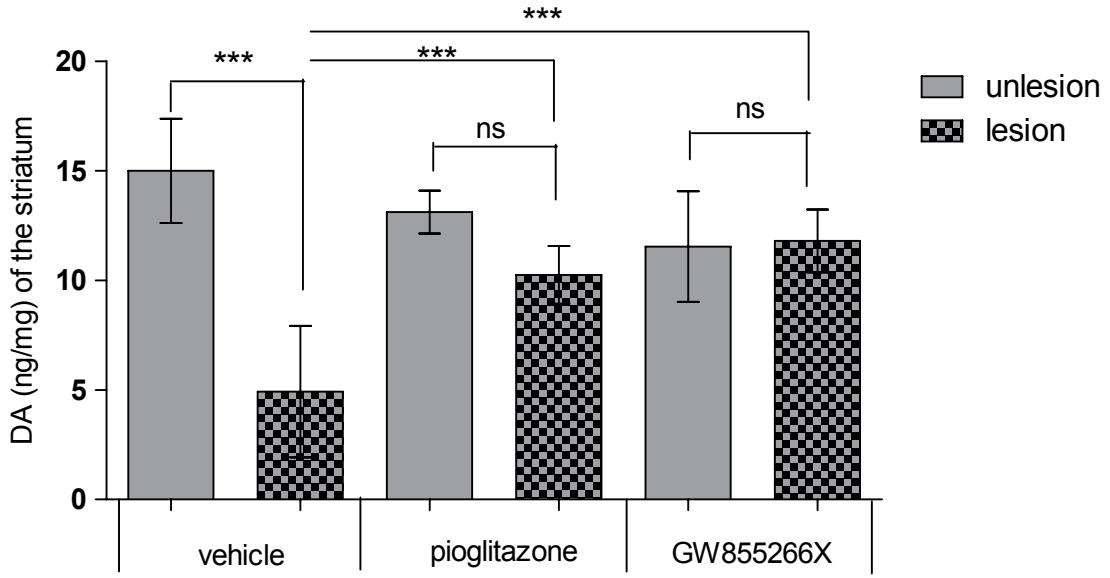

Fig 5.4 Protective effect of treatment with pioglitazone and GW855266X administered 7 days post 6-OHDA lesion induction on nigrostriatal functionality in the lesioned hemisphere compared to the lesioned hemisphere in the vehicle treated animals. Graph demonstrates the concentration of striatal dopamine ng/mg in different groups of treatment.

In vehicle treated animals the striatal dopamine content was significantly decreased in the lesioned hemisphere compared to the unlesioned hemisphere following 6-OHDA lesion induction. However, post 6-OHDA lesion treatment with pioglitazone (20mg/kg) and GW855266X (5mg/kg) led to a significant preservation of the dopamine content in the striatum in the lesioned hemisphere compared to the lesioned hemisphere in the vehicle treated 6-OHDA lesioned animals. Results are presented as mean striatal dopamine ng/mg of wet tissue weight ±SEM. * p<0.5 ** *p<0.01*, *** *p< 0.001*, *ns*= not significant. Number of animals was 6/group per treatment group. ***Treatment regime:***

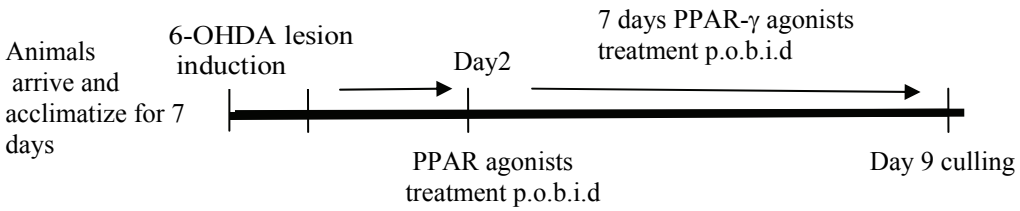

	DOPAC (ng/mg)	HVA (ng/mg)	Dopamine turnover (pmol/mg)
Vehicle	Lesion: 0.924 ± 0.40 Unlesion: 2.61 ± 0.33 *p<0.5*	Lesion: 0.48 ± 0.19 Unlesion: 0.99 ± 0.08 *P<0.5*	Lesion: 30.03 ± 8.5 Unlesion: 11.96 ± 0.95 *p<0.1*
GW855266X (5mg/kg)	Lesion: 1.19 ± 0.67 Unlesion: 1.55 ± 0.62 *p<0.5*	Lesion: 0.46 ± 0.11 Unlesion: 0.45 ± 0.17 *p>0.5*	Lesion: 10.70 ± 1.71 Unlesion: 8.68 ± 1.07 *P>0.5*
Pioglitazone (20mg/kg)	Lesion: 1.03 ± 0.10 Unlesion: 1.59 ± 0.32 *p>0.5*	Lesion: 0.90 ± 0.12 Unlesion: 1.12± 0.58 *p>0.5*	Lesion: 10.09 ± 2.42 Unlesion: 11.97 ± 1.71 *p>0.5*

Table 5.2 Treatment with pioglitazone and GW855266X administered for 7 days post 6-OHDA lesion induction led to preservation of the mean concentration of striatal dopamine metabolites: DOPAC and HVA in addition to dopamine turnover in the lesioned hemisphere compared to the unlesioned hemisphere in drug and vehicle treated animals.

Table shows that in the vehicle treated animals striatal levels of dopamine metabolites, DOPAC and HVA were significantly decreased in the 6-OHDA lesioned hemisphere compared to the unlesioned hemisphere. In addition in these animals following 6-OHDA lesion induction striatal dopamine turn over increased significantly in the lesioned hemisphere compared to the unlesioned hemisphere. Treatment with GW855266X (5mg/kg) and pioglitazone (20mg/kg) for 7 days administered post 6-OHDA lesion induction led to a significant preservation of both DOPAC and HVA in the lesioned hemisphere compared to the lesioned hemisphere in the vehicle treated animals. That was concurrent with a normalisation of striatal dopamine turn over in the 6-OHDA lesioned hemisphere compared to lesioned hemisphere. Concentration of striatal dopamine metabolites are shown as ng/mg of wet tissue weight ±SEM. Mean striatal monoamine turnover ratio was calculated using the expression ((DOPAC+HVA)/DA). Number of animals was 6/group per treatment group. *p<0.5* was considered significant.

5.3.3.2 Effects of GW855266X (5mg/kg) and pioglitazone (20mg/kg) on the number of TH+ve dopaminergic neurons in the SNc administered for 7 days following 6-OHDA lesion induction

TH+ve cell counts revealed that in the vehicle treated animals, a significant number of TH+ve dopaminergic neurons were lost in the lesioned hemisphere compared to the control unlesioned hemisphere following 6-OHDA lesioning (lesioned: 35.5 ± 2.97, unlesioned: 66.0 ± 4.46, $p<0.001$) (Fig 5.5). However, 7 days treatment with GW855266X (5mg/kg) p.o.b.i.d starting 2 days after 6-OHDA lesioning led to amelioration of nigral TH+ve dopaminergic cell death in the lesioned side compared to the lesioned side of the vehicle treated animals (Drug treated-lesioned: 61.67± 3.25 , vehicle treated-lesioned: 35.5 ± 2.97 , $p<0.001$) (Fig 5.5). Thus, post-lesion 7 day continuous treatment with GW855266X (5mg/kg) protected the integrity of the nigrostriatal tract. In parallel, pioglitazone treatment led to a significant amelioration of nigral TH+ve dopaminergic neuronal demise following 6-OHDA lesioning. 7 days treatment with pioglitazone (20mg/kg) p.o.b.i.d starting 2 days after 6-OHDA lesioning led to a significant protection of TH+ve dopaminergic neurons in the SNc in the lesioned hemisphere compared to the lesioned hemisphere in vehicle treated animals (Drug treated-lesioned: 61.67± 3.25 , vehicle treated-lesioned: 35.5 ± 2.97, $p>0.05$) (Fig 5.5).

Thus, treatment with GW855266X (5mg/kg) and pioglitazone (20mg/kg) starting 2 days post 6-OHDA lesion induction was shown to have significant neuroprotective properties in the SNc and inhibit dopamine depletion in the striatum. To further assess the effects of treatments on the state of inflammation in the SNc, activation of microglia/macrophages were studied, the data are presented in the following section.

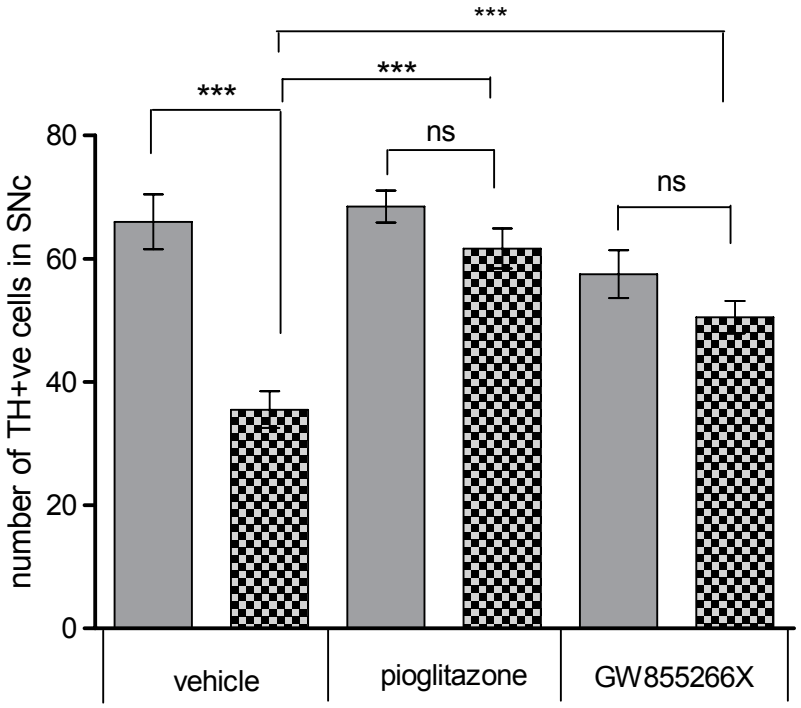

Fig 5.5 Treatment with pioglitazone and GW855266X administered for 7 days post 6-OHDA lesion induction protected nigral TH+ve dopaminergic neurons in the lesioned hemisphere compared to the lesioned hemisphere in the vehicle treated animals. Graph demonstrates the number mean number of TH+ve dopaminergic neurons in the SNc of different treatment groups

In vehicle treated animals the number of TH+ve dopaminergic neurons significantly decreased in the lesioned hemisphere compared to the unlesioned hemisphere following 6-OHDA lesion induction. However, treatment with both pioglitazone (20mg/kg) and GW855266X (5mg/kg) for 7 days after lesion induction led to a significant decrease in TH+ve dopaminergic neuronal cell demise in the lesioned hemisphere compared to the lesioned hemisphere in vehicle treated 6-OHDA lesioned animals. Results are presented as mean number of cells ±SEM. * $p<0.5$ ** $p<0.01$, *** $p< 0.001$, *ns*= not significant. Number of animals was 6/group per treatment group.

5.3.4 Continuous 7 day treatment with GW855266X and pioglitazone after 6-OHDA lesion induction exerted anti-inflammatory properties

5.3.4.1 Continuous 7 day treatment with GW855266X (5mg/kg) and pioglitazone (20mg/kg) decreased the number of activated OX6+ve and CD68+ve microglia/macrophages in the SNc following 6-OHDA lesion induction

To assess the effect of treatment with GW855266X (5mg/kg) and pioglitazone (20mg/kg) on the number of activated microglia/macrophages in the SNc following 6-OHDA lesion induction, cell counts for OX6 and CD68+ve cells was carried out. In vehicle treated animals, the number of OX6+ve microglial cells significantly increased in the SNc in the lesioned side compared to the unlesioned side after 6-OHDA lesioning (lesioned: 32.25 ± 6.45, unlesioned: 3.0 ± 0.95, $p<0.001$) (Fig 5.6A). Activated OX6+ve microglia not only increased in number but had an activated morphology characterised by an enlarged somas and thickened processes. OX6+ve microglia focally accumulated in both the lateral and medial portions of the SNc ipsilateral to the lesioned hemisphere. In parallel, the number of CD68+ve cells was significantly increased in the SNc in the lesioned side compared to the unlesioned side following 6-OHDA lesion induction (lesioned: 16.0 ± 4.41, unlesioned: 0.0, $p<0.001$) (Fig 5.6B). CD68+ve macrophages had a predominant amoeboid macrophage-like appearance with presence of granular staining in the lysosomal membranes indicating phagocytic activity. Localisation of CD68+ve macrophages was very similar to OX6+ve microglia in the lateral and medial portions of the SNc. Interestingly, 7 days treatment with GW855266X (5mg/kg) p.o.b.i.d starting 2 days after 6-OHDA lesioning led to a significant decrease in the number of OX6+ve activated microglia in the SNc in the lesioned hemisphere compared to the lesioned hemisphere in vehicle treated group (Drug treated-lesioned: 10.83 ±1.53, vehicle treated-lesioned: 32.25 ± 6.45, $p<0.001$) (Fig 5.6A). The decrease in the number of activated microglia was observed in both lateral and medial portions of the SNc. The remaining OX6+ve microglial cells showed a morphologically active phenotype with enlarged cell bodies and shortened processes. In addition, activation of CD68+ve macrophages was fully blocked by GW855266X and no CD68+ve cells were present in medial and lateral portions of the SNc. Thus, post-lesion treatment with GW855266X (5mg/kg), exerted anti-inflammatory properties by blocking the activation of OX6+ve and CD68+ve microglia/macrophages in the SNc. In parallel, 7 day pioglitazone

treatment p.o.b.i.d starting 2 days after 6-OHDA lesion induction also led to a significant reduction in the number of activated microglia/macrophages similar to the effect observed following treatment with GW855266X. Cell counts in the SNc revealed that the number of OX6+ve microglia decreased significantly in the medial and lateral portions of the SNc in the lesioned hemisphere compared to the lesioned hemisphere of vehicle treated group after pioglitazone (20mg/kg) treatment (Drug treated-lesioned: 10.69 ± 2.04, vehicle treated-lesioned: 32.25 ± 6.45, $p<0.001$) (5.6 A). Concomitantly, the number of CD68+ve macrophages decreased significantly in the medial and lateral portions of the SNc in the lesioned hemisphere following pioglitazone (20mg/kg) treatment compared to the lesioned hemisphere in the vehicle treated group (Drug treated-lesioned: 5.71 ±1.92, vehicle treated-lesioned: 9.6 ± 4.49, $p<0.1$) (Fig 5.6B). Thus, continuous treatment with both GW855266X (5mg/kg) and pioglitazone (20mg/kg) post 6-OHDA lesion induction exerted neuroprotective and anti-inflammatory properties that were accompanied by preservation of the functionality of the nigrostriatal system.

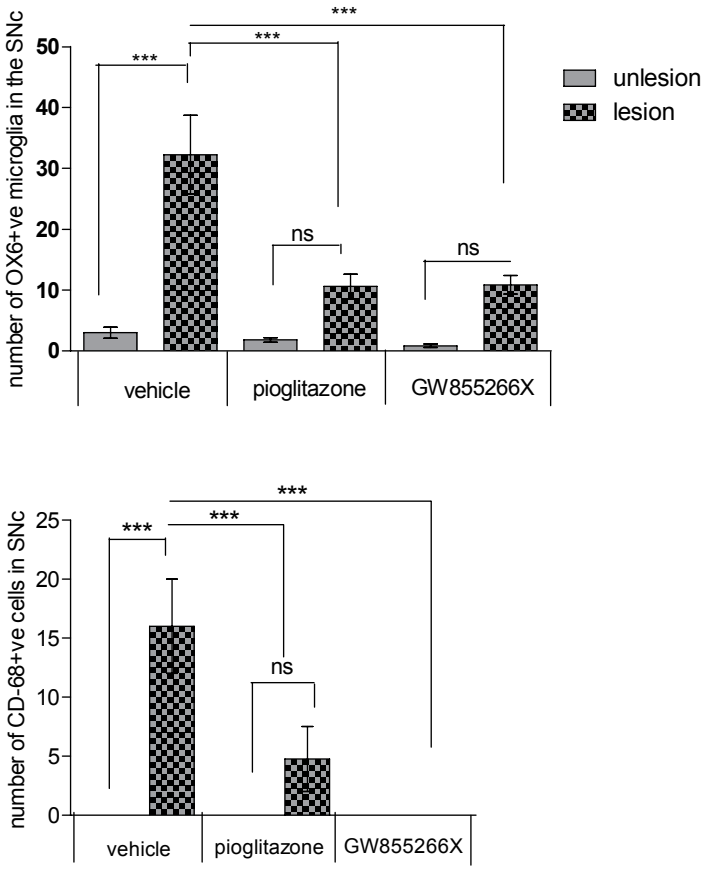

Fig 5.6 Anti-inflammatory effect of treatment with PPAR-γ agonists for 7 days starting 2 days after 6-OHDA lesion induction. This is demonstrated as significant decrease in the number of OX6+ve and CD68+ve microglia/macrophages in the SNc ipsilateral to the 6-OHDA lesioned hemisphere compared to the lesioned hemisphere in the vehicle treated animals.

Graph A: Shows the number of OX6+ve microglia in the SNc in the vehicle and PPAR-γ agonists [pioglitazone (20mg/kg) and GW855266X (5mg/kg)]. Immunohistochemistry was performed with OX6 antibody that detects the population of microglial cells expressing MHC II antigens. In the vehicle treated animals the number of OX6+ve microglial cells increased significantly following 6-OHDA lesion induction. Treatment with both pioglitazone (20mg/kg) and GW855266X (5mg/kg) resulted in a significant decrease in the number OX6+ve microglial cells in the SNc ipsilateral to 6-OHDA lesion side compared to the lesioned hemisphere in vehicle treated animals. Results are presented as mean number of cell± SEM. * p<0.5 ** *p<0.01*, *** *p< 0.001*, *ns*= not significant. Number of animals was 6/group per time point. **Graph B**: Shows the number of CD68+ve macrophages in the SNc in the vehicle and PPAR-γ agonists [pioglitazone (20mg/kg) and GW855266X (5mg/kg)]. Immunohistochemistry was performed with CD68 antibody that detects phagocytic macrophages. In the vehicle treated animals the number of OX6+ve microglial cells increased significantly following 6-OHDA lesion induction. Treatment with both pioglitazone (20mg/kg) and GW855266X (5mg/kg) resulted in a significant decrease in the number CD68+ve microglial cells in the SNc ipsilateral to 6-OHDA lesion side compared to the lesioned hemisphere in vehicle treated animals. Results are presented as mean number of cell± SEM. * p<0.5 ** *p<0.01*, *** *p< 0.001*, *ns*= not significant. Number of animals was 6/group per time point.

5.3.5 Treatment with GW855266X and pioglitazone for 7 days post 6-OHDA lesion induction suppresses the expression of MMP-3 and MMP-9 in the SNc after 6-OHDA lesioning

5.3.5.1 GW855266X (5mg/kg) and pioglitazone (20mg/kg) suppress the activation of MMP-3 and MMP-9 expressing cells in the SNc after 6-OHDA lesion induction

To investigate the effects of GW855266X (5mg/kg) and pioglitazone (20mg/kg) on the expression of two members of matrix metalloproteinases, MMP-3 and MMP- 9, cell counts were carried out for both MMP-3+ve and MMP-9+ve cells in the SNc following 6-OHDA lesion induction. Cell counts in the SNc demonstrated that in the vehicle treated animals the number of MMP-3+ve cells increased significantly in the lesioned hemisphere compared to the unlesioned hemisphere following 6-OHDA lesion induction (lesioned: 25.27 ±2.05, unlesioned: 8.01 ±1.02, $p<0.001$) (Fig 5.7A). MMP-3+ve cells were present in clusters in the ventrolateral and medial portions of the SNc.

Similarly, cell counts for MMP-9+ve cells in the SNc, revealed that in the vehicle treated group the number of MMP-9+ve cells significantly increased in the 6-OHDA lesioned side compared to the unlesioned side (lesioned: 19.0± 1.35, unlesioned: 8.09± 0.87, $p<0.001$) (Fig 5.7B). Identical to MMP-3 localisation, MMP-9+ve cells were also present in the ventrolateral and medial parts of the SNc. However, 7 days treatment p.o.b.i.d with GW855266X (5mg/kg) starting 2 days after 6-OHDA lesion induction led to a significant decrease in the number of MMP-3+ve cells in the SNc in the 6-OHDA lesioned side compared to the lesioned side in vehicle treated group (Drug treated- lesioned: 14.08 ± 1.31, vehicle treated-lesioned: 25.27 ±2.05, $p<0.001$) (Fig 5.7A). In parallel cell counts for MMP-9 +ve cells revealed a significant decrease in the number of MMP-9+ve cells in the SNc in the 6-OHDA lesioned side compared to the lesioned side in vehicle treated group (Drug treated- lesioned: 12.77 ± 0.80, vehicle treated-lesioned: 19.0± 1.35, $p<0.001$) (Fig 5.7B). Reduction in the number of MMP-3 and MMP-9+ve cells occurred in ventrolateral and medial portions of the SNc. These observations indicated that continuous 7 day treatment with GW855266X (5mg/kg) after 6-OHDA lesion induction partially, yet significantly, inhibited both MMP-3 and MMP-9 activation in the SNc, suggesting a significant decrease in the signals for microglial activation in the SNc following 6-OHDA challenge. Very similar effects were also observed when animals were treated for 7 days

with pioglitazone (20mg/kg) p.o.b.i.d starting 2 days after 6-OHDA lesioning. Following pioglitazone treatment (20mg/kg) cell counts in the SNc demonstrated that the number of MMP-3+ve cells significantly decreased in the lesioned hemisphere compared to the lesioned hemisphere in vehicle treated animals (Drug treated- lesioned: 13.92 ± 1.38, vehicle treated-lesioned: 25.27 ±2.05, $p<0.001$) (Fig 5.7A). Not surprisingly, MMP-9+ve cells were also reduced in number in the lesioned hemisphere following pioglitazone (20mgkg) treatment compared to the vehicle treated group (Drug treated- lesioned: 13.89 ± 0.90, vehicle treated-lesioned: 19.0 ±1.35, $p<0.001$) (Fig 5.7B).

Taken together, our data demonstrated that continuous 7 day treatment with both GW855266X (5mg/kg) and pioglitazone (20mg/kg) post 6-OHDA lesion induction was neuroprotective and exerted anti-inflammatory properties that was characterised by reduction in the number of activated microglia/macrophages in the SNc and reflected in the suppression of both MMP-3+ve and MMP-9+ve cells.

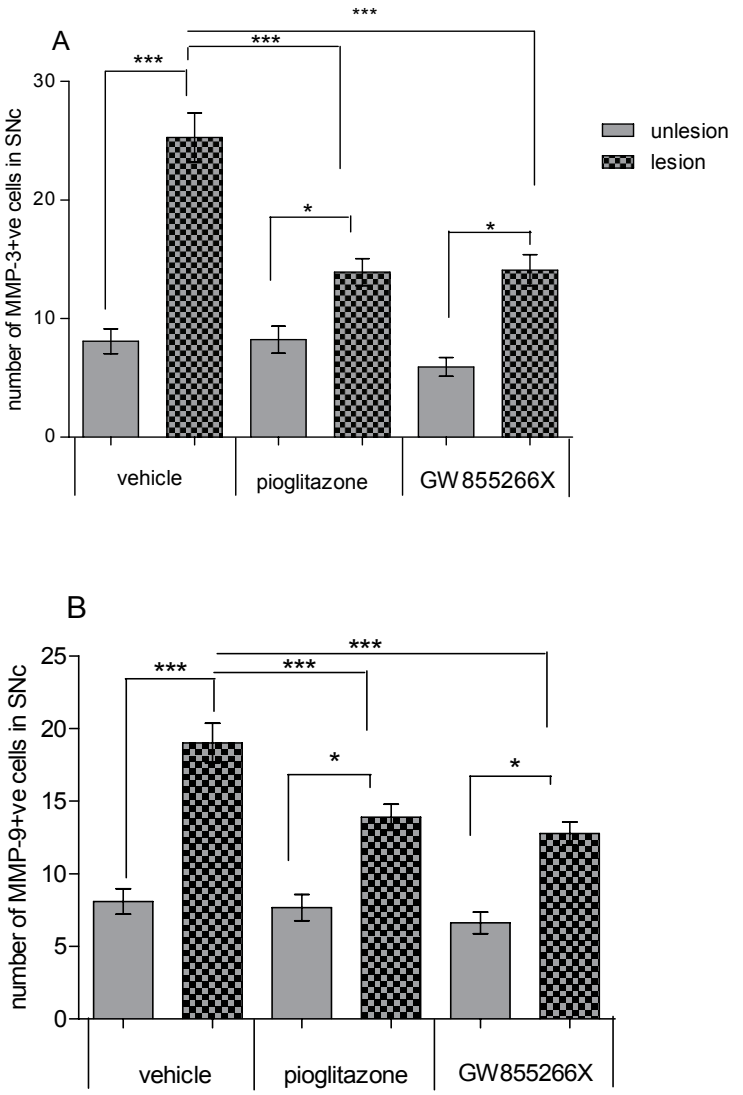

Fig 5.7 Treatment with PPAR-γ agonists for 7 days starting 2 days after 6-OHDA lesion induction leads to significant reduction in the number of both MMP-3+ve and MMP-9+ve cells in the SNc in the lesioned hemisphere compared to the lesioned hemisphere in vehicle treated animals.

Graph A: Shows the number of MMP-3+ve cells in the SNc in the vehicle and PPAR-γ agonists [pioglitazone (20mg/kg) and GW855266X (5mg/kg)] treated animals. Immunohistochemistry was performed with MMP-3 antibody that detects the expression of the active form of MMP-3 in cells. In the vehicle treated animals, the number of MMP-3+ve cells increased significantly following 6-OHDA lesion induction. Treatment with both pioglitazone (20mg/kg) and GW855266X (5mg/kg) resulted in a significant decrease in the number MMP-3+ve cells in the SNc ipsilateral to 6-OHDA lesion side compared to the lesioned hemisphere in vehicle treated animals. Results are presented as mean number of cell± SEM. * p<0.5 ** *p<0.01*, *** *p< 0.001*, *ns*= not significant. Number of animals was 6/group per time point. **Graph B**: Shows the number of MMP-9+ve cells in the SNc in the vehicle and PPAR-γ agonists [pioglitazone (20mg/kg) and GW855266X (5mg/kg)] treated animals. Immunohistochemistry was performed with MMP-9 antibody that detects the expression of the active form of MMP-9 in cells. In the vehicle treated animals, the number of MMP-9+ve cells increased significantly following 6-OHDA lesion induction. Treatment with both pioglitazone (20mg/kg) and GW855266X (5mg/kg) resulted in a significant decrease in the number MMP-9+ve cells in the SNc ipsilateral to 6-OHDA lesion side compared to the lesioned hemisphere in vehicle treated animals. Results are presented as mean number of cell± SEM. * p<0.5 ** *p<0.01*, *** *p< 0.001*, *ns*= not significant. Number of animals was 6/group per time point.

5.3.6 Continuous presence of GW855266X and pioglitazone was vital for the treatments to be neuroprotective

5.3.6.1 The effects of withdrawal of GW855266X (5mg/kg) and pioglitazone (20mg/kg) after 7 days of treatment on the dopamine content in the striatum following 6-OHDA lesion induction

To evaluate whether the effects of treatment with GW855266X and pioglitazone were long lasting, treatments were administered starting 2 days after 6-OHDA lesion induction p.o.b.i.d. for 7 consecutive days. Thereafter, drugs were withdrawn for 7 days and brains were collected on day 16 after 6-OHDA lesioning. In vehicle treated animals, striatal dopamine levels significantly decreased by ~63% in the lesioned hemisphere compared to the unlesioned hemisphere following 6-OHDA lesion induction [lesioned: 5.0 ± 1.25 (ng/mg), unlesioned: 13.56 ± 0.63 (ng/mg), $p<0.001$] (Fig 5.8). This was concomitant with depletion of dopamine metabolite, DOPAC and HVA in the lesioned hemisphere compared to the unlesioned hemisphere by ~ 55% and ~59% respectively [(Table 5.3)]. In animals treated with GW855266X (5mg/kg) for 7 days, drug withdrawal for 7 days led to the loss of neuroprotective effects of the treatment. This was reflected in significant depletion of striatal dopamine levels in the lesioned hemisphere that reached similar levels to the lesioned hemisphere of the vehicle treated animals [Drug treated- lesioned: 4.75± 2.29 (ng/mg), vehicle treated -lesioned: 7.23 ± 1.55 (ng/mg), $p>0.05$] (Fig 5.8). Striatal dopamine metabolites, DOPAC and HVA were also significantly depleted by ~60% and ~56% respectively in the lesioned hemisphere (Table 5.3). Thus, these observations indicated that the continuous presence of GW855266X (5mg/kg) following 6-OHDA lesion induction was necessary for neuroprotective properties of this compound to be maintained. In parallel, withdrawal of pioglitazone (20mg/kg) for 7 days led to a similar loss neuroprotective properties of this compound following 6-OHDA lesion induction. This was evident in the levels of striatal dopamine, where a significant depletion in the striatal dopamine content in the lesioned hemisphere was observed which was even more pronounced than the loss of striatal dopamine in the lesioned hemisphere in the vehicle treated animals (Drug treated lesioned: 4.62 ±2.47 (ng/mg), vehicle treated-lesioned: 7.23 ± 1.55 (ng/mg), $p>0.05$). Dopamine metabolites, DOPAC and HVA were also significantly depleted by ~85% and 83% respectively following pioglitazone withdrawal for 7 days in 6-

OHDA lesioned animals; however dopamine turn over in these animals did not increase (Table 5.3).

Hence, continuous presence GW855266X and pioglitazone was vital through out the time course of the study after 6-OHDA lesion induction in order to protect dopaminergic neurons and preserve dopamine concentration in the striatum.

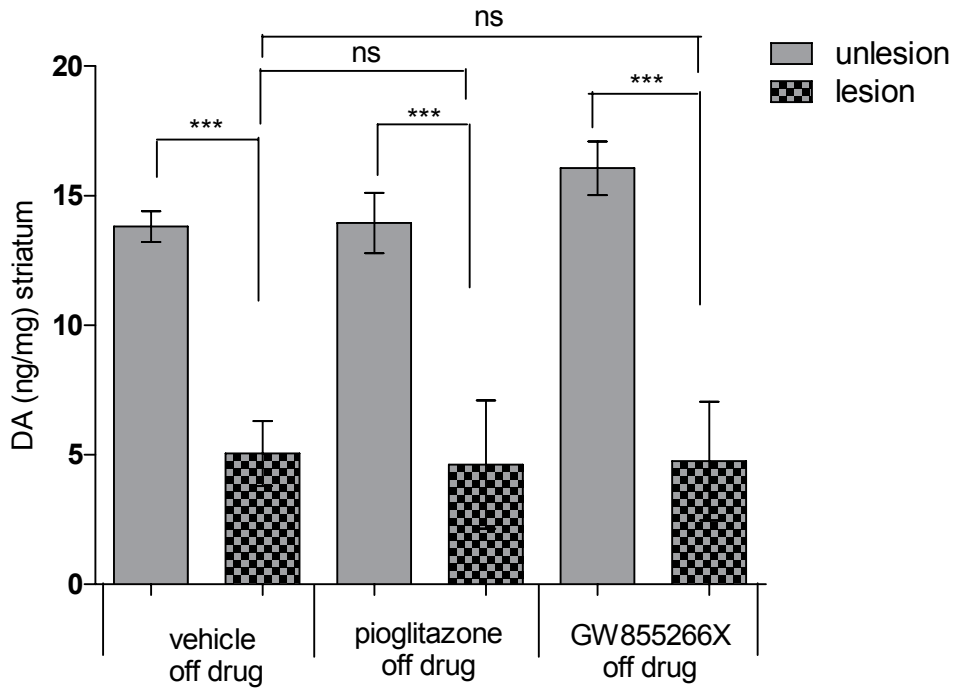

Fig 5.8 Loss of protective effect of pioglitazone and GW855266X on the nigrostriatal functionality following withdrawal of the treatments for 7 days after 6-OHDA lesion induction. 6-OHDA lesion induction in the lesioned hemisphere compared to the lesioned hemisphere in vehicle treated animals. Graph demonstrates the concentration of striatal dopamine ng/mg in different groups of treatment off drug.

In vehicle treated animals the striatal dopamine content was significantly decreased in the lesioned hemisphere compared to the unlesioned hemisphere following 6-OHDA lesion induction. Withdrawal of treatment with pioglitazone (20mg/kg) and GW855266X (5mg/kg) for 7 days led to a significant depletion of the dopamine content in the striatum in the lesioned hemisphere that represented the same levels dopamine compared to the lesioned hemisphere in the vehicle treated 6-OHDA lesioned animals. Results are presented as mean striatal dopamine ng/mg of wet tissue weight ±SEM. * p<0.5 ** *p<0.01*, *** *p< 0.001*, *ns*= not significant. Number of animals was 6/group per treatment group. ***Treatment regime:***

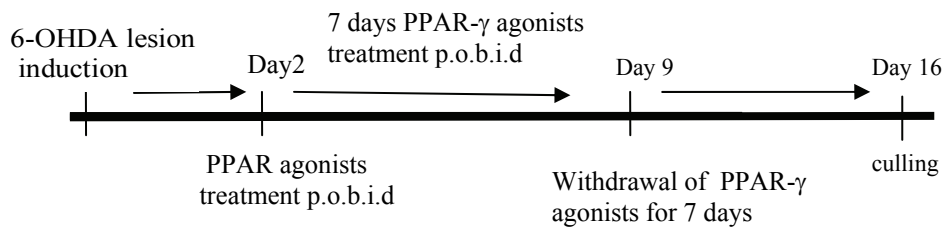

	DOPAC (ng/mg)	HVA (ng/mg)	Dopamine turnover (pmol/mg)
Vehicle	Lesion: 0.81 ± 0.47 Unlesion: 1.8 ± 0.11 *p<0.5*	Lesion: 0.13± 0.05 Unlesion: 0.32 ± 0.02 *p<0.5*	Lesion: 32.15 ± 4.46 Unlesion: 17.41 ± 2.43 *p<0.1*
GW855266X (5mg/kg)	Lesion: 0.41 ± 0.18 Unlesion: 1.02 ± 0.08 *p<0.5*	Lesion: 0.10 ± 0.04 Unlesion: 0.23 ± 0.02 *p<0.5*	Lesion: 5.29 ± 1.56 Unlesion: 8.44 ± 2.42 *p>0.5*
Pioglitazone (20mg/kg)	Lesion: 0.29± 0.20 Unlesion: 2.22 ± 0.64 *p<0.5*	Lesion: 0.05 ± 0.02 Unlesion: 0.30± 0.03 *p<0.5*	Lesion: 5.66 ± 3.68 Unlesion: 18.65 ± 4.07 *p>0.5*

Table 5.3 Withdrawal of treatment with pioglitazone and GW855266X administered for 7 days post 6-OHDA lesion induction led to depletion of the mean concentration of striatal dopamine metabolites: DOPAC and HVA that was very similar to the vehicle treated group. Dopamine turnover did not change significantly following the withdrawal of treatment in the 6-OHDA lesioned hemisphere compared to the unlesioned hemisphere in drug treated and lesioned hemisphere in the vehicle treated animals.

Table shows that in the vehicle treated animals striatal levels of dopamine metabolites, DOPAC and HVA were significantly decreased in the 6-OHDA lesioned hemisphere compared to the unlesioned hemisphere. In addition in these animals following 6-OHDA lesion induction striatal dopamine turn over increased significantly in the lesioned hemisphere compared to the unlesioned hemisphere. Withdrawal of treatment with GW855266X (5mg/kg) and pioglitazone (20mg/kg) for 7 days led to a significant depletion of both DOPAC and HVA in the 6-OHDA lesioned hemisphere compared to the unlesioned hemisphere. However, normalisation of striatal dopamine turn over in the 6-OHDA lesioned hemisphere was still observed after withdrawal of the treatments compared to the unlesioned hemisphere. Concentration of striatal dopamine metabolites are shown as ng/mg of wet tissue weight ±SEM. Mean striatal monoamine turnover ratio was calculated using the expression ((DOPAC+HVA)/DA). Number of animals was 6/group per treatment group. *p<0.5* was considered significant.

5.3.6.2 The effects of withdrawal of GW855266X (5mg/kg) and pioglitazone (20mg/kg) after 7 days of treatment on the number of TH+ve dopaminergic neurons in the SNc following 6-OHDA lesion induction

To evaluate whether the effect of treatment with of GW855266X (5mg/kg) and pioglitazone was long lasting, the treatments were administered starting 2 days after 6-OHDA lesion induction p.o.b.i.d. for 7 consecutive days. Thereafter, drugs were withdrawn for 7 days and brains were collected on day 16 after 6-OHDA lesioning. Cell counts in the SNc on day 16 revealed that in vehicle treated animals a significant number of TH+ve dopaminergic neurons were lost in lesioned hemisphere compared to the control unlesioned hemisphere following 6-OHDA lesion induction (lesioned: 37.25 ± 3.20, unlesioned: 72.5 ± 6.53, $p<0.001$) (Fig. 5.9) Withdrawal of treatment with GW855266X (5mg/kg) for 7 days following 6-OHDA lesion induction led to the loss of observed neuroprotective properties of this compound in the SNc. Nigral TH+ve dopaminergic cell counts revealed that the extent of TH+ve dopaminergic neuronal loss in these animals reached the level of loss observed in the lesioned hemisphere of the vehicle treated group (Drug treated- lesioned: 30.0± 4.30, vehicle treated -lesioned: 37.25 ± 3.20, $p>0.05$) (Fig 5.9).

This observation further indicated that the neuroprotective effects of GW855266X were not long lasting after drug withdrawal and continuous presence of this compound is necessary to maintain neuroprotection. In parallel, TH+ve cell counts in the SNc revealed that after pioglitazone withdrawal for 7 consecutive days, a significant number of TH+ve dopaminergic neurons were lost following 6-OHDA lesioning. The degree of cells death was similar to the loss seen in the lesioned hemisphere of the vehicle treated animals (Drug treated lesioned: 38.2 ±7.59, vehicle treated-lesioned: 37.25 ± 3.20, $p>0.05$) (Fig 5.9).

Taken together, our findings suggested that continuous presence of GW855266X and pioglitazone is necessary for their neuroprotective properties in the SNc and preservation of dopamine and its metabolites in the striatum following 6-OHDA lesion induction.

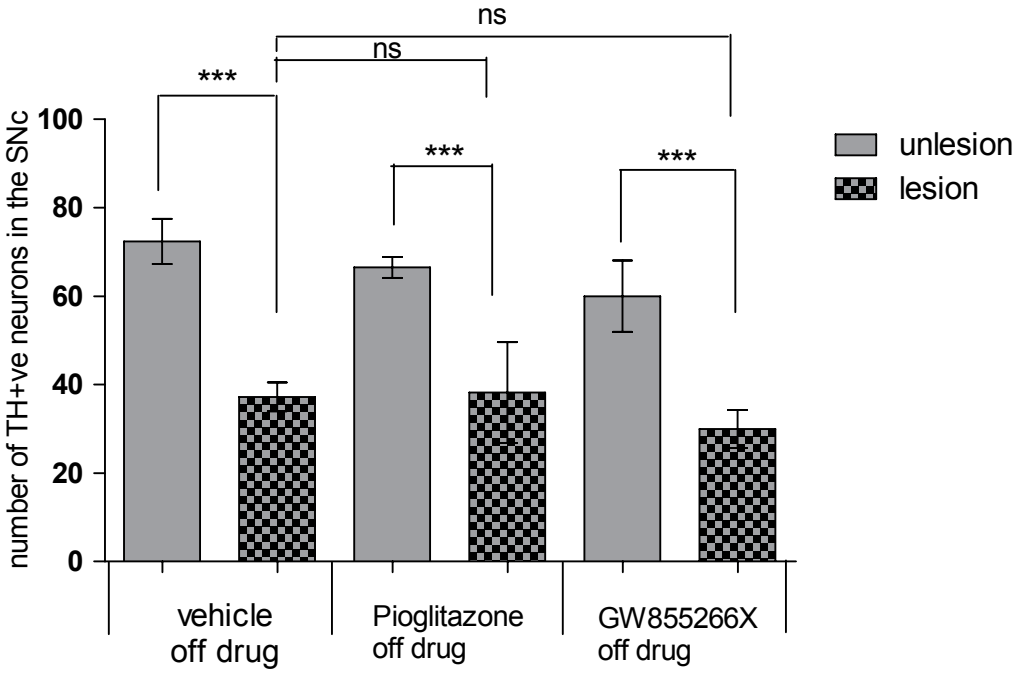

Fig 5.9 Loss of neuroprotective effect of pioglitazone and GW855266X when withdrawn for 7 days after therapy for 7 days post 6-OHDA lesion induction. The extent of nigral TH+ve dopaminergic neuronal loss in the lesioned hemisphere was similar to the lesioned hemisphere in the vehicle treated animals. Graph demonstrates the number mean number of TH+ve dopaminergic neurons in the SNc of different treatment groups

In vehicle treated animals the number of TH+ve dopaminergic neurons significantly decreased in the lesioned hemisphere compared to the unlesioned hemisphere following 6-OHDA lesion induction. Withdrawal of treatment with both pioglitazone (20mg/kg) and GW855266X (5mg/kg) for 7 days after lesion induction led to a significant decrease in TH+ve dopaminergic neuronal cell number in the lesioned hemisphere similar to the lesioned hemisphere in vehicle treated 6-OHDA lesioned animals. Results are presented as mean number of cells ±SEM. * p<0.5 ** *p<0.01*, *** *p< 0.001*, *ns*= not significant. Number of animals was 6/group per treatment group.

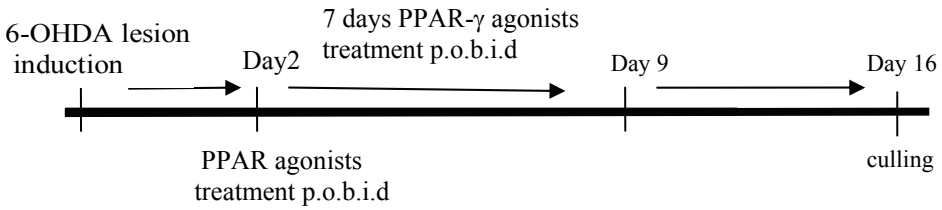

5.3.7 Continuous presence of GW855266X and pioglitazone was necessary for the exertion of anti-inflammatory properties

5.3.7.1 Withdrawal of GW855266X (5mg/kg) and pioglitazone (20mg/kg) for 7 days led to loss of suppressive effect on the activated OX6+ve and CD68+ve microglia/macrophages in the SNc following 6-OHDA lesioning

To evaluate whether continuous presence of GW855266X (5mg/kg) and pioglitazone (20mg/kg) was necessary to maintain suppression of inflammation in the SNc following 6-OHDA lesion induction, treatments were administered p.o.b.i.d. for 7 consecutive days starting from day 2 after 6-OHDA lesion induction, thereafter the drugs were withdrawn for days and brains were collected on day 16. In the vehicle treated group cell counts in the SNc revealed that the number of OX6+ve microglial cells significantly increased in the 6-OHDA lesioned hemisphere compared to the unlesioned hemisphere (lesioned: 31.50± 7.97, unlesioned: 0.83± 0.30, $p<0.001$) (Fig 5.10A). OX6+ve microglia appeared morphologically active with enlarged somas and thickened processes. These cells focally accumulated in the medial and lateral portions of the SNc in the lesioned hemisphere. Interestingly, in the drug treated groups withdrawal of GW855266X (5mg/kg) for 7 days led to loss of its suppressive effect on OX6+ve microglia. A significant activation of OX6+ve microglia, which was characterised by increase in their number and activated phenotype, following drug withdrawal was observed in the SNc. The extent and localisation of microglial activation in these animals was similar to the lesioned hemisphere in the vehicle treated group (Drug treated-lesioned: 21.0± 6.37, vehicle treated-lesioned: 31.50± 7.97, $p>0.05$) (Fig 5.10A). In parallel, in the vehicle treated animals cell counts in the SNc revealed that the number of CD68+ve macrophages increased significantly in the lesioned hemisphere following 6-OHDA lesioning compared to the unlesioned hemisphere (lesioned: 33.63 ±5.15, unlesioned: 0.0. $p<0.001$). CD68+ve macrophages had an amoeboid macrophage-like appearance with accumulation of granular staining in the lysosomal membranes indicating phagocytic activity. Localisation of CD68+ve cells was very similar to OX6+ve microglia in the lateral and medial portions of the SNc. Withdrawal of GW855266X (5mg/kg) for 7 days led to loss of suppressive effect on CD68+ve macrophages in the SNc. This was characterised by a significant increase in the number of activated CD68+ve macrophages in the SNc in the lesioned hemisphere. In these animals, the extent of CD68+ve macrophage activation in the lesioned side reached a similar number

as observed in the vehicle treated animals (Drug-treated lesioned: 37.67 ±6.17, vehicle treated-lesioned: 33.63 ±5.15, $p>0.05$) (Fig 5.10B).

Thus, these data suggest that the continuous treatment with GW855266X was essential for the drug to be able to exert significant anti-inflammatory hence neuroprotective properties in the SNc.

Pioglitazone withdrawal for 7 days following 6-OHDA lesion induction also led a loss of suppressive effect of this drug on inflammation in the SNc. Following drug withdrawal, a significant increase in the number of OX6+ve microglia in the SNc was observed. The extent and localisation of microglial activation in the lesioned hemisphere was similar to the lesioned hemisphere in the vehicle treated group (Drug treated-lesioned: 32.60± 6.04, vehicle treated-lesioned: 31.50± 7.97, $p>0.05$). Concomitantly, cell counts for CD68+ve macrophages showed a significant increase the extent of CD68+ve macrophages activation that reached a similar proportion to the lesioned hemisphere in vehicle treated animals (Drug-treated lesioned: 26.20 ±4.69, vehicle treated-lesioned: 33.63 ±5.15, $p>0.05$). Hence, withdrawal of pioglitazone (20mg/kg) treatment after 6-OHDA lesion induction resulted in exacerbation of microglia/macrophage reactivity that was characterised by increases in their number and activated morphology.

Taken together, the continuous presence of GW855266X (5mg/kg) and pioglitazone (20mg/kg) was necessary to maintain a suppressive effect on the activated OX6+ve and CD68+ve microglia/macrophages in the SNc following 6-OHDA lesion induction.

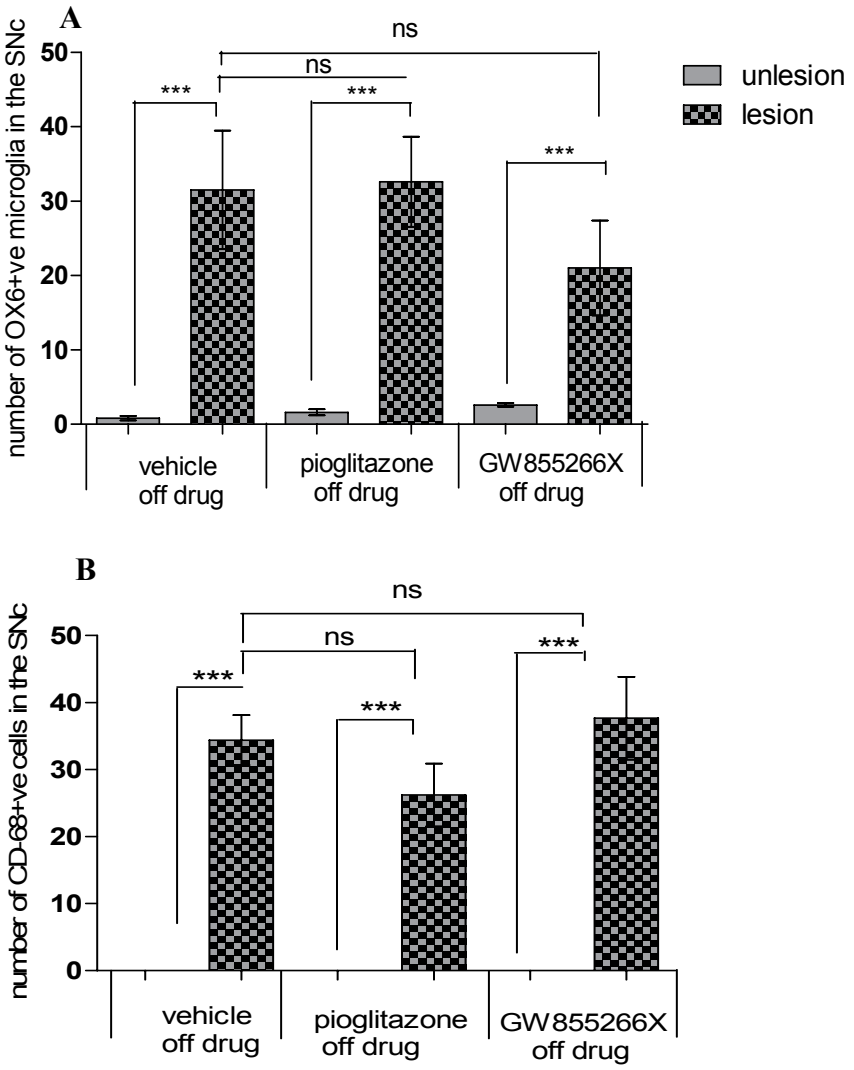

Fig 5.10 Loss of anti-inflammatory effect of treatment with PPAR-γ agonists after 7 days of withdrawal of treatments following 6-OHDA lesion induction. This is demonstrated as significant increase in the number of OX6+ve and CD68+ve microglia/macrophages in the SNc ipsilateral to the 6-OHDA lesioned hemisphere to a similar extent as the lesioned hemisphere in the vehicle treated animals.

Graph A: Shows the number of OX6+ve microglia in the SNc in the vehicle and PPAR-γ agonists [pioglitazone (20mg/kg) and GW855266X (5mg/kg)]. Immunohistochemistry was performed with OX6 antibody that detects the population of microglial cells expressing MHC II antigens. In the vehicle treated animals, the number of OX6+ve microglial cells increased significantly following 6-OHDA lesion induction. Withdrawal of both pioglitazone (20mg/kg) and GW855266X (5mg/kg), after 7 days of treatment, resulted in a significant increase in the number OX6+ve microglial cells in the SNc ipsilateral to 6-OHDA lesion side that reached similar proportion to the lesioned hemisphere in vehicle treated animals. Results are presented as mean number of cell± SEM. * $p<0.5$ ** $p<0.01$, *** $p< 0.001$, *ns*= not significant. Number of animals was 6/group per time point.

Graph B: Shows the number of CD68+ve macrophages in the SNc in the vehicle and PPAR-γ agonists [pioglitazone (20mg/kg) and GW855266X (5mg/kg)]. Immunohistochemistry was performed with CD68 antibody that detects phagocytic macrophages. In the vehicle treated animals the number of CD68+ve microglial cells increased significantly following 6-OHDA lesion induction. Withdrawal of both pioglitazone (20mg/kg) and GW855266X (5mg/kg), after 7 days of treatment, resulted in a significant increase in the number CD68+ve macrophages in the SNc ipsilateral to 6-OHDA lesion side that reached a similar proportion to the lesioned hemisphere in vehicle treated

animals. Results are presented as mean number of cell± SEM. * p<0.5 ** *p<0.01*, *** *p< 0.001*, *ns*= not significant. Number of animals was 6/group per time point.

5.3.7.1 Withdrawal of GW855266X (5mg/kg) and pioglitazone (20mg/kg) for 7 days led to loss of suppressive effect on both MMP-3 and MMP-9 expressing cells in the SNc following 6-OHDA lesioning

To assess whether the inhibitory affects of GW855266X (5mg/kg) and pioglitazone (20mg/kg) on MMP-3 and 9 +ve cells was reliant on its continuous presence in the brain throughout out the duration of the study the animals were treated with GW855266X (5mg/kg) and pioglitazone (20mg/kg) p.o.b.i.d. for 7 consecutive days starting from day 2 after 6-OHDA lesion induction. Thereafter treatments were withdrawn for 7 days after 6-OHDA lesioning. In vehicle treated animals, cell counts in the SNc on day 16 after lesion induction showed a significant increase in the number of MMP-3+ve cells in the 6-OHDA lesioned hemisphere compared to the unlesioned hemisphere (lesioned: 25.17 ±2.05, unlesioned: 9.0 ± 2.04 , $p<0.001$) (Fig 5.11 A). Interestingly, in the GW855266X (5mg/kg) treated group drug withdrawal for 7 days following 6-OHDA lesion induction led to loss of inhibitory effect of GW855266X on the number of MMP-3 expressing cells. The number of MMP-3+ve cells significantly increased in the SNc on the side of the lesion that reached similar levels to the lesioned hemisphere in the vehicle treated group following drug withdrawal (Drug treated-lesioned: 23.33 ± 1.74, vehicle treated-lesioned: 25.17 ±2.05, $p>0.5$) (Fig 5.11A). A similar effect was also observed following withdrawal of pioglitazone (20mg/kg) for 7 days after 6-OHDA lesion induction. In pioglitazone (20mg/kg) treated group drug withdrawal led to a significant increase in the number of MMP-3+ve cells in the SNc on the side of the 6-OHDA lesion, the number of these cells reached similar levels to the lesioned hemisphere in the vehicle treated animals (Drug treated-lesioned: 20.00 ± 1.29, vehicle treated-lesioned: 25.17 ±2.05, $p>0.5$) (Fig 5.11A).

In parallel, in vehicle treated animals, MMP-9+ve cells increased in number significantly on the side of the lesion compared to the unlesioned side following 6-OHDA lesion induction (lesioned: 25.82 ± 2.57, unlesioned: 10.64 ±1.01, $p<0.001$) (Fig 5.11B). Not surprisingly, in GW855266X (5mg/kg) treated group drug withdrawal for 7 days following 6-OHDA lesion induction resulted in a significant increase in the number of MMP-9+ve cells in the SNc on the side of the lesion that reached similar levels to the lesioned hemisphere in the vehicle treated animals (Drug treated-lesioned: 23.29 ± 2.74, vehicle treated-lesioned: 25.82 ± 2.57, $p>0.5$) (Fig 5.11B). Similarly in pioglitazone (20mg/kg) treated group drug withdrawal for 7 consecutive days following 6-OHDA lesion induction resulted in a significant increase in the number of MMP-9+ve cells in the SNc in the lesioned hemisphere that reached similar levels to the lesioned hemisphere in the vehicle

treated group (Drug treated-lesioned: 24.50 ± 2.14, vehicle treated-lesioned: 25.82 ± 2.57, *p>0.5*) (Fig 5.11B).

Taken together, our data demonstrated that continuous presence of GW855266X and pioglitazone after 6-OHDA lesion induction was crucial for the anti-inflammatory and neuroprotective properties of these compounds in the SNc and the striatum.

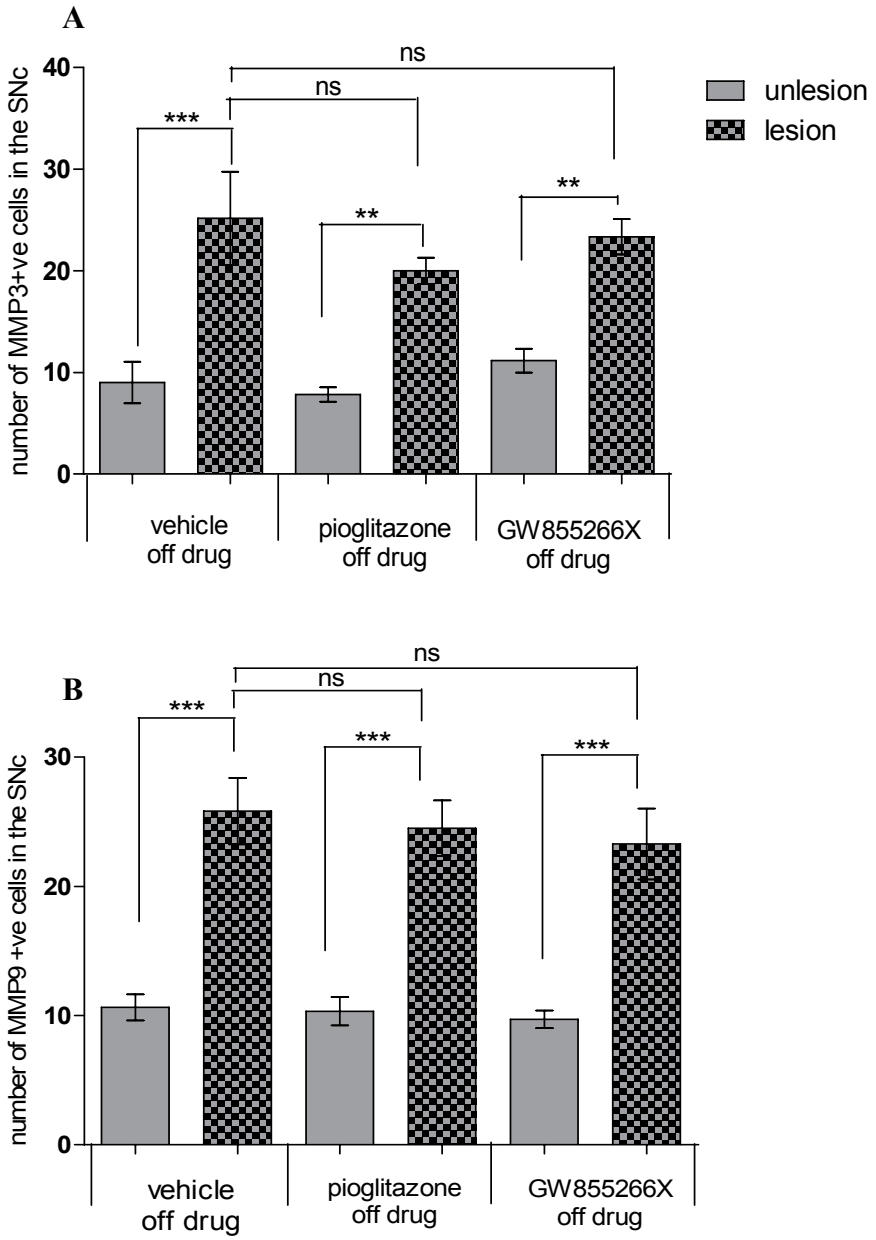

Fig 5.11 Loss of inhibitory effect on MMP-3 and MMP-9 expressing cell after withdrawal of PPAR-γ agonists for 7 days starting 2 days after 6-OHDA lesion induction leads to significant reduction in the number of both MMP-3+ve and MMP-9+ve cells in the SNc in the lesioned hemisphere compared to the lesioned hemisphere in vehicle treated animals.

Graph A: Shows the number of MMP-3+ve cells in the SNc in the vehicle and PPAR-γ agonists [pioglitazone (20mg/kg) and GW855266X (5mg/kg)] treated animals. Immunohistochemistry was performed with MMP-3 antibody that detects the expression of the active form of MMP-3 in cells. In the vehicle treated animals the number of MMP-3+ve cells increased significantly following 6-OHDA lesion induction. Treatment with both pioglitazone (20mg/kg) and GW855266X (5mg/kg) resulted in a significant decrease in the number MMP-3+ve cells in the SNc ipsilateral to 6-OHDA lesion side compared to the lesioned hemisphere in vehicle treated animals. Results are presented as mean number of cell± SEM. * p<0.5 ** *p<0.01*, *** *p< 0.001*, *ns*= not significant. Number of animals was 6/group per time point. **Graph B**: Shows the number of MMP-9+ve cells in the SNc in the vehicle and PPAR-γ agonists [pioglitazone (20mg/kg) and GW855266X (5mg/kg)] treated

animals. Immunohistochemistry was performed with MMP-9 antibody that detects the expression of the active form of MMP-9 in cells. In the vehicle treated animals the number of MMP-9+ve cells increased significantly following 6-OHDA lesion induction. Treatment with both pioglitazone (20mg/kg) and GW855266X (5mg/kg) resulted in a significant decrease in the number MMP-9+ve cells in the SNc ipsilateral to 6-OHDA lesion side compared to the lesioned hemisphere in vehicle treated animals. Results are presented as mean number of cell± SEM. * p<0.5 ** *p<0.01*, *** *p< 0.001*, *ns*= not significant. Number of animals was 6/group per time point.

5.4 Discussion

To elucidate the significance of the inflammatory response in the SNc, this study was designed to explore the effects of modulation of glial activity via activation of PPAR-γ sub-type following 6-OHDA induced lesion into the MFB. Therefore, 6-OHDA lesioned male SD rats were treated with two PPAR-γ agonists and for comparison purposes, one PPAR-δ agonist using different treatment regimes. The first compound studied, GW855266X, was developed by GSK and was administered with an effective dose of (5mg/kg), recommended by GSK from their internal *in vitro* studies. The next compound was pioglitazone that belongs to the family of TZDs and is a clinically prescribed drug for treatment of type 2 diabetes. Pioglitazone was used as a reference compound in our study. The final compound that was a PPAR-δ agonist (GW610742X) also developed by GSK was administered with a dose of (10mg/kg), recommended by GSK from their internal *in vitro* studies.

Our initial study was designed to determine whether the compounds exert neuroprotective and anti-inflammatory effects in the 6-OHDA model of PD. Since very little is known about the time course of action of these compounds our study was designed to treat the animals with each of the compounds for 7 days prior to 6-OHDA lesion induction and continue for 7 day afterwards. As demonstrated in preceding chapters activated microglial cells are present in the SNc from day 2 after 6-OHDA lesion induction and increase in a time dependent manner. Therefore, in this study we tested whether presence of GW855266X and pioglitazone prior to 6-OHDA lesioning and continued for further 7 days after 6-OHDA lesion induction would halt inflammation hence yield neuroprotection.

Treatment with GW855266X and pioglitazone before and after 6-OHDA lesion induction preserved striatal dopamine and protected dopaminergic neurons in the SNc. Indicating that continuous presence of GW855266X or pioglitazone before and after 6-OHDA lesion induction exerted significant neuroprotective effect with preservation of the functionality of the nigrostriatal tract. Concomitantly, the number OX6 and CD68+ve microglia/macrophages decreased significantly yet partially following treatments before and after 6-OHDA lesion induction. However, treatment with PPAR-δ agonist did not show any preservation of dopamine concentration in the striatum, hence it was not protective

following 6-OHDA lesioning; confirming the effect of PPAR agonists is via the γ receptor sub-type. It is noteworthy however that a recent study demonstrating that a PPAR-δ selective agonists exerted neuroprotective effects in MPTP mouse model of PD when it was focally injected into the brain's ventricles (Iwashita et al., 2007). This could indicate that the PPAR-δ agonist we tested had poor BBB permeability. These preliminary findings led us to study GW855266X and pioglitazone in a more clinically relevant treatment regime where treatments were administered p.o.b.i.d 2 days after 6-OHDA lesion induction for 7 consecutive days. The findings from this study are discussed in the following sections.

5.4.1 Continuous treatment with GW855266X or pioglitazone starting 2 days after 6-OHDA lesion induction was neuroprotective and anti-inflammatory

The choice of treating the animals on day 2 after 6-OHDA lesion induction was made because as described in the previous chapters glial response in the SNc is detectable from day 2 after 6-OHDA lesion induction. Therefore, to achieve beneficial effects it is feasible to aim for modulation of glial activity upon their activation. The experiment was terminated on day 9 after lesioning because on day 9 significant loss of TH+ve dopaminergic neurons started to manifest in the SNc and dopamine depletion in striatum was also significant.

As demonstrated in our results, treatment with GW855266X and pioglitazone starting 2 days after 6-OHDA lesion induction for 7 consecutive days attenuated TH+ve dopaminergic neuronal cell death in the SNc, hence protected the integrity of dopaminergic neurons in this area. This was concomitant with prevention of dopamine depletion in the striatum following 6-OHDA lesion induction. This observation further indicated that PPAR-γ agonists (GW855266X and pioglitazone) preserved the functional activity of the nigrostriatal tract and protected dopaminergic neuronal terminals in the striatum on day 9 after lesion induction compared to vehicle treated group.

In parallel, our data demonstrated that treatment with GW855266X and pioglitazone 2 days after 6-OHDA lesion induction significantly decreased the glial response in the SNc. The glial response as mentioned in the previous chapters was characterised by increase in the number of activated OX6 and CD68+ve microglia/macrophage as well as their immunophenotypic changes in the SNc. As discussed in Chapter 3 (*see section 3.5.1*) activated microglia/macrophages undergo morphological changes and transform from a resting ramified morphology to an amoeboid morphology with short and thick processes

(Kreutzberg, 1996). Presence of OX6+ve microglia indicated that this sub-population of activated microglia underwent immunological changes acquiring the ability to process and present antigens. Treatment with GW855266X (5mg/kg) or pioglitazone (20mg/kg) for 7 days led to significant and partial decrease in the number of activated OX6+ve microglia in the medial and lateral portions of the SNc. This supports the significance of microglial activation and their association with dopaminergic neuronal cell death following 6-OHDA lesion induction. Indeed, other studies have shown that oral treatment with the PPAR-γ agonist pioglitazone reduced OX6+ve microglial cell number in the SNc and protected dopaminergic neurons in the SNc following LPS injection into the striatum (Hunter et al., 2007). In addition, several other studies have shown that oral administration of PPAR-γ agonists partially protected dopaminergic neurons against MPTP administration and this was associated with inhibition of glial response in the SNc (Teismann and Ferger 2001; Breidert et al. 2002; Feng et al. 2002; Dehmer et al. 2004).). In our study partial inhibition of microglial activation was associated with a significant protection of dopaminergic neurons and preserved striatal dopamine content. Indicating that reactive gliosis could be damaging if microglia are over- activated (Streit et al., 1999).

GW855266X and pioglitazone treatment after 6-OHDA lesion induction, not only affected the number of OX6+ve microglia but there was also a total inhibition of CD68+ve macrophages in the SNc following GW855266X treatment. The amount of CD68 expression in a single cell can be correlated to phagocytic activity of the respective cell type (Damoiseaux et al., 1994). One possible explanation for the absence/ reduction of CD68 expressing phagocytic macrophages in the SNc following treatment with GW855266X and pioglitazone could be the almost total protection of dopaminergic neurons in the SNc where no cell debris or apoptotic neurons were present to stimulate phagocytic activity and clearance. In addition, PPAR-γ agonists might have inhibited the phenotypic conversion of monocytes to macrophages in the SNc (Ricote et al., 1998). PPAR-γ is expressed on cells of monocyte/macrophage lineage including brain resident microglia (Ricote et al., 1998; Bernardo et al., 2002). Evidence suggests that PPAR-γ receptor stimulation inhibits the activation of macrophages by interfering with the transcriptional induction of genes involved in their differentiation, such as MMP-9 which is up regulated during macrophage activation and contributes to tissue damage in acute and chronic inflammation (Welgus, 1990; Matrisian, 1992) and iNOS (Ricote et al., 1998). Differentiation of the bone marrow

derived monocytes into OX6 and CD68+ve microglia/macrophages in the SNc following MPTP administration (Rodriguez et al., 2007) was blocked by PPAR-γ agonists that has been shown to be a negative regulator of microglia/ macrophage activation and differentiation, (Ricote et al., 1998). PPARγ agonists were also found to inhibit production of inflammatory cytokines such as TNF-α in monocytes (Jiang et al., 1998).

In line with these findings, our data further demonstrated that concurrent with a reduction in the microglial response, treatment with GW855266X and pioglitazone led to decrease in the number of MMP-3 and MMP-9+ve cells in the SNc. As demonstrated in Chapter 4 neuronal MMP-3 and 9 expressions increased significantly prior to dopaminergic neuronal loss and was associated with microglial activation (*see Chapter 4, section 4.3.1*). A decrease in the number of both MMP-3 and 9+ve cells following GW855266X or pioglitazone treatment reflects their role in the local activation of microglia. However, the number of MMP-3 and MMP-9+ve cells was not entirely eliminated by GW855266X and pioglitazone. Evidence suggests that MMPs are involved in microglial activation and differentiation in the SNc (Kim et al., 2005; Kim et al., 2007). Hence, partial inhibition of MMP-3 and 9 by GW855266X and pioglitazone could be one possible explanation for partial inhibition of 6-OHDA induced OX6+ve activated microglia in the SNc. The mechanism by which MMPs specifically MMP-3 and MMP-9 leads to microglial activation is not yet fully understood. Indeed, ECM molecules such as laminin and fibronectin, are substrates for MMPs being modified or cleaved by MMPs to release their soluble forms which regulate microglia/macrophages function (Chamak and Mallat, 1991; Tate et al., 2007). In support of our findings, a recent study has demonstrated that neuroprotection and reduction in the infarct size in a model of stroke was associated with decreased MMP-9 expression following treatments with a non TZD PPAR-γ agonist (Pereira et al., 2005).

Treatment with GW855266X and pioglitazone after 6-OHDA lesion induction protected > 90% of dopaminergic neurons in the SNc however, activated microglial cells namely OX6+ve microglia were only partially inhibited by ~68%. Interestingly, even partial inhibition of activated microglia protected dopaminergic neurons from 6-OHDA toxicity further emphasising the detrimental effects of microglial response in the SNc. Alternatively, there may also be a direct protective effect of GW855266X and pioglitazone on dopaminergic nerve cells leading secondary reduction in MMP-3 and 9 expressions and microglial activation. Pioglitazone is currently used as an antidiabetic agent that enhances basal glucose uptake by regulation of glucose transporters in peripheral tissue (Smith et al.,

2001). In neuronal tissue, the effects of pioglitazone and other members of thiazolidinediones on glucose homeostasis has not yet been investigated. However, following 6-OHDA lesion induction, reduced glucose metabolism has been observed on the lesioned side of the brain (Carlson et al., 1999; Casteels et al., 2008). Therefore, it is feasible to suggest that GW855266X and pioglitazone could induce an increase in glucose uptake which could partially protect dopaminergic neurons from death inducing effects of hypoglycemia (*For review see*, Suh et al., 2007). Such effects could be investigated in *vitro* studies.

It is beyond the scope of this thesis to explore these mechanisms in detail. However , PPAR-γ activation leads to regulation of gene expression by heterodimerization with another nuclear receptor, the retinoid X receptor α (RXR), and this complex binds to specific DNA sequence elements termed peroxisome proliferator response elements (PPREs) on target genes, leading to responsive gene expression (Kleiwer et al., 1992). On the other hand, PPARs also act to inhibit pro-inflammatory gene expression and do so through mechanisms which are not reliant upon their DNA binding ability. Through various mechanisms, PPARs can suppress the activities of many distinct families of transcription factor. In most cases, agonist-induced activation of the PPAR is required for effective transrepression to occur, regardless of the specific controlling mechanism that is being induced.

Ghisletti and colleagues (2007) have recently described a novel mechanism of PPAR-γ mediated transrepression of NFκB regulated inflammatory genes. NFκB-regulated inflammatory genes are maintained in a repressed state through their association with nuclear receptor co repressor (N-CoR) containing complexes. Upon exposure to pro-inflammatory stimuli this complex is dissociated and gene expression initiated. If PPAR-γ agonists are present they bind to the PPAR-γ and this ligand–receptor complex is then modified by the addition of a Small Ubiquitin-related Modifier (SUMO) moiety. This modified receptor then binds to N-CoR complexes that are resident on the promoters of NFκB-regulated genes and prevents the dismissal of the co repressor complex, thus preventing inflammatory gene expression (Pascual et al., 2005). This proposed mechanism is supported by in *vivo* studies in the MPTP model of PD, where an increase in expression of the inhibitory protein-kappa-B alpha (IκBα) and inhibition of translocation of the NFκB subunit p65 to the nucleus in dopaminergic neurons, glial cells and astrocytes correlates

with the protective effects of pioglitazone via blockade of NFκB activation and iNOS induction (Dehmer et al., 2004).

Despite the substantial amount of data, including our study, that demonstrate the anti-inflammatory effects of PPAR-γ agonists being the main property of these compounds that leads to neuroprotection, other mechanisms of neuroprotection could not be ruled out. Indeed a recent study demonstrated that PPAR-γ agonist rosiglitazone protected hippocampal and dorsal root ganglion neurons by a mechanism involving Bcl-2 up-regulation and inhibition of neuronal apoptosis (Fuenzalida et al., 2007). As demonstrated in chapter 3 (see *section 3.4.5.1*) Caspase-3+ve apoptotic neurons were present in the SNc following 6-OHDA lesioning. In addition, PPAR-γ agonists might modulate excitotoxic effects of excess glutamate in the SNc, by increasing the expression of GLT1/EAAT2, glutamate transporter in the SNc hence, removing excess extracellular glutamate and protect neurons from excitotoxicity and death (Romera et al., 2007).

Taken together, continuous treatment with GW855266X (5mg/kg) and pioglitazone (20mg/kg) starting 2 days after 6-OHDA lesion induction protected dopaminergic neurons in the SNc and preserved dopamine content in the striatum. The observed neuroprotective properties were at least partly mediated via inhibition of the inflammatory response following 6-OHDA lesion induction.

5.4.2 Continuous treatment with GW855266X or pioglitazone was crucial for the treatments to be neuroprotective and anti-inflammatory

In order to address the question whether the effects observed with either pioglitazone or GW855266X treatment were long lasting, animals were treated with GW855266X (5mg/kg) or pioglitazone (20mg/kg) starting 2 days after 6-OHDA lesion induction for 7 consecutive days. The treatments were withdrawn for further 7 consecutive days and the brains were collected on day 16 after 6-OHDA lesioning. This study mainly demonstrated that withdrawal of treatment with pioglitazone and GW855266X after 6-OHDA lesion induction led to a return of significant dopaminergic neuronal cell death in the SNc and a depletion of dopamine in the striatum. However, unlike the vehicle treated group in these animals, dopamine turnover did not increase on day 16 after 6-OHDA lesioning. The reason for this is not clear in our study but could be due to direct effect of PPAR-γ agonists on dopamine itself, further studies in which treatments are given on their

without 6-OHDA lesion would be useful in determining the effects of PPAR-γ agonists on dopamine and its metabolites. The extent of neuronal cell loss and dopamine depletion reached similar levels observed in the vehicle treated animals suggesting that the effects of GW855266X and pioglitazone completely negated after 7 days of treatment withdrawal. In addition, withdrawal of treatment for 7 consecutive days led to an increase in the number of activated OX6 and CD68+ve macrophages in the SNc after 6-OHDA administration that were morphologically active. OX6 and CD68+ve microglia/macrophages had hypertrophied cell bodies and thickened processes. The extent of microglial activation reached similar levels to that observed in the vehicle treated animals 16 days after 6-OHDA suggesting that the anti-inflammatory effects of GW855266X and pioglitazone were not long lasting when the compounds were withdrawn. These findings were also reflected in the significant increase in the number MMP-3 and MMP-9+ve cells in the SNc, indicating that inflammation in the SNc following 6-OHDA lesion induction is an ongoing process and continuous presence of PPAR-γ agonist is essential in order to maintain its anti-inflammatory and hence neuroprotective properties. Time course studies in Chapter 3 and 4 indicate that on day 15 after 6-OHDA lesion induction active microglia are still present in the SNc and further studies in which PPAR-γ agonist treatment is extended past this window may be more beneficial in halting microglial activation. Our data indirectly supports the mode of action of PPAR-γ agonists that are ligand dependent nuclear receptors and continuous presence of the ligand is necessary to evoke cellular changes. Therefore, treatment with PPAR-γ agonists relies on adequate presence of its ligand in order to be beneficial and maintain its anti-inflammatory and neuroprotective effect.

Thus, oral administration of PPAR-γ agonists activates a cascade of events involving PPAR-γ activation, inhibition of NFκB and iNOS expression in microglia resulting in the reduction of active gliosis that leads to protection of dopaminergic neurons in the SNc and protects the integrity of the nigrostriatal tract.

Conclusions

This study provides robust evidence that inflammation plays a significant role in the initiation and progression of damage to dopaminergic neurons. This was mirrored in the neuroprotective and anti-inflammatory effects of PPAR-γ agonists, GW855266X and

pioglitazone, in the SNc, following 6-OHDA lesion induction. This study further supports potential therapeutic benefits of manipulation of inflammation in PD.

Chapter 6 -General Discussion and Future work

6.1 A brief overview of the project

One of the most challenging and unmet need in PD is to understand the events leading to neuronal degeneration. Such information could lead to the development of novel drugs that could possibly slow down or even arrest the neurodegenerative process in PD. Post-mortem studies have revealed some useful information and insight into the pathogenesis of PD, indeed they have demonstrated an association of an innate inflammatory response with the neurodegenerative process. Our knowledge of factors contributing to the neurodegenerative process is hampered to some degree by the fact that donated human tissue for research is often from advanced PD patients, thus precluding the examination of factors in the early phases of neurodegeneration. Consequently, it is very difficult to judge the true role in the neurodegenerative process of factors e.g. microglial activation, found in the terminal stage of the disease. Therefore, this project utilized an animal model of PD, namely the 6-OHDA model, to examine the role of the innate inflammatory response during initiation and progression of damage to dopaminergic neurons. In light of knowledge gained from the time course of the inflammatory response in relation to dopaminergic neuronal cell death this project further investigated whether manipulation of the inflammatory cascade with anti-inflammatory agents would be neuroprotective and lead to preservation of dopamine content in striatum.

6.2 The summary of the key findings presented in this thesis

1- Activation of microglia/macrophages, characterised by their morphological and immunophenotypic transformation, preceded dopaminergic neuronal cell death in the SNc following unilateral 6-OHDA lesion induction into the MFB. Activated microglia/macrophages were in close vicinity or attached to dopaminergic neurons in the SNc from day 3 following lesioning with significant dopaminergic neuronal cell loss only occurring from day 9 after 6-OHDA lesion induction concomitant with depletion of striatal dopamine. This suggests an active involvement by microglia in the initiation and progression of dopaminergic neuronal cell death in the SNc. Furthermore, our data demonstrated early phagocytosis of apoptotic neurons by CD68+ve macrophages preventing a potential recovery of these neurons. Dopaminergic neuronal cell death was

observed up to day 15 after 6-OHDA lesion induction and was associated with an increased numbers of CD68+ve phagocytic macrophages. However, MHC II expressing microglia decreased in number from day 9 onwards. This result indicates that the microglial response might be self limiting phenomenon that activates a pro-inflammatory cascade leading to further dopaminergic neuronal death in the SNc. Hence, future studies would be necessary to investigate longer survival time points even up to 6 months.

2- Up-regulation of MMP-3 and MMP-9 following 6-OHDA lesion induction was concomitant with microglia/macrophage activation in the SNc prior to dopaminergic neuronal cell death. The time course of MMP-3 up-regulation was similar to the appearance of MHC II expressing microglia and decreased by day 15 after lesion induction. However, up-regulation of MMP-9 expressing cells was maintained up to day 15 after lesioning. It is possible that MM-9 might act as a trigger for further pro-inflammatory changes in the SNc leading to the progression of dopaminergic neuronal cell death. Indeed, the interaction between the ECM and neurons plus neuron-glia interactions play an important role in microglial activation. This was evident in our findings that demonstrated a temporal relationship between neuronal expression of both MMP-3 and MMP-9 and microglial activation prior to dopaminergic neuronal cell death after 6-OHDA lesioning. These observations were concomitant with up-regulation of CD200R expression, further suggesting that once the ECM is challenged and neurons are damaged, signalling factors are released that are rapidly recognised by microglia leading to their activation and consequently neuronal damage and eventually death.

3- The significance of inflammatory response following 6-OHDA lesion induction was evident when treatment with Pioglitazone and PPAR-γ agonist (GW855266X) either before or after lesion induction led to the down regulation of microglial response and protection of dopaminergic neurons in the SNc with preservation of striatal dopamine content. Indeed, down regulation of both MMP-3 and MMP-9 concomitant with inhibition of microglial response was indicative of their signalling role in microglial activation. Furthermore, to maintain the neuroprotective properties of PPAR-γ agonists their continuous presence was vital as once the drug were withdrawn for 7 days the neuroprotective /anti-inflammatory effect were not maintained.

Taken together, this study for the first time demonstrated that in the 6-OHDA model of PD, inflammation that is at least partly triggered by activation of MMP-3 and MMP-9 prior to dopaminergic neuronal cell death, is deleterious to dopaminergic

neurons. In parallel, the neuron-microglia interaction that keeps microglia quiescence was disturbed leading to decreased inhibitory effect of neurons on microglial response following 6-OHDA lesioning. This was characterised by a time dependent increase in the number of CD200R+ve cells that under normal condition are bound to their ligand the CD200 glycoprotein present on neurons. Furthermore, for the first time we demonstrated that inhibition of microglial response via activation of the anti-inflammatory PPAR-γ sub-type, using a novel agonist (GW855266X) and pioglitazone as a reference compound, leads to robust neuroprotection in the SNc with preservation of dopamine in the striatum.

The findings presented herein are of significant interest, especially since they are *in vivo*; however it is noteworthy that these data must be interpreted in the context of some methodological considerations related to the experimental model of PD employed in the current study, which are discussed in the following sections.

6.3 Reappraisal of the 6-OHDA model employed in this study and some methodological considerations

In humans, PD has a slow and progressive nature, whereas the 6-OHDA-lesion models may promote rapid cell death. Therefore, different 6-OHDA-lesion rat models of PD have been developed to study different stages of PD. 6-OHDA injections into the SNc, MFB or striatum have been widely used as methods of inducing degeneration of dopaminergic neurons in the nigrostriatal pathway. Nevertheless, depending on the location of the injection site, animals present different time courses of progression and severity of lesion (Emborg et al., 2004; Deumens et al., 2002; Kirik et al., 1998). The model employed in this project was created by injection of 6-OHDA into the MFB in order to promote a time dependent partial retrograde loss of dopaminergic neurons in the SNc and partial depletion of striatal dopamine. The partial and time dependent progression of lesion of the nigrostriatal system represented the early stages of idiopathic PD in humans. In the current study, in order to ensure that a partial lesion of the nigrostriatal system was generated such that the lesion size may be closer in scale to that observed in early stage PD, use of the noradrenalin uptake inhibitor desipramine was not employed. Desipramine administration prior to 6-OHDA, leads to an almost total destruction of nigrostriatal axons and cell bodies. Desipramine, by preventing

uptake and sequestration of 6-OHDA into noradrenergic neurones may result in dopaminergic neurons being exposed to a higher concentration of 6-OHDA. This is important, since clearly it would be preferable to investigate the role of inflammation in initiation and progression of lesion in the nigrostriatal system and assess the potential neuroprotective effects of putative neuroprotective agents in a model system which mimics this clinical situation, where some of the nigrostriatal system is still preserved and may serve as a substrate for functional regeneration or neuroprotection. It is worth noting that toxin injection into the MFB induces dopaminergic cell death retrogradely. Thus, this model may provide a more prolonged temporal window for neuroprotective effects relative to 6-OHDA injection into the SNc, which probably causes a more rapid and dramatic cell death. However, this model did not demonstrate the progressive nature of PD as observed in humans. The size of lesion in the SNc did not show any sigficant progression after day 9 following 6-OHDA lesioning. This observation could be an indication that the 6-OHDA model used in this project, reflects the acute phase of dopaminergic cell death and gliosis in the SNc. Therefore, future studies are needed to examine long term effects of 6-OHDA on microglial activation and doapminergic neuronal cell death in the SNc (*see section 6.5*).

Injection of 6-OHDA to other regions, such as the SN or the striatum was not suitable for studying the time course of inflammatory events in association with dopaminergic neuronal loss for the following reasons. Studies have demonstrated that injection of 6-OHDA into the SNc can promote profound lesions with high degree of dopaminergic cell loss (Kondoh et al., 2005) that might mimic the late stages of idiopathic PD in humans. Also direction administration of 6-OHDA into the SNc would cause additional mechanical damage in the SNc, thus complicating the interpretation of the results. Furthermore, single 6-OHDA administration into the striatum only produces a mild and regional loss of dopaminergic cells in the SNc. Thus, to obtain the extent of cell loss present in newly diagnosed cases of PD it is required to administer 6-OHDA into several sites in the striatum, inducing major mechanical damage which would again complicate any results obtained. Hence, it was deemed for this study a 6-OHDA lesion to the mfb was most suitable. Indeed, there is no perfect animal model that replicates all the pathological features of human idiopathic PD, some of the limitations of the 6-OHDA model employed in this study are discussed below.

The clinical and widespread neuropathological alterations seen in PD patients are not entirely replicated by intra-cerebral injection of 6-OHDA in rodents. Although 6-OHDA induces significant decrease of dopamine and dopaminergic fibres in the striatum and leads to degeneration of dopaminergic neurons in the SN with preservation of non-dopaminergic neurons, it does not affect other brain regions that are affected in human PD such as: anterior olfactory structures, lower brain stem areas or the locus coeruleus (Betarbet et al., 2002). In addition, formation of cytoplasmic inclusion bodies, known as Lewy bodies, that are hallmarks of PD pathology are not observed in 6-OHDA lesioned animals. However, *in vivo* 6-OHDA partial lesion model has been used routinely for the purpose of screening potential therapeutic (Lundblad et al., 2002; Asin et al., 1995) and neuroprotective drugs (Datla et al., 2003). 6-OHDA robustly mimics and reflects many of the molecular changes observed in human PD including oxidative stress, altered iron metabolism, mitochondrial dysfunction etc. and it is a suitable model for studying the underlying mechanisms involved in the processes that leads to dopaminergic neuronal loss including the involvement and role of inflammation (Cicchetti et al., 2002; Depino et al., 2003). Despite the mentioned limitations of this model it is one the most reliable, reproducible and widely used models of PD. To compliment our findings, in future studies it may be informative to carry out similar experiments in other experimental models of Parkinsonism. For example, chronic treatment of rodents with the pesticide Rotenone (Betarbet et al, 2000a) or the proteasome inhibitors such as lactacystin and MG-132 (McKnaught et al, 2002; 2004) or Z-Ile-Glu(OtBu)-Ala-Leu-al (PSI) (Zeng et al, 2006), both of which appear to replicate the classical neuropathology of PD, but importantly are associated with neuropathological changes in other brain nuclei affected in PD and with the formation of Lewy body-like inclusions *in vivo*.

An additional methodological consideration of the current study may be related to the cell counting methodology employed. Indeed, this methodology may potentially lead to over or under estimation of cell numbers (neurons and glia). In the current study, the numbers of cells were quantified manually in a blind fashion throughout the rostral to caudal extent of the SNc. As the cell counting was not performed at pre-determined distance intervals as is the case in unbiased stereological methods (Hedreen et al., 1999; Baddely et al., 2001) coupled with the thickness of the tissue sections on which immunostaining and cell counting was performed (20 μM-thick) the possibility exists that the same cells may be present in two sections, leading to possible over estimation

of cell numbers. Therefore, our results could be confirmed using unbiased stereological methods of cell counting as described by others (Luquin et al., 2006; Aguirre et al., 2001). However, it is important to note that the approach used to cell counting has been employed in previously published studies to ensure that comparable rostral to caudal levels of the SNc are sampled between animals. Importantly, this approach provides robust and accurate quantification of nigral cell loss (Iravani et al., 2002,2005) and neuroprotection (Datla et al., 2001, 2004; Vernon et al., 2005; 2007). Moreover, the counting was performed blind to the treatment group and verified by a second operator, also blind to the treatment group.

6.4 General discussion of the main findings and possible future directions

Following a 6-OHDA challenge to the MFB activated microglia started to migrate and proliferate in the SNc in a time dependent manner prior to dopaminergic neuronal cell death in the SNc. The local proliferation of activated microglia was evident by expression of the Ki67 mitotic marker co-localised with the MHC II expressing microglia and their migration was observed by their relocation from the medial portion of the SNc to the ventrolateral portion in a time dependent manner. In the SNc, OX6+ve microglia appeared earlier than those labelled with CD68. Moreover, it was found throughout all time points of our study that the number of OX6+ve microglia was slightly greater than that of CD68+ve microglia suggesting that a vast proportion of the OX6 +ve cells may acquire a phagocytic phenotype. In fact, it has been demonstrated that significant proportion of OX6+ve microglial cells are CD68+ve at the site of neurodegeneration after MFB transection (Cho et al., 2003, Cho et al., 2007). It would be interesting in the future studies to assess the presence of activated microglia/macrophages at the actual site of lesion in the MFB and to determine the time course of their activation in this region and comparing it to the SNc. This may be useful in the assessment of dynamics of the microglial response in the MFB compared to the SNc. Our findings clearly demonstrated that following 6-OHDA lesion induction a significant increase in microglia/macrophages occurs in the SNc. However, whether this is a direct effect of 6-OHDA on microglia or whether it is indirectly induced via other cells, remains to be elucidated. Indeed, studies on rat primary mesencephalic cultures,

demonstrated that cell death observed following 6-OHDA exposures could be due to different factors. Namely the synergestic effect of 6-OHDA auto-oxidation derived ROS and the inhibition of the mitochondrial respiratory chain with early microglial activation followed by further increase in the amounts NADPHoxidase derived ROS constitute a relevant and early component of the 6-OHDA-induced neuronal death (Rodriguez-Pallares et al., 2007). These findings are in line with our studies presented in this thesis. However, the effect of 6-OHDA on microglial cells per se is not yet known, therefore *in vitro* studies using glial cell cultures on their own would be informative to establish whether the effect of 6-OHDA on the activation of glia mainly microglia is a direct effect or it requires the presence of neurons or other cells such as astrocytes in the culture. In addition, further studies are needed to investigate the origins of the microglia /macrophages in our model. This study would address the question of what proportion of activated microglia in the SNc are the resident macrophages in the brain and to what extent do peripheral blood derived monocytes participate in this process and mature to OX6 or CD68 expressing microglia/macrophages in the brain parenchyma. Interestingly, a study by Rodriguez et al., (2007) demonstrated that the migration of peripheral bone-marrow-derived cells (BMDCs) takes place to the brain occurs in the chronic MPTP model of PD. They demonstrated that BMDCs expressing enhanced green fluorescent protein (GFP) were present in the SNc before dopaminergic neuronal cell death and were mainly microglial cells of a peripheral origin that matured to OX6 and CD68 expressing microglia/macrophages in the SNc. Therefore, this study provides evidence of increased penetration of BMDC into brain areas before and during dopaminergic cell death. The differentiation of BMDC into microglia suggests that cells crossing the BBB may participate in the neurodegeneration process (Rodriguez et al., 2007). Furthermore, these findings imply that the transformation of microglia to antigen presenting cells, expressing MHC II antigens, that precedes their transformation to phagocytic cells, could be initiated from both the local resident population of microglia and some invading BMD cells. However, which one of these processes precedes the other is another missing link which needs to be addressed in future studies. Indeed, studies by Carvey, et al (2005) demonstrated that unilateral injections of 6-OHDA into the striatum or the MFB produced increased leakage in the BBB in the SNc and striatum, as assessed by the leakage of FITC-labelled albumin or horseradish peroxidase from the vasculature into the brain parenchyma.

The time dependent functional and morphological transformation of microglia in the SNc in parallel to dopaminergic cell death, indicates that when dopaminergic cell death occurs, the number of phagocytic macrophages also increase to clean up the debris. which on its own could be neuroprotective. Indeed initial activation of microglia/macrophages could be an attempt to protect neurons, importantly the exent and the duration of their activation are crucial factors determining the role of glia in the CNS following an insult. One of the most compelling evidence supporting a critical role of microglia in neuroprotection comes from acute axonal injury in rodents. Axotomy of facial motoneurons in the periphery triggers a microglial response in the facial nucleus almost immediately after the injury has occurred. Within a few days, axotomized perikarya are surrounded by activated microglial cells which tightly ensheath the injured neurons with their cytoplasmic processes. The number of activated microglia in the facial nucleus increases dramatically and suddenly through a proliferative burst that lasts from about day 2 to day 4 post-axotomy (Graeber et al, 1988). In addition production of transforming growth factor-b1 (TGF-β1) mRNA is increased in the facial nucleus during the first week post-axotomy and this growth factor has been localized to activated microglial cells (Lehrmann et al, 1998). Indeed, it likely that many other intercellular communication processes are mediated by the close physical apposition of microglia and neurons. Microglia constantly monitore the neuronal state of viability, which undoubtedly involves many complex signaling events (Nimmerjahn et al, 2005). In fact, it is even conceivable that upon early recognition of non-viability, microglia may actively hasten the neuron's demise through production of toxic molecules, facilitating speedy removal of a non-functional cell (Streit et al, 2002). On the other hand, the over-activation of microglia, as observed in our study, could lead to further damage and apoptosis. Apoptotic cells trigger the recruitment of phagocytic cells, so as to quickly and effectively remove the dead neurons. Such dying cells release chemoattractants, such as fractalkine, a chemokine that is predominantly expressed in the brain (Chapman et al., 2000) or the phospholipid lysophosphatidylcholine (Lauber et al., 2003) which promotes chemotaxis of primary microglia and monocytes. In the early phases of neuronal injury microglia express numerous molecules with important immune functions and may stimulate functions such as the adaptive removal of synapses from injured neurons (Graeber et al., 1993). The loss of synapses, axons and neurons following 6-OHDA lesion induction may exacerbate the inflammatory response within the central nervous system towards the site

of injury leading to progressive neuronal cell death (Hirsch et al., 1998). In a more clinical point of view, similar activation could be elicited by neuronal inclusions, Lewy bodies, plaques or viral/bacterial antigens in humans. Microglia, acquire a macrophage phenotype and take on the role of removing degenerating synaptic terminals and neuronal debris. The inflammatory response around damaged neurons or neurites could induce an indiscriminate response similar to chronic inflammation in the cartilage or myelin, as observed during autoimmune disease such as rheumatoid arthritis or multiple sclerosis (Vowinckel et al., 1997; Banati et al., 1999). This response may result in exacerbation of neuronal injury. Activated microglia could participate in the neurodegenerative process by releasing soluble factors and enzymes such as TNFα, PGE_2 , INF-γ, reactive nitrogen species ,proteases, ROS, eicosanoids and excitatory amino acids which are toxic to neurons (Block and Hong ,2005; Liu and Hong, 2003). Among these microglial derived neurotoxic factors, ROS and their downstream products have been shown by us and others to contribute significantly to neuronal cell loss in PD (Dexter et al., 1987, Dexter et al., 1994, Koutsilieri et al., 2002). It is highly likely that microglia-derived neurotoxic factors act in concert, exacerbating their effects. For example, TNFα induces the expression of inducible nitric oxide synthase (iNOS) in glia, thus amplifying the NO-mediated neuronal loss. Additionally, aging is shown to provide a pro-inflammatory environment in the brain and is another factor that amplifies the microglial response (Godbout et al., 2005). Microarray studies on post-mortem brain tissue from parkinsonian patients and controls demonstrated an increased expression of genes encoding pro-inflammatory cytokines including, the TNF receptor gene, TNF receptor super family, member 21, and the mitochondrial complex I gene, and subunits of the mitochondrial electron transport chain with decreased expression of several glutathione related genes in the SNc suggesting a molecular basis for inflammatory and oxidative damage to neurons in parkinsonian cases compared to controls (Duke et al., 2007). These findings, despite reflecting the end stage of the disease, provide clues for future studies on the involvement of inflammation in PD pathogenesis.

This project, for the first time established a potential trigger for activation of microglia/macrophage in the SNc following 6-OHDA lesion induction. We demonstrated that the microglia response, could to be at least partly mediated by expression of different matrix metalloproteinases as signalling molecules. Neuronal

expression of MMP-3 and MMP-9 showed a temporal relationship with microglial activation and dopaminergic neuronal cell death. The exact cellular and molecular events that trigger the release of MMP-3 and MMP-9 enzymes in our model are to be investigated in future studies. In addition, the full chemotaxis leading to the focal up-regulation of MMP-3 and MMP-9 in the SNc, followed by focal activation of microglia, remains to be investigated. It seems likely that pre-apoptotic neurons, which were detected by the expression of the apoptotic marker caspase-3, release significant amounts of MMP-3 and MMP-9. Up-regulation of these enzymes could destabilise the ECM that alerts and eventually activates microglial cells. Up-regulation of CD200R, which is predominantly expressed on microglia and under homeostasis conditions, is engaged with its ligand CD200 on neurons, is a further indication of a disrupted ECM and up-regulation of microglia. At this stage, neuronal inhibition of microglia is reduced or even lost as consequence of the neurons being pre-apoptotic, hence leading to microglial activation. Additional evidence for MMP-3 release from apoptotic neuronal cells was evident in studies by Kim et al., (2007) where MMP-3 was identified in degenerating primary mouse mesencephalic cultures treated with MPP^+. Furthermore, in such studies the inhibition of TNF-α release from activated microglia by the specific MMP-3 inhibitor NNGH led to neuroprotection. Up-regulation of MMP-3 and MMP-9 may contribute to changes in BBB permeability with the ingress of plasma components, which contribute in some part to microglial activation (Madena et al., 2000). The cascade of events leading to the glial response and cell death in PD following an insult, could be further investigated by examining the up-stream mechanisms that induces MMP activation in the 6-OHDA model. A search for MMP inducing factors in tumour cells has led to the identification of the extracellular matrix metalloproteinase inducer (EMMPRIN) molecule (Kataoka et al., 1993; Biswas et al., 1995). EMMPRIN is a cell surface glycoprotein composed of two Ig domains in the extracellular region. Depending on the cell system, EMMPRIN can stimulate production of MMP-1, -2, -3, and 9 (Gabison et al., 2005; Yan et al., 2005). Therefore, studies looking into the gene expression profile of this molecule and its expression following 6-OHDA lesion induction would be of interest as it could be a new target for therapy in PD that might lead to inhibition of inflammation before its initiation.

The interpretation of our findings in a clinically relevant scenario so far indicates that the process of dopaminergic neuronal degeneration in the SNc is initiated following the expression of both MMP-3 and MMP-9 with subsequent microglial activation. This

process not only enhances death of the damaged dopaminergic neurons but also cause apoptosis of the neighbouring dopaminergic neurons. This cycle may create a progressive, self-perpetuating degeneration of the dopaminergic neurons in the SNc. The progressive nature of PD is best shown in previously mentioned reports in humans who had self-administered MPTP 10 to 12 years prior to death. As mentioned in the preceding chapters, post-mortem analysis in these subjects revealed activated microglial surrounding dopaminergic neurons in the SNc (Langston et al., 1999). Therefore, the final part of this project given the significance of the inflammatory response in the SNc, explored the effects of modulation of glial activity via activation of PPAR-γ sub-type following 6-OHDA induced lesion into the MFB.

Our data presented herein demonstrated that a microglial response was evident from 2-3 days after 6-OHDA lesion induction. Hence, this is a rapid process and considering the progressive dopaminergic neuronal cell death that followed, the glial response is most likely to be more damaging than protective. Therefore, we hypothesised that inhibition or down-regulation of microglial cells could serve as a neuroprotective strategy in PD. To examine this hypothesis we used a novel PPAR-γ agonist GW855266X (licensed by GSK) and pioglitazone as a reference compound. Our data provided robust evidence that oral treatment with GW855266X and pioglitazone, either before 6-OHDA lesion induction and continued for 7 days post lesion or administered 2 days after 6-OHDA lesion induction continued for further 7 days, significantly reduced the microglial response in addition to both MMP-3 and MMP-9 expression. This was accompanied by a significant protection of dopaminergic neurons in the SNc. The nigrostriatal functionality was also preserved indicated by normal levels of striatal dopamine and its metabolites. However, continuing presence of PPAR-γ agonists was vital for the neuroprotective and anti-inflammatory effects of these compounds. As presented in our data withdrawal from this compound led to dopaminergic neuronal death and activation of microglia to the same level as the vehicle treated animals.

The exact mechanism of action of PPAR-γ agonists is not yet fully understood in the 6-OHDA model. Our drug withdrawal data indirectly supports the known mode of action of PPAR-γ agonists, which stimulate nuclear receptors and continuous presence of the ligand is necessary to evoke cellular changes. Therefore, treatment with PPAR-γ agonists relies on adequate presence of its ligand in order to be beneficial and maintain

its anti-inflammatory and neuroprotective effect. Our knowledge regarding the anti-inflammatory role of PPAR-γ would potentially be aided greatly by comparative evaluation of normal and mutant mice that lack PPAR-γ subtypes. However, complete elimination of a functional PPAR-γ gene results in embryonic lethality, therefore PPAR-γ heterozygote knockout mice ($PPAR\gamma^{+/-}$) with 50% reduction in PPAR-γ were developed. Such mice exhibit resistance to high-fat diet–induced obesity and insulin resistance (Kubota et al., 1999; Kadowaki et al., 2000). PPAR-γ mutant permits us to investigate the physiological role of PPAR-γ in the immune system that will aid in the development of better drug targets. Evidence suggests that PPAR-γ receptor stimulation inhibits the activation of macrophages by interfering with the transcriptional induction of genes involved in their differentiation, such as MMP-9 which is up regulated during macrophage activation and contributes to tissue damage in acute and chronic inflammation (Welgus, 1990; Matrisian, 1992) and iNOS (Ricote et al., 1998) (Fig 6.1). Differentiation of the bone marrow derived monocytes into OX6 and CD68+ve microglia/macrophages in the SNc following MPTP administration (Rodriguez et al., 2007) was blocked by PPAR-γ agonists which have been shown to be a negative regulator of microglia/ macrophage activation and differentiation, (Ricote et al., 1998). PPARγ agonists were also found to inhibit production of inflammatory cytokines such as TNF-α in monocytes (Jiang et al., 1998) (Fig 6.1).

Despite all this encouraging *in vivo* evidence, it is noteworthy that almost all putative neuroprotective drugs, which have shown promising neuroprotection *in vitro* and *in vivo* experimental models of PD, have failed to show neuroprotective or disease modifying effects in humans. This may reflect limitations of current experimental models of this disease (Schapira et al., 2004). One other major problem is the fact that despite evidence to suggest that inflammation, excitotoxicity, oxidative stress and UPS defects may all be potential pathogenic mechanisms in PD; we still do not know what triggers neurodegeneration in the SNc or indeed, any of the other brain regions affected in PD (Jenner and Olanow, 2006). Additionally, increasing evidence suggests that PD is not simply a single disease, but may in fact be a syndrome associated with different aetiologies, that may vary in complexity between individuals (Jenner and Olanow, 2006; Langston et al., 2006; Carvey, et al., 2006). It is apparent, that different signs and symptoms of PD manifest at different time points in different individual patients, suggesting that the involvement of pathogenic factors may also vary between individual

patients which points to the heterogeneity of PD aetiology (Jenner and Olanow, 2006). Thus, the possibility that PD is a syndrome, in which different patients may be undergoing different pathogenic mechanisms at different times and in different brain regions, it is perhaps not surprising that many neuroprotective strategies which are aimed at a specific pathogenic event or pathway implicated in PD may fail (Jenner and Olanow, 2006). Additionally, to imply anti-inflammatory/neuroprotective therapy for PD one major issue is to be able to diagnose PD before the symptoms appear. Because once symptoms are present already ~80% of dopaminergic neurons are lost hence neuroprotective strategies might not be beneficial due to the profound loss of dopaminergic neurons.. This is where biomarkers that specifically reflect onset of pathology, directly or indirectly, may have a profound impact on diagnosis making in the future. Biomarkers can also be used to determine the efficacy of novel neuroprotective strategies and for monitoring the progress of the disease. Research into finding the most relevant biomarkers that are indicative of early PD before the symptoms occur is a growing field and still there is no definite marker for this disease. Studies in this area are ongoing, for example one study using a high field strength MRI demonstrated increase of iron in the lateral portion of the SNc in early PD (Martin et al., 2008). Other possible biomarkers include biochemical markers where antibodies found in the CSF or blood of patients against certain molecules, such as α-synuclein and neuromelanin antibodies, oxidative stress and mitochondrial deficit markers. In addition, alteration in the ratio of T regulatory cells in the blood may reflect an immune reaction before any symptoms of the disease manifest (Baba et al., 2005). On the basis of findings of McGeer et al., (2004) who demonstrated immune reactions associated with cell death in the SN occur several years before the onset of symptomatic PD, it is interesting to note a study which reported PD patients rarely have a cold with high fever requiring bed rest, not only during the course of their illness but also before symptomatic disease onset (Kawaguchi et al., 1998). This observation indicates that a series of peripheral immune alterations might precede the occurrence of immune reaction-related inflammation in the brain that could be used as immune related biomarkers for PD. Thus, until these issues are resolved or we are able to identify specific subsets of PD patients with specific aetiologies and treat them accordingly to the pathogenic cascade underlying their disease, a possible useful approach to PD treatment may be the use of multi-functional or a cocktail of drugs which are able to protect neurones against multiple toxic insults (Jenner and Olanow, 2006). Indeed,

support for this idea comes from the development of novel iron chelators which are also monoamine oxidase B inhibitors and sequester free radicals result in significantly greater neuroprotection in experimental models of PD than compounds with these individual activities alone (Zheng et al, 2005; Gal et al, 2005). These data suggest that a drug with at least two mechanisms of action, targeting at multiple pathogenic mechanisms of the same disease, may offer more therapeutic benefit compared with a drug that only targets one disease aetiology (Van der Schyf et al., 2006). To this end, treatment with PPAR-γ agonist in our model targets multiple factors involved in the pathogenesis of PD. For example, as mentioned earlier the reduction in both MMP-3 and MMP-9 could stabilise the BBB, hence limiting the invasion of activated blood-derived leukocytes into the brain (Leppert et al., 2001; Avolio et al., 2003), plus the down regulation of microglia/macrophage activation in the SNc leading to the ultimate protection of dopaminergic neurons. In addition, other studies have demonstrated that PPAR-γ agonists inhibit neuronal apoptosis (Fuenzalida et al., 2007), modulate excitotoxic effects of excess glutamate in the SNc, thus protecting neurons from excitotoxicity (Romera et al., 2007), blockade of NFκB activation and iNOS induction (Dehmer et al., 2004). PPAR-γ agonists were also found to inhibit production of inflammatory cytokines such as TNF-α in monocytes (Jiang et al., 1998). Therefore, PPAR-γ agonists may be promising compounds in modifying PD in future. (Figure 6.2 shows a simplified schematic diagram of how inflammatory pathway effects dopaminergic neurons).

6.5 Future directions

The main findings of this project could be taken further to expand our knowledge on the role of immune responses in PD and to identify potential key molecules as new drug targets for neuroprotective therapy in PD. The main findings presented in this thesis demonstrated that microglial response triggered by expression of neuronal MMP-3 and MMP-9 enzymes precedes dopaminergic neuronal loss in PD. Furthermore modulation of microglial response concomitant with down regulation of MMP-3 and MMP-9 by PPAR-γ agonists reduced the inflammatory response and protected dopaminergic neurons in the SNc and restored functional activity of the nigrostriatal tract.

To take our studies further and gain more insight into the role of inflammation in PD pathogenesis in our model, later time points could be investigated to elucidate later phases of microglial activation and changes in signalling molecules both in the SNc and striatum and their association with progression of dopaminergic neuronal loss.

In addition, we could further investigate additional factors that are involved in dopaminergic neuronal cell death in the SNc following microglial activation, such as the expression profile of pro and anti-inflammatory cytokines at different time points in the SNc and striatum, following 6-OHDA lesion induction needs to be assessed. For example: Groups of animals (n=6) will be sacrificed at 1,3,5,7,9,11,13,15,21,28, 35 and 50 days post 6-OHDA lesion induction for changes in cytokine expression profiles in the SNc and the striatum. Cytokines that can be investigated utilising SearchLight (ThermoFisher Scientific) cytokine/chemokine rat Arrays (sandwich ELISA) include, the anti-inflammatory cytokines (IL-4, IL-6, IL-10, IL-11, 1L-13 and TGF-B) and pro-inflammatory cytokines (IL-1β, IL-1α, IL-2, IFNγ, TNFα and MCP-1). In addition, to gain more information on degeneration of dopaminergic neurons Fluoro-Jade C immunoreactivity which has been utilised as an early marker of degenerating neurons could also be employed to see whether the neurons are showing signs of neurodegeneration prior to the loss of TH or NeuN expression. In light of data gained from the above mentioned studies key molecules in the activation of microglia and the neurodegenerative process could be identified and used as targets for neuroprotective therapy in PD. To test whether these molecules represent suitable drug targets for neuroprotection proof of concept neuroprotective studies utilizing the 6-OHDA model would be used. However, knowing that no animal model truly represents all of the features of PD hence it is essential to pre-clinically test potential neuroprotective compounds in a variety of models displaying different features of PD so as to support their use in the clinic. This approach will also enable us to study the nature of innate immune response in different models. Therefore in addition to the 6-OHDA the lactacysteine proteasome inhibitor rat models and the MPTP mouse model should also be employed. One example of a molecule used as a target for therapy would be the expansion of our pilot studies using PPARγ agonist. As demonstrated (see *Chapter 5*) a single dose of PPAR γ agonist in the 6-OHDA model have shown a robust neuroprotective effect associated with inhibition of microglial activation after 7 days of treatment when animals were killed on drug. Neuroprotection was observed when the

PPARγ agonist was given both as a pre and post 6-OHDA treatment; however this neuroprotection was lost in animals where the drug had been withdrawn after 7 days of treatment. Therefore, future studies on this compound would be to carry out a dose response study in the 6-OHDA model and to investigate whether longer treatment results in a long lasting neuroprotection. Two days after the 6-OHDA lesioning, PPAR γ agonist (5, 10 or 20mg/kg) or drug vehicle will be administered twice daily by gavage for 15 days. 50% of the animals will be killed at the end of the 15 days treatment whilst the remainder will be killed after a further 7 days off drug. This aims to investigate whether the effect of PPAR-γ agonist would be long lasting after the microglial response is down regulated day 15. Similar to this study other potential targets that play an active role in the inflammatory/neurodegenerative process in PD could be used. However, it is important to carry out the pre-clinical studies on different models of PD such as the recent partial lesion model of MPTP in marmosets (Iravani et al., 2005).

6.6 Conclusion

Microglial activation triggered by expression of MMP-3 and MMP-9 preceded dopaminergic neuronal demise in the SNc and was associated with the initiation and the process of cell death in the 6-OHDA rat model of PD. Early modulation of glial response with PPAR-γ agonists (GW855266X- licensed by GSK) and pioglitazone down-regulated the glial response and protected dopaminergic neurons in the SNc with preservation of the functional integrity of the nigrostriatal tract. Hence, inflammation does play a deleterious role in PD pathogenesis and modulation of microglial response could serve as a neuroprotective strategy in this disease.

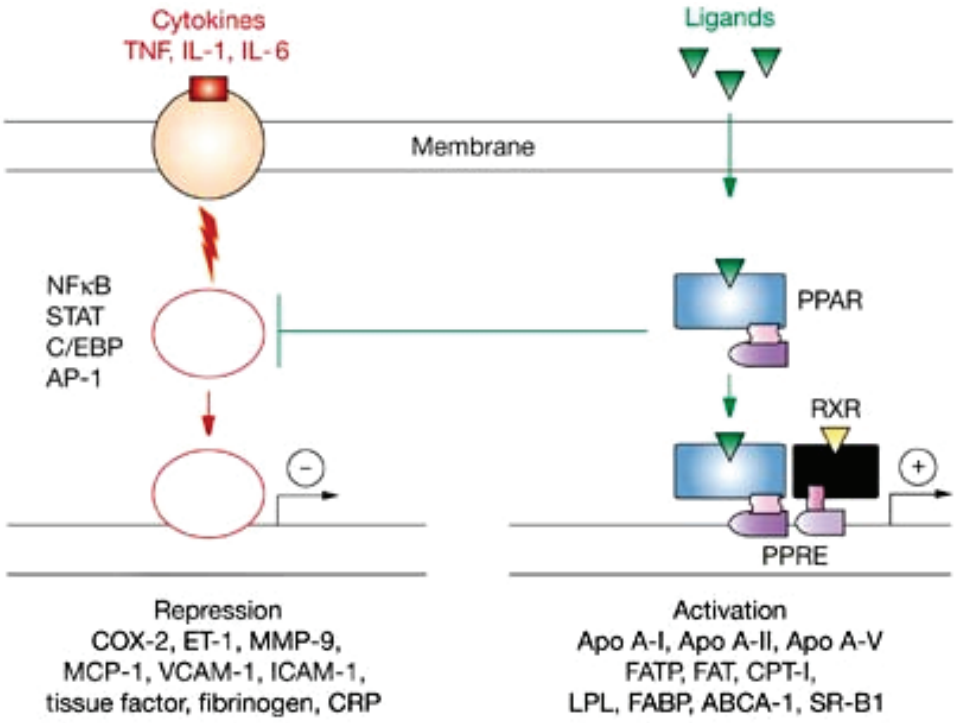

Fig 6.1 After ligand binding (A), PPARs form a PPAR–RXR heterodimeric complex, capable of binding to specific response elements, termed PPREs, located in the promoter region of target genes. In the absence of ligand, the PPAR–RXR heterodimer is associated with a multicomponent corepressor complex, which contains histone deacetylase activity and thus maintains the chromatin in an inactive state. Binding of the ligand to PPAR physically destabilizes the co-repressor complex and leads to the recruitment of a multicomponent coactivator complex, which induces chromatin remodeling by histone acetylation and activates the basal transcription machinery resulting in gene activation. PPARs may repress gene transcription by a mechanism that is independent of DNA binding (B). This mechanism includes interference by PPARs with other transcription factor pathways such as those involving NFκB, STAT, C/EBP, and AP-1, which modulate the expression of genes involved in inflammation pathways. This repression mechanism occurs by interference at different levels of these signal transduction pathways: via protein–protein interaction between PPARs and transcription factors, leading to the formation of inactive complexes; via competition with, and sequestration of, cofactors; via induction of the inhibitor of NFκB (IκB); and via downregulation of gene transcription of membrane receptors of inflammatory cytokines and activators.

Abbreviations: ABCA-1, ATP-binding cassette A1; AP-1, activator protein 1; Apo, apolipoprotein; C/EBP, CAAT enhancer binding protein; COX-2, cyclooxygenase type 2; CPT-I, carnitine palmitoyltransferase I; CRP, C-reactive protein; ET-1, endothelin 1; FABP; adipocyte fatty acid binding protein; FAT, fatty acid translocase; FATP, fatty acid transport protein; ICAM-1, intercellular adhesion molecule 1; IL-1, interleukin 1; IL-6, interleukin 6; LPL, lipoprotein lipase; MCP-1, monocyte chemoattractant protein 1; MMP-9, matrix metalloproteinase 9; NFκB, nuclear factor κB; PPAR, peroxisome proliferator-activated receptor; PPRE, peroxisome proliferative response element; RXR, retinoic X receptor; SR-B1, scavenger receptor class B1; STAT, signal transducer and activator of transcription; TNF, tumor necrosis factor; VCAM-1, vascular cell adhesion molecule. Adapted from: *Gervois P et al. (2007) Drug Insight: mechanisms of action and therapeutic applications for agonists of peroxisome proliferator-activated receptors Nat Clin Pract Endocrinol Metab* ***3:*** *145–156*

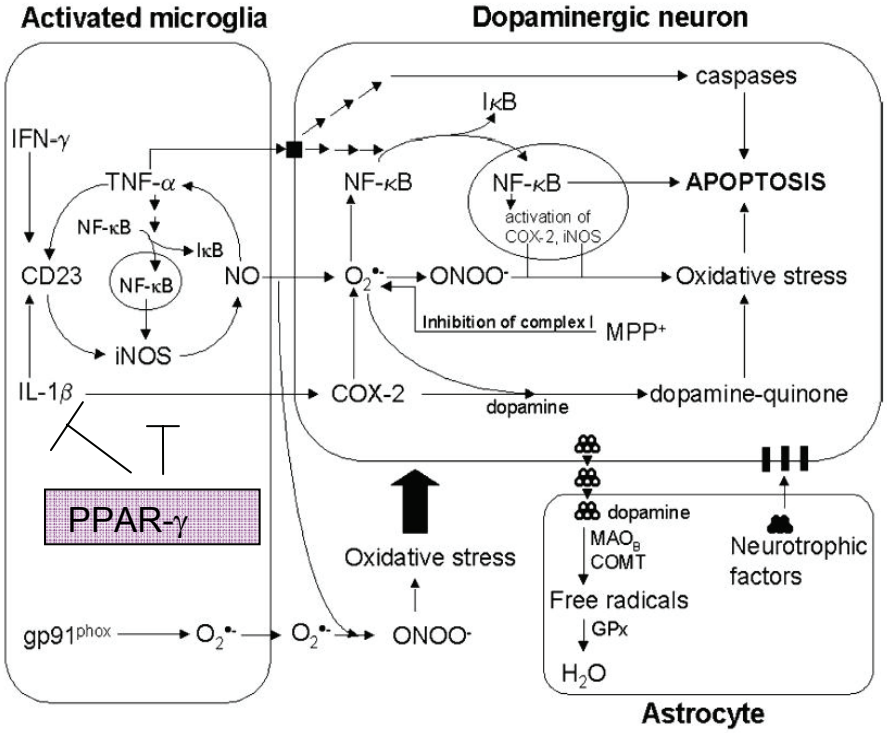

Fig 6.2 Simplified schimatic showing the inflammatory pathways contributing to dopaminergic neurodegeneration in PD.

Activated microglia releases cytotoxic compounds such as cytokines, TNF-α, IFN-γ and IL-1β. Cytokines have a direct effect on the dopaminergic neurons by activating transduction pathways that lead to apoptosis or by inducing the expression of iNOS within glial cells and the subsequent formation of NO. NO is membrane permeable and can diffuse into neighbouring dopaminergic neurons. If the neighbouring cell has elevated levels of superoxide, there is increased probability that superoxide will react with NO to form the peroxynitrite ($ONOO^-$), which can damage lipids, proteins and DNA, which ultimately leads to the death of the neurons. Astrocytes may have a neuroprotective effect acting to reduce the numbers of superoxides and neurotoxins. The inflammatory response could modulated by PPAR-γ agonists that act to inhibit different components of the inflammatory cascade leading dopaminergic neuronal cell death (The diagram was adapted from Schulz et al, 2004).

References:

1. abd-el-Basset E, Fedoroff S. Effect of bacterial wall lipopolysaccharide (LPS) on morphology, motility, and cytoskeletal organization of microglia in cultures. J Neurosci Res 1995;41(2):222-37.

2. Agid Y, Hirsch E, Anglade P, Michel P, Brugg B, Ruberg M. Aging, disease and death of nerve cells. Acta Neurol Belg 1996;96(3):219-23.

3. Agnati LF, Fuxe K. On the mechanism of the antiparkinsonian action of 1-DOPA and bromocriptine: a theoretical and experimental analysis of dopamine receptor sub- and supersensitivity. J Neural Transm Suppl 1980(16):69-81.

4. Aguirre JA, Andbjer B, Gonzalez-Baron S, Hansson A, Stromberg I, Agnati LF et al., Group I mGluR antagonist AIDA protects nigral DA cells from MPTP-induced injury. Neuroreport 2001;12(12):2615-7.

5. Ahlskog JE, Muenter MD. Frequency of levodopa-related dyskinesias and motor fluctuations as estimated from the cumulative literature. Mov Disord 2001;16(3):448-58.

6. Akiyama H, Tooyama I, Kondo H, Ikeda K, Kimura H, McGeer EG et al., Early response of brain resident microglia to kainic acid-induced hippocampal lesions. Brain Res 1994;635(1-2):257-68.

7. Allam MF, Del Castillo AS, Navajas RF. Parkinson's disease risk factors: genetic, environmental, or both? Neurol Res 2005;27(2):206-8.

8. Aloisi F, Ambrosini E, Columba-Cabezas S, Magliozzi R, Serafini B. Intracerebral regulation of immune responses. Ann Med 2001;33(8):510-5.

9. Aloisi F, De Simone R, Columba-Cabezas S, Levi G. Opposite effects of interferon-gamma and prostaglandin E2 on tumor necrosis factor and interleukin-10 production in microglia: a regulatory loop controlling microglia pro- and anti-inflammatory activities. J Neurosci Res 1999;56(6):571-80.

10. Amat JA, Ishiguro H, Nakamura K, Norton WT. Phenotypic diversity and kinetics of proliferating microglia and astrocytes following cortical stab wounds. Glia 1996;16(4):368-82.

11. Asahina M, Yoshiyama Y, Hattori T. Expression of matrix metalloproteinase-9 and urinary-type plasminogen activator in Alzheimer's disease brain. Clin Neuropathol 2001;20(2):60-3.

12. Asin KE, Bednarz L, Nikkel A, Perner R. Rotation and striatal c-fos expression after repeated, daily treatment with selective dopamine receptor agonists and levodopa. J Pharmacol Exp Ther 1995;273(3):1483-90.
13. Avolio C, Giuliani F, Liuzzi GM, Ruggieri M, Paolicelli D, Riccio P et al., Adhesion molecules and matrix metalloproteinases in Multiple Sclerosis: effects induced by Interferon-beta. Brain Res Bull 2003;61(3):357-64.
14. Baba M, Nakajo S, Tu PH, Tomita T, Nakaya K, Lee VM et al., Aggregation of alpha-synuclein in Lewy bodies of sporadic Parkinson's disease and dementia with Lewy bodies. Am J Pathol 1998;152(4):879-84.
15. Baba Y, Kuroiwa A, Uitti RJ, Wszolek ZK, Yamada T. Alterations of T-lymphocyte populations in Parkinson disease. Parkinsonism Relat Disord 2005;11(8):493-8.
16. Baddeley A. Is stereology 'unbiased'? Trends Neurosci 2001;24(7):375-6; author reply 378-80.
17. Banati RB, Daniel SE, Blunt SB. Glial pathology but absence of apoptotic nigral neurons in long-standing Parkinson's disease. Mov Disord 1998;13(2):221-7.
18. Banati RB, Goerres GW, Myers R, Gunn RN, Turkheimer FE, Kreutzberg GW et al., [11C](R)-PK11195 positron emission tomography imaging of activated microglia in vivo in Rasmussen's encephalitis. Neurology 1999;53(9):2199-203.
19. Barclay AN, Wright GJ, Brooke G, Brown MH. CD200 and membrane protein interactions in the control of myeloid cells. Trends Immunol 2002;23(6):285-90.
20. Barneoud P, Parmentier S, Mazadier M, Miquet JM, Boireau A, Dubedat P et al., Effects of complete and partial lesions of the dopaminergic mesotelencephalic system on skilled forelimb use in the rat. Neuroscience 1995;67(4):837-48.
21. Barron KD. The microglial cell. A historical review. J Neurol Sci 1995;134 Suppl:57-68.
22. Bauer J, Sminia T, Wouterlood FG, Dijkstra CD. Phagocytic activity of macrophages and microglial cells during the course of acute and chronic relapsing experimental autoimmune encephalomyelitis. J Neurosci Res 1994;38(4):365-75.
23. Benmoyal-Segal L, Soreq H. Gene-environment interactions in sporadic Parkinson's disease. J Neurochem 2006;97(6):1740-55.
24. Ben-Shachar D, Youdim MB. Intranigral iron injection induces behavioral and biochemical "parkinsonism" in rats. J Neurochem 1991;57(6):2133-5.

25. Berger K, Przedborski S, Cadet JL. Retrograde degeneration of nigrostriatal neurons induced by intrastriatal 6-hydroxydopamine injection in rats. Brain Res Bull 1991;26(2):301-7.
26. Berlett BS, Stadtman ER. Protein oxidation in aging, disease, and oxidative stress. J Biol Chem 1997;272(33):20313-6.
27. Bernardo A, Ajmone-Cat MA, Levi G, Minghetti L. 15-deoxy-delta12,14-prostaglandin J2 regulates the functional state and the survival of microglial cells through multiple molecular mechanisms. J Neurochem 2003;87(3):742-51.
28. Bernardo A, Levi G, Minghetti L. Role of the peroxisome proliferator-activated receptor-gamma (PPAR-gamma) and its natural ligand 15-deoxy-Delta12, 14-prostaglandin J2 in the regulation of microglial functions. Eur J Neurosci 2000;12(7):2215-23.
29. Bernardo A, Minghetti L. PPAR-gamma agonists as regulators of microglial activation and brain inflammation. Curr Pharm Des 2006;12(1):93-109.
30. Bernheimer H, Birkmayer W, Hornykiewicz O, Jellinger K, Seitelberger F. Brain dopamine and the syndromes of Parkinson and Huntington. Clinical, morphological and neurochemical correlations. J Neurol Sci 1973;20(4):415-55.
31. Betarbet R, Sherer TB, Greenamyre JT. Animal models of Parkinson's disease. Bioessays 2002;24(4):308-18.
32. Betarbet R, Sherer TB, MacKenzie G, Garcia-Osuna M, Panov AV, Greenamyre JT. Chronic systemic pesticide exposure reproduces features of Parkinson's disease. Nat Neurosci 2000;3(12):1301-6.
33. Birkmayer W, Hornykiewicz O. [The L-dihydroxyphenylalanine (L-DOPA) effect in Parkinson's syndrome in man: On the pathogenesis and treatment of Parkinson akinesis.]. Arch Psychiatr Nervenkr Z Gesamte Neurol Psychiatr 1962;203:560-74.
34. Biswas C, Zhang Y, DeCastro R, Guo H, Nakamura T, Kataoka H et al., The human tumor cell-derived collagenase stimulatory factor (renamed EMMPRIN) is a member of the immunoglobulin superfamily. Cancer Res 1995;55(2):434-9.
35. Block ML, Hong JS. Microglia and inflammation-mediated neurodegeneration: multiple triggers with a common mechanism. Prog Neurobiol 2005;76(2):77-98.
36. Blum D, Torch S, Lambeng N, Nissou M, Benabid AL, Sadoul R et al., Molecular pathways involved in the neurotoxicity of 6-OHDA, dopamine and MPTP: contribution to the apoptotic theory in Parkinson's disease. Prog Neurobiol 2001;65(2):135-72.

37. Bonifati V, Fabrizio E, Vanacore N, De Mari M, Meco G. Familial Parkinson's disease: a clinical genetic analysis. Can J Neurol Sci 1995;22(4):272-9.
38. Braak H, Del Tredici K, Rub U, de Vos RA, Jansen Steur EN, Braak E. Staging of brain pathology related to sporadic Parkinson's disease. Neurobiol Aging 2003;24(2):197-211.
39. Braak H, Ghebremedhin E, Rub U, Bratzke H, Del Tredici K. Stages in the development of Parkinson's disease-related pathology. Cell Tissue Res 2004;318(1):121-34.
40. Breidert T, Callebert J, Heneka MT, Landreth G, Launay JM, Hirsch EC. Protective action of the peroxisome proliferator-activated receptor-gamma agonist pioglitazone in a mouse model of Parkinson's disease. J Neurochem 2002;82(3):615-24.
41. Carlson JD, Pearlstein RD, Buchholz J, Iacono RP, Maeda G. Regional metabolic changes in the pedunculopontine nucleus of unilateral 6-hydroxydopamine Parkinson's model rats. Brain Res 1999;828(1-2):12-9.
42. Carman LS, Gage FH, Shults CW. Partial lesion of the substantia nigra: relation between extent of lesion and rotational behavior. Brain Res 1991;553(2):275-83.
43. Carson MJ, Doose JM, Melchior B, Schmid CD, Ploix CC. CNS immune privilege: hiding in plain sight. Immunol Rev 2006;213:48-65.
44. Casteels C, Lauwers E, Bormans G, Baekelandt V, Van Laere K. Metabolic-dopaminergic mapping of the 6-hydroxydopamine rat model for Parkinson's disease. Eur J Nucl Med Mol Imaging 2008;35(1):124-34.
45. Cenci MA, Whishaw IQ, Schallert T. Animal models of neurological deficits: how relevant is the rat? Nat Rev Neurosci 2002;3(7):574-9.
46. Chamak B, Mallat M. Fibronectin and laminin regulate the in vitro differentiation of microglial cells. Neuroscience 1991;45(3):513-27.
47. Chambers AF, Matrisian LM. Changing views of the role of matrix metalloproteinases in metastasis. J Natl Cancer Inst 1997;89(17):1260-70.
48. Chapman GA, Moores K, Harrison D, Campbell CA, Stewart BR, Strijbos PJ. Fractalkine cleavage from neuronal membranes represents an acute event in the inflammatory response to excitotoxic brain damage. J Neurosci 2000;20(15):RC87.
49. Charlett A, Dobbs RJ, Dobbs SM, Weller C, Brady P, Peterson DW. Parkinsonism: siblings share Helicobacter pylori seropositivity and facets of syndrome. Acta Neurol Scand 1999;99(1):26-35.

50. Chen H, Jacobs E, Schwarzschild MA, McCullough ML, Calle EE, Thun MJ et al., Nonsteroidal antiinflammatory drug use and the risk for Parkinson's disease. Ann Neurol 2005;58(6):963-7.

51. Chew LJ, Takanohashi A, Bell M. Microglia and inflammation: impact on developmental brain injuries. Ment Retard Dev Disabil Res Rev 2006;12(2):105-12.

52. Cho BP, Song DY, Sugama S, Shin DH, Shimizu Y, Kim SS et al., Pathological dynamics of activated microglia following medial forebrain bundle transection. Glia 2006;53(1):92-102.

53. Cho BP, Sugama S, Shin DH, DeGiorgio LA, Kim SS, Kim YS et al., Microglial phagocytosis of dopamine neurons at early phases of apoptosis. Cell Mol Neurobiol 2003;23(4-5):551-60.

54. Choi DK, Pennathur S, Perier C, Tieu K, Teismann P, Wu DC et al., Ablation of the inflammatory enzyme myeloperoxidase mitigates features of Parkinson's disease in mice. J Neurosci 2005;25(28):6594-600.

55. Chung CY, Seo H, Sonntag KC, Brooks A, Lin L, Isacson O. Cell type-specific gene expression of midbrain dopaminergic neurons reveals molecules involved in their vulnerability and protection. Hum Mol Genet 2005;14(13):1709-25.

56. Cicchetti F, Brownell AL, Williams K, Chen YI, Livni E, Isacson O. Neuroinflammation of the nigrostriatal pathway during progressive 6-OHDA dopamine degeneration in rats monitored by immunohistochemistry and PET imaging. Eur J Neurosci 2002;15(6):991-8.

57. Clark AW, Krekoski CA, Bou SS, Chapman KR, Edwards DR. Increased gelatinase A (MMP-2) and gelatinase B (MMP-9) activities in human brain after focal ischemia. Neurosci Lett 1997;238(1-2):53-6.

58. Colton CA, Keri JE, Chen WT, Monsky WL. Protease production by cultured microglia: substrate gel analysis and immobilized matrix degradation. J Neurosci Res 1993;35(3):297-304.

59. Combs CK, Johnson DE, Karlo JC, Cannady SB, Landreth GE. Inflammatory mechanisms in Alzheimer's disease: inhibition of beta-amyloid-stimulated proinflammatory responses and neurotoxicity by PPARgamma agonists. J Neurosci 2000;20(2):558-67.

60. Conant K, St Hillaire C, Nagase H, Visse R, Gary D, Haughey N et al., Matrix metalloproteinase 1 interacts with neuronal integrins and stimulates dephosphorylation of Akt. J Biol Chem 2004;279(9):8056-62.

61. Coons AH, Leduc EH, Connolly JM. Studies on antibody production. I. A method for the histochemical demonstration of specific antibody and its application to a study of the hyperimmune rabbit. J Exp Med 1955;102(1):49-60.
62. Croisier E, Moran LB, Dexter DT, Pearce RK, Graeber MB. Microglial inflammation in the parkinsonian substantia nigra: relationship to alpha-synuclein deposition. J Neuroinflammation 2005;2:14.
63. Damier P, Hirsch EC, Agid Y, Graybiel AM. The substantia nigra of the human brain. II. Patterns of loss of dopamine-containing neurons in Parkinson's disease. Brain 1999;122 (Pt 8):1437-48.
64. Datla KP, Bennett RD, Zbarsky V, Ke B, Liang YF, Higa T et al., The antioxidant drink effective microorganism-X (EM-X) pre-treatment attenuates the loss of nigrostriatal dopaminergic neurons in 6-hydroxydopamine-lesion rat model of Parkinson's disease. J Pharm Pharmacol 2004;56(5):649-54.
65. Datla KP, Christidou M, Widmer WW, Rooprai HK, Dexter DT. Tissue distribution and neuroprotective effects of citrus flavonoid tangeretin in a rat model of Parkinson's disease. Neuroreport 2001;12(17):3871-5.
66. de Lau LM, Breteler MM. Epidemiology of Parkinson's disease. Lancet Neurol 2006;5(6):525-35.
67. de Rijk MC, Launer LJ, Berger K, Breteler MM, Dartigues JF, Baldereschi M et al., Prevalence of Parkinson's disease in Europe: A collaborative study of population-based cohorts. Neurologic Diseases in the Elderly Research Group. Neurology 2000;54(11 Suppl 5):S21-3.
68. Dehmer T, Heneka MT, Sastre M, Dichgans J, Schulz JB. Protection by pioglitazone in the MPTP model of Parkinson's disease correlates with I kappa B alpha induction and block of NF kappa B and iNOS activation. J Neurochem 2004;88(2):494-501.
69. Depino AM, Earl C, Kaczmarczyk E, Ferrari C, Besedovsky H, del Rey A et al., Microglial activation with atypical proinflammatory cytokine expression in a rat model of Parkinson's disease. Eur J Neurosci 2003;18(10):2731-42.
70. Desvergne B, Wahli W. Peroxisome proliferator-activated receptors: nuclear control of metabolism. Endocr Rev 1999;20(5):649-88.
71. Deumens R, Blokland A, Prickaerts J. Modeling Parkinson's disease in rats: an evaluation of 6-OHDA lesions of the nigrostriatal pathway. Exp Neurol 2002;175(2):303-17.

72. Dexter DT, Carter CJ, Wells FR, Javoy-Agid F, Agid Y, Lees A et al., Basal lipid peroxidation in substantia nigra is increased in Parkinson's disease. J Neurochem 1989;52(2):381-9.

73. Dexter DT, Holley AE, Flitter WD, Slater TF, Wells FR, Daniel SE et al., Increased levels of lipid hydroperoxides in the parkinsonian substantia nigra: an HPLC and ESR study. Mov Disord 1994;9(1):92-7.

74. Dexter DT, Wells FR, Lees AJ, Agid F, Agid Y, Jenner P et al., Increased nigral iron content and alterations in other metal ions occurring in brain in Parkinson's disease. J Neurochem 1989;52(6):1830-6.

75. Dluzen D. Estrogen decreases corpus striatal neurotoxicity in response to 6-hydroxydopamine. Brain Res 1997;767(2):340-4.

76. Du Y, Ma Z, Lin S, Dodel RC, Gao F, Bales KR et al., Minocycline prevents nigrostriatal dopaminergic neurodegeneration in the MPTP model of Parkinson's disease. Proc Natl Acad Sci U S A 2001;98(25):14669-74.

77. Dubal DB, Kashon ML, Pettigrew LC, Ren JM, Finklestein SP, Rau SW et al., Estradiol protects against ischemic injury. J Cereb Blood Flow Metab 1998;18(11):1253-8.

78. Duke DC, Moran LB, Kalaitzakis ME, Deprez M, Dexter DT, Pearce RK et al., Transcriptome analysis reveals link between proteasomal and mitochondrial pathways in Parkinson's disease. Neurogenetics 2006;7(3):139-48.

79. Elbaz A, Bower JH, Maraganore DM, McDonnell SK, Peterson BJ, Ahlskog JE et al., Risk tables for parkinsonism and Parkinson's disease. J Clin Epidemiol 2002;55(1):25-31.

80. Emborg ME. Evaluation of animal models of Parkinson's disease for neuroprotective strategies. J Neurosci Methods 2004;139(2):121-43.

81. Escher P, Braissant O, Basu-Modak S, Michalik L, Wahli W, Desvergne B. Rat PPARs: quantitative analysis in adult rat tissues and regulation in fasting and refeeding. Endocrinology 2001;142(10):4195-202.

82. Fadok VA, Chimini G. The phagocytosis of apoptotic cells. Semin Immunol 2001;13(6):365-72.

83. Farrer MJ. Genetics of Parkinson disease: paradigm shifts and future prospects. Nat Rev Genet 2006;7(4):306-18.

84. Faulk WP, Taylor GM. An immunocolloid method for the electron microscope. Immunochemistry 1971;8(11):1081-3.

85. Faull RL, Laverty R. Changes in dopamine levels in the corpus striatum following lesions in the substantia nigra. Exp Neurol 1969;23(3):332-40.

86. Feng ZH, Wang TG, Li DD, Fung P, Wilson BC, Liu B et al., Cyclooxygenase-2-deficient mice are resistant to 1-methyl-4-phenyl1, 2, 3, 6-tetrahydropyridine-induced damage of dopaminergic neurons in the substantia nigra. Neurosci Lett 2002;329(3):354-8.

87. Ferger B, Leng A, Mura A, Hengerer B, Feldon J. Genetic ablation of tumor necrosis factor-alpha (TNF-alpha) and pharmacological inhibition of TNF-synthesis attenuates MPTP toxicity in mouse striatum. J Neurochem 2004;89(4):822-33.

88. Fetler L, Amigorena S. Neuroscience. Brain under surveillance: the microglia patrol. Science 2005;309(5733):392-3.

89. Forman BM, Tontonoz P, Chen J, Brun RP, Spiegelman BM, Evans RM. 15-Deoxy-delta 12, 14-prostaglandin J2 is a ligand for the adipocyte determination factor PPAR gamma. Cell 1995;83(5):803-12.

90. Forno LS. Neuropathologic features of Parkinson's, Huntington's, and Alzheimer's diseases. Ann N Y Acad Sci 1992;648:6-16.

91. Forno LS. Neuropathology of Parkinson's disease. J Neuropathol Exp Neurol 1996;55(3):259-72.

92. Fowlkes JL, Suzuki K, Nagase H, Thrailkill KM. Proteolysis of insulin-like growth factor binding protein-3 during rat pregnancy: a role for matrix metalloproteinases. Endocrinology 1994;135(6):2810-3.

93. Frank M, Wolburg H. Cellular reactions at the lesion site after crushing of the rat optic nerve. Glia 1996;16(3):227-40.

94. Friedman JH. Progressive parkinsonism in boxers. South Med J 1989;82(5):543-6.

95. Fuenzalida K, Quintanilla R, Ramos P, Piderit D, Fuentealba RA, Martinez G et al., Peroxisome proliferator-activated receptor gamma up-regulates the Bcl-2 anti-apoptotic protein in neurons and induces mitochondrial stabilization and protection against oxidative stress and apoptosis. J Biol Chem 2007;282(51):37006-15.

96. Gabison EE, Hoang-Xuan T, Mauviel A, Menashi S. EMMPRIN/CD147, an MMP modulator in cancer, development and tissue repair. Biochimie 2005;87(3-4):361-8.

97. Gal S, Zheng H, Fridkin M, Youdim MB. Novel multifunctional neuroprotective iron chelator-monoamine oxidase inhibitor drugs for neurodegenerative diseases. In vivo selective brain monoamine oxidase inhibition and prevention of MPTP-induced striatal dopamine depletion. J Neurochem 2005;95(1):79-88.

98. Gao HM, Jiang J, Wilson B, Zhang W, Hong JS, Liu B. Microglial activation-mediated delayed and progressive degeneration of rat nigral dopaminergic neurons: relevance to Parkinson's disease. J Neurochem 2002;81(6):1285-97.
99. Gao HM, Liu B, Zhang W, Hong JS. Critical role of microglial NADPH oxidase-derived free radicals in the in vitro MPTP model of Parkinson's disease. FASEB J 2003;17(13):1954-6.
100. Gasser T. Genetics of Parkinson's disease. Clin Genet 1998;54(4):259-65.
101. Gebicke-Haerter PJ. Microglia in neurodegeneration: molecular aspects. Microsc Res Tech 2001;54(1):47-58.
102. Gelb DJ, Oliver E, Gilman S. Diagnostic criteria for Parkinson disease. Arch Neurol 1999;56(1):33-9.
103. Gerlach M, Riederer PF. Time sequences of dopaminergic cell death in Parkinson's disease: indications for neuroprotective studies. Adv Neurol 1999;80:219-25.
104. Gervois P, Fruchart JC, Staels B. Drug Insight: mechanisms of action and therapeutic applications for agonists of peroxisome proliferator-activated receptors. Nat Clin Pract Endocrinol Metab 2007;3(2):145-56.
105. Ghaemi M, Rudolf J, Schmulling S, Bamborschke S, Heiss WD. FDG- and Dopa-PET in postencephalitic parkinsonism. J Neural Transm 2000;107(11):1289-95.
106. Ghisletti S, Huang W, Ogawa S, Pascual G, Lin ME, Willson TM et al., Parallel SUMOylation-dependent pathways mediate gene- and signal-specific transrepression by LXRs and PPARgamma. Mol Cell 2007;25(1):57-70.
107. Gibbons HM, Dragunow M. Microglia induce neural cell death via a proximity-dependent mechanism involving nitric oxide. Brain Res 2006;1084(1):1-15.
108. Gillies GE, Murray HE, Dexter D, McArthur S. Sex dimorphisms in the neuroprotective effects of estrogen in an animal model of Parkinson's disease. Pharmacol Biochem Behav 2004;78(3):513-22.
109. Glezer I, Lapointe A, Rivest S. Innate immunity triggers oligodendrocyte progenitor reactivity and confines damages to brain injuries. FASEB J 2006;20(6):750-2.
110. Glinka Y, Gassen M, Youdim MB. Mechanism of 6-hydroxydopamine neurotoxicity. J Neural Transm Suppl 1997;50:55-66.
111. Glinka Y, Tipton KF, Youdim MB. Nature of inhibition of mitochondrial respiratory complex I by 6-Hydroxydopamine. J Neurochem 1996;66(5):2004-10.

112. Godbout JP, Chen J, Abraham J, Richwine AF, Berg BM, Kelley KW et al., Exaggerated neuroinflammation and sickness behavior in aged mice following activation of the peripheral innate immune system. FASEB J 2005;19(10):1329-31.
113. Goldman SM, Tanner CM, Oakes D, Bhudhikanok GS, Gupta A, Langston JW. Head injury and Parkinson's disease risk in twins. Ann Neurol 2006;60(1):65-72.
114. Goldstein DS, Holmes CS, Dendi R, Bruce SR, Li ST. Orthostatic hypotension from sympathetic denervation in Parkinson's disease. Neurology 2002;58(8):1247-55.
115. Goldstein DS, Li ST, Kopin IJ. Sympathetic neurocirculatory failure in Parkinson disease: Evidence for an etiologic role of alpha-synuclein. Ann Intern Med 2001;135(11):1010-1.
116. Gorrell JM, DiMonte D, Graham D. The role of the environment in Parkinson's disease. Environ Health Perspect 1996;104(6):652-4.
117. Graeber MB. Microglia, macrophages and the blood-brain barrier. Clin Neuropathol 1993;12(5):296-7.
118. Graeber MB, Streit WJ, Kreutzberg GW. Axotomy of the rat facial nerve leads to increased CR3 complement receptor expression by activated microglial cells. J Neurosci Res 1988;21(1):18-24.
119. Greene JG, Dingledine R, Greenamyre JT. Gene expression profiling of rat midbrain dopamine neurons: implications for selective vulnerability in parkinsonism. Neurobiol Dis 2005;18(1):19-31.
120. Halliday GM, Blumbergs PC, Cotton RG, Blessing WW, Geffen LB. Loss of brainstem serotonin- and substance P-containing neurons in Parkinson's disease. Brain Res 1990;510(1):104-7.
121. Haro H, Crawford HC, Fingleton B, MacDougall JR, Shinomiya K, Spengler DM et al., Matrix metalloproteinase-3-dependent generation of a macrophage chemoattractant in a model of herniated disc resorption. J Clin Invest 2000;105(2):133-41.
122. He Y, Appel S, Le W. Minocycline inhibits microglial activation and protects nigral cells after 6-hydroxydopamine injection into mouse striatum. Brain Res 2001;909(1-2):187-93.
123. Hedreen JC. Unbiased stereology? Trends Neurosci 1999;22(8):346-7.
124. Hefti F, Melamed E, Wurtman RJ. Partial lesions of the dopaminergic nigrostriatal system in rat brain: biochemical characterization. Brain Res 1980;195(1):123-37.

125. Heikkila R, Cohen G. Inhibition of biogenic amine uptake by hydrogen peroxide: a mechanism for toxic effects of 6-hydroxydopamine. Science 1971;172(989):1257-8.
126. Heneka MT, Feinstein DL, Galea E, Gleichmann M, Wullner U, Klockgether T. Peroxisome proliferator-activated receptor gamma agonists protect cerebellar granule cells from cytokine-induced apoptotic cell death by inhibition of inducible nitric oxide synthase. J Neuroimmunol 1999;100(1-2):156-68.
127. Heneka MT, Klockgether T, Feinstein DL. Peroxisome proliferator-activated receptor-gamma ligands reduce neuronal inducible nitric oxide synthase expression and cell death in vivo. J Neurosci 2000;20(18):6862-7.
128. Heppner FL, Skutella T, Hailer NP, Haas D, Nitsch R. Activated microglial cells migrate towards sites of excitotoxic neuronal injury inside organotypic hippocampal slice cultures. Eur J Neurosci 1998;10(10):3284-90.
129. Herrera AJ, Tomas-Camardiel M, Venero JL, Cano J, Machado A. Inflammatory process as a determinant factor for the degeneration of substantia nigra dopaminergic neurons. J Neural Transm 2005;112(1):111-9.
130. Hirsch EC, Hunot S, Damier P, Faucheux B. Glial cells and inflammation in Parkinson's disease: a role in neurodegeneration? Ann Neurol 1998;44(3 Suppl 1):S115-20.
131. Hirt UA, Leist M. Rapid, noninflammatory and PS-dependent phagocytic clearance of necrotic cells. Cell Death Differ 2003;10(10):1156-64.
132. Hoek RM, Ruuls SR, Murphy CA, Wright GJ, Goddard R, Zurawski SM et al., Down-regulation of the macrophage lineage through interaction with OX2 (CD200). Science 2000;290(5497):1768-71.
133. Holloway RG, Shoulson I, Fahn S, Kieburtz K, Lang A, Marek K et al., Pramipexole vs levodopa as initial treatment for Parkinson disease: a 4-year randomized controlled trial. Arch Neurol 2004;61(7):1044-53.
134. Huang CC, Weng YH, Lu CS, Chu NS, Yen TC. Dopamine transporter binding in chronic manganese intoxication. J Neurol 2003;250(11):1335-9.
135. Hubbard AK, Rothlein R. Intercellular adhesion molecule-1 (ICAM-1) expression and cell signaling cascades. Free Radic Biol Med 2000;28(9):1379-86.
136. Hunter RL, Dragicevic N, Seifert K, Choi DY, Liu M, Kim HC et al., Inflammation induces mitochondrial dysfunction and dopaminergic neurodegeneration in the nigrostriatal system. J Neurochem 2007;100(5):1375-86.

137. Huynh ML, Fadok VA, Henson PM. Phosphatidylserine-dependent ingestion of apoptotic cells promotes TGF-beta1 secretion and the resolution of inflammation. J Clin Invest 2002;109(1):41-50.

138. Iravani MM, Kashefi K, Mander P, Rose S, Jenner P. Involvement of inducible nitric oxide synthase in inflammation-induced dopaminergic neurodegeneration. Neuroscience 2002;110(1):49-58.

139. Iravani MM, Syed E, Jackson MJ, Johnston LC, Smith LA, Jenner P. A modified MPTP treatment regime produces reproducible partial nigrostriatal lesions in common marmosets. Eur J Neurosci 2005;21(4):841-54.

140. Issemann I, Green S. Activation of a member of the steroid hormone receptor superfamily by peroxisome proliferators. Nature 1990;347(6294):645-50.

141. Iwanaga K, Wakabayashi K, Yoshimoto M, Tomita I, Satoh H, Takashima H et al., Lewy body-type degeneration in cardiac plexus in Parkinson's and incidental Lewy body diseases. Neurology 1999;52(6):1269-71.

142. Iwashita A, Muramatsu Y, Yamazaki T, Muramoto M, Kita Y, Yamazaki S et al., Neuroprotective efficacy of the peroxisome proliferator-activated receptor delta-selective agonists in vitro and in vivo. J Pharmacol Exp Ther 2007;320(3):1087-96.

143. Jackson-Lewis V, Jakowec M, Burke RE, Przedborski S. Time course and morphology of dopaminergic neuronal death caused by the neurotoxin 1-methyl-4-phenyl-1,2,3,6-tetrahydropyridine. Neurodegeneration 1995;4(3):257-69.

144. Jankovic J. Searching for a relationship between manganese and welding and Parkinson's disease. Neurology 2005;64(12):2021-8.

145. Jellinger LK. Pathologic correlates of dementia in Parkinson's disease. Arch Neurol 1987;44(7):690-1.

146. Jenmalm MC, Cherwinski H, Bowman EP, Phillips JH, Sedgwick JD. Regulation of myeloid cell function through the CD200 receptor. J Immunol 2006;176(1):191-9.

147. Jenner P. Oxidative stress in Parkinson's disease and other neurodegenerative disorders. Pathol Biol (Paris) 1996;44(1):57-64.

148. Jenner P, Olanow CW. Oxidative stress and the pathogenesis of Parkinson's disease. Neurology 1996;47(6 Suppl 3):S161-70.

149. Jenner P, Olanow CW. Understanding cell death in Parkinson's disease. Ann Neurol 1998;44(3 Suppl 1):S72-84.

150. Jenner P, Olanow CW. The pathogenesis of cell death in Parkinson's disease. Neurology 2006;66(10 Suppl 4):S24-36.

151. Jeon BS, Jackson-Lewis V, Burke RE. 6-Hydroxydopamine lesion of the rat substantia nigra: time course and morphology of cell death. Neurodegeneration 1995;4(2):131-7.

152. Jiang C, Ting AT, Seed B. PPAR-gamma agonists inhibit production of monocyte inflammatory cytokines. Nature 1998;391(6662):82-6.

153. Kadowaki T. Insights into insulin resistance and type 2 diabetes from knockout mouse models. J Clin Invest 2000;106(4):459-65.

154. Kataoka H, DeCastro R, Zucker S, Biswas C. Tumor cell-derived collagenase-stimulatory factor increases expression of interstitial collagenase, stromelysin, and 72-kDa gelatinase. Cancer Res 1993;53(13):3154-8.

155. Kaur C, Ling EA. Activation and re-expression of surface antigen in microglia following an epidural application of kainic acid in the rat brain. J Anat 1992;180 (Pt 2):333-42.

156. Kawaguchi N , Yamada T, Hattori T, Rare tendency of catching cold in Parkinson's disease. Parkinsonism and related disorders 1998;4(4):207-9.

157. Kielian T, Drew PD. Effects of peroxisome proliferator-activated receptor-gamma agonists on central nervous system inflammation. J Neurosci Res 2003;71(3):315-25.

158. Kim WG, Mohney RP, Wilson B, Jeohn GH, Liu B, Hong JS. Regional difference in susceptibility to lipopolysaccharide-induced neurotoxicity in the rat brain: role of microglia. J Neurosci 2000;20(16):6309-16.

159. Kim YS, Choi DH, Block ML, Lorenzl S, Yang L, Kim YJ et al., A pivotal role of matrix metalloproteinase-3 activity in dopaminergic neuronal degeneration via microglial activation. FASEB J 2007;21(1):179-87.

160. Kim YS, Kim SS, Cho JJ, Choi DH, Hwang O, Shin DH et al., Matrix metalloproteinase-3: a novel signaling proteinase from apoptotic neuronal cells that activates microglia. J Neurosci 2005;25(14):3701-11.

161. Kirik D, Rosenblad C, Bjorklund A. Characterization of behavioral and neurodegenerative changes following partial lesions of the nigrostriatal dopamine system induced by intrastriatal 6-hydroxydopamine in the rat. Exp Neurol 1998;152(2):259-77.

162. Kliewer SA, Forman BM, Blumberg B, Ong ES, Borgmeyer U, Mangelsdorf DJ et al., Differential expression and activation of a family of murine peroxisome proliferator-activated receptors. Proc Natl Acad Sci U S A 1994;91(15):7355-9.

163. Knott C, Stern G, Wilkin GP. Inflammatory regulators in Parkinson's disease: iNOS, lipocortin-1, and cyclooxygenases-1 and -2. Mol Cell Neurosci 2000;16(6):724-39.

164. Kondo T. Initial therapy for Parkinson's disease: levodopa vs. dopamine receptor agonists. J Neurol 2002;249 Suppl 2:II25-9.

165. Kondoh T, Bannai M, Nishino H, Torii K. 6-Hydroxydopamine-induced lesions in a rat model of hemi-Parkinson's disease monitored by magnetic resonance imaging. Exp Neurol 2005;192(1):194-202.

166. Kopito RR. Aggresomes, inclusion bodies and protein aggregation. Trends Cell Biol 2000;10(12):524-30.

167. Koutsilieri E, Scheller C, Grunblatt E, Nara K, Li J, Riederer P. Free radicals in Parkinson's disease. J Neurol 2002;249 Suppl 2:II1-5.

168. Kreutzberg GW. Microglia: a sensor for pathological events in the CNS. Trends Neurosci 1996;19(8):312-8.

169. Kubota N, Terauchi Y, Miki H, Tamemoto H, Yamauchi T, Komeda K et al., PPAR gamma mediates high-fat diet-induced adipocyte hypertrophy and insulin resistance. Mol Cell 1999;4(4):597-609.

170. Kumar R, Seth RK, Sekhon MS, Bhargava JS. Serum lipid peroxide and other enzyme levels of patients suffering from thermal injury. Burns 1995;21(2):96-7.

171. Kurkowska-Jastrzebska I, Wronska A, Kohutnicka M, Czlonkowski A, Czlonkowska A. MHC class II positive microglia and lymphocytic infiltration are present in the substantia nigra and striatum in mouse model of Parkinson's disease. Acta Neurobiol Exp (Wars) 1999;59(1):1-8.

172. Lang AE, Obeso JA. Challenges in Parkinson's disease: restoration of the nigrostriatal dopamine system is not enough. Lancet Neurol 2004;3(5):309-16.

173. Langston JW. Parkinson's disease: current and future challenges. Neurotoxicology 2002;23(4-5):443-50.

174. Langston JW, Ballard P, Tetrud JW, Irwin I. Chronic Parkinsonism in humans due to a product of meperidine-analog synthesis. Science 1983;219(4587):979-80.

175. Langston JW, Forno LS, Tetrud J, Reeves AG, Kaplan JA, Karluk D. Evidence of active nerve cell degeneration in the substantia nigra of humans years after 1-methyl-4-phenyl-1,2,3,6-tetrahydropyridine exposure. Ann Neurol 1999;46(4):598-605.

176. Lauber K, Bohn E, Krober SM, Xiao YJ, Blumenthal SG, Lindemann RK et al., Apoptotic cells induce migration of phagocytes via caspase-3-mediated release of a lipid attraction signal. Cell 2003;113(6):717-30.

177. Lawson LJ, Perry VH, Dri P, Gordon S. Heterogeneity in the distribution and morphology of microglia in the normal adult mouse brain. Neuroscience 1990;39(1):151-70.

178. Lehmann JM, Lenhard JM, Oliver BB, Ringold GM, Kliewer SA. Peroxisome proliferator-activated receptors alpha and gamma are activated by indomethacin and other non-steroidal anti-inflammatory drugs. J Biol Chem 1997;272(6):3406-10.

179. Leppert D, Lindberg RL, Kappos L, Leib SL. Matrix metalloproteinases: multifunctional effectors of inflammation in multiple sclerosis and bacterial meningitis. Brain Res Brain Res Rev 2001;36(2-3):249-57.

180. Liberatore GT, Jackson-Lewis V, Vukosavic S, Mandir AS, Vila M, McAuliffe WG et al., Inducible nitric oxide synthase stimulates dopaminergic neurodegeneration in the MPTP model of Parkinson disease. Nat Med 1999;5(12):1403-9.

181. Ling Z, Gayle DA, Ma SY, Lipton JW, Tong CW, Hong JS et al., In utero bacterial endotoxin exposure causes loss of tyrosine hydroxylase neurons in the postnatal rat midbrain. Mov Disord 2002;17(1):116-24.

182. Lippa CF, Fujiwara H, Mann DM, Giasson B, Baba M, Schmidt ML et al., Lewy bodies contain altered alpha-synuclein in brains of many familial Alzheimer's disease patients with mutations in presenilin and amyloid precursor protein genes. Am J Pathol 1998;153(5):1365-70.

183. Liu B, Gao HM, Hong JS. Parkinson's disease and exposure to infectious agents and pesticides and the occurrence of brain injuries: role of neuroinflammation. Environ Health Perspect 2003;111(8):1065-73.

184. Liu B, Jiang JW, Wilson BC, Du L, Yang SN, Wang JY et al., Systemic infusion of naloxone reduces degeneration of rat substantia nigral dopaminergic neurons induced by intranigral injection of lipopolysaccharide. J Pharmacol Exp Ther 2000;295(1):125-32.

185. Lorenzl S, Calingasan N, Yang L, Albers DS, Shugama S, Gregorio J et al., Matrix metalloproteinase-9 is elevated in 1-methyl-4-phenyl-1,2,3,6-tetrahydropyridine-induced parkinsonism in mice. Neuromolecular Med 2004;5(2):119-32.

186. Lundblad M, Andersson M, Winkler C, Kirik D, Wierup N, Cenci MA. Pharmacological validation of behavioural measures of akinesia and dyskinesia in a rat model of Parkinson's disease. Eur J Neurosci 2002;15(1):120-32.

187. Luquin MR, Saldise L, Guillen J, Belzunegui S, San Sebastian W, Izal A et al., Does increased excitatory drive from the subthalamic nucleus contribute to dopaminergic neuronal death in Parkinson's disease? Exp Neurol 2006;201(2):407-15.

188. Luthman J, Fredriksson A, Sundstrom E, Jonsson G, Archer T. Selective lesion of central dopamine or noradrenaline neuron systems in the neonatal rat: motor behavior and monoamine alterations at adult stage. Behav Brain Res 1989;33(3):267-77.

189. Maeda A, Sobel RA. Matrix metalloproteinases in the normal human central nervous system, microglial nodules, and multiple sclerosis lesions. J Neuropathol Exp Neurol 1996;55(3):300-9.

190. Mannello F, Luchetti F, Falcieri E, Papa S. Multiple roles of matrix metalloproteinases during apoptosis. Apoptosis 2005;10(1):19-24.

191. Manning-Bog AB, McCormack AL, Li J, Uversky VN, Fink AL, Di Monte DA. The herbicide paraquat causes up-regulation and aggregation of alpha-synuclein in mice: paraquat and alpha-synuclein. J Biol Chem 2002;277(3):1641-4.

192. Martin WR, Wieler M, Gee M. Midbrain iron content in early Parkinson disease: a potential biomarker of disease status. Neurology 2008;70(16 Pt 2):1411-7.

193. Matrisian LM. The matrix-degrading metalloproteinases. Bioessays 1992;14(7):455-63.

194. McCormack AL, Thiruchelvam M, Manning-Bog AB, Thiffault C, Langston JW, Cory-Slechta DA et al., Environmental risk factors and Parkinson's disease: selective degeneration of nigral dopaminergic neurons caused by the herbicide paraquat. Neurobiol Dis 2002;10(2):119-27.

195. McGeer EG, Klegeris A, McGeer PL. Inflammation, the complement system and the diseases of aging. Neurobiol Aging 2005;26 Suppl 1:94-7.

196. McGeer PL, Itagaki S, Boyes BE, McGeer EG. Reactive microglia are positive for HLA-DR in the substantia nigra of Parkinson's and Alzheimer's disease brains. Neurology 1988;38(8):1285-91.

197. McGeer PL, Schwab C, Parent A, Doudet D. Presence of reactive microglia in monkey substantia nigra years after 1-methyl-4-phenyl-1,2,3,6-tetrahydropyridine administration. Ann Neurol 2003;54(5):599-604.

198. McNaught KS, Belizaire R, Jenner P, Olanow CW, Isacson O. Selective loss of 20S proteasome alpha-subunits in the substantia nigra pars compacta in Parkinson's disease. Neurosci Lett 2002;326(3):155-8.

199. McNaught KS, Bjorklund LM, Belizaire R, Isacson O, Jenner P, Olanow CW. Proteasome inhibition causes nigral degeneration with inclusion bodies in rats. Neuroreport 2002;13(11):1437-41.

200. McNaught KS, Jenner P. Proteasomal function is impaired in substantia nigra in Parkinson's disease. Neurosci Lett 2001;297(3):191-4.

201. McNaught KS, Olanow CW, Halliwell B, Isacson O, Jenner P. Failure of the ubiquitin-proteasome system in Parkinson's disease. Nat Rev Neurosci 2001;2(8):589-94.

202. McNaught KS, Perl DP, Brownell AL, Olanow CW. Systemic exposure to proteasome inhibitors causes a progressive model of Parkinson's disease. Ann Neurol 2004;56(1):149-62.

203. McNaught KS, Shashidharan P, Perl DP, Jenner P, Olanow CW. Aggresome-related biogenesis of Lewy bodies. Eur J Neurosci 2002;16(11):2136-48.

204. Michalik L, Auwerx J, Berger JP, Chatterjee VK, Glass CK, Gonzalez FJ et al., International Union of Pharmacology. LXI. Peroxisome proliferator-activated receptors. Pharmacol Rev 2006;58(4):726-41.

205. Min KJ, Yang MS, Kim SU, Jou I, Joe EH. Astrocytes induce hemeoxygenase-1 expression in microglia: a feasible mechanism for preventing excessive brain inflammation. J Neurosci 2006;26(6):1880-7.

206. Mirza B, Hadberg H, Thomsen P, Moos T. The absence of reactive astrocytosis is indicative of a unique inflammatory process in Parkinson's disease. Neuroscience 2000;95(2):425-32.

207. Mogi M, Harada M, Narabayashi H, Inagaki H, Minami M, Nagatsu T. Interleukin (IL)-1 beta, IL-2, IL-4, IL-6 and transforming growth factor-alpha levels are elevated in ventricular cerebrospinal fluid in juvenile parkinsonism and Parkinson's disease. Neurosci Lett 1996;211(1):13-6.

208. Mogi M, Harada M, Riederer P, Narabayashi H, Fujita K, Nagatsu T. Tumor necrosis factor-alpha (TNF-alpha) increases both in the brain and in the cerebrospinal fluid from parkinsonian patients. Neurosci Lett 1994;165(1-2):208-10.

209. Mogi M, Togari A, Tanaka K, Ogawa N, Ichinose H, Nagatsu T. Increase in level of tumor necrosis factor (TNF)-alpha in 6-hydroxydopamine-lesioned striatum in rats

without influence of systemic L-DOPA on the TNF-alpha induction. Neurosci Lett 1999;268(2):101-4.

210. Mor G, Nilsen J, Horvath T, Bechmann I, Brown S, Garcia-Segura LM et al., Estrogen and microglia: A regulatory system that affects the brain. J Neurobiol 1999;40(4):484-96.

211. Murphy MP, Krueger MJ, Sablin SO, Ramsay RR, Singer TP. Inhibition of complex I by hydrophobic analogues of N-methyl-4-phenylpyridinium (MPP+) and the use of an ion-selective electrode to measure their accumulation by mitochondria and electron-transport particles. Biochem J 1995;306 (Pt 2):359-65.

212. Murray HE, Pillai AV, McArthur SR, Razvi N, Datla KP, Dexter DT et al., Dose- and sex-dependent effects of the neurotoxin 6-hydroxydopamine on the nigrostriatal dopaminergic pathway of adult rats: differential actions of estrogen in males and females. Neuroscience 2003;116(1):213-22.

213. Nagase H, Visse R, Murphy G. Structure and function of matrix metalloproteinases and TIMPs. Cardiovasc Res 2006;69(3):562-73.

214. Nakane PK, Pierce GB, Jr. Enzyme-labeled antibodies: preparation and application for the localization of antigens. J Histochem Cytochem 1966;14(12):929-31.

215. Neumann H. The immunological microenvironment in the CNS: implications on neuronal cell death and survival. J Neural Transm Suppl 2000;59:59-68.

216. Neumann H. Control of glial immune function by neurons. Glia 2001;36(2):191-9.

217. Neumann H, Wekerle H. Neuronal control of the immune response in the central nervous system: linking brain immunity to neurodegeneration. J Neuropathol Exp Neurol 1998;57(1):1-9.

218. Niino M, Iwabuchi K, Kikuchi S, Ato M, Morohashi T, Ogata A et al., Amelioration of experimental autoimmune encephalomyelitis in C57BL/6 mice by an agonist of peroxisome proliferator-activated receptor-gamma. J Neuroimmunol 2001;116(1):40-8.

219. Nimmerjahn A, Kirchhoff F, Helmchen F. Resting microglial cells are highly dynamic surveillants of brain parenchyma in vivo. Science 2005;308(5726):1314-8.

220. Nussbaum RL, Ellis CE. Alzheimer's disease and Parkinson's disease. N Engl J Med 2003;348(14):1356-64.

221. Nutt JG. Clinical pharmacology of levodopa-induced dyskinesia. Ann Neurol 2000;47(4 Suppl 1):S160-4; discussion S164-6.

222. Obeso JA, Rodriguez-Oroz MC, Rodriguez M, Lanciego JL, Artieda J, Gonzalo N et al., Pathophysiology of the basal ganglia in Parkinson's disease. Trends Neurosci 2000;23(10 Suppl):S8-19.

223. Ogata A, Tashiro K, Nukuzuma S, Nagashima K, Hall WW. A rat model of Parkinson's disease induced by Japanese encephalitis virus. J Neurovirol 1997;3(2):141-7.

224. Ogata Y, Enghild JJ, Nagase H. Matrix metalloproteinase 3 (stromelysin) activates the precursor for the human matrix metalloproteinase 9. J Biol Chem 1992;267(6):3581-4.

225. Olanow CW. Manganese-induced parkinsonism and Parkinson's disease. Ann N Y Acad Sci 2004;1012:209-23.

226. Olanow CW, Perl DP, DeMartino GN, McNaught KS. Lewy-body formation is an aggresome-related process: a hypothesis. Lancet Neurol 2004;3(8):496-503.

227. Olanow CW, Tatton WG. Etiology and pathogenesis of Parkinson's disease. Annu Rev Neurosci 1999;22:123-44.

228. Palmer CN, Hsu MH, Griffin KJ, Raucy JL, Johnson EF. Peroxisome proliferator activated receptor-alpha expression in human liver. Mol Pharmacol 1998;53(1):14-22.

229. Park EJ, Park SY, Joe EH, Jou I. 15d-PGJ2 and rosiglitazone suppress Janus kinase-STAT inflammatory signaling through induction of suppressor of cytokine signaling 1 (SOCS1) and SOCS3 in glia. J Biol Chem 2003;278(17):14747-52.

230. Pascual G, Fong AL, Ogawa S, Gamliel A, Li AC, Perissi V et al., A SUMOylation-dependent pathway mediates transrepression of inflammatory response genes by PPAR-gamma. Nature 2005;437(7059):759-63.

231. Paul R, Lorenzl S, Koedel U, Sporer B, Vogel U, Frosch M et al., Matrix metalloproteinases contribute to the blood-brain barrier disruption during bacterial meningitis. Ann Neurol 1998;44(4):592-600.

232. Pearson J, Goldstein M, Markey K, Brandeis L. Human brainstem catecholamine neuronal anatomy as indicated by immunocytochemistry with antibodies to tyrosine hydroxylase. Neuroscience 1983;8(1):3-32.

233. Pereira MP, Hurtado O, Cardenas A, Alonso-Escolano D, Bosca L, Vivancos J et al., The nonthiazolidinedione PPARgamma agonist L-796,449 is neuroprotective in experimental stroke. J Neuropathol Exp Neurol 2005;64(9):797-805.

234. Perry TL, Yong VW. Idiopathic Parkinson's disease, progressive supranuclear palsy and glutathione metabolism in the substantia nigra of patients. Neurosci Lett 1986;67(3):269-74.
235. Perry VH. A revised view of the central nervous system microenvironment and major histocompatibility complex class II antigen presentation. J Neuroimmunol 1998;90(2):113-21.
236. Perry VH, Gordon S. Macrophages and the nervous system. Int Rev Cytol 1991;125:203-44.
237. Perumal AS, Gopal VB, Tordzro WK, Cooper TB, Cadet JL. Vitamin E attenuates the toxic effects of 6-hydroxydopamine on free radical scavenging systems in rat brain. Brain Res Bull 1992;29(5):699-701.
238. Pickel VM, Joh TH, Reis DJ. Regional and ultrastructural localization of tyrosine hydroxylass by immunocytochemistry in dopaminergic neurons of the mesolimbic and nigroneostriatal systems. Adv Biochem Psychopharmacol 1977;16:321-9.
239. Plassman BL, Havlik RJ, Steffens DC, Helms MJ, Newman TN, Drosdick D et al., Documented head injury in early adulthood and risk of Alzheimer's disease and other dementias. Neurology 2000;55(8):1158-66.
240. Podkletnova I, Alho H. Neonatal noradrenaline depletion prevents the transition of Bergmann glia in the developing cerebellum. J Chem Neuroanat 1998;14(3-4):167-73.
241. Podkletnova I, Rothstein JD, Helen P, Alho H. Microglial response to the neurotoxicity of 6-hydroxydopamine in neonatal rat cerebellum. Int J Dev Neurosci 2001;19(1):47-52.
242. Polazzi E, Contestabile A. Reciprocal interactions between microglia and neurons: from survival to neuropathology. Rev Neurosci 2002;13(3):221-42.
243. Porter CC, Totaro JA, Stone CA. Effect of 6-hydroxydopamine and some other compounds on the concentration of norepinephrine in the hearts of mice. J Pharmacol Exp Ther 1963;140:308-16.
244. Priyadarshi A, Khuder SA, Schaub EA, Shrivastava S. A meta-analysis of Parkinson's disease and exposure to pesticides. Neurotoxicology 2000;21(4):435-40.
245. Puistola U, Ronnberg L, Martikainen H, Turpeenniemi-Hujanen T. The human embryo produces basement membrane collagen (type IV collagen)-degrading protease activity. Hum Reprod 1989;4(3):309-11.
246. Qin L, Wu X, Block ML, Liu Y, Breese GR, Hong JS et al., Systemic LPS causes chronic neuroinflammation and progressive neurodegeneration. Glia 2007;55(5):453-62.

247. Rabey JM, Sagi I, Huberman M, Melamed E, Korczyn A, Giladi N et al., Rasagiline mesylate, a new MAO-B inhibitor for the treatment of Parkinson's disease: a double-blind study as adjunctive therapy to levodopa. Clin Neuropharmacol 2000;23(6):324-30.

248. Raivich G, Bohatschek M, Kloss CU, Werner A, Jones LL, Kreutzberg GW. Neuroglial activation repertoire in the injured brain: graded response, molecular mechanisms and cues to physiological function. Brain Res Brain Res Rev 1999;30(1):77-105.

249. Ramos-DeSimone N, Hahn-Dantona E, Sipley J, Nagase H, French DL, Quigley JP. Activation of matrix metalloproteinase-9 (MMP-9) via a converging plasmin/stromelysin-1 cascade enhances tumor cell invasion. J Biol Chem 1999;274(19):13066-76.

250. Ravichandran KS. "Recruitment signals" from apoptotic cells: invitation to a quiet meal. Cell 2003;113(7):817-20.

251. Richardson JR, Quan Y, Sherer TB, Greenamyre JT, Miller GW. Paraquat neurotoxicity is distinct from that of MPTP and rotenone. Toxicol Sci 2005;88(1):193-201.

252. Ricote M, Li AC, Willson TM, Kelly CJ, Glass CK. The peroxisome proliferator-activated receptor-gamma is a negative regulator of macrophage activation. Nature 1998;391(6662):79-82.

253. Rinaman L, Milligan CE, Levitt P. Persistence of fluoro-gold following degeneration of labeled motoneurons is due to phagocytosis by microglia and macrophages. Neuroscience 1991;44(3):765-76.

254. Rodriguez M, Barroso-Chinea P, Abdala P, Obeso J, Gonzalez-Hernandez T. Dopamine cell degeneration induced by intraventricular administration of 6-hydroxydopamine in the rat: similarities with cell loss in parkinson's disease. Exp Neurol 2001;169(1):163-81.

255. Rodriguez-Pallares J, Parga JA, Munoz A, Rey P, Guerra MJ, Labandeira-Garcia JL. Mechanism of 6-hydroxydopamine neurotoxicity: the role of NADPH oxidase and microglial activation in 6-hydroxydopamine-induced degeneration of dopaminergic neurons. J Neurochem 2007;103(1):145-56.

256. Romera C, Hurtado O, Mallolas J, Pereira MP, Morales JR, Romera A et al., Ischemic preconditioning reveals that GLT1/EAAT2 glutamate transporter is a novel

PPARgamma target gene involved in neuroprotection. J Cereb Blood Flow Metab 2007;27(7):1327-38.

257. Rosenberg GA. Matrix metalloproteinases in neuroinflammation. Glia 2002;39(3):279-91.

258. Sachs C, Jonsson G. Mechanisms of action of 6-hydroxydopamine. Biochem Pharmacol 1975;24(1):1-8.

259. Salo T, Sorsa T, Lauhio A, Konttinen YT, Ainamo A, Kjeldsen L et al., Matrix metalloproteinases, their endogenous inhibitors, and microbial activators in gingival crevicular fluid and saliva of HIV(+)-subjects. Ann N Y Acad Sci 1994;732:476-8.

260. Sauer H, Oertel WH. Progressive degeneration of nigrostriatal dopamine neurons following intrastriatal terminal lesions with 6-hydroxydopamine: a combined retrograde tracing and immunocytochemical study in the rat. Neuroscience 1994;59(2):401-15.

261. Savill J, Fadok V. Corpse clearance defines the meaning of cell death. Nature 2000;407(6805):784-8.

262. Schapira AH. Etiology of Parkinson's disease. Neurology 2006;66(10 Suppl 4):S10-23.

263. Schapira AH. The use of rasagiline in Parkinson's disease. J Neural Transm Suppl 2006(71):157-61.

264. Schapira AH, Cooper JM, Dexter D, Clark JB, Jenner P, Marsden CD. Mitochondrial complex I deficiency in Parkinson's disease. J Neurochem 1990;54(3):823-7.

265. Schapira AH, Cooper JM, Dexter D, Jenner P, Clark JB, Marsden CD. Mitochondrial complex I deficiency in Parkinson's disease. Lancet 1989;1(8649):1269.

266. Schiefer J, Kampe K, Dodt HU, Zieglgansberger W, Kreutzberg GW. Microglial motility in the rat facial nucleus following peripheral axotomy. J Neurocytol 1999;28(6):439-53.

267. Schlondorff J, Blobel CP. Metalloprotease-disintegrins: modular proteins capable of promoting cell-cell interactions and triggering signals by protein-ectodomain shedding. J Cell Sci 1999;112 (Pt 21):3603-17.

268. Schmidt OI, Heyde CE, Ertel W, Stahel PF. Closed head injury--an inflammatory disease? Brain Res Brain Res Rev 2005;48(2):388-99.

269. Schulz JB, Falkenburger BH. Neuronal pathology in Parkinson's disease. Cell Tissue Res 2004;318(1):135-47.

270. Schwab JM, Schluesener HJ, Seid K, Meyermann R. IL-16 is differentially expressed in the developing human fetal brain by microglial cells in zones of neuropoesis. Int J Dev Neurosci 2001;19(1):93-100.

271. Schwarting RK, Huston JP. The unilateral 6-hydroxydopamine lesion model in behavioral brain research. Analysis of functional deficits, recovery and treatments. Prog Neurobiol 1996;50(2-3):275-331.

272. Sedgwick JD, Schwender S, Imrich H, Dorries R, Butcher GW, ter Meulen V. Isolation and direct characterization of resident microglial cells from the normal and inflamed central nervous system. Proc Natl Acad Sci U S A 1991;88(16):7438-42.

273. Sethi KD. Clinical aspects of Parkinson disease. Curr Opin Neurol 2002;15(4):457-60.

274. Sherer TB, Betarbet R, Testa CM, Seo BB, Richardson JR, Kim JH et al., Mechanism of toxicity in rotenone models of Parkinson's disease. J Neurosci 2003;23(34):10756-64.

275. Sherman MY, Goldberg AL. Cellular defenses against unfolded proteins: a cell biologist thinks about neurodegenerative diseases. Neuron 2001;29(1):15-32.

276. Shohami E, Gallily R, Mechoulam R, Bass R, Ben-Hur T. Cytokine production in the brain following closed head injury: dexanabinol (HU-211) is a novel TNF-alpha inhibitor and an effective neuroprotectant. J Neuroimmunol 1997;72(2):169-77.

277. Silva RM, Ries V, Oo TF, Yarygina O, Jackson-Lewis V, Ryu EJ et al., CHOP/GADD153 is a mediator of apoptotic death in substantia nigra dopamine neurons in an in vivo neurotoxin model of parkinsonism. J Neurochem 2005;95(4):974-86.

278. Simard AR, Rivest S. Neuroprotective properties of the innate immune system and bone marrow stem cells in Alzheimer's disease. Mol Psychiatry 2006;11(4):327-35.

279. Smith U. Pioglitazone: mechanism of action. Int J Clin Pract Suppl 2001(121):13-8.

280. Spillantini MG, Schmidt ML, Lee VM, Trojanowski JQ, Jakes R, Goedert M. Alpha-synuclein in Lewy bodies. Nature 1997;388(6645):839-40.

281. Sriram K, Matheson JM, Benkovic SA, Miller DB, Luster MI, O'Callaghan JP. Mice deficient in TNF receptors are protected against dopaminergic neurotoxicity: implications for Parkinson's disease. FASEB J 2002;16(11):1474-6.

282. Sriram K, Matheson JM, Benkovic SA, Miller DB, Luster MI, O'Callaghan JP. Deficiency of TNF receptors suppresses microglial activation and alters the susceptibility of brain regions to MPTP-induced neurotoxicity: role of TNF-alpha. FASEB J 2006;20(6):670-82.

283. Stence N, Waite M, Dailey ME. Dynamics of microglial activation: a confocal time-lapse analysis in hippocampal slices. Glia 2001;33(3):256-66.

284. Stern MB. Head trauma as a risk factor for Parkinson's disease. Mov Disord 1991;6(2):95-7.

285. Streit WJ, Kreutzberg GW. Response of endogenous glial cells to motor neuron degeneration induced by toxic ricin. J Comp Neurol 1988;268(2):248-63.

286. Streit WJ, Walter SA, Pennell NA. Reactive microgliosis. Prog Neurobiol 1999;57(6):563-81.

287. Stricker TP, Dumin JA, Dickeson SK, Chung L, Nagase H, Parks WC et al., Structural analysis of the alpha(2) integrin I domain/procollagenase-1 (matrix metalloproteinase-1) interaction. J Biol Chem 2001;276(31):29375-81.

288. Sugama S, Cho BP, Degiorgio LA, Shimizu Y, Kim SS, Kim YS et al., Temporal and sequential analysis of microglia in the substantia nigra following medial forebrain bundle axotomy in rat. Neuroscience 2003;116(4):925-33.

289. Suh SW, Hamby AM, Swanson RA. Hypoglycemia, brain energetics, and hypoglycemic neuronal death. Glia 2007;55(12):1280-6.

290. Sung JY, Park SM, Lee CH, Um JW, Lee HJ, Kim J et al., Proteolytic cleavage of extracellular secreted {alpha}-synuclein via matrix metalloproteinases. J Biol Chem 2005;280(26):25216-24.

291. Suzumura A, Sawada M, Takayanagi T. Production of interleukin-12 and expression of its receptors by murine microglia. Brain Res 1998;787(1):139-42.

292. Swerdlow RH, Parker WD, Currie LJ, Bennett JP, Harrison MB, Trugman JM et al., Gender ratio differences between Parkinson's disease patients and their affected relatives. Parkinsonism Relat Disord 2001;7(2):129-133.

293. Takahashi H, Wakabayashi K. The cellular pathology of Parkinson's disease. Neuropathology 2001;21(4):315-22.

294. Tan J, Town T, Paris D, Mori T, Suo Z, Crawford F et al., Microglial activation resulting from CD40-CD40L interaction after beta-amyloid stimulation. Science 1999;286(5448):2352-5.

295. Tanner CM, Aston DA. Epidemiology of Parkinson's disease and akinetic syndromes. Curr Opin Neurol 2000;13(4):427-30.

296. Tate CC, Garcia AJ, LaPlaca MC. Plasma fibronectin is neuroprotective following traumatic brain injury. Exp Neurol 2007;207(1):13-22.

297. Tate CC, Tate MC, LaPlaca MC. Fibronectin and laminin increase in the mouse brain after controlled cortical impact injury. J Neurotrauma 2007;24(1):226-30.

298. Tatton NA, Kish SJ. In situ detection of apoptotic nuclei in the substantia nigra compacta of 1-methyl-4-phenyl-1,2,3,6-tetrahydropyridine-treated mice using terminal deoxynucleotidyl transferase labelling and acridine orange staining. Neuroscience 1997;77(4):1037-48.

299. Tatton NA, Maclean-Fraser A, Tatton WG, Perl DP, Olanow CW. A fluorescent double-labeling method to detect and confirm apoptotic nuclei in Parkinson's disease. Ann Neurol 1998;44(3 Suppl 1):S142-8.

300. Taylor CA, Saint-Hilaire MH, Cupples LA, Thomas CA, Burchard AE, Feldman RG et al., Environmental, medical, and family history risk factors for Parkinson's disease: a New England-based case control study. Am J Med Genet 1999;88(6):742-9.

301. Teismann P, Ferger B. Inhibition of the cyclooxygenase isoenzymes COX-1 and COX-2 provide neuroprotection in the MPTP-mouse model of Parkinson's disease. Synapse 2001;39(2):167-74.

302. Tsai CH, Lo SK, See LC, Chen HZ, Chen RS, Weng YH et al., Environmental risk factors of young onset Parkinson's disease: a case-control study. Clin Neurol Neurosurg 2002;104(4):328-33.

303. Tsirka SE, Rogove AD, Bugge TH, Degen JL, Strickland S. An extracellular proteolytic cascade promotes neuronal degeneration in the mouse hippocampus. J Neurosci 1997;17(2):543-52.

304. Tu PH, Galvin JE, Baba M, Giasson B, Tomita T, Leight S et al., Glial cytoplasmic inclusions in white matter oligodendrocytes of multiple system atrophy brains contain insoluble alpha-synuclein. Ann Neurol 1998;44(3):415-22.

305. Turpeenniemi-Hujanen T, Ronnberg L, Kauppila A, Puistola U. Laminin in the human embryo implantation: analogy to the invasion by malignant cells. Fertil Steril 1992;58(1):105-13.

306. Uhl GR, Walther D, Mash D, Faucheux B, Javoy-Agid F. Dopamine transporter messenger RNA in Parkinson's disease and control substantia nigra neurons. Ann Neurol 1994;35(4):494-8.

307. Uversky VN. Neurotoxicant-induced animal models of Parkinson's disease: understanding the role of rotenone, maneb and paraquat in neurodegeneration. Cell Tissue Res 2004;318(1):225-41.

308. Uversky VN, Li J, Fink AL. Pesticides directly accelerate the rate of alpha-synuclein fibril formation: a possible factor in Parkinson's disease. FEBS Lett 2001;500(3):105-8.

309. Van der Schyf CJ, Gal S, Geldenhuys WJ, Youdim MB. Multifunctional neuroprotective drugs targeting monoamine oxidase inhibition, iron chelation, adenosine receptors, and cholinergic and glutamatergic action for neurodegenerative diseases. Expert Opin Investig Drugs 2006;15(8):873-86.

310. Vernon AC, Palmer S, Datla KP, Zbarsky V, Croucher MJ, Dexter DT. Neuroprotective effects of metabotropic glutamate receptor ligands in a 6-hydroxydopamine rodent model of Parkinson's disease. Eur J Neurosci 2005;22(7):1799-806.

311. Vernon AC, Zbarsky V, Datla KP, Dexter DT, Croucher MJ. Selective activation of group III metabotropic glutamate receptors by L-(+)-2-amino-4-phosphonobutryic acid protects the nigrostriatal system against 6-hydroxydopamine toxicity in vivo. J Pharmacol Exp Ther 2007;320(1):397-409.

312. Vijitruth R, Liu M, Choi DY, Nguyen XV, Hunter RL, Bing G. Cyclooxygenase-2 mediates microglial activation and secondary dopaminergic cell death in the mouse MPTP model of Parkinson's disease. J Neuroinflammation 2006;3:6.

313. Vila M, Jackson-Lewis V, Guegan C, Wu DC, Teismann P, Choi DK et al., The role of glial cells in Parkinson's disease. Curr Opin Neurol 2001;14(4):483-9.

314. Vila M, Przedborski S. Targeting programmed cell death in neurodegenerative diseases. Nat Rev Neurosci 2003;4(5):365-75.

315. Vilhardt F. Microglia: phagocyte and glia cell. Int J Biochem Cell Biol 2005;37(1):17-21.

316. Vincent VA, Tilders FJ, Van Dam AM. Inhibition of endotoxin-induced nitric oxide synthase production in microglial cells by the presence of astroglial cells: a role for transforming growth factor beta. Glia 1997;19(3):190-8.

317. Vowinckel E, Reutens D, Becher B, Verge G, Evans A, Owens T et al., PK11195 binding to the peripheral benzodiazepine receptor as a marker of microglia activation in multiple sclerosis and experimental autoimmune encephalomyelitis. J Neurosci Res 1997;50(2):345-53.

318. Wakabayashi K, Yoshimoto M, Tsuji S, Takahashi H. Alpha-synuclein immunoreactivity in glial cytoplasmic inclusions in multiple system atrophy. Neurosci Lett 1998;249(2-3):180-2.

319. Wang T, Pei Z, Zhang W, Liu B, Langenbach R, Lee C et al., MPP+-induced COX-2 activation and subsequent dopaminergic neurodegeneration. FASEB J 2005;19(9):1134-6.

320. Wang XJ, Ye M, Zhang YH, Chen SD. CD200-CD200R regulation of microglia activation in the pathogenesis of Parkinson's disease. J Neuroimmune Pharmacol 2007;2(3):259-64.

321. Wassef M, Berod A, Sotelo C. Dopaminergic dendrites in the pars reticulata of the rat substantia nigra and their striatal input. Combined immunocytochemical localization of tyrosine hydroxylase and anterograde degeneration. Neuroscience 1981;6(11):2125-39.

322. Welgus HG, Campbell EJ, Cury JD, Eisen AZ, Senior RM, Wilhelm SM et al., Neutral metalloproteinases produced by human mononuclear phagocytes. Enzyme profile, regulation, and expression during cellular development. J Clin Invest 1990;86(5):1496-502.

323. Wells GM, Catlin G, Cossins JA, Mangan M, Ward GA, Miller KM et al., Quantitation of matrix metalloproteinases in cultured rat astrocytes using the polymerase chain reaction with a multi-competitor cDNA standard. Glia 1996;18(4):332-40.

324. Whitehouse PJ, Hedreen JC, White CL, 3rd, Price DL. Basal forebrain neurons in the dementia of Parkinson disease. Ann Neurol 1983;13(3):243-8.

325. Wilkin GP, Knott C. Glia: a curtain raiser. Adv Neurol 1999;80:3-7.

326. Willson TM, Lambert MH, Kliewer SA. Peroxisome proliferator-activated receptor gamma and metabolic disease. Annu Rev Biochem 2001;70:341-67.

327. Wilms H, Rosenstiel P, Sievers J, Deuschl G, Zecca L, Lucius R. Activation of microglia by human neuromelanin is NF-kappaB dependent and involves p38 mitogen-activated protein kinase: implications for Parkinson's disease. FASEB J 2003;17(3):500-2.

328. Witting A, Muller P, Herrmann A, Kettenmann H, Nolte C. Phagocytic clearance of apoptotic neurons by Microglia/Brain macrophages in vitro: involvement of lectin-, integrin-, and phosphatidylserine-mediated recognition. J Neurochem 2000;75(3):1060-70.

329. Wright GJ, Cherwinski H, Foster-Cuevas M, Brooke G, Puklavec MJ, Bigler M et al., Characterization of the CD200 receptor family in mice and humans and their interactions with CD200. J Immunol 2003;171(6):3034-46.

330. Wu DC, Jackson-Lewis V, Vila M, Tieu K, Teismann P, Vadseth C et al., Blockade of microglial activation is neuroprotective in the 1-methyl-4-phenyl-1,2,3,6-tetrahydropyridine mouse model of Parkinson disease. J Neurosci 2002;22(5):1763-71.
331. Wu DC, Teismann P, Tieu K, Vila M, Jackson-Lewis V, Ischiropoulos H et al., NADPH oxidase mediates oxidative stress in the 1-methyl-4-phenyl-1,2,3,6-tetrahydropyridine model of Parkinson's disease. Proc Natl Acad Sci U S A 2003;100(10):6145-50.
332. Wyss-Coray T, Mucke L. Inflammation in neurodegenerative disease--a double-edged sword. Neuron 2002;35(3):419-32.
333. Yahr MD, Duvoisin RC. Medical therapy of Parkinsonism. Mod Treat 1968;5(2):283-300.
334. Yan L, Zucker S, Toole BP. Roles of the multifunctional glycoprotein, emmprin (basigin; CD147), in tumour progression. Thromb Haemost 2005;93(2):199-204.
335. Yong VW, Krekoski CA, Forsyth PA, Bell R, Edwards DR. Matrix metalloproteinases and diseases of the CNS. Trends Neurosci 1998;21(2):75-80.
336. Youdim MB, Lavie L, Riederer P. Oxygen free radicals and neurodegeneration in Parkinson's disease: a role for nitric oxide. Ann N Y Acad Sci 1994;738:64-8.
337. Youdim MB, Riederer P. The role of iron in senescence of dopaminergic neurons in Parkinson's disease. J Neural Transm Suppl 1993;40:57-67.
338. Yuan H, Sarre S, Ebinger G, Michotte Y. Histological, behavioural and neurochemical evaluation of medial forebrain bundle and striatal 6-OHDA lesions as rat models of Parkinson's disease. J Neurosci Methods 2005;144(1):35-45.
339. Zbarsky V, Datla KP, Parkar S, Rai DK, Aruoma OI, Dexter DT. Neuroprotective properties of the natural phenolic antioxidants curcumin and naringenin but not quercetin and fisetin in a 6-OHDA model of Parkinson's disease. Free Radic Res 2005;39(10):1119-25.
340. Zeng BY, Iravani MM, Lin ST, Irifune M, Kuoppamaki M, Al-Barghouthy G et al., MPTP treatment of common marmosets impairs proteasomal enzyme activity and decreases expression of structural and regulatory elements of the 26S proteasome. Eur J Neurosci 2006;23(7):1766-74.
341. Zhang B, Berger J, Hu E, Szalkowski D, White-Carrington S, Spiegelman BM et al., Negative regulation of peroxisome proliferator-activated receptor-gamma gene expression contributes to the antiadipogenic effects of tumor necrosis factor-alpha. Mol Endocrinol 1996;10(11):1457-66.

342. Zhang J, Graham DG, Montine TJ, Ho YS. Enhanced N-methyl-4-phenyl-1,2,3,6-tetrahydropyridine toxicity in mice deficient in CuZn-superoxide dismutase or glutathione peroxidase. J Neuropathol Exp Neurol 2000;59(1):53-61.
343. Zheng H, Weiner LM, Bar-Am O, Epsztejn S, Cabantchik ZI, Warshawsky A et al., Design, synthesis, and evaluation of novel bifunctional iron-chelators as potential agents for neuroprotection in Alzheimer's, Parkinson's, and other neurodegenerative diseases. Bioorg Med Chem 2005;13(3):773-83.
344. Zhu JH, Kulich SM, Oury TD, Chu CT. Cytoplasmic aggregates of phosphorylated extracellular signal-regulated protein kinases in Lewy body diseases. Am J Pathol 2002;161(6):2087-98.